DRAFT

SOLAR RADIATION STATISTICAL PROPERTIES

A Technical Report of Task 9:

Solar Radiation and Pyranometry Studies

August 1992

INTERNATIONAL ENERGY AGENCY
Solar Heating & Cooling Programme

THE INTERNATIONAL ENERGY AGENCY
SOLAR HEATING AND COOLING PROGRAMME

International Energy Agency

The international Energy Agency, headquartered in Paris, was formed in November 1974 as an autonomous body withim the framework of the Organization for Economic Cooperation and Development to establish cooperation in the area of energy policy. Twenty-one countries are presently members, with the Commission of the European Communities participating under a special arrangement.

Collaboration in the research, development and demonstration of new energy technologies to help reduce dependence on oil and to increase long-term energy security has been an important part of the Agency's programme. The IEA R&D activities are headed by the Committee on Research and Development (CRD) wich is supported by a small Secretariat staff. In addition, four Working Parties (in Conservation, Fossil Fuels, Renewwable Energy and Fusion) are charged with monitoring the various collaborative energy Agreements, identifying new areas for cooperation and advising the CRD on policy matters.

Solar Heating and Cooling Programme

On of the first collaborative R&D agreements was the IEA Solar Heating and Cooling Programme which was initiated in 1977 to conduct joint projects in active and passive solar technologies, primarily for building applications. The eighteen members of the Programme are:

Australia	Germany	Norway
Austria	Finland	Spain
Belgium	Italy	Sweden
Canada	Japan	Switzerland
Denmark	The Netherlands	United Kingdom
European Community	New Zealand	United States

A total of eighteen projects or "Tasks" have been undertaken sice the beginning of the Programme. The overall programme is managed by an Executive Committee composed of one representative from each of the member countries, while the leadership and management of the individual Tasks is the responsability of Operating Agents. These Tasks and their respective Operating Agents are:

* **Task 1:** Investigation of the Performance of Solar Heating and Cooling Systems – Denmark
* **Task 2:** Coordination of Research and Development on Solar Heating and Cooling – Japan
* **Task 3:** Performance Testing of Solar Collectors – United Kingdom
* **Task 4:** Development of an Insolation Handbook and Instrument Package – Unated States
* **Task 5:** Use of Existing Meteorological Information for Solar Energy Application – Sweden
* **Task 6:** Solar Heating, Cooling, and Hot Water System Using Evacuated Collectors – Unated States
* **Task 7:** Central Solar Heating Plants with Seasonal Storage – Sweden
* **Task 8:** Passive and Hybrid Solar Low Energy Building – United States
* **Task 9:** Solar Radiation and Pyranometry Studies – Germany
* **Task 10:** Material Research and Testing – Japan
* **Task 11:** Passive and Hybrid Solar Commercial Buildings – Switzerland

Task 12: Building Energy Analysis and Design Tools for Solar Applications – United States

Task 13: Advanced Solar Low Energy Buildings – Norway

Task 14: Advanced Active Solar System – Canada

Task 15: Advanced Central Solar Heating Plants (In Planning Stage)

Task 16: Photovoltaics in Buildings – Germany

Task 17: Measuring and Modelling Spectral Radiation – Germany

Task 18: Advanced Glazing Materials – United Kingdom

* Completed Task

Brief Description of Task 9:

SOLAR RADIATION AND PYRANOMETRY STUDIES

As activity in the field of solar energy research and application increased, a need was identified for more accurate solar radiation and meteorological data to aid in resource assessment, system design and evaluation, and solar collector testing. Task 9 was initiated to address this need and to expand on the work accomplished in earlier IEA meteorological Tasks (4 and 5). The first phase of the Task ran from October 1982 until June 1987 and consisted of three Subtasks, each coordinated by a lead country;

- Subtask A: Small–scale Time and Space Variability of Solar Radiation (Austria);
- Subtask B: Validation of Solar Irradiance Simulation Models (Canada);
- Subtask C: Pyranometry (Canada).

The second phase of the Task ran from July 1987 until June 1991. The work is divided into the following Subtask:

- Subtask D: Techniques for Supplementing Network Data for Solar Energy Applications (Switzerland);
- Subtask E: Rrepresentative Design Years for Solar Ebergy Applications (Denmark);
- Subtask F: Irradiance Measurement for Solar Collector Testing (Canada).

Based on some of th eresults obtained in Subtask A and B, Subtask D was evaluating techniques for estimating solar energy radiation resources at locations between network sites, using both measured and synthetic data. In addition to the calassical statistical techniques for deriving solar radiation data received at the earth's surface (e.g., interpolation and extrapolation), new methods, such as satellite–based techniques, were investigated.
As an alternative to measured meteorological data, several techniques have been developed recently for simulating representative hourly data over the year using statistical techniques. This approach is particularly suited to simplified design techniques since there are no uncontrolled variables. Subtask E was concerned with developing recommendations on the most appropriate methods for producing representative design years as input to solar energy system and building energy system simulation models.
Building on the work of Subtask C, Subtask F focused on demonstrating the improved quality of solar radiation measurements now available. Participants developed guidelines on solar radiation measurement for solar energy engineers and rpedicted achievable accuracies for such measurements. Further experimental work on characterization of pyranometers were conducted, and the improvement of terrestrial (longwave) radiation measurement for solar collector testing was investigated.

Report No. IEA-SCHP-9E-4

SOLAR RADIATION

STATISTICAL PROPERTIES

Roberto Festa

Corrado F. Ratto

Dipartimento di Fisica,
Università di Genova,
Via Dodecaneso 33,
16146 Genova ITALY

FINAL DRAFT

August 1992

This report documents work performed within the IEA Solar Heating and Cooling Programme
Task 9: Solar Radiation and Pyranometry Studies
Subtask E: Representative Design Years for Solar Energy Applications
Volume printed by the Ufficio Documentazione of the Department of Physics of the Genoa University

Additional Copies may be ordered from:
Ufficio Documentazione
Dipartimento di Fisica,
Università di Genova,
Via Dodecaneso 33,
16146 Genova ITALY

Distribution Category: Unrestricted

Contents

List of Figures

NOMENCLATURE

Researchers in solar climatology often use very different symbols to indicate the same quantities, and sometimes the same symbols to indicate different quantities.

Eleven years ago, Solar Energy magazine published a paper signed by some of the most reknown researchers in the field, members of the *Ad-hoc Committee on Education and Standardization,* ISES [31]. In the paper standard symbols were suggested; nevertheless the use of personal notations has continued. This phenomenon, which is possibly due to the fact that the subject is still young, does not cause too many problems in a specific work report, but can produce some misunderstanding and cause continuous cumbersome explanations in a review paper. Thus, in this review we chose to use a unified "rational" (we hope) set of symbols. Of course, this implies that our symbols will be sometimes different from those used in the original paper which we will refer to.

I) Irradiation symbols

Unless otherwise specified the global, diffuse, beam, atmospheric and extra-atmospheric irradiation values (see below) refer to horizontal surfaces.

Each irradiation (or meteorological) quantity will be indicated by a two letter symbol "XY", where X indicates the time interval to which the irradiation refers and Y the type of irradiation (or of the other meteorological parameter considered):

$X = I$ instantaneous (one second to few minutes average) irradiation (i.e. *irradiance*)

$X = H$ hourly irradiation

$X = D$ daily irradiation

$X = M$ monthly irradiation

$X = Y$ yearly irradiation

Note that in notations suggested by Beckman *et al.* the irradiances are indicated with G and all irradiations with H.

$Y = G$ global (D+B) irradiation or irradiance

$Y = G_{cs}$ global irradiation under clear sky condition

$Y = G_{cls}$ global irradiation under cloudless sky condition

$Y = D$ diffuse irradiation

$Y = D_{cs}$ diffuse irradiation under clear sky condition

$Y = B$ beam (direct) irradiation

$Y = B_{cs}$ beam irradiation under clear sky condition

$Y = E$ extra-atmospheric irradiation

$Y = S$ sunshine time length

$Y = S_o$ astronomical sunshine time length

$Y = C$ fractional cloud cover

$Y = R$ relative humidity

$Y = T$ air temperature

In notations suggested by Beckman *et al.* the global irradiances and irradiations are indicated by only G and H, respectively, while the beam irradiances and irradiations are indicated by the subscript b (*i.e.* G_b and H_b, respectively) and the diffuse irradiances and irradiations are indicated by the subscript d (G_d and H_d, respectively).

With the notations used here, DG means daily global irradiation, HR means hourly relative humidity, and so on.

II) Statistical symbols

We will use systematically $f(x|y,z,...)$ to indicate the frequency (or probability) density function (*fdf*) of the random quantity X *under the condition* that the quantities $Y, Z, \ldots$ have given fixed values $y, z, \ldots$, i.e.

$$f(x|y,z,...)\,dx \;=\; Prob\{x \le X < x+dx \mid Y=y, Z=z, \ldots\}.$$

We will use the symbol $F(x|y,z,...)$ for the corresponding cumulative frequency (or probability) function (*cff*) for X, i.e.

$$F(x|y,z,...) \;=\; \int_{-\infty}^{x} dt\; f(t|y,z,...).$$

The anticumulative frequency function (*acff*)

$$1 - F(x|y,z,...)$$

will sometimes be used.

For example, $F(x|\langle x\rangle, j)$ can indicate the *cff* of a random quantity X *given* that its expected value $\langle x\rangle$ is known and that, for instance, the concerned month is j (j=1,...,12).

The symbol $\langle \ldots \rangle$ will be used to indicate expected values of a random quantity. Sometimes, mainly when reference is made to single-month frequency distributions (see the following Introduction), average values will be indicated by an overbar (as $\overline{x}$ for the average values of x).

We will often colloquially use the term *distribution* to mean a fdf or the corresponding cff.

When a distribution is not subjected to particular explicit constrains, (this is, in fact, never the case from a theoretical point of view) we will indicate its fdf and cff by $f(x)$ or $F(x)$ respectively.

III)Shortening notations

We will use the symbol

$$x \;=\; a(b)c$$

to indicate that the variable x takes the values a, $a+b$, $a+2b$,...,c. Moreover, the symbol

$$x \;=\; a[b]c$$

will mean that the range $[a, c]$ of the variable x has been partitioned into a number of intervals of width b, i.e. $[a, a+b]$, $[a+b, a+2b]$, and so on, and that a given value of x is classified according to the interval to which it belongs. Specifications about the right or left closure of the intervals, i.e. about the four possible cases $[a, c]$, $[a, c[$, $]a, c]$, $]a, c[$ (for instance, $x \in [a, c[$ means $a \leq x < c$) will be given explicitly if they are relevant.

PREFACE

Ackermann [1] ascribes to H.B. de Saussure the invention of the flat plate solar collector in the second half of the 18th century. Throughout the 19th century sporadic examples of the use of this "technological" solar energy converter are reported. More recently, during the first half of our century, both experimental and theoretical investigations on solar energy conversion methods and tests on the efficiency of the related conversion devices increased in number and continuity. At the same time a similar trend was experienced in the market of those technologies.

In spite of the long history of research into solar energy, the question of solar irradiation climatology only gained substance in the late nineteen fifties. This was probably due both to the extension of solar energy utilisation in many sparsed countries around the world and to the awareness that a better knowledge of solar availability (both in space and time) was needed in order to improve the efficiency estimation of the various conversion methods. Nevertheless, from the very beginning solar climatology took two distinct paths.

The first, which can be identified as the "physical sky modelling" route, led to important developments in the knowledge and schematization of the interactions between solar radiation and atmosphere, and produced models which satisfactorily accounted for the measured solar irradiation at the ground in terms of a number of physical and meteorological parameters (water vapour content, dust, aerosols, clouds and cloud types, and so on).

The second path, which could be called the "statistical solar climatology" route, arose mainly as a tool to help reach immediate goals in solar energy utilization, though rapidly became an autonomous field of both applicative and fundamental investigations. This second path can be ideally subdivided into four topics:

a) descriptive statistical analysis, for each locality and period of the year, of the main quantities of interest (such as hourly or daily global, diffuse or beam solar irradiation, etc.) and statistical modelling of the observed empirical frequency distributions;

b) investigations on the statistical interrelationships between the main solar quantities measurements (for instance diffuse versus beam

irradiaton) in order to break down the information, often in fact rather incomplete, needed for applications. The same goal also regards questions about the spatial correlation between simultaneous solar data at different localities;

c) investigation on the statistical interrelationships between some commonly available meteorological parameters (such as hours of sunshine, cloudiness, temperature and so on) and the simultaneous corresponding value of the main solar irradiation quantities;

d) statistical analysis of the underlying rules and parameters which can account for the observed stochastic features of the time sequences of solar irradiation data on a given time step (mainly the hour or the day).

Of course, the "physical" and "statistical" routes to solar meteorology are not unrelated to each other. On the one hand, the parameters which govern a physical model of the sky take, hour by hour or day by day, values which fluctuate according to the fluctuating changes in the meteorological and environmental situations. Thus, if one is interested in using a physical model in order to account for the real data, statistics must be introduced at the level of the model parameters.

On the other hand, any rough statistical analysis which does not carefully choose the "right" quantities to be invesigated — taking into account their fundamental physical and meteorological relationships — is destined to give trivial and/or useless results (and sometimes misleading suggestions).

In this report we will give a synthetical description of the state of the art attained in the last two or three decades about topics a), c) and d) above. Although we have tried to point out the main steps accomplished we do not claim quotation completeness nor complete explanation of all details of the quoted works. With regard to the latter, the reader can make reference to the Bibliography at the end of this report, whereas for the former we can only apologize to the unquoted researchers for the (almost unavoidable) omissions.

INTRODUCTION

We assume that the climate of a given locality is fully described by a set of (possibly interrelated) *stochastic processes*

$$x(t),\ y(t),\ z(t),...$$

each representing the stochastically determined time evolution of a specific climatological quantity (solar irradiance, wind velocity and direction, temperature, humidity, pressure, and so on). Since no secular changes in climatic conditions are considered, the set of processes is *stochastically periodic* (with period equal to one year) or *ciclostationary*, i.e. with probabilistic parameters periodically varying in time.

In particular, the *solar* climate consists of the subset of processes which are related to the solar global, diffuse and beam irradiance on the ground and/or to other solar quantities which are connected with those, such as the sunshine index, the ratios of the various irradiances with the simultaneous extraatmospheric irradiance on a parallel plane, etc.

According to the different climatological goals, the continuous stochastic processes $x(t)$, $y(t)$, $z(t)$, ... can be substituted by *stochastic sequences* (i.e. stochastic processes with discrete time parameter t), obtained by averaging, integrating or sampling them on an appropriate time basis (for instance the hour or the day).

Thus, for example, each daily observed quantity (say the daily global irradiation or the diffuse irradiation from 9 a.m. to 10 a.m.) is represented by a ciclostationary stochastic sequence with time step one day and period one year. Even with this simplification, a great number of measured years is needed in order to obtain a satisfactory statistical knowledge of the behaviour of the concerned sequences. Unfortunately, such a great number of measured years is in general not available.

Therefore, one usually more or less implicitly assumes that the daily observed climatological sequences are *stepwise* stationary, i.e. that, in spite of the intrinsic ciclostationarity, during appropriately chosen partitions of the year the subsequences are approximately stationary. This way their stochastic characteristics (relative to each

partition) can be evaluated on the basis of a fictitious larger sample (number of allowable years times the number of days in the partition). This of course implies the assumption that single realizations of daily-based stochastic sequences during each chosen section of the year, are stochastically representative, independently from the considered year, of the *ensemble* of all the possible analogous realizations.

Normally the chosen sections of the year are months, both for practical and theoretical reasons, but other sectioning procedures can be found in literature.

Thus, concepts such as "monthly frequency distribution" of a given daily referred quantity arise in the statistical analysis. Some caution must be applied to this topic, since the "monthly frequency distribution" of a daily quantity may represent its frequency distribution over a specified 30-day period (for instance, November 1977 in a given locality) or its frequency distribution over all statistically available Novembers (theoretically all conceivable Novembers, in that locality, disregarding *secular* climatical changes).

In the following we will use the words *ensemble* monthly distribution in the latter and *single* monthly distribution in the former case, avoiding the word $long-term$ as synonimous of *ensemble* (since "long" and "short", referred to the number of necessary years to obtain satisfactory estimates, depend on a variety of factors).

One can investigate, for instance, if the single January monthly frequency distributions of the hourly global irradiation between 11 a.m. and midday during the period 1958-1968, i.e. eleven different distributions, are statistically consistent to each other or each one to the ensemble January monthly distribution (all January's together).

Note, moreover, that both ensemble and single month frequency distributions are found in literature, which only refer to months which show specific statistical characteristics, for instance monthly distributions of daily global irradiation with a given daily global irradiation average value.

In the following chapters we report the main results obtained in the last three decades regarding the concerned topics. In the first chapter, frequency distributions of a number of solar climatological variables are described as they have been studied and modelled by the researchers in the field. In chapter two, some statistical relation-

ships between solar irradiation and other climatological quantities (sunshine, cloud cover, relative humidity, and so on) are discussed. In the third chapter, methods and results are reviewed concerning the time series analysis and modelling of solar irradiation quantities. Finally, in the fourth chapter, methods are described used to disaggregate global solar irradiation into diffuse and beam irradiation.

Chapter 1

FREQUENCY DISTRIBUTIONS

1.1 Relative Sunshine Durations (DS/DS_o)

The sunshine measurements obtained, for instance, with the well known Campbell–Stokes solarimeter, are the more likely solar irradiation related measurements available around the world, mainly for the distant and recent past.

Regression formulae for daily irradiations (mainly DG/DE, though even DB/DE, DD/DE and DG/DG_{cs}) versus DS/DS_o for many locations, meteorological conditions, different periods of the year, and so on, are very frequently found in literature, starting from the Angstrom work on this topic [14] [13] [12].

Ensemble frequency distributions of DS/DS_o can be easily obtained from the available measured time series.

A feature common to these distributions is a *bimodality*, or — when this is absent — a marked *skewness*, (i.e. asymmetry with respect to the *mean*), as reported for example by Lestienne [156] in his work on the *dichotomic* DS/DS_o time series at Odeillo, France, based on about three years of measurements (see Fig. 1.1). [1]

[1] This bimodality, is known to be typical not only for DS/DS_o but also for cloud cover and short-period beam irradiation distributions, two quantities intuitively related with the former.

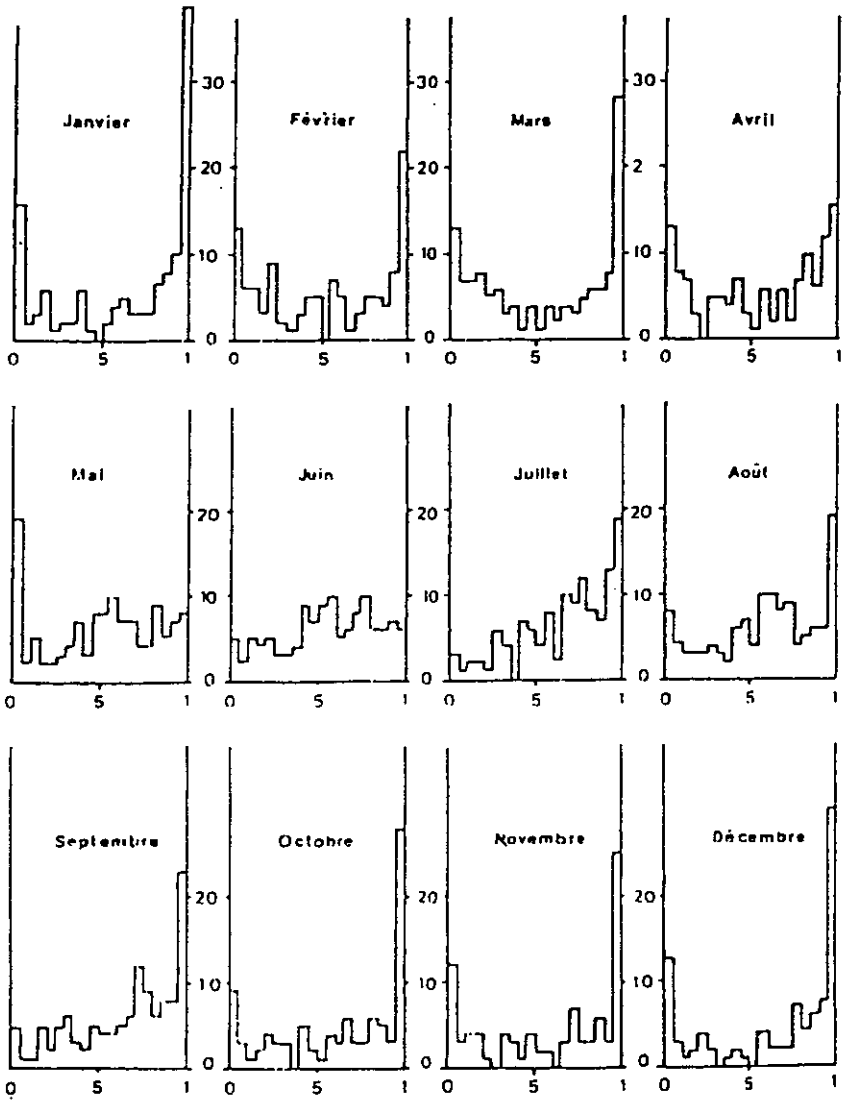

Figure 1.1: Monthly distributions of DS/DS_o relative to Odeillo, France. The bimodality and the skewness are evident. From Lestienne (79)

Goussebaile *et al.* [112] report the twelve ensemble monthly *acff*'s (with $DS/DS_o = 0.00[0.02]1.00$) based on the data of Perpignan (France) for the years 1949-1975. These curves confirm the previously noted main features. The authors try to fit the monthly curves with third degree polynomyals (coefficients are not reported), obtaining a reasonable coherence (see Fig. 1.2).

Andretta *et al.* [11], while evaluating the errors made in estimating the global solar irradiation from the relative sunshine measurements, report examples of DS/DS_o seasonal frequency distributions which confirm their customary skewness and bimodality (see Fig. 1.3).

Barbaro *et al.* [20] show, using four years of daily data for eleven Italian locations, that the single monthly *fdf*'s for DS/DS_o for any *given* locality only depend on the corresponding average value $\overline{DS/DS_o}$ (the F-test [226] with $\alpha = 0.05$ is used to support this statement). See Fig. 1.4.

The authors claim that the same dependence holds for the ensemble monthly *fdf*'s of DS/DS_o. The distributions, both *fdf*'s and *cdf*, are scanned with DS/DS_o=0.0[0.1]0.9.

In a subsequent work Barbaro *et al.* [23] examine, using the same scanning intervals and the same data base, the possible location dependence of the monthly distributions, examining 11 Italian locations. Using the Kolmogorov-Smirnov test [88] at a confidence level $\alpha = 0.05$, they find that, apart few exceptions, for each given $\langle DS/DSo \rangle$ no location dependence can be shown. Thus, they can give (see Fig. 1.5) a set of reference *cff*'s $F(DS/DSo|\langle DS/DSo \rangle)$ almost valid for all Italian locations.

The authors compare the obtained curves with the set of Bendt-like curves

$$F(x \mid \langle x \rangle) = \frac{exp(\gamma\, x) - exp(\gamma\, x_{min})}{exp(\gamma\, x_{max}) - exp(\gamma\, x_{min})}$$

where $x = DS/DS_o$.

They set $x_{min} = 0.01$ and x_{max} equal to the maximum observed value: x_{max} is allowed to vary from month to month. The γ value is iteratively calculated in terms of $\langle DS/DSo \rangle$, x_{min}, x_{max}, imposing

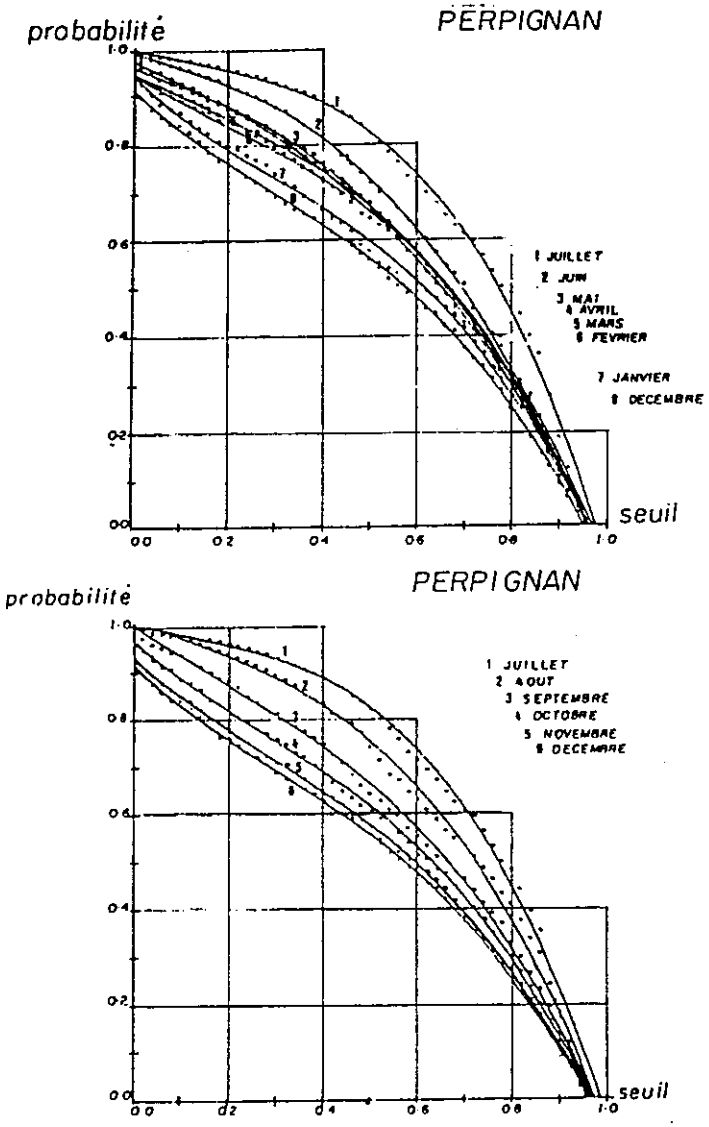

Figure 1.2: Monthly *acff's* of DS/DS_o, based on the data measured in months from December to July (above) and from July to December (below) in Perpignan, France, in years 1949–1975. The continuous lines give the smoothed frequencies obtained by fitting the empirical points by means of a third degree polynomium. From Goussebaile (79).

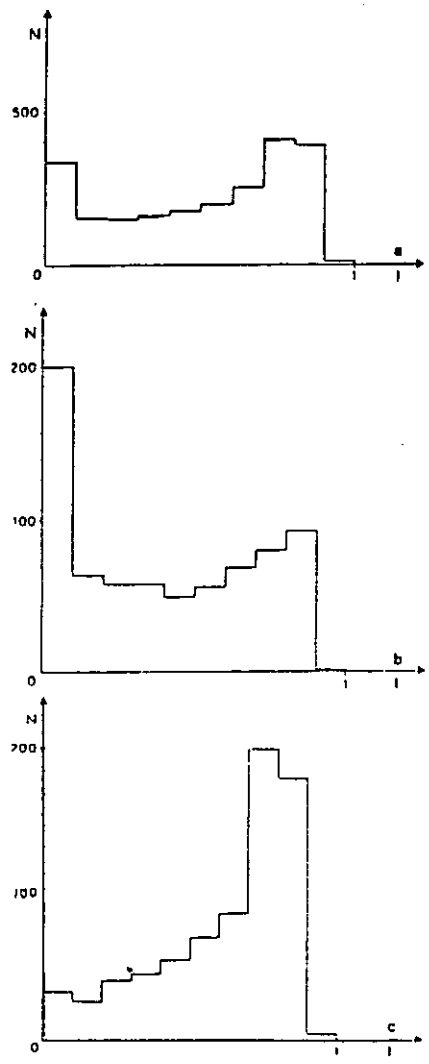

Figure 1.3: Typical frequency distributions of DG/DG_{cs} values in Italy: (a) througout the year; (b) winter (December–March); (c) summer (June–September). From Andretta (82).

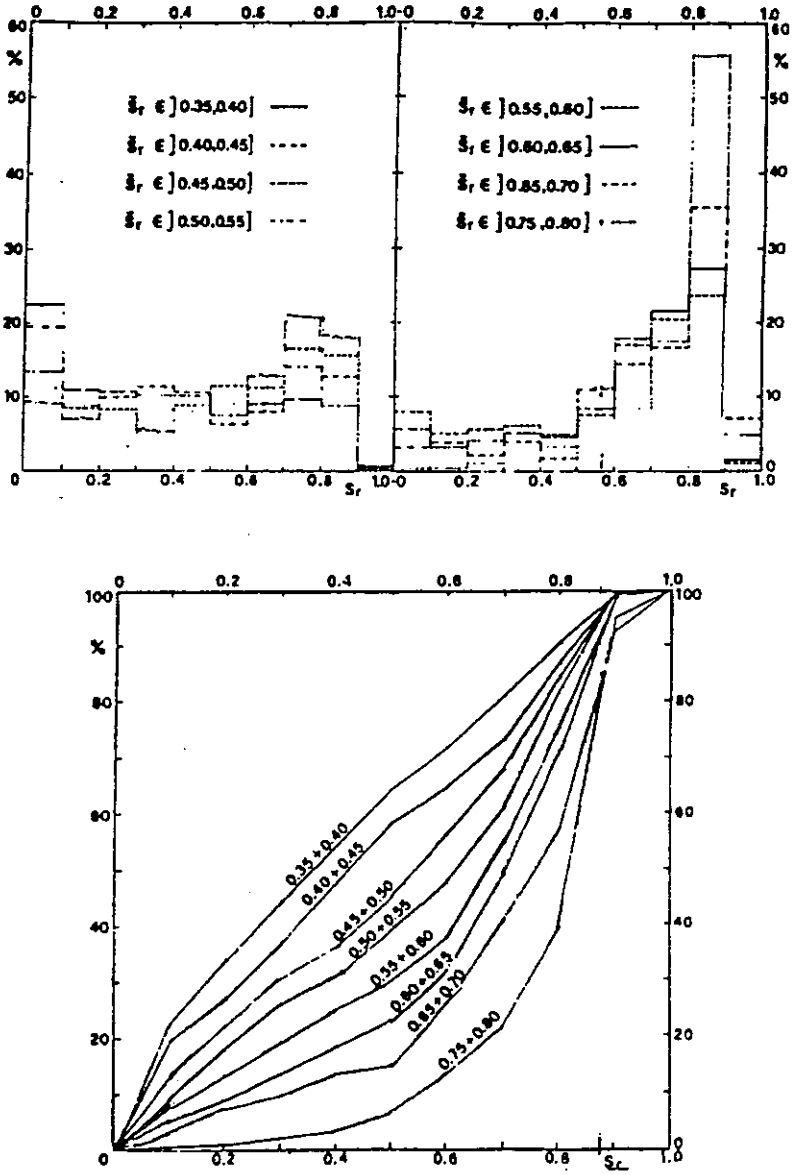

Figure 1.4: Frequency distributions (diagrams above) and the corresponding *cff's* (diagram below) of DS/DS_o for Palermo (Italy). From Barbaro (83).

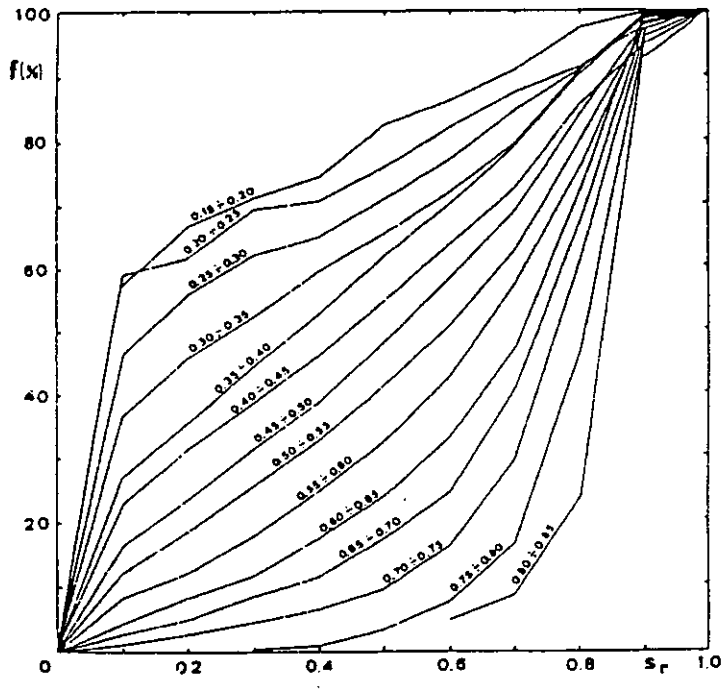

Figure 1.5: Cumulative frequency distributions of DS/DS_o relative to 11 Italian locations. From Barbaro (84).

that:

$$\langle x \rangle = \frac{\int_{x_{min}}^{x_{max}} dx\ x\ exp(\gamma\ x)}{exp(\gamma\ x_{max}) - exp(\gamma\ x_{min})}$$

i.e.

$$\langle x \rangle = \frac{x_{max}\ exp(\gamma\ x_{max}) - x_{min}\ exp(\gamma\ x_{min})}{exp(\gamma\ x_{max}) - exp(\gamma\ x_{min})} - \frac{1}{\gamma}.$$

A not so bad agreement is obtained, as one can see in Fig. 1.6.

1.2 Global irradiation

1.2.1 Daily global irradiation (DG)

Among the solar irradiation measurements, the daily global values have been for a long period (and possibly are still nowadays) the most frequently recorded data. Nevertheless they have not usually been treated by statistical methods or even graphically shown, since a previous *normalization* by the corresponding extra-atmospheric irradiation values DE has recently become a customary detrendizing practice (see next sections).

By analyzing the monthly ensemble DG frequency distributions for many U.S. stations, Bennet [39] [38] pointed out that they are negatively skewed and occasionally bimodal, and suggested that, due to these features, the *median* and the *interquartile* range give better information on the distributions than the *mean* and the *standard variance* (but, if one is interested in long term irradiation totals in a given locality, the *mean* retains of course its worth).

Klink [147] confirms the observations of Bennet, pointing out that the monthly DG frequency distributions (eleven years at St. Paul, Canada) are *negatively skewed* (i.e. with a left tail), *platycurtic* (i.e. less peaked that the gaussian *fdf*) and tend to be *bimodal.*

Baker and Klink [17], investigating such deviations from the *normality*, explicitely show the differences between the *mean* and the *median* for six monitored localities in the North-Central U.S. regions. They find that the skewness decreases as cloud cover increases and

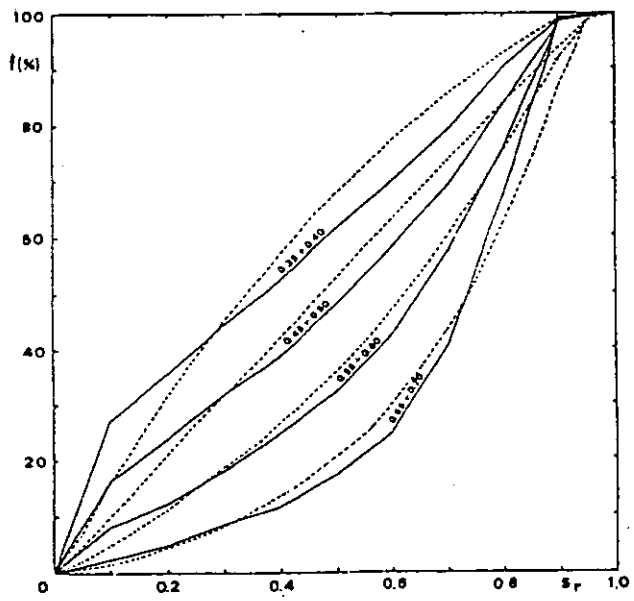

Figure 1.6: Comparison between experimental (—) and calculated (...) cfd's of DS/DS_o relative to 11 Italian localities. From Barbaro (84).

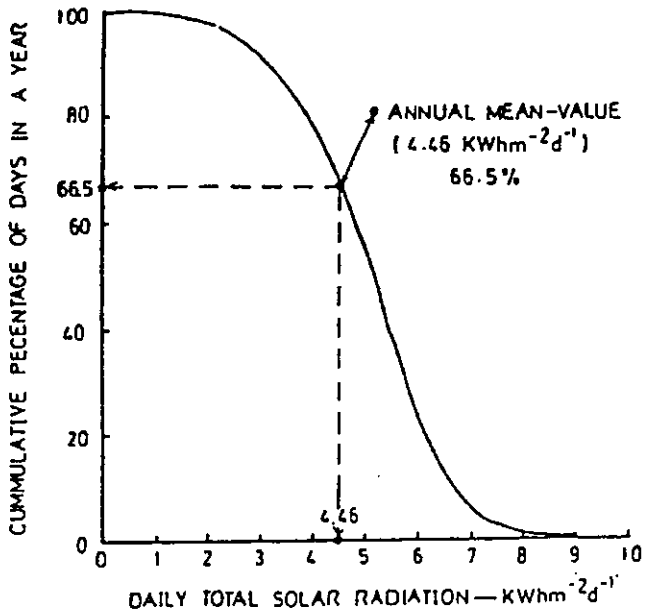

Figure 1.7: Yearly *cff* of *DG* relative to Singapore. From Rao (78).

that, even in Winter , more *skewed* distributions are found for stations with little cloud cover [2].

Rao and Lim [209] report the ensemble (10 years) yearly *acff* and *fdf* of *DG* relative to Singapore. (see Fig. 1.7), the ensemble monthly distributions with the DG values classified in three broad classes, and the percentiles (0.05(0.05)0.95) for monthly distributions.

Other sparsed examples of *DG* frequency distributions, mainly relative to single years, can be found in some solar climatological overviews such as, for instance, that given by Goh [102] for Singapore, which also reports the *short − term* (five years) monthly *DG* distribution with $DG = 0[100]600$ *cal/sqcm*. See Fig.s 1.8 and 1.9.

[2] By using the Smirnov statistics, these authors demonstrate that at least six years of data are needed to obtain stable estimates of ensemble monthly frequency distributions.

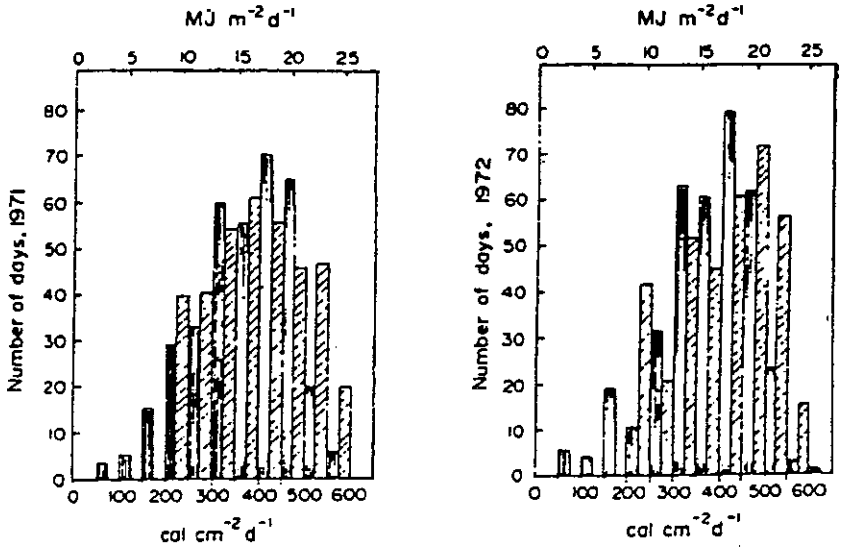

Figure 1.8: Comparison of distributions of measured and estimated values of DG. From Goh (79).

1.2.2 Scaled Daily Global Irradiation ($DG/\overline{DG}$)

The most well known example of *scaled DG* distributions is attributed to Liu and Jordan [164]. Using five years of daily data from 27 U.S. localities they were able to draw a set of generalized ensemble monthly *cff* for $DG/\overline{DG}$, each corresponding to a given value of $\langle DG/DE \rangle$ (see Fig.s 1.10, 1.11, and Fig. 1.12). These curves are not conceptually different from the more famous $\langle DG/DE \rangle$-parametrized DG/DE ensemble monthly *cff*'s (see sec.2.2.4), but are of some relevance — as one can see in Fig. 1.10. The figure, in fact, refers to vertical south facing surfaces — for their similarity with the corresponding $HG/\overline{HG}$ curves which are used to calculate the monthly "utilizability" for solar collectors. Indeed, this similarity had already been recognized by Hottel and Whillier [123].

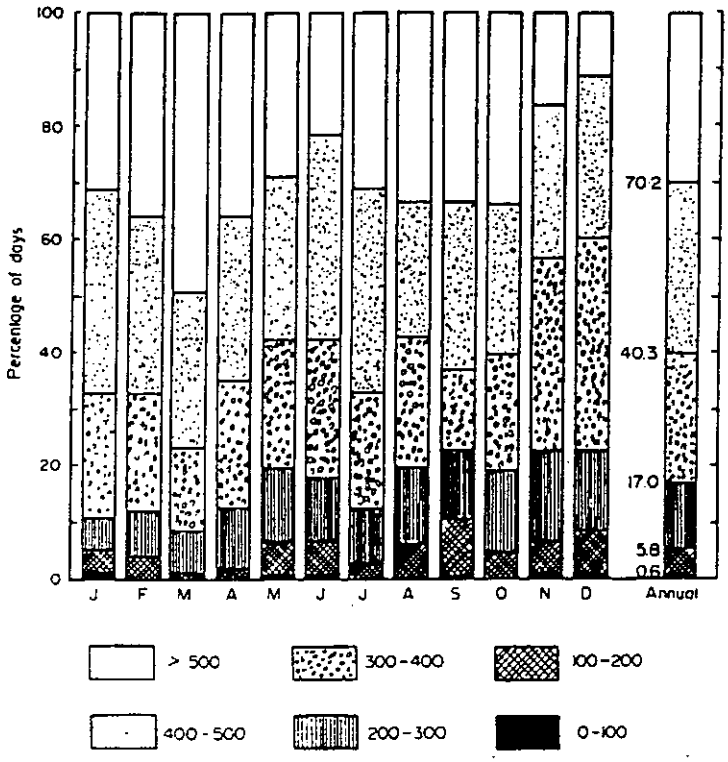

Figure 1.9: Percentage of days in a month with values of DG in various ranges (in $mWh\ cm^{-2}\ d^{-1}$). From Goh (79).

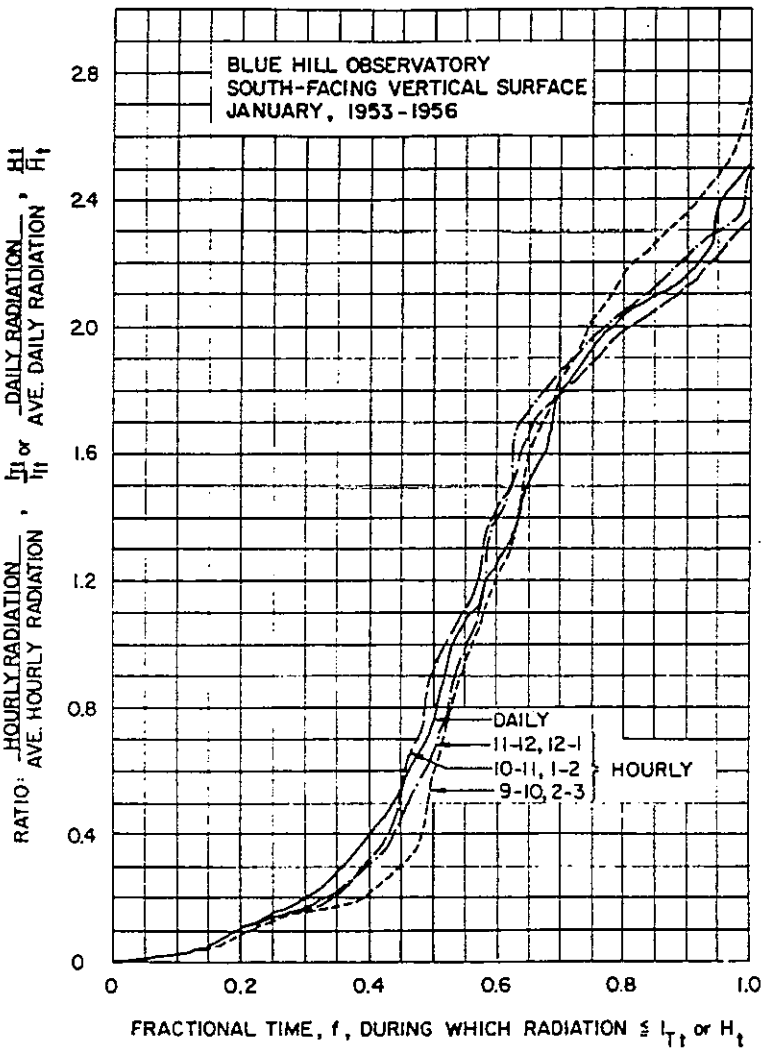

Figure 1.10: Distribution curves of $DG/\overline{DG}$ and $HG/\overline{HG}$, for a south–facing surface at Blue Hill. From Liu (63).

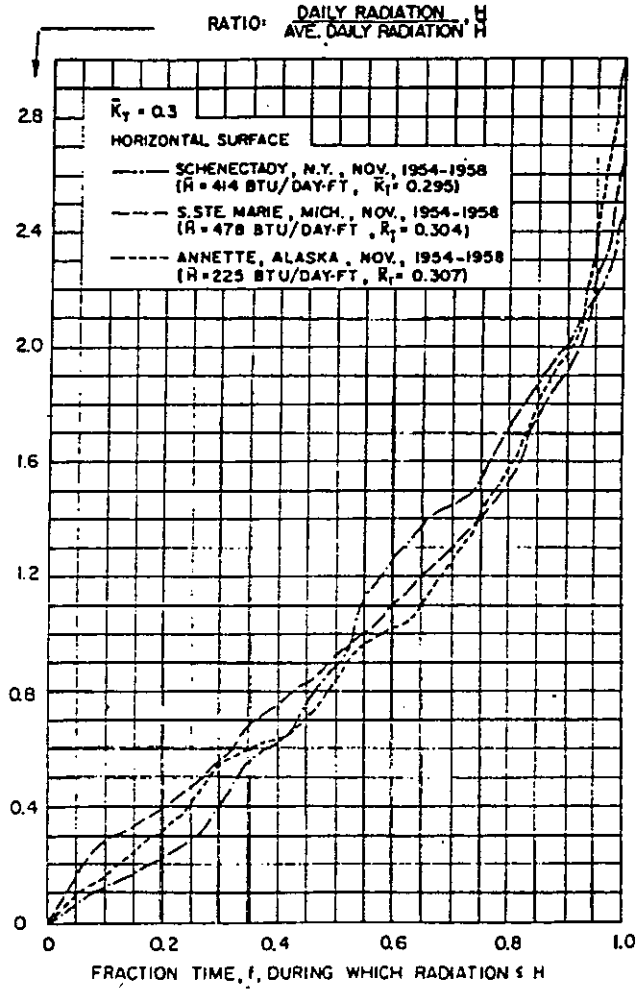

Figure 1.11: Comparison of distribution curves relative to $DG/\overline{DG}$ at Schenectady, S.Ste.Marie and Annette (for months with $\langle DG/DE \rangle = 0.3$). From Liu (63).

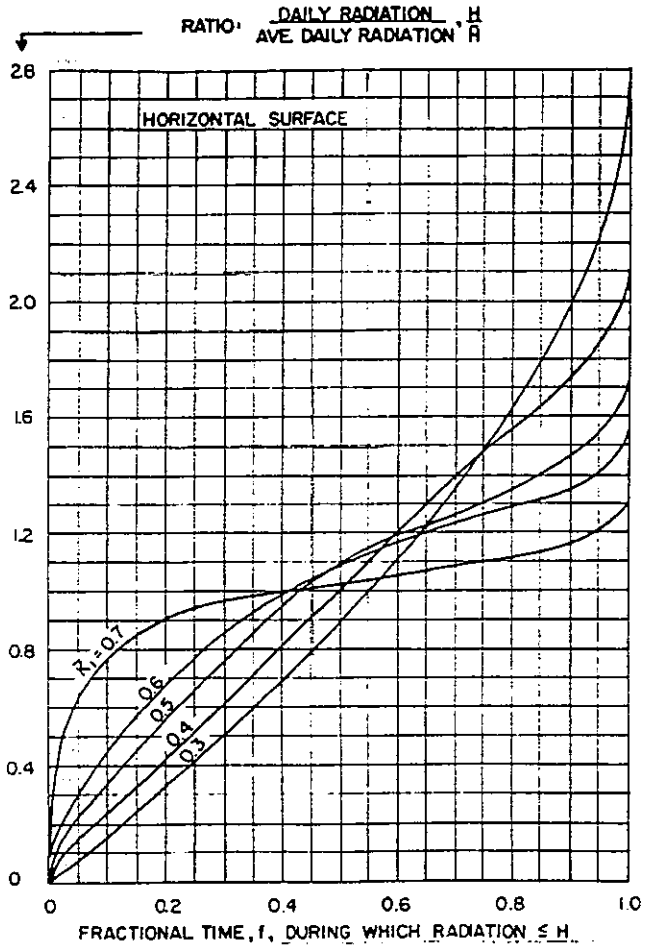

Figure 1.12: The generalized distribution curves of $DG/\overline{DG}$ for a horizontal surface relative to various $\overline{DG/DE}$. From Liu (63).

1.2.3 Scaled Daily Global Irradiation (DG/DG_{cs})

Bois *et al.* [53] [54] suggest that in order to compare the DG distributions relative to different localities or different seasons it would be appropriate to normalize DG by the *potential* or *clear sky* global daily irradiation DG_{cs}; a quantity which can be calculated using some atmospheric model or simply estimated from the data by enveloping the maximum values of DG, and which depends, for a given locality, on the time of the year. They also report the monthly *acff*'s for some months at Carpentras (France) (see Fig. 1.13).

The distributions of the *scaled DG* , i.e. DG/DG_{cs}, have been investigated by Exell [84].

Exell calculates DG_{cs} by the empirical Fourier formula

$$DG_{cs} = c_0 + \sum_{i=1}^{3} c_i \cos(i\,t) + \sum_{i=1}^{3} c_{3+i} \cos(i\,t)$$

where

$$t = 360\,\frac{n_d - 80}{365}$$

(n_d is the day number), which reproduces for suitable chosen c-values (which are in turn polynomial functions of the latitude) the values of DG_{cs} tabulated for tropical latitudes by Schuepp [227].

He divides the year into 8 periods (semi-seasons of about 45 days) and for each period tries to fit the DG/DG_{cs} distribution with a $\overline{DG/DG_{cs}}$ parametrized binomial distribution

$$f(DG/DG_{cs} \mid \overline{DG/DG_{cs}}) = 100 \binom{9}{s} p^s (1-p)^{9-s}$$

with

$$p = \frac{10\,\overline{DG/DG_{cs}} - 1}{9}$$

and $s = 0, 1, ..., 9$. See Fig. 1.14.

1.2.4 Daily Global Clearness Index (DG/DE)

Except for some previous studies by Whillier [256] the importance of the daily clearness index DG/DE in solar climatological research dates from the fundamental work of Liu and Jordan [163].

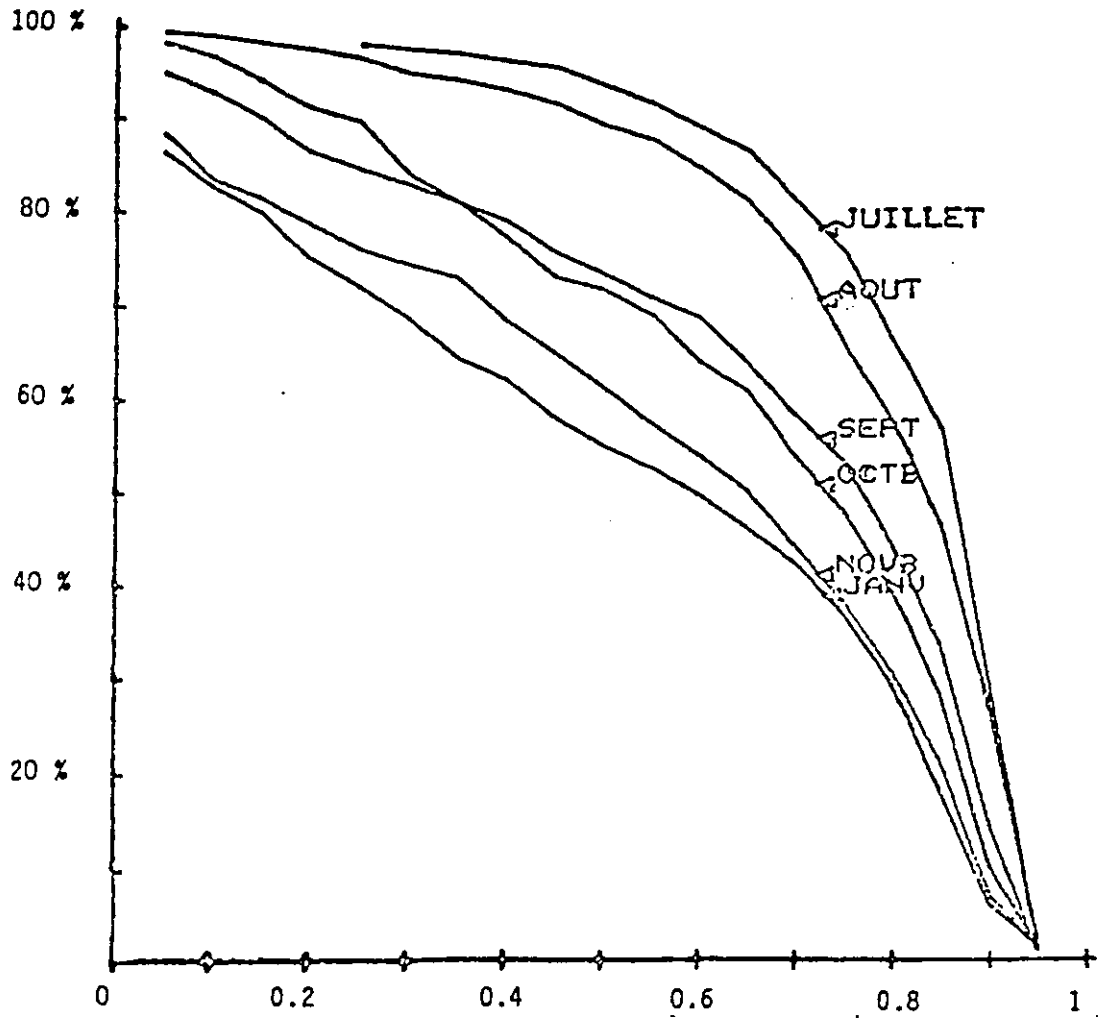

Figure 1.13: Monthly *acff*'s relative to DG/DG_{cs} for months from July to January at Carpentras, France. From Bois (78).

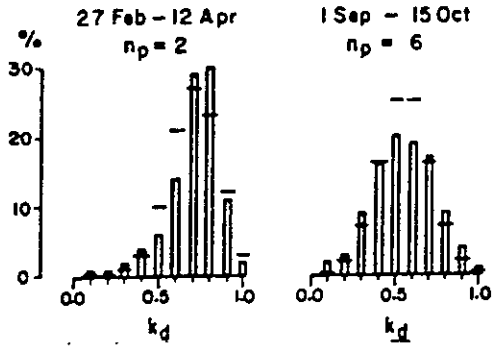

Figure 1.14: Frequency distribution of DG/DG_{cs} at Bangkok. Vertical bars: actual percentages; horizontal lines: calculated percentages. From Exell (81).

Liu and Jordan discovered, among other relevant relations, that the ensemble monthly *cff* curves for DG/DE do not vary significantly with the name of the month or the locality, but mainly depend on the single month average $\overline{DG/DE}$ in the considered month (see Fig. 1.15). In fact, they analyzed the quantity DG/DE_*, where DE_* represents the daily extra-atmospheric irradiation during a "central" day of the concerned month: note that this can cause some anomalously high DG/DE values.

In their analysis they used 5 years of data for 27 U.S. localities, with latitudes between about 19 and 55 degrees North (but mainly between 25 and 50), and deduced a set of generalized monthly ensemble *cff*s

$$F = F(x \mid \overline{x})$$

with

$$x = 0.04(0.04)1.00$$

and

$$\overline{x} = 0.3(0.1)0.7.$$

where $x = DG/DE$.

The values of $F(x \mid \overline{x})$ and the corresponding curves are shown in Fig. 1.16 and Fig. 1.17). The authors suggested that, due to the large interval of latitudes and to the variety of climatic conditions, these

curves have some approximate though universal validity (nevertheless they do not fit them with any mathematical formula).

From the Liu and Jordan paper onwards, almost every researcher concerned with the daily global irradiation statistics has been obliged to compare and/or test his own monthly distribution with the L-J curves. For instance, Ambrosone *et al.* [10] reported in 1978, i.e. about twenty years later, the *fdf*s for DG/DE=0.0(0.2)1.0 relative to four Italian localities, with $\overline{DG/DE}$= 0.30(0.05)0.70 (no explanation of the fitting curves is reported) (see Fig. 1.18).

In the late seventies, Bartoli *et al.* [27], used three years of DG measurements for 17 Italian stations in order to calculate the DG/DE frequency distributions relative to *each* individually considered month. Comparing them, they showed, using the F-test for variance comparison [226] at a confidence level $\alpha = 0.05$, that — for each given locality — months, with the same $\overline{DG/DE}$=0.25(0.05)0.75 values, have the same DG/DE frequency distribution. Moreover, they show, using the Smirnov test [88] at the same confidence level, that the $\overline{DG/DE}$ parametrization also holds for months measured in different Italian localities. These results allow the authors to build monthly generalized *cff*s and *fdf*s for DG/DE, for DG/DE=0.0(0.1)1.0 and with the $\overline{DG/DE}$ values above reported (Fig. 1.19).

One must mention on the other hand that Theilacker and Klein [247], by re-examining the Liu and Jordan data twenty years later, suggest that some site dependence in fact does exist.

An interesting feature of the DG/DE monthly frequency distributions is their marked non normality.

For instance, Graham *et al.* [113] show that the *skewness coefficient* and the *excess kurtosis* of some analyzed DG/DE distributions are by far incompatible with normality. In Fig. 1.20 the values of the DG/DE ***monthly average***, ***standard deviation***, ***skewness***, ***kurtosis***, minimum and maximum values are reported for each month.

This is why, starting from the eighties, many authors looked for formulae fitting the DG/DE monthly frequency distribution.

In 1981 Bendt *et al.* [36] repeat the analysis performed in 1960 by Liu and Jordan, using data recorded in 90 stations in the contiguous U.S. and for approximately twenty years of observation, in

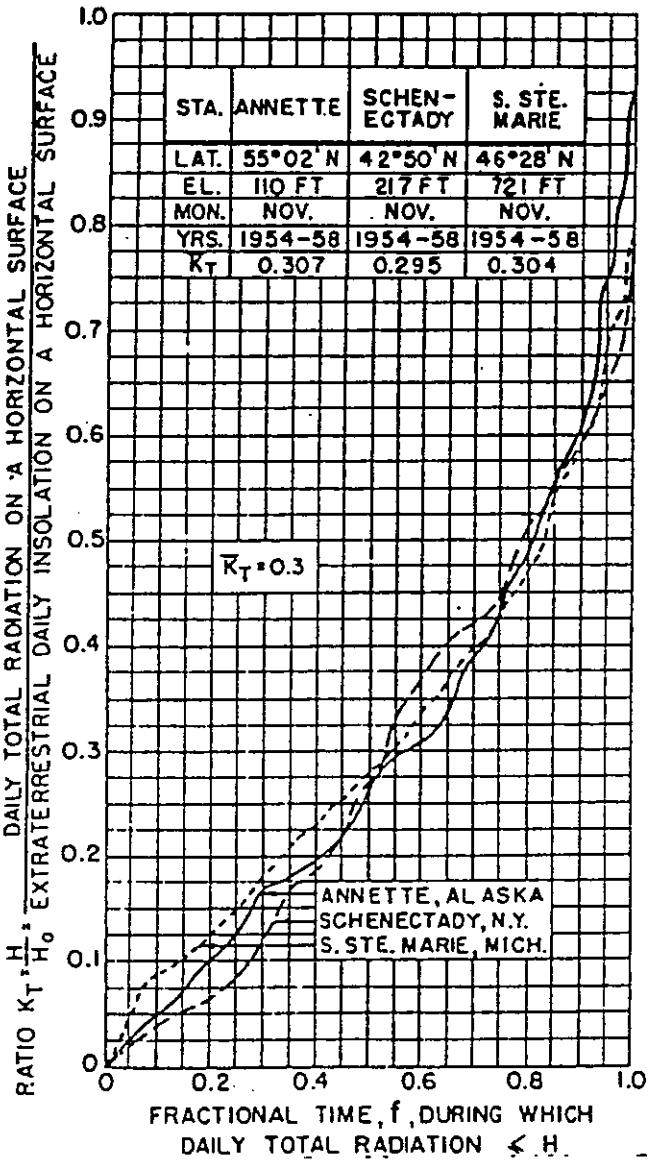

Figure 1.15: Frequency distribution curves of DG/DE for months with $\overline{DG/DE} = 0.3$. From Liu (60).

K_T	Value of f for $\bar{K}_T$ =				
	.3	.4	.5	.6	.7
.04	.073	.015	.001	.000	.000
.08	.162	.070	.023	.008	.000
.12	.245	.129	.045	.021	.007
.16	.299	.190	.082	.039	.007
.20	.395	.249	.121	.053	.007
.24	.496	.298	.160	.076	.007
.28	.513	.346	.194	.101	.013
.32	.579	.379	.234	.126	.013
.36	.628	.438	.277	.152	.027
.40	.687	.493	.323	.191	.034
.44	.748	.545	.358	.235	.047
.48	.793	.601	.400	.269	.054
.52	.824	.654	.460	.310	.081
.56	.861	.719	.509	.360	.128
.60	.904	.760	.614	.410	.161
.64	.936	.827	.703	.467	.228
.68	.953	.882	.792	.538	.295
.72	.967	.931	.873	.648	.517
.76	.979	.967	.945	.758	.678
.80	.986	.981	.980	.884	.859
.84	.993	.997	.993	.945	.940
.88	.995	.999	1.000	.985	.980
.92	.998	.999		.996	1.000
.96	.998	1.000		.999	
1.00	1.000			1.000	

Figure 1.16: Table relative to the generalized monthly cff curves for DG/DE for various $\overline{DG/DE}$ values. From Liu (60).

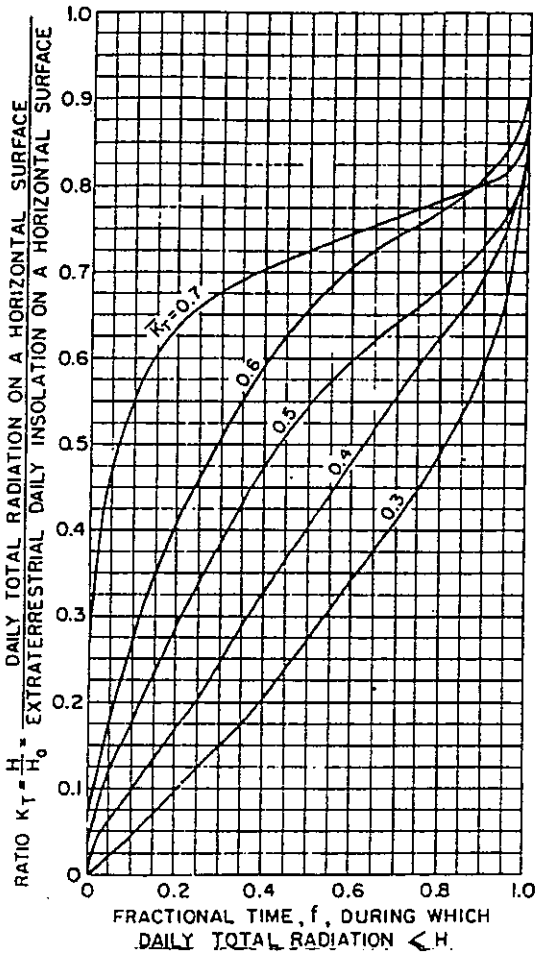

Figure 1.17: Generalized monthly cumulative frequency distribution curves of DG/DE for various $\overline{DG/DE}$ values. From Liu (60).

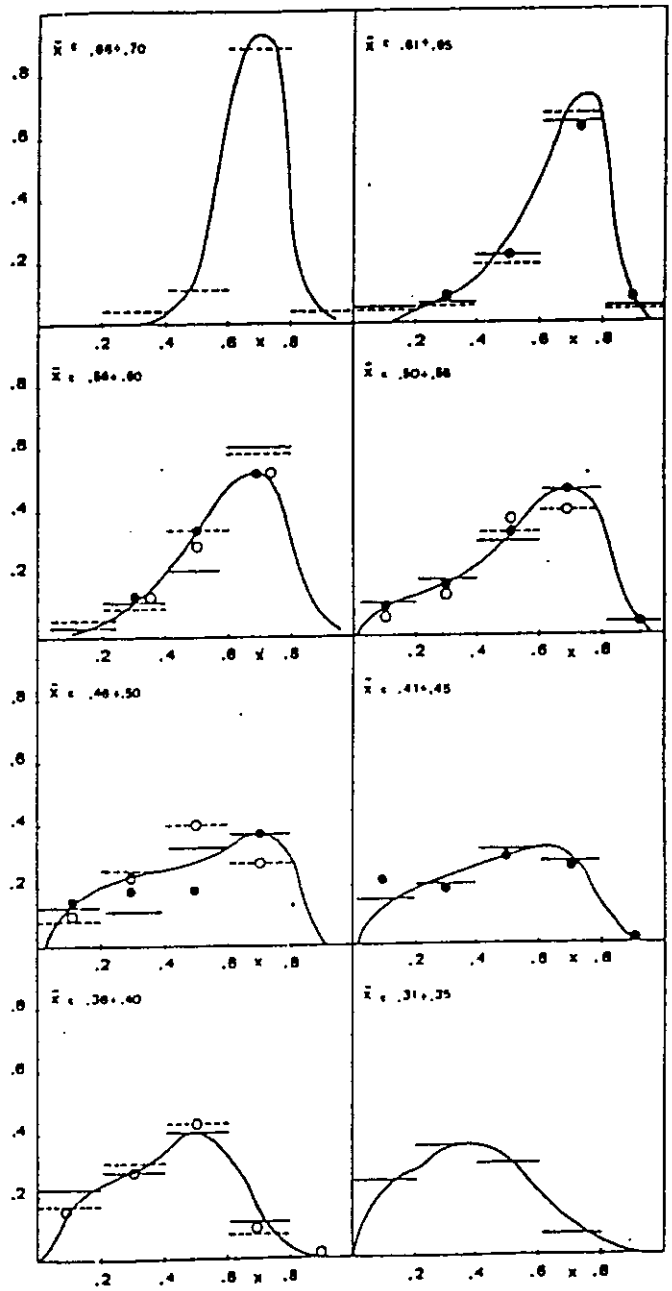

Figure 1.18: Monthly frequency distribution curves of DG/DE for months with $\overline{DG/DE} = 0.30(0.05)0.70$. From Ambrosone (78).

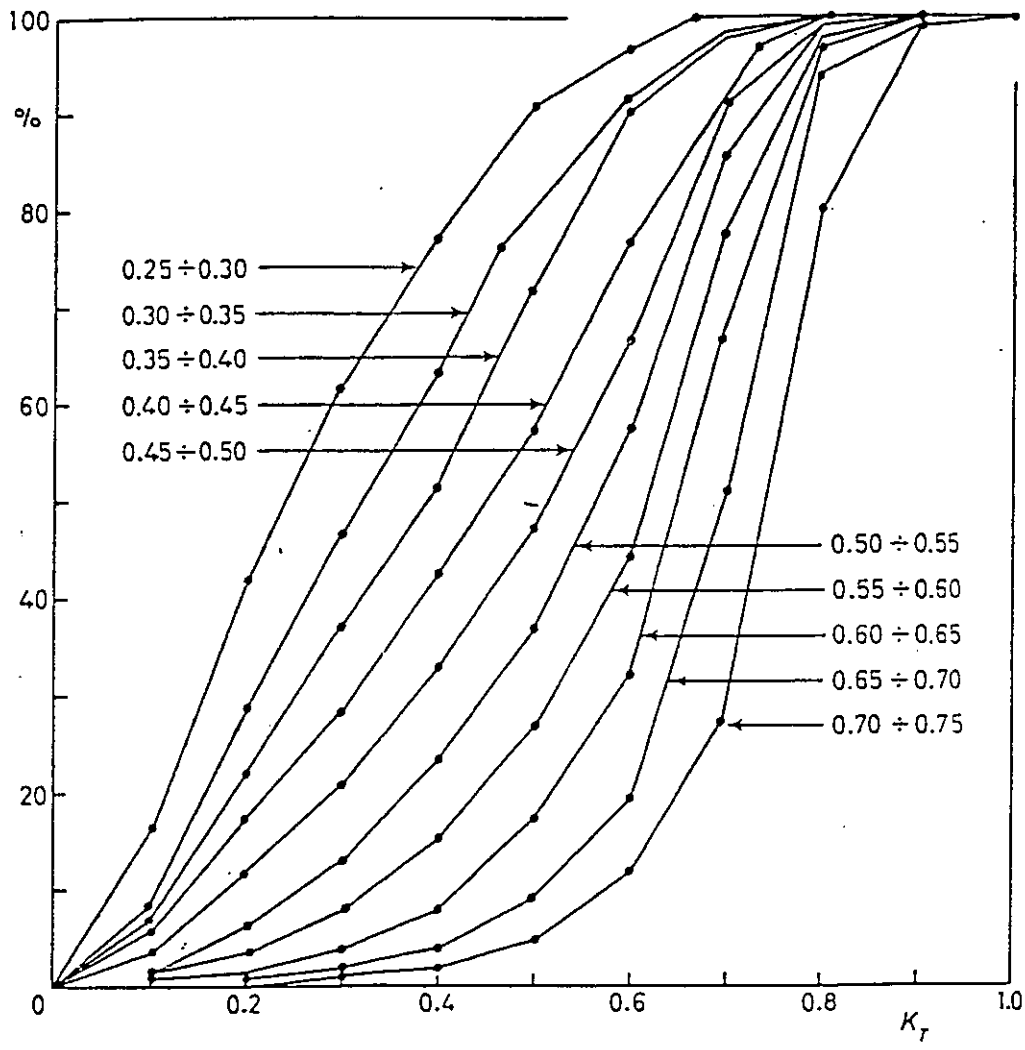

Figure 1.19: Generalized monthly frequency distribution curves of DG/DE. From Bartoli (79).

	K_t	σ_{K_t}	g_1	g_2	K_{tl}	K_{tn}
Jan	0.297	0.197	0.532	−0.971	0.023	0.751
Feb	0.390	0.228	0.184	−1.375	0.031	0.770
Mar	0.433	0.234	−0.051	−1.495	0.041	0.786
Apr	0.478	0.204	−0.291	−1.217	0.079	0.796
May	0.527	0.183	−0.683	−0.659	0.061	0.782
Jun	0.510	0.194	−0.586	−0.915	0.078	0.767
Jul	0.575	0.177	−1.149	0.148	0.072	0.768
Aug	0.535	0.183	−0.765	−0.597	0.065	0.760
Sep	0.528	0.204	−0.797	−0.695	0.066	0.773
Oct	0.412	0.228	−0.182	−1.480	0.027	0.749
Nov	0.321	0.198	0.335	−1.115	0.037	0.736
Dec	0.275	0.192	0.678	−0.771	0.017	0.772

Figure 1.20: Summary statistics of monthly DG/DE data, relative to Vancouver: month, monthly average DG/DE, standard deviation, skewness, kurtosis, minimum DG/DE, maximum DG/DE. From Graham (88).

order to confirm the previous results. They consider about 21600 single monthly frequency distributions (remember that work of Liu and Jordan was based on five years data only), from which they extract those *fdf*'s whose monthly averages $\overline{DG/DE}$ are near enough to the values 0.3(0.1)0.7 (differences of 0.01 are allowed).

An overall comparison of the long-term parametrized distributions with those of Liu and Jordan reveals a good agreement (see Fig. 1.21) except for high values of the daily clearness index (this is easily explained by the fact that Liu and Jordan use the same fixed DE value for all days of a month). Moreover, the authors are able to show the existence of a systematical seasonal trend by dividing months into three seasonal groups with the same $\overline{DG/DE}$ value.

Bendt *et al.* chose the following "seasons": May, June , July and August (MJJA), September, October and March, April (SOMA) and November, December, January and February (NDJF). Finally, for each $\overline{DG/DE}$, they compare all the individual *cff*'s (single location and month) with the general *cff* with the same $\overline{DG/DE}$ and calculate,

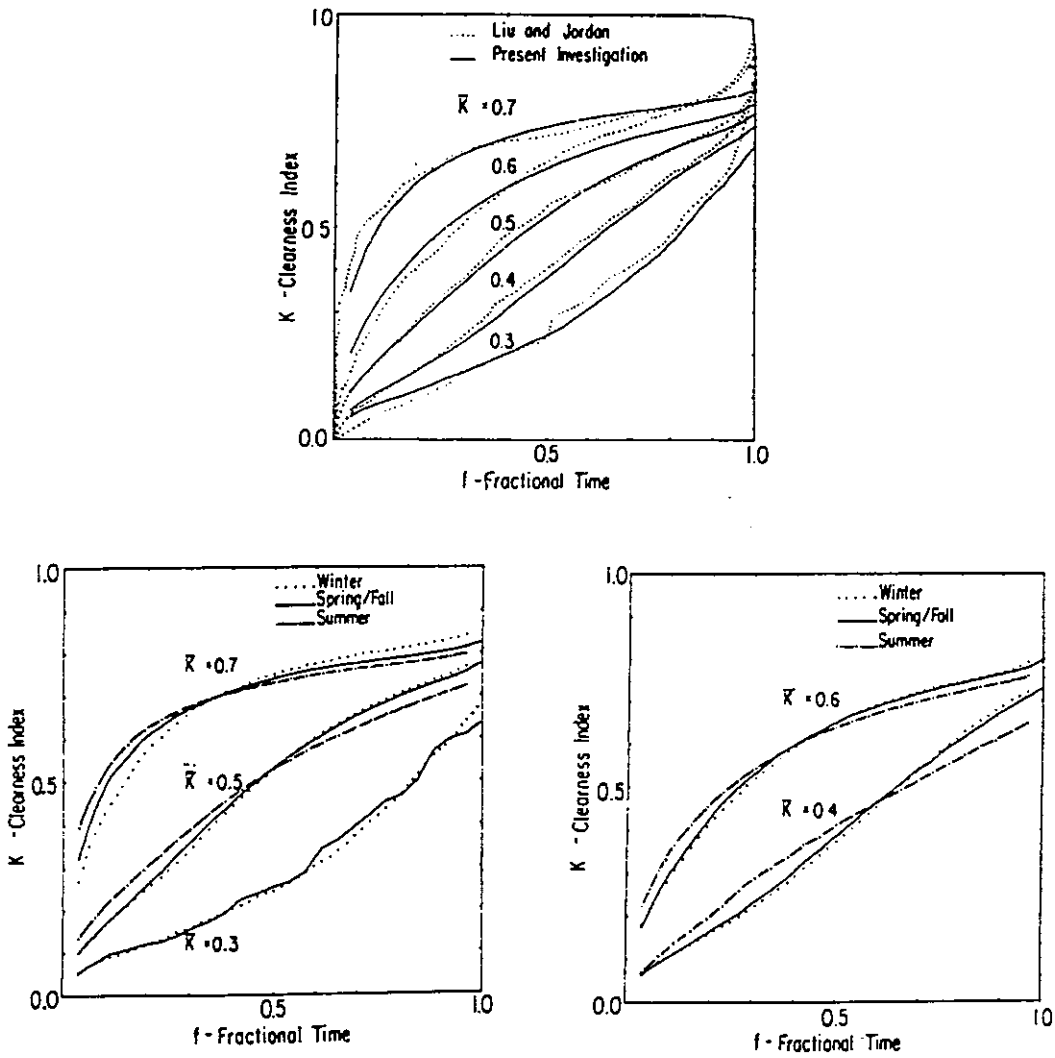

Figure 1.21: Monthly *cff*'s of DG/DE parametrized by $\overline{DG/DE}$ (above). Seasonal dependence of the same curves (below). From Bendt (81).

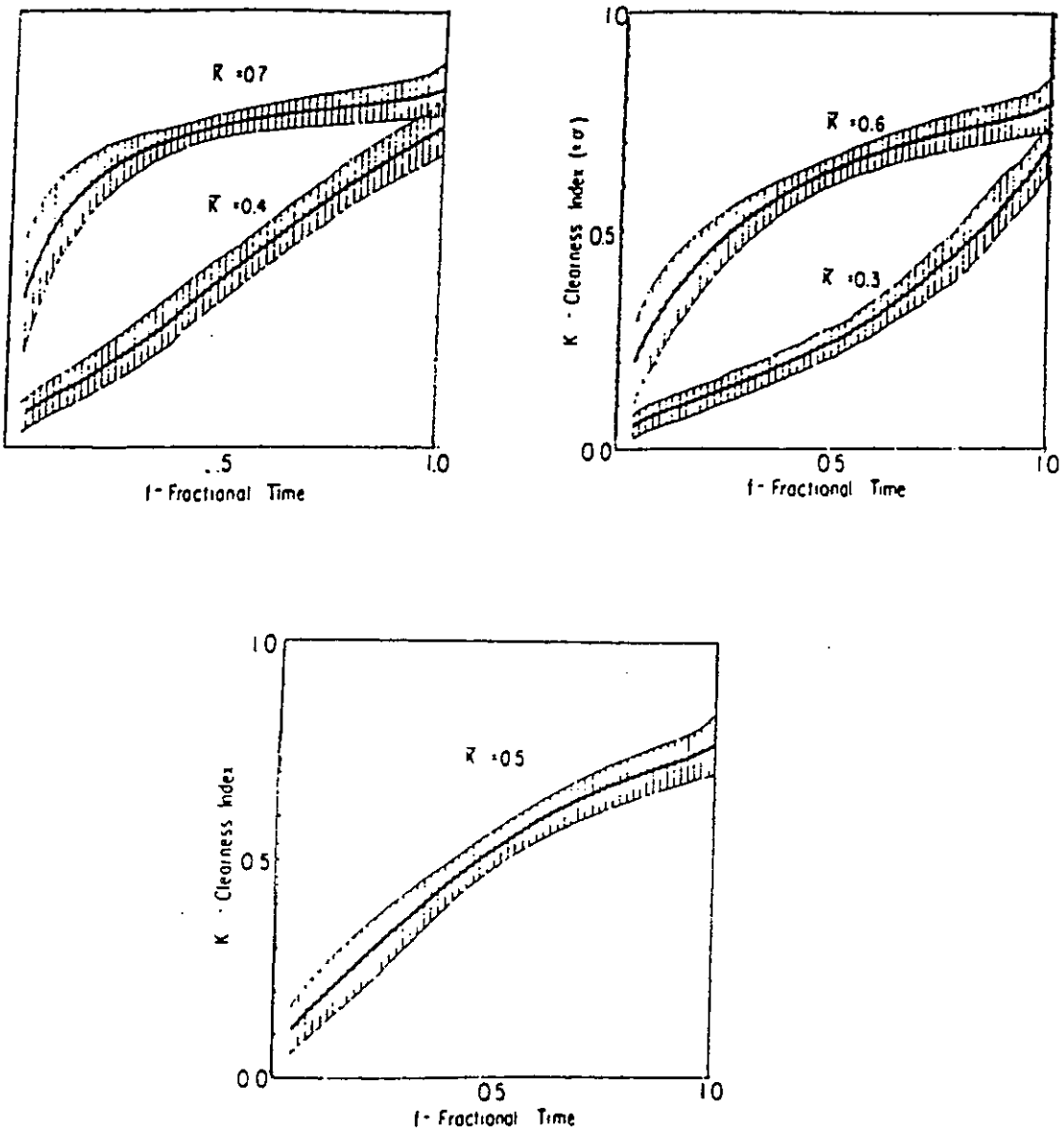

Figure 1.22: Standard deviations of the monthly *cff*'s for DG/DE parametrized by $\overline{DG/DE}$ (above). From Bendt (81).

for each value of the cumulative frequency F, the standard deviation of the corresponding set of values DG/DE. Thus the indeterminacy of the "generalized" *cff* has been investigated and estimated (see Fig. 1.22).

To conclude their work, the authors analyze, with an approximate asymptotic calculation, the "monthly" frequency distributions which would arise if a (very long) DG/DE "month" was constituted by a purely random sequence of DG/DE days — with uniform probability distribution between 0 and 1 — with the sole constrain that the final $\overline{DG/DE}$ has to assume a specified value. Bendt *et al.* deduce the density (in the following $x = DG/DE$)

$$f(x \mid \overline{x}) \;=\; \frac{\gamma \, \exp(\gamma \, x)}{\exp(\gamma \, x_{max}) \;-\; \exp(\gamma \, x_{min})}$$

in the range $x_{min} \leq x \leq x_{max}$, where $x_{min} = 0.05$, x_{max} is appropriately chosen for each month, and γ is implicitly given by the already seen average value expression:

$$\overline{x} \;=\; \frac{x_{max} \; exp(\gamma \, x_{max}) \;-\; x_{min} \; exp(\gamma \, x_{min})}{exp(\gamma \, x_{max}) \;-\; exp(\gamma \, x_{min})} \;-\; \frac{1}{\gamma}.$$

The corresponding *cff* is then given by:

$$F(x \mid \overline{x}) \;=\; \frac{\exp(\gamma \, x_{max}) \;-\; \exp(\gamma \, x_{min})}{\exp(\gamma \, x_{max}) \;-\; \exp(\gamma \, x_{min})}$$

Comparison with the experimental curves, taking x_{max} suitably dependent on $\overline{x}$, shows a good agreement (see Fig. 1.23).

A few years later Reddy *et al.* [217] suggest the choice

$$x_{max} \;=\; 0.362 \;+\; 0.597 \, \overline{x}$$

In 1981, Biga and Rosa [46], analyzing eight years of daily data for Lisbon, considered, month by month, the average $\overline{DG/DE}^{(N)}$ over periods of N = 1, 5, 15 and 25 consecutive days [3]. They investigated, for each N and, given the monthly $\overline{DG/DE}$, the frequency distributions of $\overline{DG/DE}^{(N)}$ (Fig. 1.24). They found that, to any given cumulative

[3] It is evident that the one–day average of DG/DE, i.e. $\overline{DG/DE}^{(1)}$, coincides with the measured DG/DE.

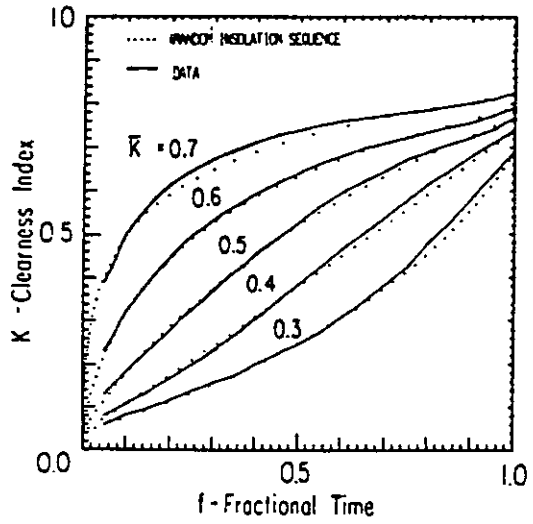

Figure 1.23: Comparison between the *cff*s of real insolation data and random insolation sequences. From Bendt (81).

frequency F=0.1(0.1)0.9, the corresponding DG/DE value is given by

$$[DG/DE](F,N) \;=\; a(F,N)\;\overline{DG/DE}^{(N)} \;+\; b(F,N)$$

For example, the median (F=0.5) of the "one day" DG/DE frequency distribution for a month with $\overline{DG/DE} = 0.4$ is given by

$$[DG/DE](0.5,1) \;=\; a(0.5,1)\;0.4 \;+\; b(0.5,1)\;.$$

Biga and Rosa tabulate and draw by interpolation the two functions $a(F,N)$ and $b(F,N)$. Furthermore they derived the corresponding *cff*s for $\overline{DG/DE}^{(N)}$, given $\overline{DG/DE}$. Comparison with the Liu and Jordan curves show a fairly good agreement.

Suercke and McCormick [243] indicate an explicit and very good approximate explicit formula for γ in the Bendt frequency distribution, given by

$$\gamma \;=\; A\;tg(\pi\;\frac{\overline{x} \;-\; \frac{x_{max}\,-\,x_{min}}{2}}{x_{max} \;-\; x_{min}})$$

where, for $x_{min} = 0.05$,

$$A \;=\; 15.51 \;-\; 20.63\;x_{max} \;+\; 9.00\;x_{max}^2 \quad .$$

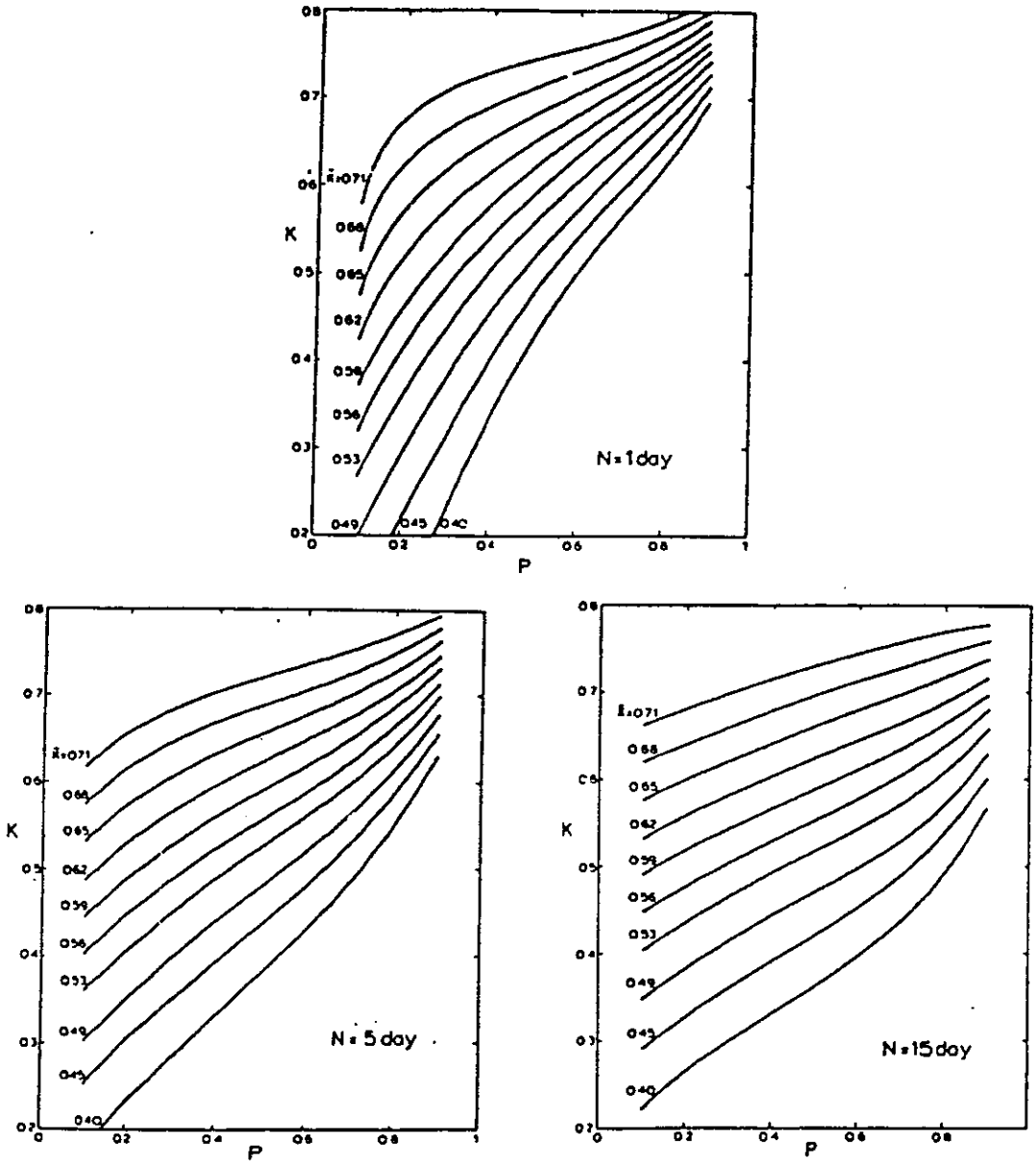

Figure 1.24: Monthly *cff*s of $\overline{DG/DE}^{(N)}$ (see text for the definition of this quantity) parametrized by $\overline{DG/DE}$. From Biga (81).

One can note that, since the Bendt formula for γ can be written

$$\frac{\overline{x} - x_{min}}{x_{max} - x_{min}} = \frac{1}{1 - exp\left[-\gamma\left(x_{max} - x_{min}\right)\right]} - \frac{1}{\gamma\left(x_{max} - x_{min}\right)}$$

then γ results in a function of $(x_{max} - x_{min})$ and of the *normalized clearness index*

$$\Phi = \frac{x - x_{min}}{x_{max} - x_{min}} \quad .$$

In 1983, Hollands and Huget [120], in a general article about the probabilistic distributions of the global clearness indices, assert that, among the standard handbook forms for the *fdf*s, the function which gives the best fit for the Liu and Jordan curves (assumed to range between 0 and their an empirical upper bound x_{max}) is the modified Gamma density

$$f(x \mid \overline{x}) = C\left(1 - \frac{x}{x_{max}}\right) exp(\lambda\, x)$$

where, as before, $x = DG/DE$. This distribution accounts for a reasonable vanishing of the *fdf*when the variable tends to its maximum value. C is a normalization factor which depends, in an analytical form, on λ and x_{max}; furthermore λ can be iteratively calculated from the formula

$$\overline{x} = \frac{\left(\frac{2}{\lambda} + x_{max}\right)\left(1 - exp(\lambda\, x_{max})\right) + 2\, x_{max}\, exp(\lambda\, x_{max})}{exp(\lambda\, x_{max}) - 1 - \lambda\, x_{max}}$$

The λ dependence on $\overline{x}$ and x_{max} is found to be very closely approximated by

$$\lambda = \frac{2\,\Gamma - 17.59\, exp(-1.3118\,\Gamma) - 1062\, exp(-5.0426\,\Gamma)}{x_{max}}$$

where $\Gamma = x_{max}/(x_{max} - \overline{x})$.

By best fitting the 1963 L-J curves, Hollands and Huget fix $x_{max} = 0.864$ and give a table for C and λ for $\overline{x}$=0.300(0.005)0.700. See Fig.s 1.25 and 1.26.

The agreement with the Liu and Jordan curves is good, the observed differences being of the same order as the location-to-location

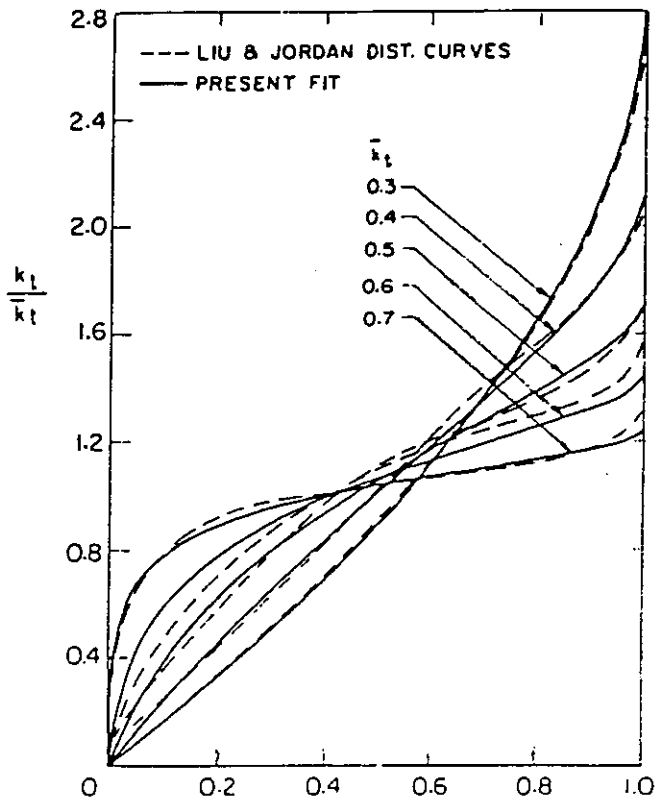

Figure 1.25: The Liu and Jordan *fdf* of $DG/\overline{DG}$ (here replaced by $DG/DE/\overline{DG/DE}$) compared with the proposed generalized *fdf* of $DG/DE/\overline{DG/DE}$. From Hollands (83).

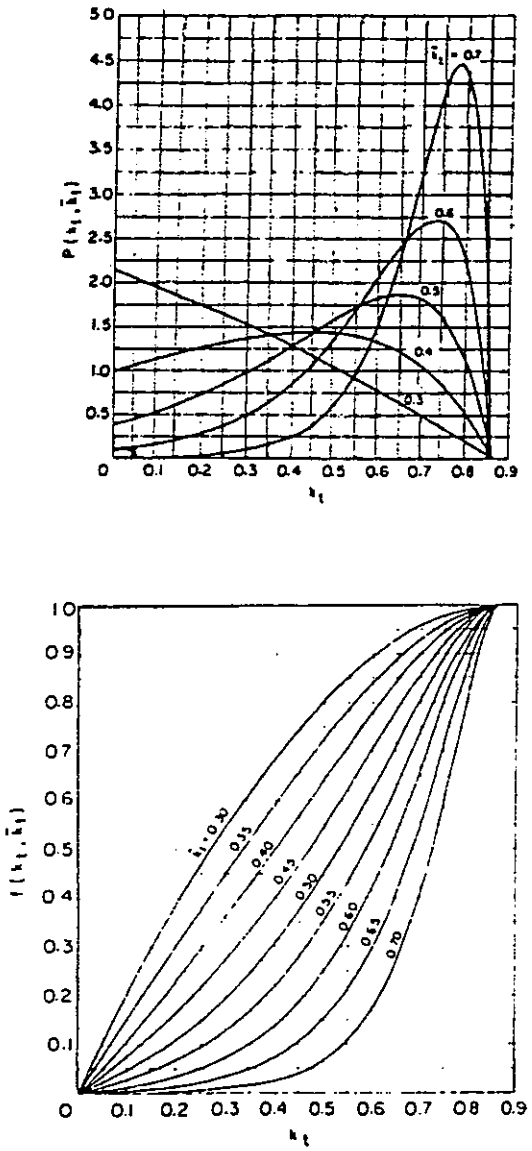

Figure 1.26: The proposed generalized *fdf*s (above) and *cdf*s (below) of DG/DE, given $\overline{DG/DE}$. From Hollands (83).

or month-to-month variability reported by Liu and Jordan. Though the comparison is performed with the *daily* clearness index curves, the authors claim to believe that the given formula holds better for the clearness index relative to one hour or less. On the other hand, they recall that Liu and Jordan found very little difference, in practice, between the two kinds of distributions.

A further formula for the DG/DE distributions was proposed in 1984 by Olseth and Skartveit [190]. As a result of the clear bimodality of the cloud cover distribution within the temperate storm belts, they suggest a formula given by a mixture of two modified Gamma distributions ("clear sky" and "overcast sky" distributions).

Their work is based on a very rich sample of daily values relative to 8 locations close to the sea, with latitudes ranging from 49.3 to 69.7, covering twenty seven years (development sample) and nineteen years (verification sample) respectively. They consider the *uniformized daily clearness index* ($x = DG/DE$)

$$\Phi \;=\; \frac{x \;-\; x_{min}}{x_{max} \;-\; x_{min}}$$

where x_{min} ranges between 0.02 and 0.05 and x_{max} ranges between 0.7 and 0.8, depending on the month. Examination of the data with $\overline{\Phi}$ partitioned into intervals of width 0.1 is performed. The bimodality of the observed frequency densities is accounted for with the formula

$$f(\Phi \mid \overline{\Phi}) \;=\; w\; G(\Phi, \lambda_1) \;+\; (1 \;-\; w)\; G(\Phi, \lambda_2)$$

where $0 \leq w \leq 1$ and G is the Gamma density:

$$G(\Phi, \lambda) \;=\; \frac{(1 \;-\; \Phi)\; exp(\lambda\; \Phi))}{\int_0^1 d\Phi\; (1 \;-\; \Phi)\; exp(\lambda\; \Phi)}$$

The λ_1 and λ_2 parameters are determined by the best fit, which gives:

$$\lambda_1 \;=\; -6.0 \;+\; 21.3\; \overline{\Phi}$$

$$\lambda_2 \;=\; 3.7 \;+\; 35\; exp(-5.3\; \overline{\Phi})$$

The weighting factor w is determined by probabilistic constraints to be

$$w \simeq 0.81 - 0.432\,\overline{\Phi};+ (\overline{\Phi} - 0.377)^3 - 23.8\,(\overline{\Phi} - 0.415)^4$$

(see [190] for greater details).

The authors compare both their model and that of Hollands-Huget with the *fdf* extracted from the verification sample, using all data together and separating different localities, and find an excellent agreement between their model and the data (Figs. 1.27 and 1.28).

Saunier *et al.* [222] question the presumed universal validity of the Liu and Jordan curves, mainly for tropical regions. Thus they suggest a single monthly distribution model for DG/DE [4]. They find that neither the L–J DG/DE distributions nor that of Bendt (with fixed DG/DE_{max}) fit the data close enough for Bangkok (five years of measurements). Same misfits are claimed to exist for Chiang Mai and for Indian localities such as Madras and Calcutta [115]. Thus, they suggest modifing the Bendt formula to take into account higher order terms in the theoretical calculation of Bendt *et al.* [36] and propose

$$f(x \mid \overline{x}) = \frac{x\,(1 - x)\,exp(\gamma\,x)}{\int_0^1 dx\; x\,(1-x)\,exp(\gamma\,x)}$$

where $x = (DG/DE)/(DG/DE_{max})$ and γ is given implicitly by

$$\langle x \rangle = \frac{exp(\gamma)\,(\gamma^2 - 4\,\gamma + 6) - 2\,\gamma - 6}{\gamma\,[exp(\gamma)\,(\gamma - 2) + \gamma + 2]}\,.$$

The authors compare, both monthly and yearly, for Bangkok, Chiang Mai and Bet Degan (Israel) the *weighted standard deviations* (wsd) given by

$$wsd^2 = \frac{1}{N-1} \sum_{i=1}^{N} x_i^2\,[f_{calc}(x_i \mid \overline{x}) - f_{obs}(x_i \mid \overline{x})]^2$$

finding a general improvement using their model with respect to the Bendt model (see Fig.s 1.29 and 1.30).

[4] More precisely, the distribution function is obtained examining the individual experimental monthly distributions and not distributions relative to ensembles of choosen months of many years.

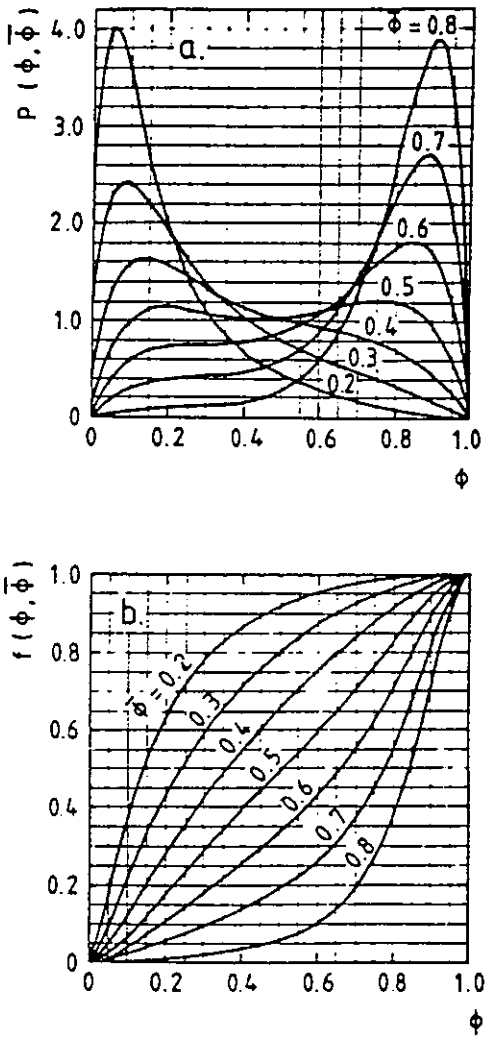

Figure 1.27: The proposed *fdf*'s (a) and *cdf*'s (b) of the *uniformized daily global irradiation* Φ (see the text) for various values of $\overline{\Phi}$. From Olseth (84).

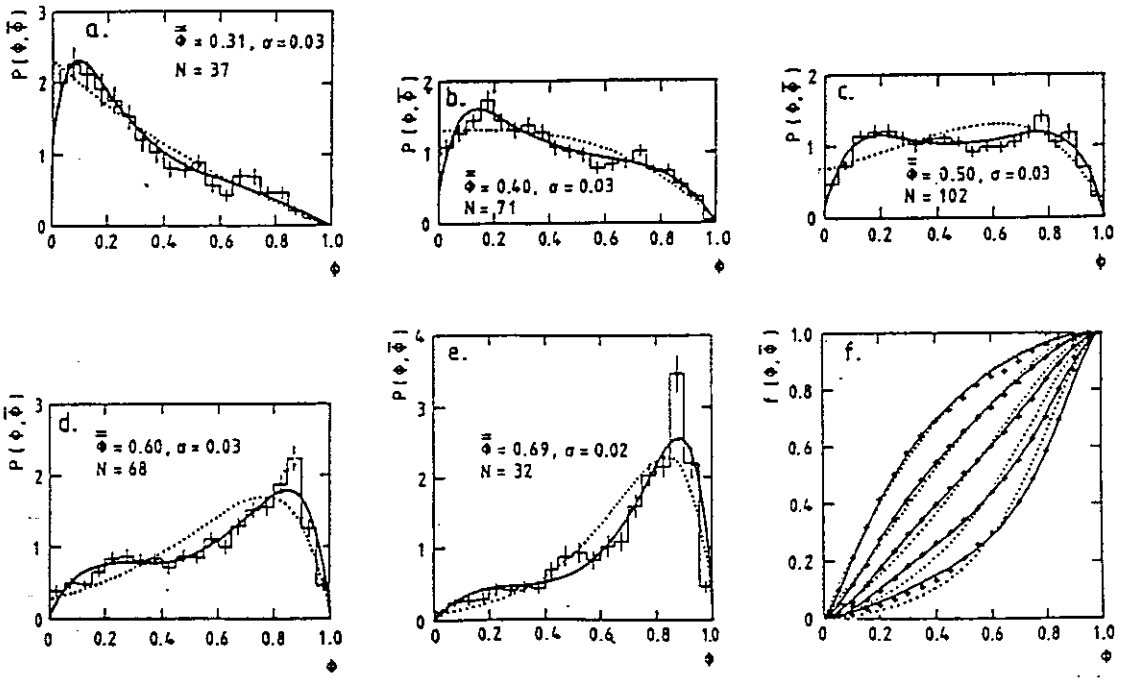

Figure 1.28: Comparison between the observed and the proposed *fdf*s of the parameter Φ (see the text) for various values of $\overline{\Phi}$. From Olseth (84).

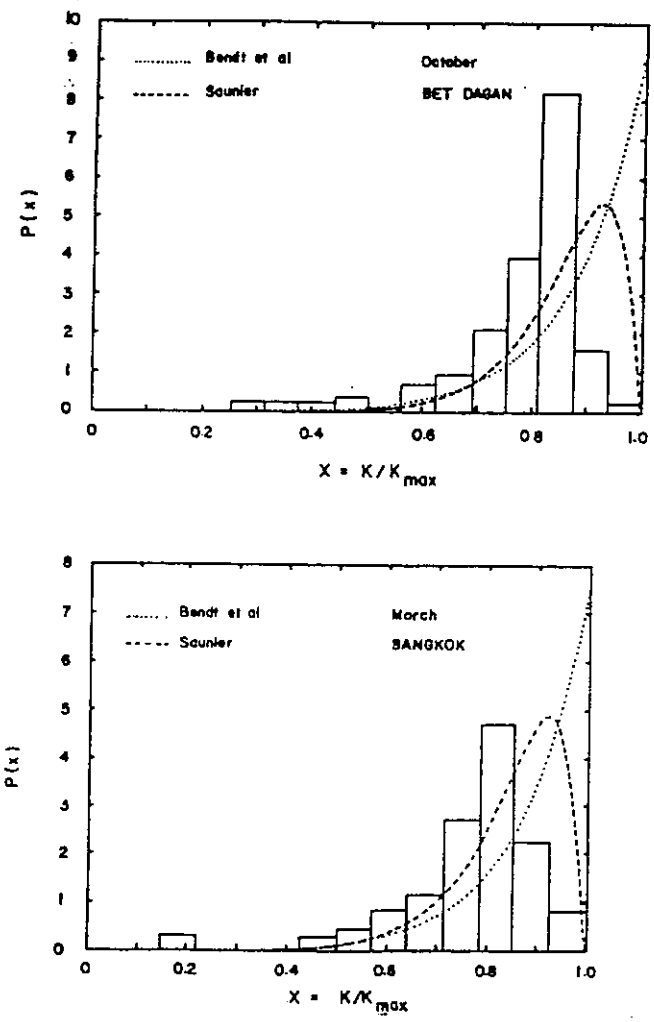

Figure 1.29: Cumulative frequency curves(*cff*'s) of DG/DE on a horizontal surface at Bangkok, as a function of $\overline{DG/DE}$. (best fit) means that a best fit on K_{max} has been performed. From Saunier (87).

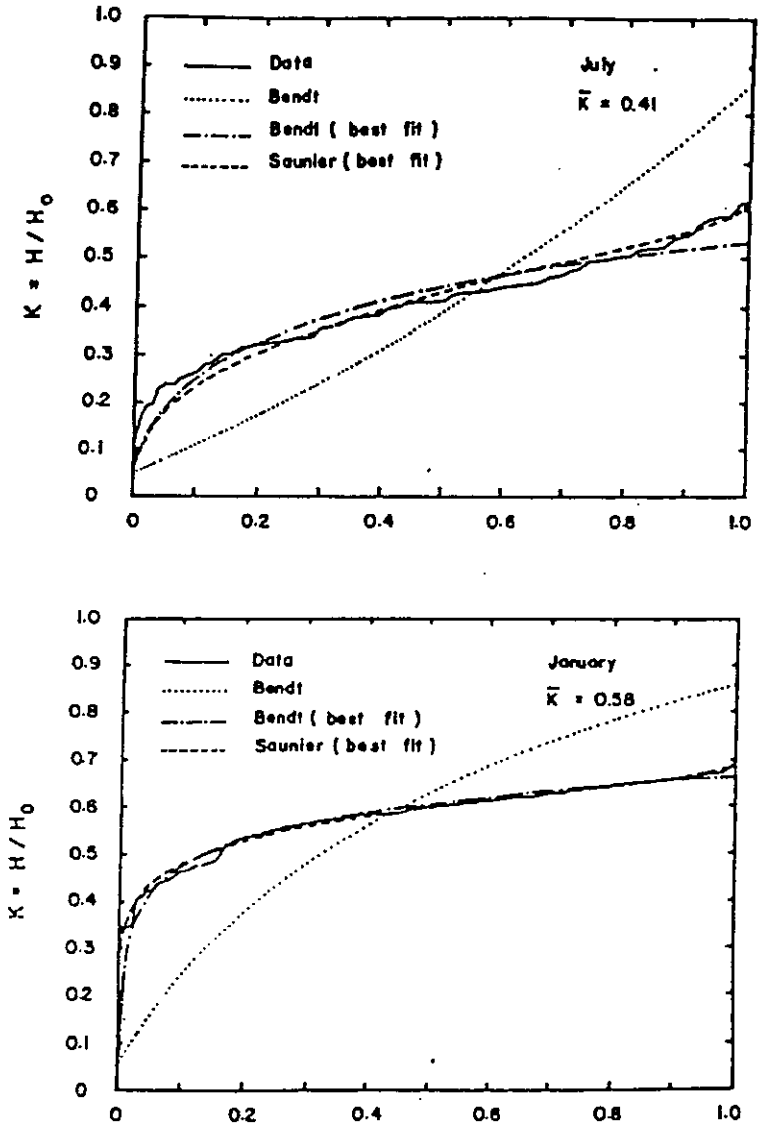

Figure 1.30: Comparison between theoretical and experimental *fdf*'s of the parameter $x = (DG/DE)/(DG/DE_{max})$ (see the text). From Saunier (87).

Gordon and Reddy [111] suggest the general formula

$$f(x) = A\, x^n \left(1 - \frac{x}{x_{max}} \right)$$

for

$$x = \frac{DG/DE}{\overline{DG/DE}} ,$$

where $\overline{DG/DE}$ is the single month average. The parameters A, n and x_{max} are determined, using the normalization condition and knowing the values of the mean $\overline{x} = 1$ and of the variance $\sigma^2(x)$, as

$$x_{max} = \frac{n+3}{n+1}$$

$$A = \frac{(n+1)\,(n+2)}{{x_{max}}^{n+1}}$$

$$n = -2.5 + 0.5\,(9. + \frac{8}{\sigma^2(x)})^{\frac{1}{2}} .$$

The authors note that the *single* monthly average $\overline{DG/DE}$ and the *single* monthly variance of DG/DE are seldom available to the designer. Thus they suggest the use of the previous frequency distribution with the ensemble monthly average and variance (see Fig. 1.31). Nevertheless, recognizing that even the knowledge of the ensemble monthly variance is not so customary, they can only suggest that the single monthly variances should be recorded in future together with the single monthly averages.

Gordon and Reddy claim that the use of the variance as a second parameter for the DG/DE frequency distributions can help to more adequately describe universal curves, largely independent from the various climates.

1.2.5 Hourly Global Irradiation (HG) and Hourly Mean Irradiance ($\overline{IG}$)

In the past, estimations of the HG monthly frequency distributions have been performed mainly in order to assess, on a monthly

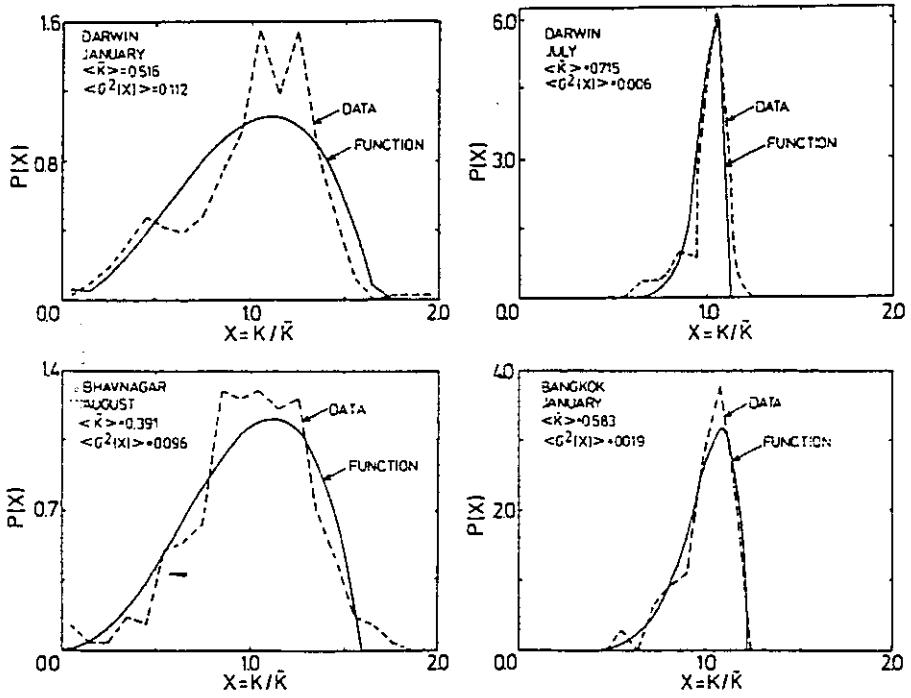

Figure 1.31: Comparison between theoretical and experimental *fdf*'s of the parameter $(DG/DE)/(\overline{DG/DE})$ considering not only the monthly average $\overline{DG/DE}$ but also the monthly variance of $(DG/DE)/(\overline{DG/DE})$. From Gordon (88).

basis, the "utilizability" of global solar irradiation (i.e. the useful energy collectable by some solar energy conversion device with a lower threshold).

In fact, these assesments has been done by many authors by replacing the ensemble monthly *cdf* of solar irradiance, IG (power per unit surface), on the ground, with the ensemble monthly *cdf* of the corresponding hourly averaged irradiances ($\overline{IG} = HG/3600$ with, for instance, HG in $joule\ sqm^{-1}$ and $\overline{IG}$ in $watt\ sqm^{-1}$).

More significantly, one can use the curve which describes the *monthly mean time per day*, t, corresponding to solar irradiance $\overline{IG}$ greater than a given value. Inverting this relation, that is expressing $\overline{IG}$ as a function of t, the useful collected solar energy is in this case simply expressed by

$$\int_0^{t_c} dt\,(\overline{IG}(t) - \overline{IG}_c)$$

where $\overline{IG}_c$ is the threshold irradiance and t_c the corresponding *monthly mean time per day* (in seconds).

Gicquel [100] gives a few exemples (for Nice, La Rochelle and Rennes) of a single monthly curve of this type $\overline{IG} = \overline{IG}(n_h)$, where n_h represents the *monthly mean time per day* measured in hours. He also tries to fit the curves with a power formula

$$\overline{IG} = 25\,(\,\frac{14 - n_h}{d}\,)^e$$

where d and e are fitting parameters whose variability is attributed to astronomical and/or meteorological local conditions (see Fig. 1.32).

In a subsequent work [99] he prefers the fitting of formula

$$\overline{IG} = \frac{S_1}{S_2\,\exp(B\,n_h) + 1} - A_0$$

and points out that this formula (known as *logistic curve*) has an intuitive meaning and is mathematically tractable with some ease (see Fig. 1.33). Nevertheless, due to "some inherent fitting imprecision", the same Gicquel *et al.* [2] finally propose a fifth order polynomial fit (the coefficient values are not reported). See Fig. 1.34.

Bedel [32] compares the hourly and six-minutes measurements of average IG, taken at Carpentras on various sloping surfaces and for

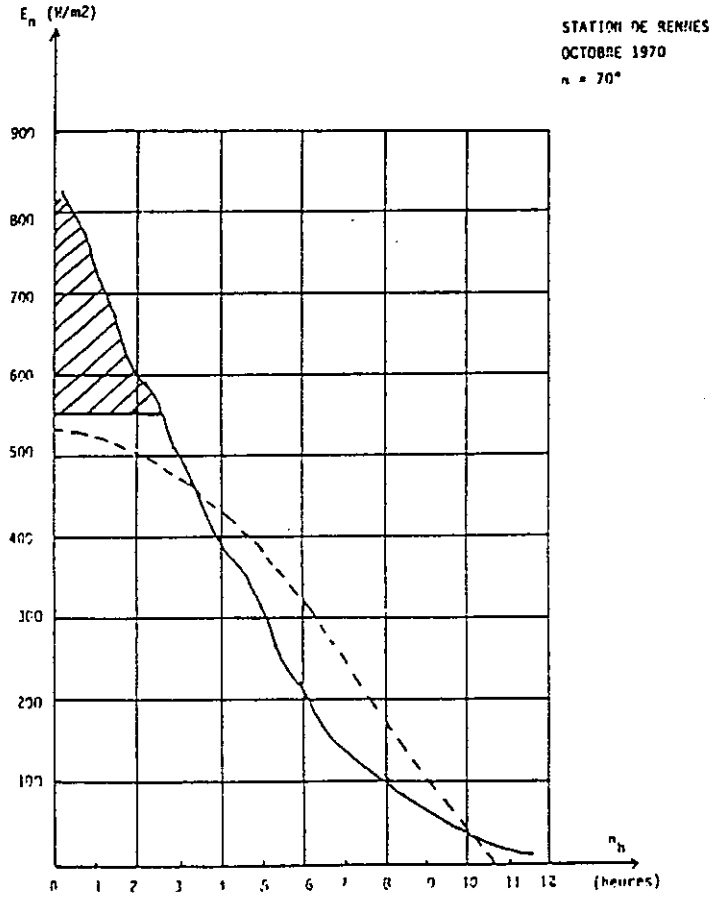

Figure 1.32: Monthly *acff*'s of the parameter $\overline{IG}$ (see the text) before (continuous line) and after (dashed line) having performed a monthly mean of $\overline{IG}$, hour by hour. From Gicquel (79).

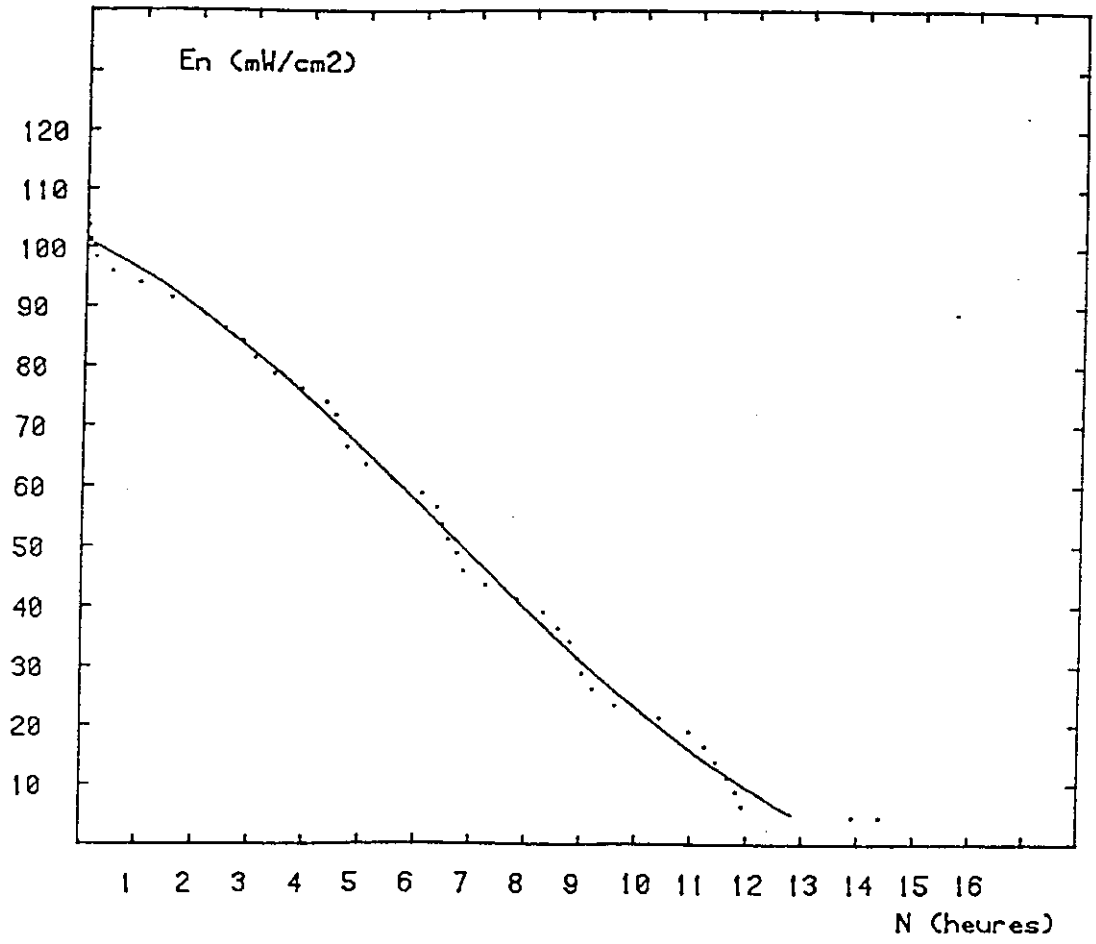

Figure 1.33: Comparison between the experimental and the theoretical (four parameter logistic curve) monthly *acff*'s of the parameter $\overline{IG}$ (see the text). From Gicquel (79).

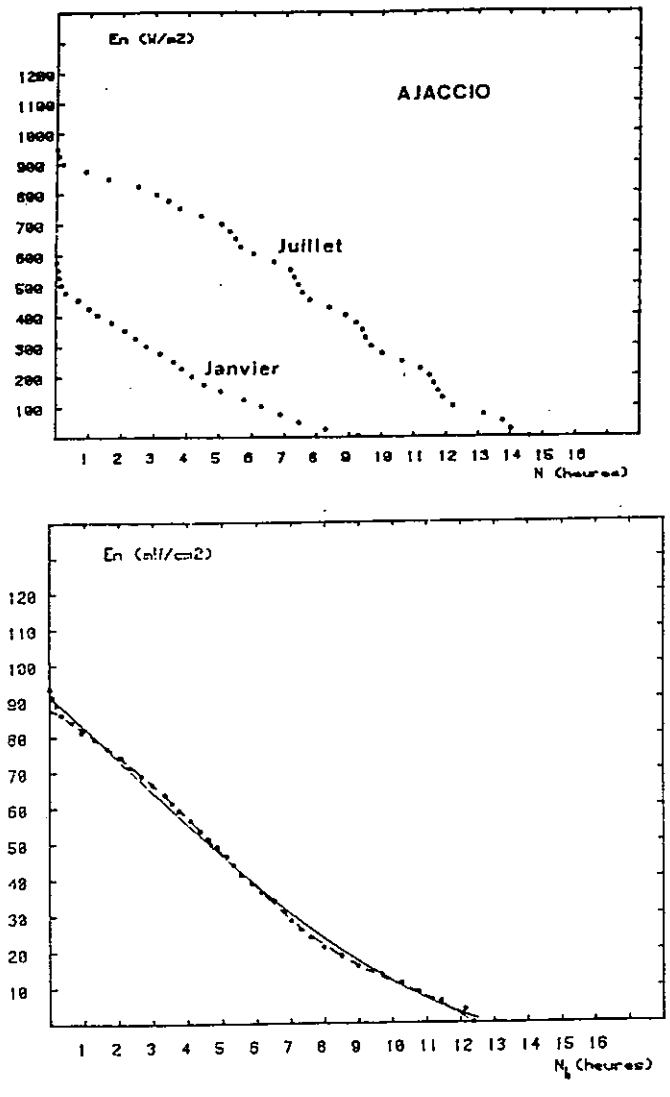

Figure 1.34: Comparison between the experimental (dotted lines), the four parameter logistic curve (continuous line) and the fifth order polynomium (dashed line) monthly *acf*'s of the parameter $\overline{IG}$. From Adnot (79).

different months, showing that minor differences exist between the two series of measurements, more or less evident depending on the considered month and slope angle. Thus, hourly averaged $\overline{IG}$'s seem to be sufficiently precise for accurate evaluation of the utilizable solar irradiance during a day.

Bourges and Lasnier [56] examine the same kind of curves by Principal Component Factor Analysis and find that they depend on four parameters:

- maximal irradiance IG_{max} (solar noon, clear day);
- day length d;
- mean daily irradiation $\overline{DG}$;
- secondary climatic and geographical factors ϵ_2 [5].

For the French localities, they propose the formula

$$n_h = d\,(1-y)\,(1 + B_1\,y + B_2\,y^2 + B_3\,y^3 + B_4\,y^4)$$

where $y = \overline{IG}/IG_{max}$ and the B-coefficients are linear functions of ϵ_2 and of the first, second and third powers of $\overline{DG}/(IG_{max}\,d)$.

It is worth noticing that all these monthly *irradiance–time* curves may be easily modified to get the monthly *acff*'s for HG (all hours of the day together). In fact, the previous values of n_h divided by the daylength in hours (costant daylength is assumed) also represent the fraction of hours in the concerned month with hourly global irradiation greater then the corresponding (hourly averaged) $\overline{IG}$ value multiplied by 3600 sec (i.e. HG).

Negative skewness and tendency to the bimodality, typical of the short period beam irradiation, are reported for HG by Baloutkis and Tsalides [18] — see Fig. 1.35.

1.2.6 Scaled Hourly Global Irradiation (HG/HG_{cs})

Distributions for HG/HG_{cs} during a day, *given* $DG/DG-cs$, are reported by Exell and Huq [86]. Exell [84] suggests frequency

[5] These parameters are not better defined in the quoted paper.

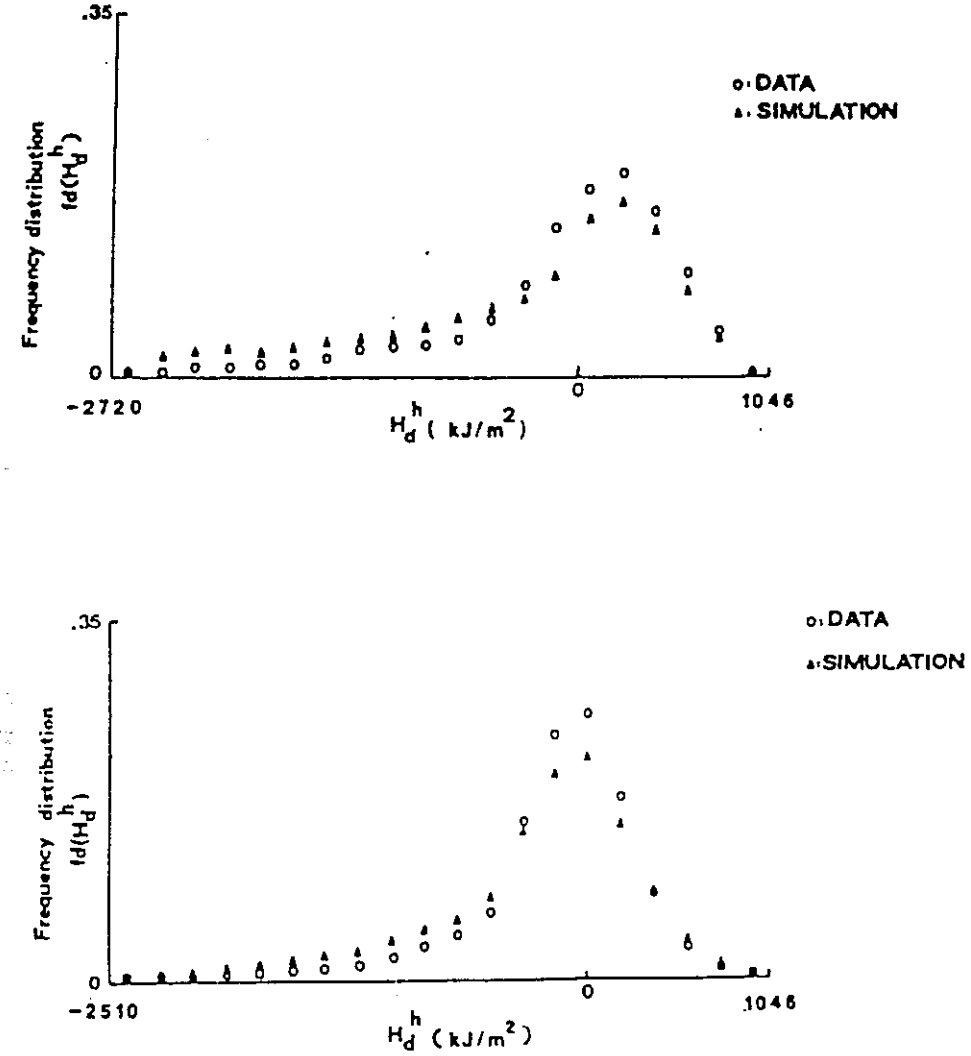

Figure 1.35: Yearly (above) and monthly (below; for April) examples of *fdf*'s of the parameter $HG - \langle HG \rangle$ where $\langle HG \rangle$ is the long term average of HG in the considered day and in the considered hour in Athens (Greece). From Baloutkis (86).

distributions of HG/HG_{cs} analogous to those already suggested in the same [84] paper for DG/DG_{cs}.

Engels *et al.* [81] observe that the standardized HG (i.e. HG/HG_{cs}) frequency distribution for the single hour midday to 1 p.m., examined for each day of March during the period 1953-1975 shows, in fact, the same characteristics as the daily data (as shown by Bennet [38]) and even weekly data (as shown by Baker and Klink [17]). The authors particularly point out the existence of negative skewness and occasional bimodality.

A confirmation of these facts can be found in the work of Olseth and Skarveit [191], who propose, also for the hourly normalized clearness index HG/HG_{cs} (HG_{cs} is calculated using a clear sky transmittance model) the same formula previously used by the authors to fit the daily data distribution [190]. The hourly curves, parametrized by the expected value $\langle\Phi\rangle$ of the uniformized clearness index, are based on 43627 hourly measurements (data from 1965 to 1979) and show more evident bimodality with respect to the corresponding daily *fdf*s (see Sec 2.2.4).

1.2.7 Hourly Global Clearness Index (HG/HE)

As already said, Liu and Jordan [164] found little difference, *in practice*, between the daily and the hourly clearness index ensemble monthly distributions, mainly for the central hours of the day, In fact Hollands and Huget propose their formula *mainly* for HG/HE.

Negative skewness and tendency to the bimodality, typical of the short period beam irradiation, are reported for HG/HE by many other authors, for instance Mustacchi *et al.* [181] — see Fig. 1.36 —, Cammarata *et al.* [64] — see Fig. 1.37.

1.2.8 "Instantaneous" Global Clearness Index (IG/IE)

The origin of the bimodality of the clearness index distributions is investigated by Suehrcke and McCormick [245], who analyze about one year of "instantaneous" global irradiation values IG (with an instrumental relaxation time of about 4 seconds) performed every

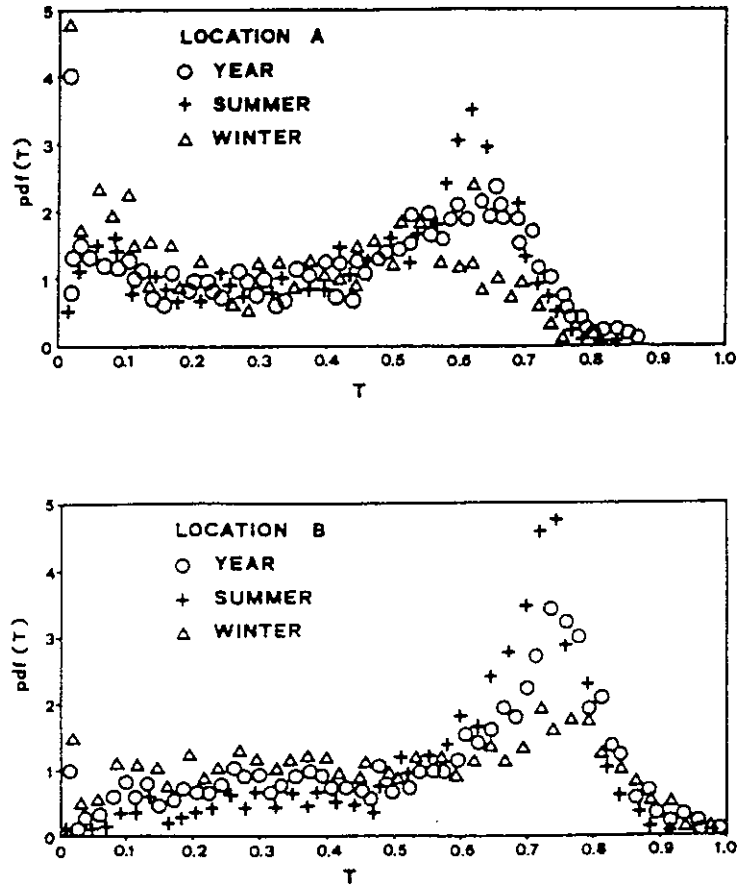

Figure 1.36: Probability density functions (*fdf*) of HG/HE at Ispra (above) and Vigna di Valle (below), both in Italy. From Mustacchi (79).

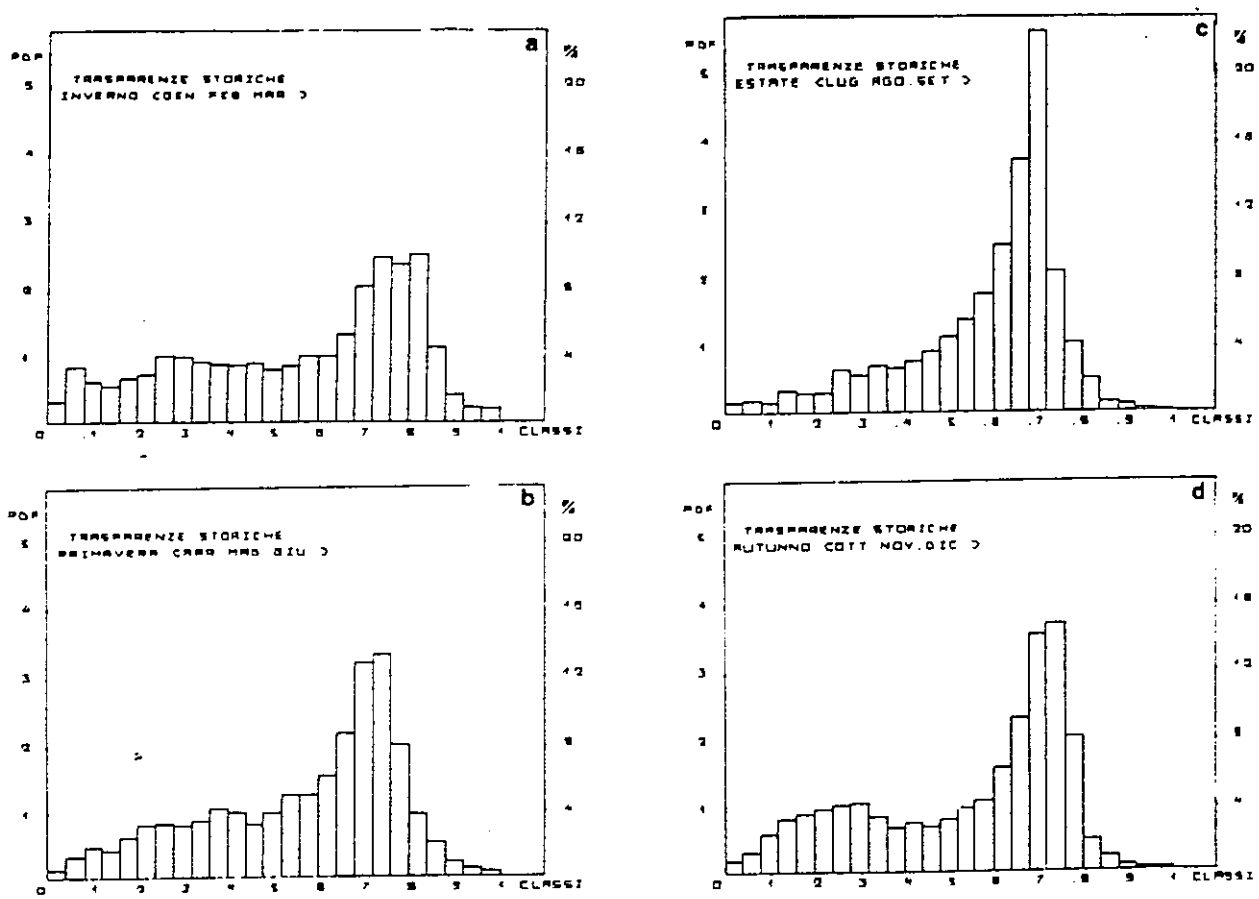

Figure 1.37: The four seasonal *fdf*s of HG/HE in Catania (Italy). From Cammarata (82).

minute at Perth (Australia). They convert the data to IG/IE dividing by the corresponding calculated extra-atmospheric irradiation and separate the obtained values into four subsets according to the four air mass intervals [1.,1.1], [1.4,1.6], [1.8,2.2] and [2.7,3.3]. The existence of a quasi-unique IG/IE frequency distribution with parameters $\overline{IG/IE}$ and m (air mass) is investigated. The experimental *cff*s show distinct sudden steps at intermediate values of IG/IE, which are not evident in the DG/DE or HG/HE frequency distributions, and values of IG/IE exceeding one (see Figs. 1.38, and 1.39). The latter effect can be easily explained as a cloud diffuse reflection effect, while the former is shown to gradually disappear as the integration time increases from 1 to 60 minutes.

The authors demonstrate that the "step effect" and its disappearing can be accounted for by supposing that the relative irradiation, say k, during a very short time interval, ranges between two given values k_{min} and k_{max} and has a discontinuous "square well" *fdf*, $q(k)$, which takes three constant values, with jumps at two given values k_1 and k_2 (see Fig. 1.40).

By supposing that any finite time measurement takes a value given by the average over a very long purely random sequence of "instantaneous" contributions, Suehrcke and McCormick find for IG/IE the theoretical fdf

$$f(IG/IE) \;=\; C\; q(IG/IE)\; exp(\gamma\; IG/IE)$$

By best fitting the IG/IE frequency distributions they are able to calculate $k_{min} = 0.03$, $k_1 = 0.550\; exp(-0.129\; m)$, $k_2 = 0.857\; exp(-0.103\; m)$ and $k_{max} = 0.905\; exp(-0.074\; m)$. The three constant value for $q(k)$ are found to be 1, $0.14\; exp(-0.202\; m)$ and 1.83. The solution for γ requires an iterative procedure, but a good approximation is given by

$$\gamma \;=\; \frac{(\overline{k} \;-\; k_{mid})\;(6.6\;\overline{k}^2 \;+\; (0.39\;m \;-\; 3.79)\;\overline{k} \;-\; 2.4)}{(\overline{k} \;-\; k_{min})\;(\overline{k} \;-\; k_{max})}$$

where k_{mid} is the value of k when $\gamma \;=\; 0$ in the exact solution (see Fig. 1.41).

With this work, the bimodality of the global irradiation distributions relative to a not too long time interval is satisfactorily explained,

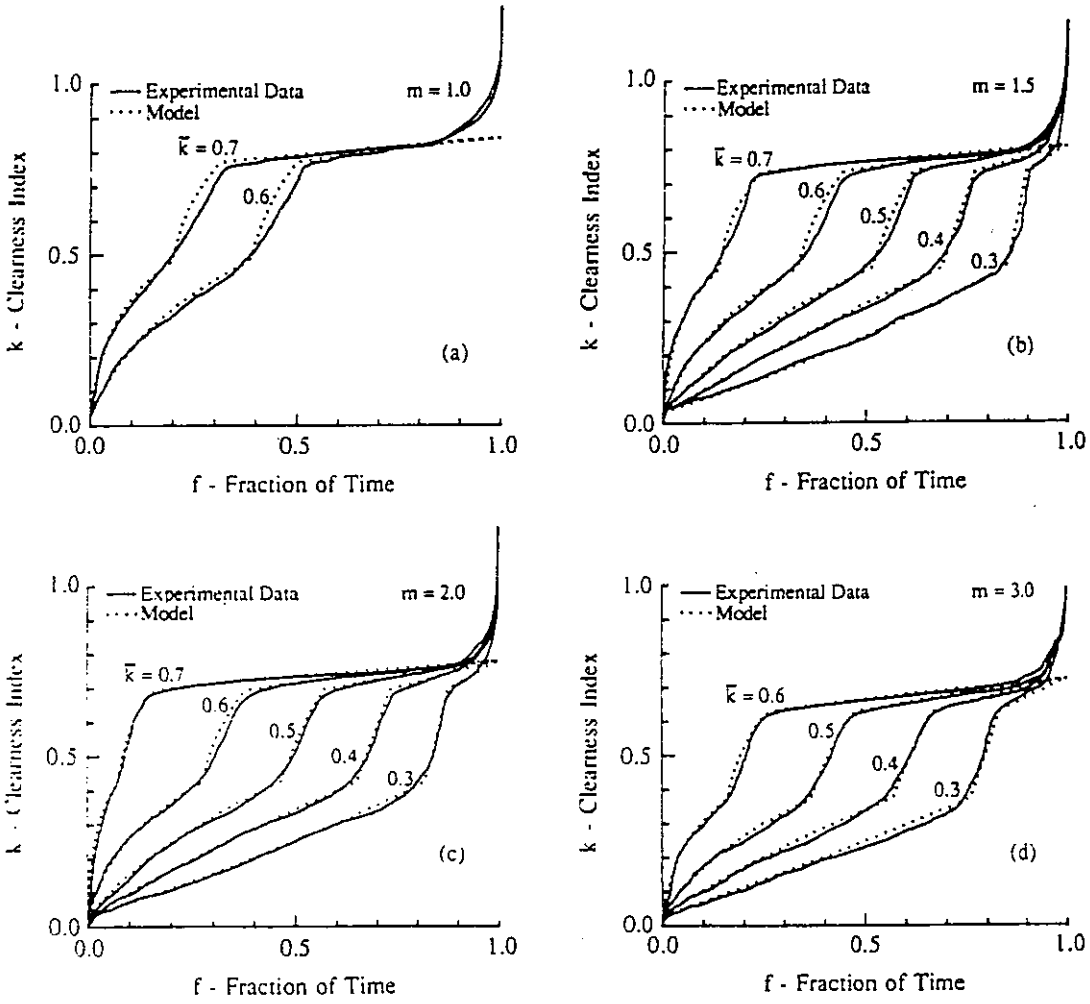

Figure 1.38: Comparison between experimental and theoretical *fdf*s (fractional time distributions) of IG/IE for various $\overline{IG/IE}$ and air mass m values. From Suehrcke (88a).

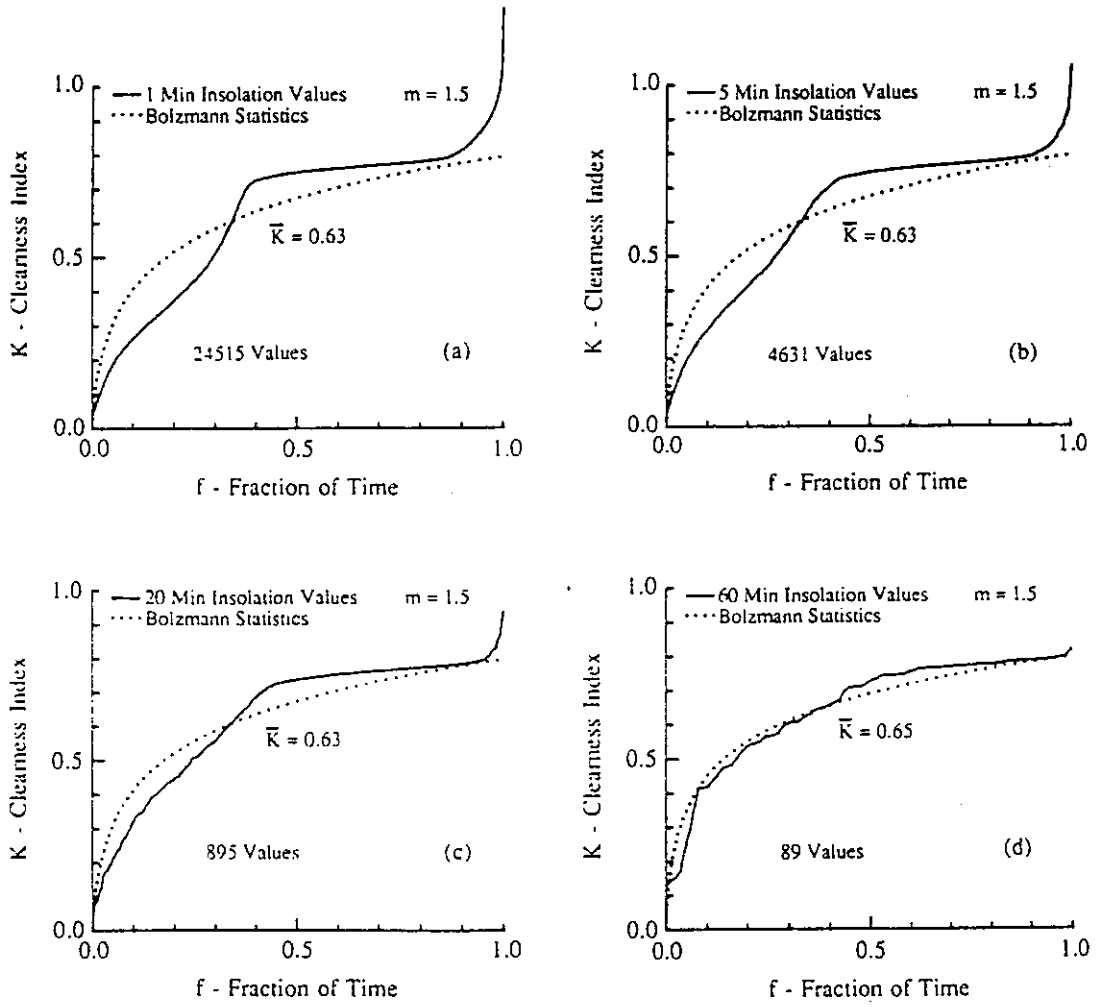

Figure 1.39: The effect of the averaging time interval of $\overline{IG/IE}$ on its *fdf*: (a) 1 min, (b) 5 min, (c) 20 min and (d) 60 min. From Suehrcke (88a).

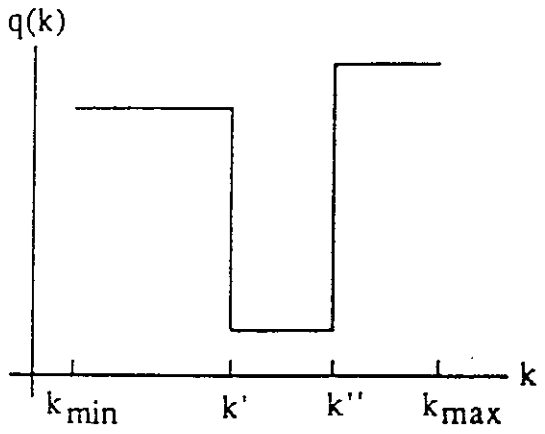

Figure 1.40: The square well probability density of IG/IE. From Suehrcke (88a).

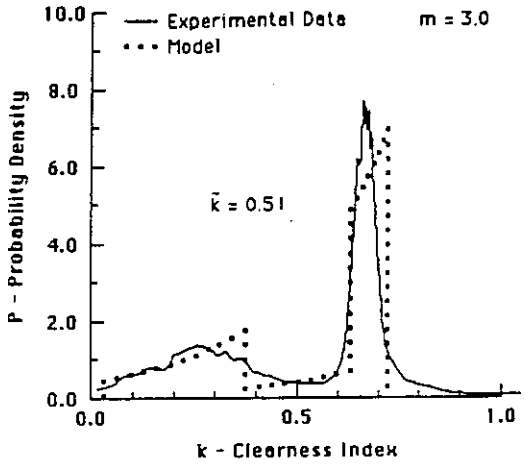

Figure 1.41: The *fdf* of IG/IE calculated from data with $\overline{IG/IE} = 0.51$ and air mass $m = 3.0$, compared with the corresponding theoretical *fdf*. From Suehrcke (88a).

even if some improvement can, eventually, be obtained by considering some *autocorrelation* in the *underlying time series*, i.e. in the time series used to generate the distribution of the very short time irradiations.

1.3 Beam Irradiation

1.3.1 Daily Beam Irradiation (DB)

Since solar tracking devices are expensive and often give some maintenance problems, direct DB measurements are seldom available. Usually the DB values are obtained by subtracting the daily diffuse irradiation DD (which can be obtained by obscuring the sun with semifix shadow bands) from the corresponding daily global DG.

Moreover, as happens for the DG values, direct statistics on DB are not so frequent in literature, due to customary standardization of this quantity by DE.

Examples of DB frequency distributions are given by Tricaud

et al. [248] for the single monthly acff, for some months in 1982 at Odeillo, France (see Fig. 1.42).

1.3.2 Daily Beam Clearness Index (DB/DE)

The linear correlation between the daily relative sunshine DS/DS_o and DG/DE is a classical topic in solar irradiation climatology. Less customary is the (possibly more fundamental) correlation between DB/DE and DS/DS_o.

Lestienne [156] [158] reports the four seasonal DB/DE fdf's built with three years of daily data at Odeillo (France), and shows that they can be considered mixtures of "bad" day ($DS/DSo \leq 0.5$) exponential densities

$$\frac{1}{m}\, exp(\frac{-DB/DE}{m})$$

and "good" day normal densities

$$\frac{1}{\sigma_b \sqrt{2\,\pi}}\, exp(-\frac{(DB/DE\ -\ b)^2}{2\,{\sigma_b}^2})$$

The distributions are parametrized with the "bad" day average m as follows

$season$	b	σ_b
DJF	$4.56m$	$1.23m$
MAM	$4.36m$	$1.21m$
JJA	$4.05m$	$1.19m$
SON	$5.57m$	$1.62m$

The resulting fit shows a good, even if not excellent, agreement. The bimodality is somewhat clearly accounted for (see Fig. 1.43).

1.3.3 Hourly Beam Irradiation (DB) and Mean Irradiance

The performance evaluation for some solar conversion devices, mainly concentrating systems, can profit from the knowlwdge of the beam irradiance distributions. Since mainly DB or HB distributions are

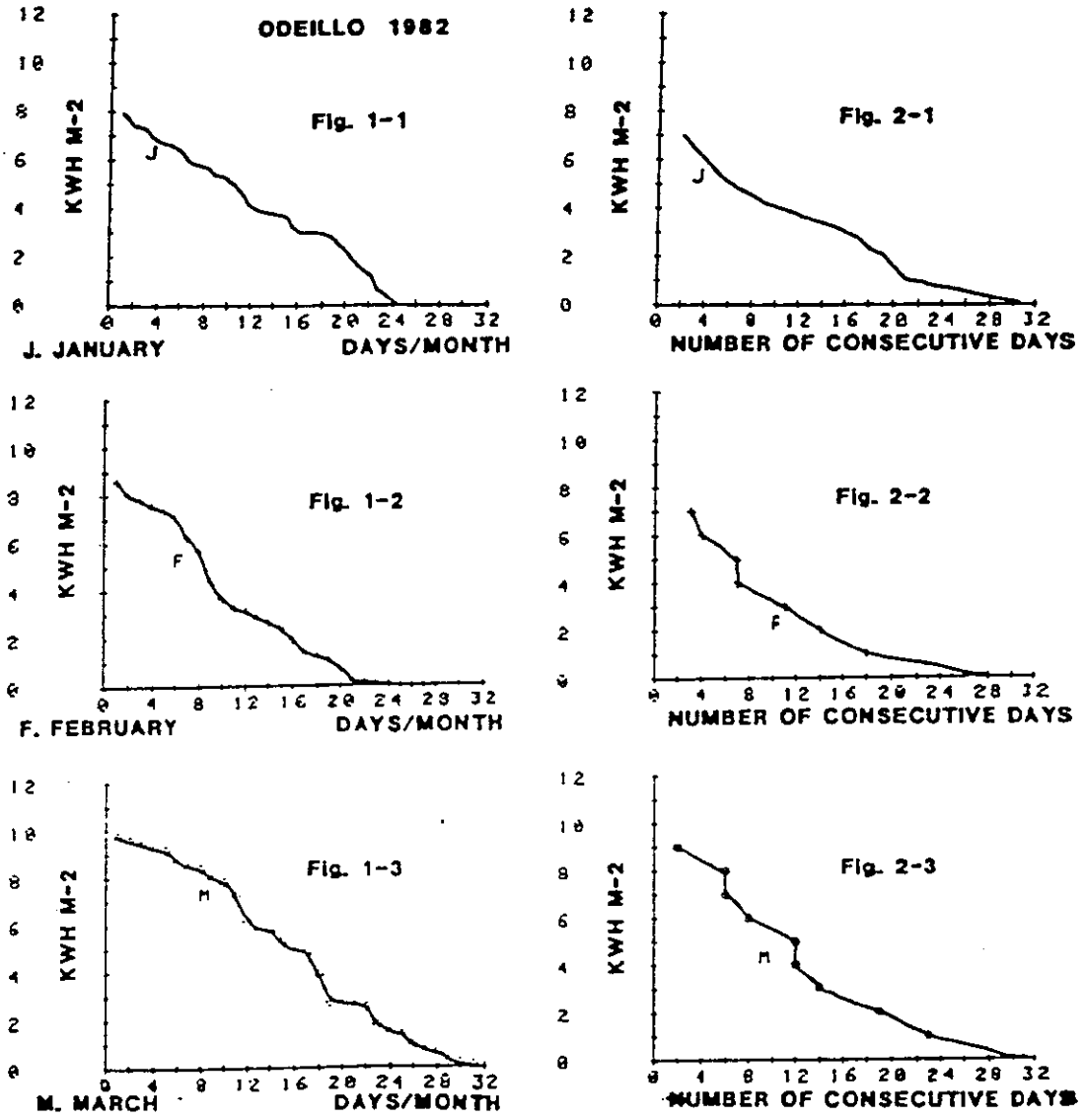

Figure 1.42: Cumulative frequency curves of DB values (left column). Number of consecutive days with DB values above given thresholds (right column). From Tricaud (82).

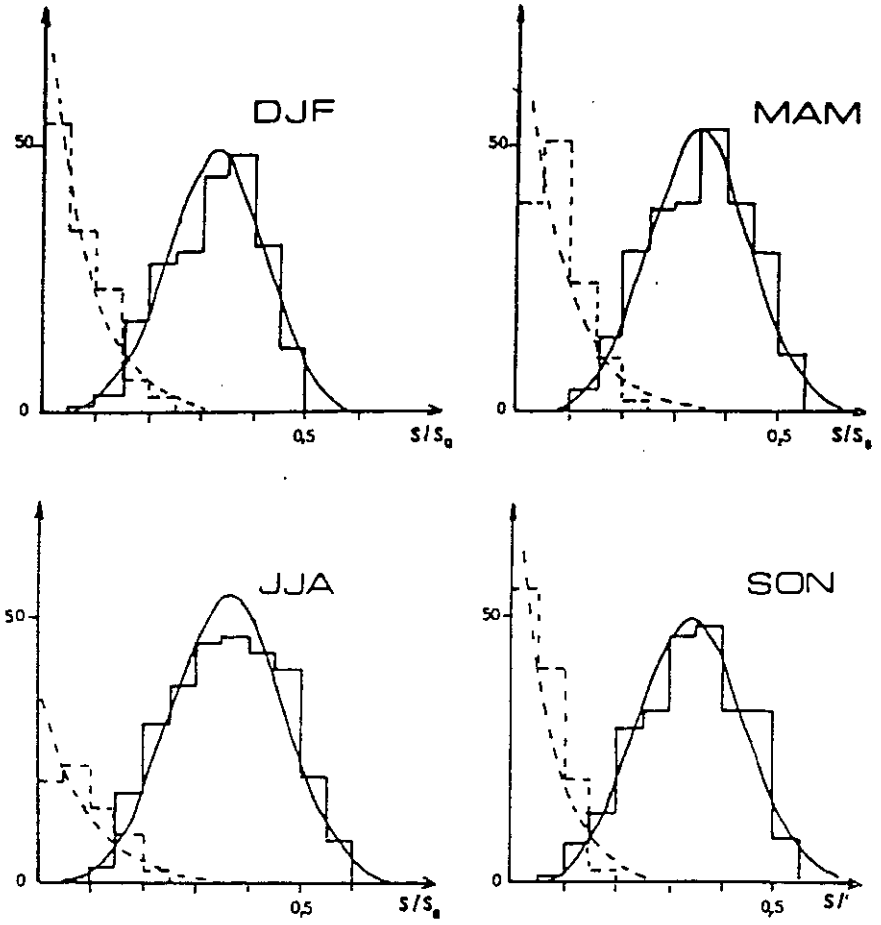

Figure 1.43: The four seasonals *fdf*'s of DB/DE, relative to good weather (—) and bad weather (- - -). From Lestienne (79b).

available (or, equivalently, mean daily or hourly irradiance distributions), the question arises if they well represent the original not averaged information on irradiance.

Bois and Mejon [54] have studied the differences between averaged irradiance distributions when the irradiance is averaged over different time basis. They used data collected during some months at a station near Marseille (France), only considering the days with no missing measurements (the sunrise and sunset hours were in fact never considered). The data base consists of "instantaneous" (less then one minute) measures of beam irradiation sampled at time intervals of 2, 4, 10, 15, 30 and 60 minutes, together the corresponding integrated measurements over 1, 2, 4, 10, 15, 30 and 60 minutes. Comparisons between the two sets of data have been performed with different criteria: considering all data together, on a monthly basis and during typical days (overcast, clear and with intermittency in cloudiness). The averages, the variances relative to the daily averages and the frequencies on a partition in subintervals of width 100 w/sqm have been compared for different choices of data.

The authors find a decrease in the daily averages variance of about 8 % when passing from 1 minute to 60 minute time basis, indicating some loss of detail (see Fig. 1.44).

The corresponding fdf differ, in the same range, for some percent (for instance, the probability of daily average irradiances less then 100 w/sqm on the hourly measurement basis is 3 % lower than the corresponding probability on the one-minute basis). They conclude that integrated measurements on a 15 minute basis gives a good accuracy, while the 60 minute basis give less reliable estimates of the daily averages, mainly during the "mixed cloudiness" days.

1.3.4 Hourly Beam Clearness Index (HB/HE)

Hourly *normal* beam irradiation has been studied by Gordon and Hochman [110], who base their investigation on eleven years of hourly measurements at Bet Degan Israel. They try to extend to the HB/HE frequency distributions the HG/HE formula given Bendt *et al.*, taking into account the existence of a finite probability p for vanishing HB/HE. Thus, both for monthly and yearly HBE distributions, they

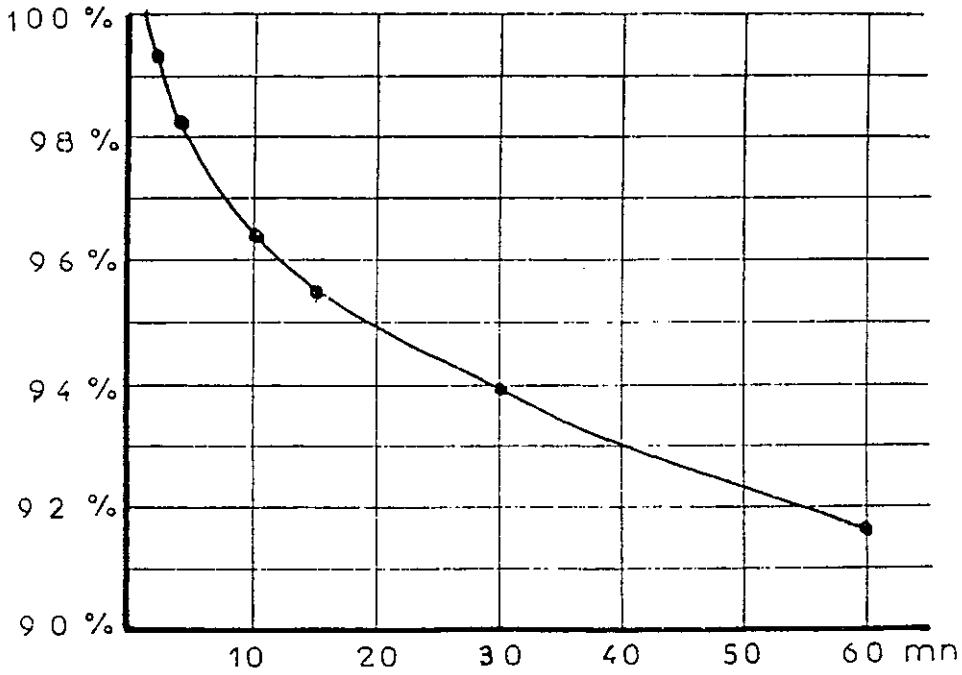

Figure 1.44: Ratio between the variance of data after integration over different time intervals (abscissa) and the variance of the one minute data. From Bois (79).

propose the formula

$$f(x) = p\,\delta(x) + (1-p)\,\frac{B\,exp(B\,x)}{exp(B\,x_{max}) - 1}$$

or the corresponding CFF

$$F(x) = p + (1-p)\,\frac{exp(B\,x) - 1}{exp(B\,x_{max}) - 1}$$

where $x = HB/HE/\overline{HB/HE}$ and $\delta(x)$ is the Dirac's delta function.

Given the probability p for overcast hours, B can be iteratively calculated by

$$B = (1-p)\,\frac{(B\,x_{max} - 1)\,exp(B\,x_{max}) + 1}{exp(B\,x_{max}) - 1}$$

A different formula for the HB/HE frequency distributions is given by Stuart and Hollands [242]. They analyze ten years of data for Toronto (Canada) and verify the results of the investigation using five years for Winnipeg, Charlottetown and Vancouver(Canada). The hourly data are first subdivided into 136 groups, each characterized by month of the year and hour of the day. For each group the average $\langle HB/HE \rangle$ and the mean air mass is calculated, and the HB/HE values are grouped into 20 intervals of width 0.05. For each group the fdf is then evaluated. These frequency densities show some bimodality, with a large percentage of small (i.e. between 0.00 and 0.05) HB/HE values and no values greater then 0.8. The maximum value for each group is found to depend on the air mass with the law

$$HB/HE_{max} = 0.55 + 0.45\,exp(-0.34\,m)$$

and the probability of small HB/HE values is evaluated as

$$\delta = 15.6 - 37.2\,\langle HB/HE \rangle$$

for $0 \leq \langle HB/HE \rangle \leq 0.485$ and zero otherwise.

The authors also propose a compound polynomial model, given by

$$f(HB/HE \mid \langle HB/HE \rangle) = a + b\,x + c\,x^2 + d\,x^3$$

for $0.05 \leq HB/HE \leq HB/HE_{max}$ and by δ for lower values, where $x = (HB/HE - 0.05)/(HB/HE_{max} - 0.05)$. By imposing probabilistic constraints a, b and c can be expressed in terms of d, which is given by best fitting as a linear function of $\langle HB/HE \rangle$

$$d = 5.23 - 56.6 \langle HB/HE \rangle \ .$$

See Fig. 1.45.

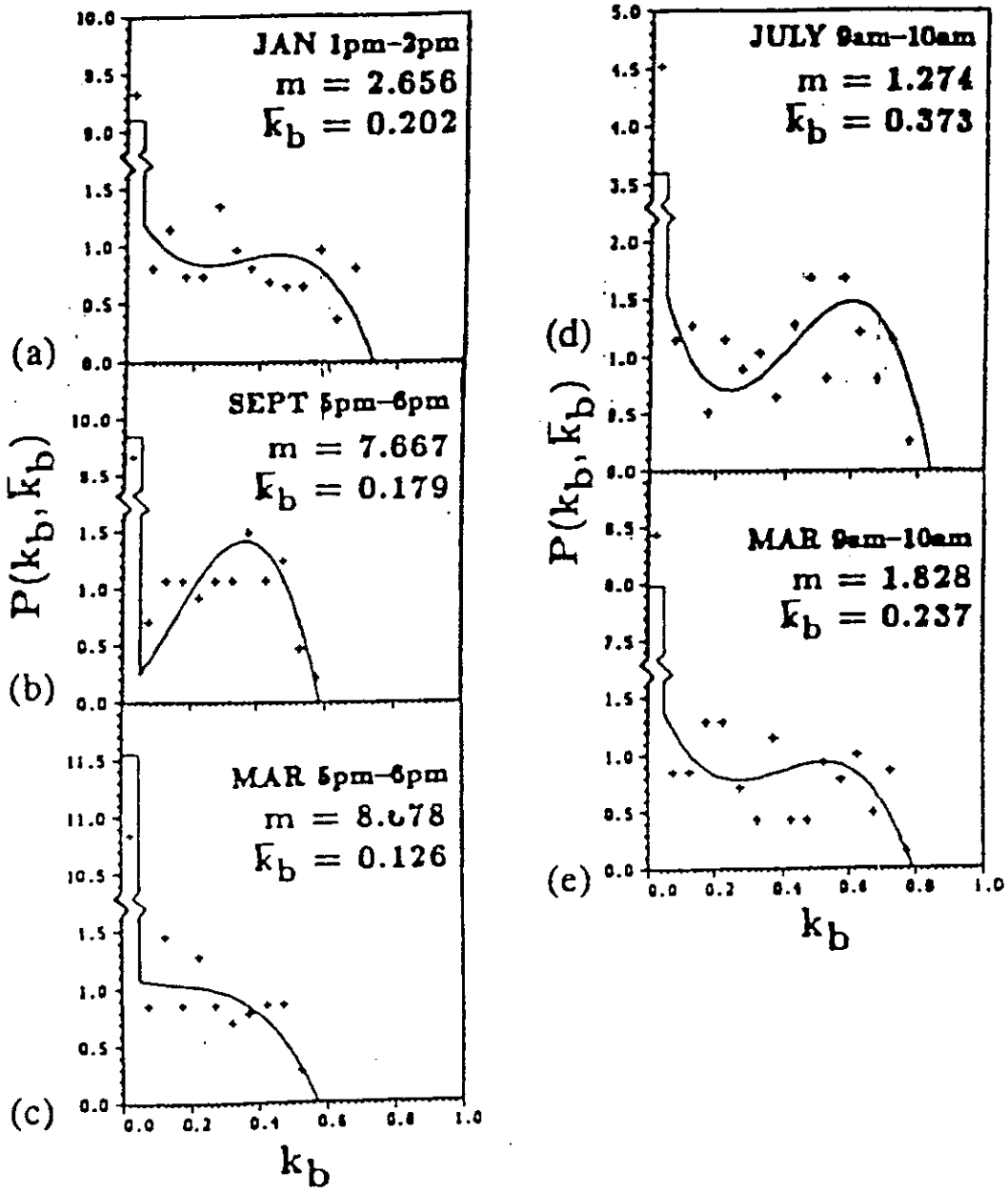

Figure 1.45: The *fdf*'s of HB/HE for different values of m and $\langle HB/HE \rangle$: data (+) and proposed model (—). From Stuart (88).

Chapter 2

IRRADIATION FROM OTHER DATA

2.1 Introduction

It is not a rare occurrence that solar irradiation values are needed for sites where no irradiation measuring instrument is installed. Typical is the case of mapping the solar climate for a large region starting from a measured irradiation data base relative to a few isolated stations.

A similar problem arises when instruments have been working for a very short time, such as one year or less, so that reliable frequency distributions or even statistical averages are not available to designers or researchers.

Thus, inquiries about the existence of relationships between solar irradiation and other available meteorological parameters (such as relative sunshine, relative humidity, cloudiness, temperature, and so on) are very interesting.

Due to the complexity of the deterministic dependence of solar irradiance at ground level on the physical properties of the atmosphere, and because of the great variability of the status of the sky, one expects that such relationships would be *statistical* in their nature, i.e. *regressed* relationships. Moreover, even if some of these regressed laws give satisfactory correlations, they can refer to meteorological parameters which are not always available, so that one is sometimes compelled to use less satisfactory correlations between the irradiation

values and whatever data is available.

For these reasons researchers have generally proposed *simple* mathematical formulae (mainly linear and quadratic forms) which *empirically* account for the statistical dependence of suitably averaged irradiation values from analogously averaged climatical parameters, without looking for more precise correlation laws which would require knowledge of many parameters or unjustified computational efforts. For instance, one can try to evaluate if a satisfactory simple regression exists between individual monthly averages such as $\overline{DG}$ or the corresponding ensemble average $< \overline{DG} >$[1] and analogously averaged climatical parameters such as DT (daily average temperature) or DR (daily average relative humidity) or DC(daily average cloud cover).

One must expect, of course, that the parameters which appear in these empirical regressions would change dependig on site and season. Nevertheless, the information which can be extracted from these formulae can be very useful, in the absence of direct measurements, to infer more complete knowledge. For instance, if one can estimate in any way $\overline{DG}$, the previously discussed monthly frequency distributions, assumed to depend on $\overline{DG}/\overline{DE}$, can be used with an appropriate degree of confidence.

In this chapter we briefly review some of the more useful statistical relationships between global, diffuse and direct irradiations and quantity such as percent sunshine (S/S_o), cloudiness (C, in oktas or tenths), relative humidity (R), water vapour content (W), and temperature (T). Some statistical relationships which have been found among such quantities will be also reviewed.

[1] In the following we will indicate ensemble-time averages such as $< \overline{X} >$ by the simpler notation $[X]$. Unless otherwise specified, the time averaging period will be the *month*.

2.2 Irradiation values vs. percent sunshine

2.2.1 Ångström-like regressions

The climatological quantity which most obviously is expected to be correlated with the solar irradiation relative to a given period is the percent relative sunshine during the same period.

About sixty years ago, Ångström [14] [13] [12], developing the ideas of Kimball [145], suggested fitting the simple linear relationship

$$\frac{[DG]}{[DG_{cs}]} = a + (1-a)\frac{[DS]}{[DS_o]}$$

where $[DG_{cs}]$ represents the daily global irradiation under cloudless sky conditions during the concerned period, and $[DS]$, $[DS_o]$ respectively the experimental daily sunshine and the maximum possible daily sunshine, both averaged over the same period. In practice, one identifies $[DS_o]$ with the astronomically determined average daylength or, more shortly, with the daylength calculated for a suitable chosen day within the period.

The determination of $[DG_{cs}]$ can be made both empirically, by enveloping the maxima of the DG values in the data base, or with a clear sky trasmittance model which requires more information (such as latitude, relative humidity, atmospheric dust content and so on). Note that *clear sky* is usually taken as equivalent to *cloudless sky*, even if the latter can be not perfecly *clear*, due to possible excess of dust and water vapour content. We will distinguish the cases by using indices *cls* for cloudless, and *cs* both for calculated values and for values estimated by regressions (see below).

Even if the case $[DS] = 0$ never occurs in practice (if the concerned period is not too short), the coefficient a of the above equation gives a rough estimate of the ratio $[DG_{ov}]/[DG_{cs}]$ (i.e. $[DD_{ov}]/[DG_{cs}]$), where the index *ov* means *completely overcast day*[2]. In this sense

[2]In fact the lower limit for $[DS]/[DS_o]$ which can give reasonable estimates strongly depends on the averaging time period, due to the influence of this choice on the validity of the linear regression.

the coefficient a could be assumed as a parameter defining the solar transmission within clouds and experimentally ranging between 0.33 in low latitudes and 0.55 in high latitudes.

Note that the Ångström's formula can be rewritten as

$$[DG] = [DG_{ov}] + ([DG_{cs}] - [DG_{ov}])\frac{[DS]}{[DS_o]}$$

with both $[DG_{ov}]$ and $[DG_{cs}]$ intended as regression parameters. We will speak in the following of Ångström-like regressions (A-regressions) to indicate formulae of the type

$$[DG] = [DG_{cs}]\ f([\sigma],[\xi])$$

where

$$[\sigma] = [DS]/[DS_o]$$

and $[\xi]$ (which can be absent) stands for the average of one ore more additional climatological variables. Unless otherwise specified, the function f will be assumed to be a first degree polynomial in the variable $[\sigma]$.

The original Ångström regression has been subsequently and variously modified by other researchers.

Fritz and McDonald [93], analyzing data measured at 11 stations in USA for a period of 10 years, suggest the overall formula

$$[DG] = [DG_{cls}]\ (0.35 + 0.61\ [\sigma])$$

which gives a correlation coefficient $r = 0.88$ between computed and observed values. It is evident that the Ångström condition regarding the coefficients of the linear regression, i.e. that they must sum up to 1, has been relaxed[3].

De Boer [77] uses hourly values measured during five years at Debilt (Holland) to fit, for each month and each hour of the day, the values

$$[HG] = [HG_{cs}]\ (\alpha + (1-\alpha)\ \frac{[HS]}{[HS_o]})$$

[3]When, later in this section, we will loosely speak of a and b coefficients of an A-regression, we will refer to the linear general formula $[DG] = [DG_{cs}]\ (a + b\ [\sigma])$.

where $[HG_{cs}]$ and α are determined by regression.

Mani *et al.* [175], assume that the corrected Ångström formula holds

$$\frac{DG}{DG_{cs}} = a + (1-a)\,[\sigma']$$

where σ' is the relative sunshine corrected as suggested by Hay [118] for threshold sensitivity of the Campbell-Stokes instruments(see below).

Chia [68] and Leong [155] both study the behaviour of the A-regression at Singapore on a monthly basis, using data measured respectively from 1961 to 1967 and from 1968 to 1970.
For equations covering yearly periods, the estimated coefficients a, b range in $[0.234, 0.274]$ and $[0.422, 0.494]$. The $a+b$ values corresponding to the four extremes are $0.727, 0.745, 0.681, 0.739$.
The same coefficients oscillate in wider ranges, from 0.231 to 0.284 and from 0.411 to 0.500, for regressions covering monthly periods.

We recall that Leong also relates directely DG to DS for the whole three year period, obtaining

$$DG = 8.92 + 1.39\,DS \qquad [MJ\ m^{-2}\ day^{-1}]$$

with correlation coefficient $r = 0.90$ and standard error of estimate 2.12 $MJ\ m^{-2}\ day^{-1}$, which corresponds to a very poor forcasting performance.

Exell [85] [83] calculates $[DG_{cs}]$ using the Schuepp's formula [227] for standard atmospheric conditions (precipitable water: 2 cm, pressure: 1000 mb, ozone content: 0.34 cm NTP, turbidity: 0). He uses 5 years of measurements at Chiang Mai and Bangkok (Thailand) and takes as averaging time intervals eight 1.5-month periods during the year. He obtains the results reported in Fig. 2.1.

Since parameters a and b are expected to vary with latitude and climate (see [165]), Exell compares his results with other results relative to Calcutta and Madras (India), which have latitudes and climates similar to those of the cities analyzed in Thailand, and obtains a good agreement. The author claims that estimates for $[DG]$ using his parameters give errors less than 1.3 $MJ\ m^{-2}\ day^{-1}$.
Exell uses the obtained formula to estimate $[DD]$ (identified with $a\,[DG_{cs}]$) and $[DG_{cls}]$ (identified with $(a+b)\,[DG_{cs}]$). Starting from

	Q_m MJ $m^{-2}d^{-1}$	S_m h d^{-1}	a	b	a + b	s
Chiang Mai						
Feb 27 - Apr 12	26.90	11.70	0.271	0.560	0.831	0.071
May 29 - Jul 15	29.95	12.82	0.351	0.536	0.887	0.059
Sep 1 - Oct 15	26.57	11.70	0.319	0.605	0.924	0.071
Nov 30 - Jan 13	19.95	10.66	0.323	0.559	0.882	0.058
Bangkok						
Feb 27 - Apr 12	27.70	11.70	0.272	0.566	0.838	0.074
May 29 - Jul 15	29.08	12.52	0.332	0.488	0.820	0.065
Sep 1 - Oct 15	27.32	11.70	0.307	0.538	0.845	0.102
Nov 30 - Jan 13	22.12	10.96	0.322	0.519	0.841	0.090

Figure 2.1: Coefficients and data for A-regressions for Chiang Mai and Bangkok. From Exell (76).

the quantity $a + b$ estimations of the atmospheric turbidity are performed which result close to the experimental pyrheliometric values measured in India.

Bois *etal.* [53] fit the linear regression

$$1 - \frac{DG}{DG_{cls}} = a\,(1 - \sigma) + b$$

using 10 years of individual daily values for Davos. Twelve regressions are performed, for each month of the year. Results and some examples of scatter diagrams are reported in Fig.2.2 and Fig.2.3.

The authors also try to improve the correlation by introducing at the r.h.s. other three terms

$$c_1\,N_1 + c_2\,N_2 + c_3\,N_3$$

where N_i $(i = 1, 2, 3)$ represent the observed cloud covers at morning, noon and afternoon respectively. No relevant improvement is obtained.

Estimation of DG from the calculated parameters, compared with independent data (May to August 1972), gives a fair agreement but for low values of σ.

Adnot *et al.* [2] test a formula similar to that of De Boer for the hourly irradiation values measured at Trappes (France) during one year. In the regression equation

$$[HG] = [HG_{cs}]\,(a + b\,\frac{[HS]}{[HS_o]})$$

the *clear sky* hourly global irradiation is determined as

$$[HG_{cs}] = 342.5\,(sin\ h)^{1.15} \quad [J\ cm^{-2}\ h^{-1}]$$

where h is the solar altitude. They find $a + b \simeq 1$, and assume, for $sin\ h \geq 0.1$, the relationships:

$$a = 0.5 - \frac{0.35}{h} \qquad if \quad 0.1 \leq sin\ h \leq 0.4$$

$$a = 0.36 \qquad if \quad 0.4 < sin\ h$$

Mois	r	a	b
JAN	.90	.442	.142
FEV	.91	.443	.109
MARS	.91	.405	.075
AVRIL	.86	.401	.063
MAI	.85	.462	.059
JUIN	.90	.579	.052
JUILLET	.94	.63	.079
AOUT	.94	.63	.122
SEPT	.94	.59	.145
OCT	.94	.52	.152
NOV	.91	.46	.157
DEC	.91	.43	.168

Figure 2.2: Regression coefficients for $1 - DG/DG_{cs}$ vs σ. From Bois (78).

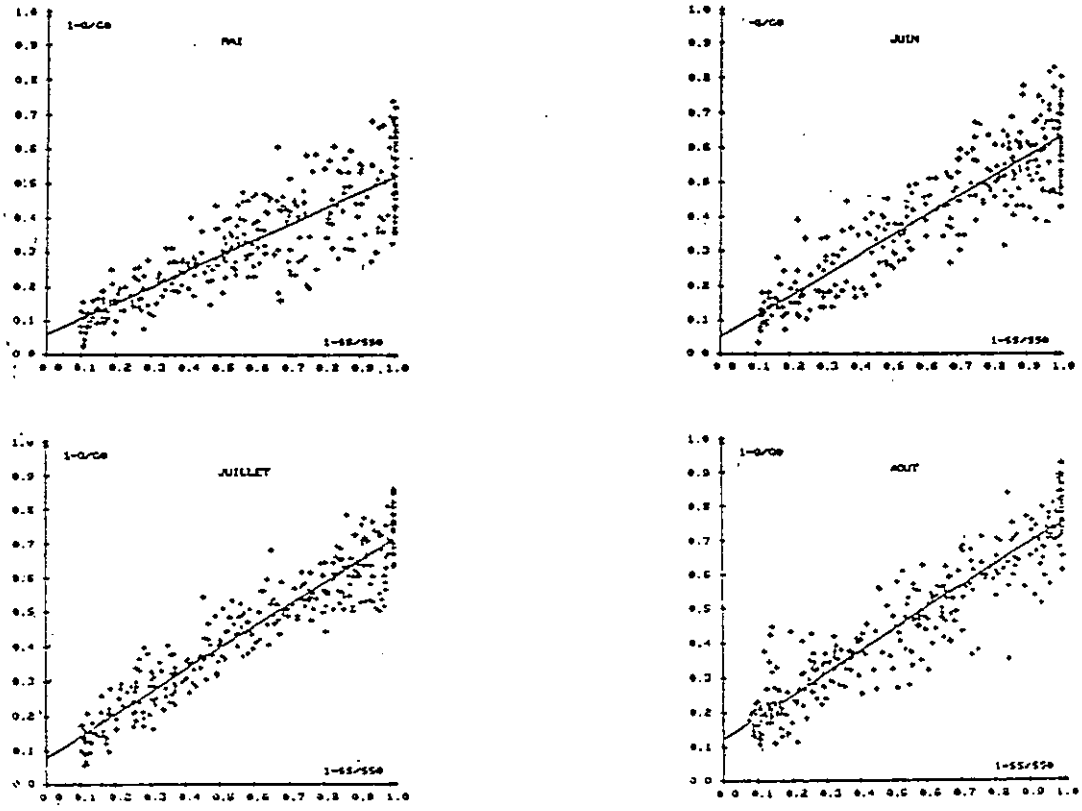

Figure 2.3: Scattering diagrams for $1 - DG/DG_{cs}$ vs σ. From Bois (78).

$$b = 1 - a$$

The obtained correlation coefficient is $r = 0.91$. Nevertheless the authors complain that the scatter of the experimental points is quite large.

Berger [41] uses Duffie's formula [80] to calculate the *clear sky* hourly average irradiance:

$$\overline{IG_{cs}} = 1350\ 0.70\ sin\ h \qquad [W\ m^{-2}]$$

Using data from Nice (France) he notices that the relationship between DG/DG_{cs} and σ does not appear to be linear at all (see Fig. 2.4). He proposes the fitting formula

$$DG = DG_{cs}\ \{0.3 + 0.7\ \sigma + 0.24\ \sigma(1 - \sigma)\}$$

Mejon *et al.* [179], assume, for latitudes between 42° N and 50° N, the empirical formula:

$$DG_{cs} = 85\ (105 - \Phi) + 1.75\ \delta\ (38 + \Phi),$$

where Φ is the latitude and δ the solar declination (both in degrees). The authors fit the A-regression using data from Carpentras, Nice and Ajaccio (France) relative to 5 to 12 years and calculate a and b coefficients for each month and each locality, obtaining accounted variances between 90% and 95% and relative errors between 3% and 6% mainly depending on the month. The introduction in the regression formula of four cloud cover variables (representing cloud cover values measured at four times during the day) does not significatively implement the determination.
The authors also try to fit the data with two different formulae:

$$\frac{DG}{DG_{cs}} = a\ \sqrt{\sigma + b} + c$$

and

$$\frac{DG}{DG_{cs}} = a\ \sigma^2 + b\ \sigma + c$$

and notice a small improvement in the accounted variance (see Fig.2.5)

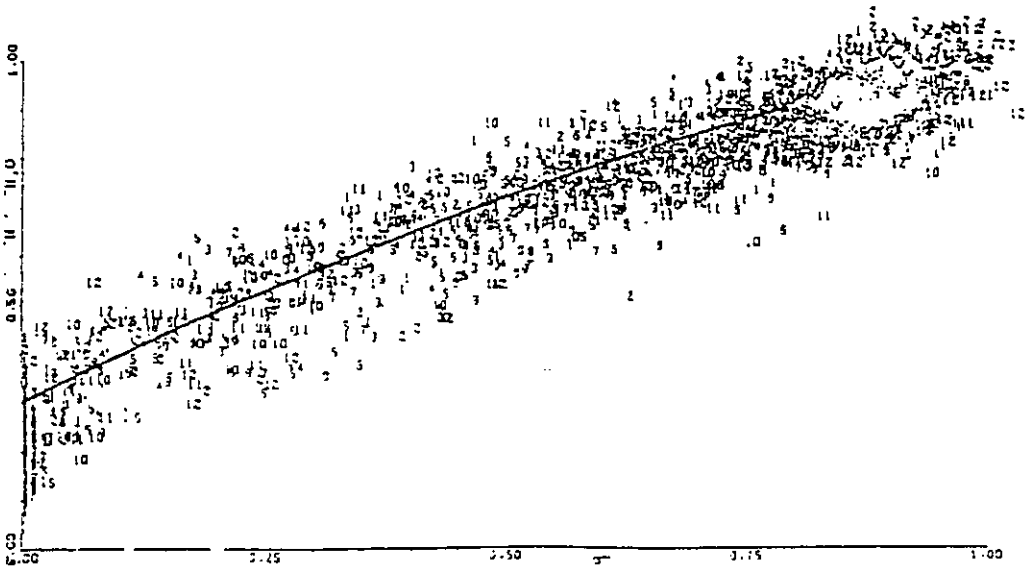

Figure 2.4: Scattering diagram *clear sky* hourly average irradiance vs. σ. From Berger (79).

MOIS	a	b	R^2	MOIS	a	b	c	R^2
JANV.	0.4850	0.1901	0.91	JANV.	0.598	0.035	0.031	0.93
FEV.	0.5555	0.1544	0.95	FEV.	0.716	0.055	-0.057	0.97
MARS	0.5596	0.1892	0.93	MARS	0.726	0.065	-0.040	0.95
AVRIL	0.5692	0.1838	0.94	AVRIL	0.789	0.095	-0.099	0.95
MAI	0.5426	0.2141	0.93	MAI	0.902	0.250	-0.027	0.94
JUIN	0.5461	0.2084	0.95	JUIN	0.814	0.115	-0.127	0.96
JUIL.	0.4795	0.2493	0.92	JUIL.	1.085	0.700	-0.693	0.92
AOUT	0.4916	0.2288	0.92	AOUT	0.896	0.275	-0.303	0.93
SEPT.	0.5348	0.1963	0.93	SEPT.	0.737	0.070	-0.060	0.94
OCT.	0.4877	0.2064	0.90	OCT.	0.637	0.035	0.019	0.92
NOV.	0.4574	0.2075	0.92	NOV.	0.772	0.295	-0.232	0.93
DEC.	0.4605	0.1935	0.91	DEC.	0.499	0.000	0.117	0.95

Figure 2.5: Linear and quadratic A-regression coefficients for DG/DG_{cs} vs. σ. From Mejon (79).

They also fit the standardized variables

$$X = \frac{\frac{DG}{DG_{cs}} - \left[\frac{DG}{DG_{cs}}\right]}{s_{\frac{DG}{DG_{cs}}}}$$

and

$$Y = \frac{\sigma - [\sigma]}{s_\sigma}$$

where the averages and standard deviations refer to the month to which the concerned day belongs.
All daily values in the period 1971–1975 for Carpentras are used. A linear correlation coefficient $r = 0.96$ is obtained (see Fig. 2.6).
Tests of the obtained relationships vs. independent measured data show correlation coefficients between observed and calculated values between 0.96 (linear fit) and about 0.97 (parabolic fit).

Chuah and Lee [72] fit A-regression to daily data measured at Kuala Lumpur, Penang and Kota Bahru (Malaysia) over four years. They calculate DG_{cs} with the Schuepp [227] prescriptions under standard atmosphere (see above). They find a and b coefficients varying month by month and for the three localities in the ranges 0.22 ($a + b = 0.86$) to 0.39 ($a + b = 0.86$) for a and 0.38 ($a + b = 0.77$) to 0.62 ($a + b = 0.96$) for b, with less fluctuations for each individual locality and/or each single month.
The authors use the obtained coefficients to compare estimated and observed $[DG]$ for Ipoh, Malacca and Kuala Trengganu (Malaysia), using only 1 to 2 years of measurments. They observe that, but for the third site during two months, the percentage error does not exceed 10%.

Lewis [162], while comparing various formulae to estimate $[DG]$ from $[\sigma]$, tests the A-regression on the data measured during one year at Lusaka (Zambia) using the Fritz [92] coefficients

$$\frac{[DG]}{[DG_{cs}]} = 0.35 + 0.61\,[\sigma]$$

He deduces $[DG_{cs}]$ from charts presented in a standard book [80] and finds for $[DG]$ an overall percentage error of -1%.

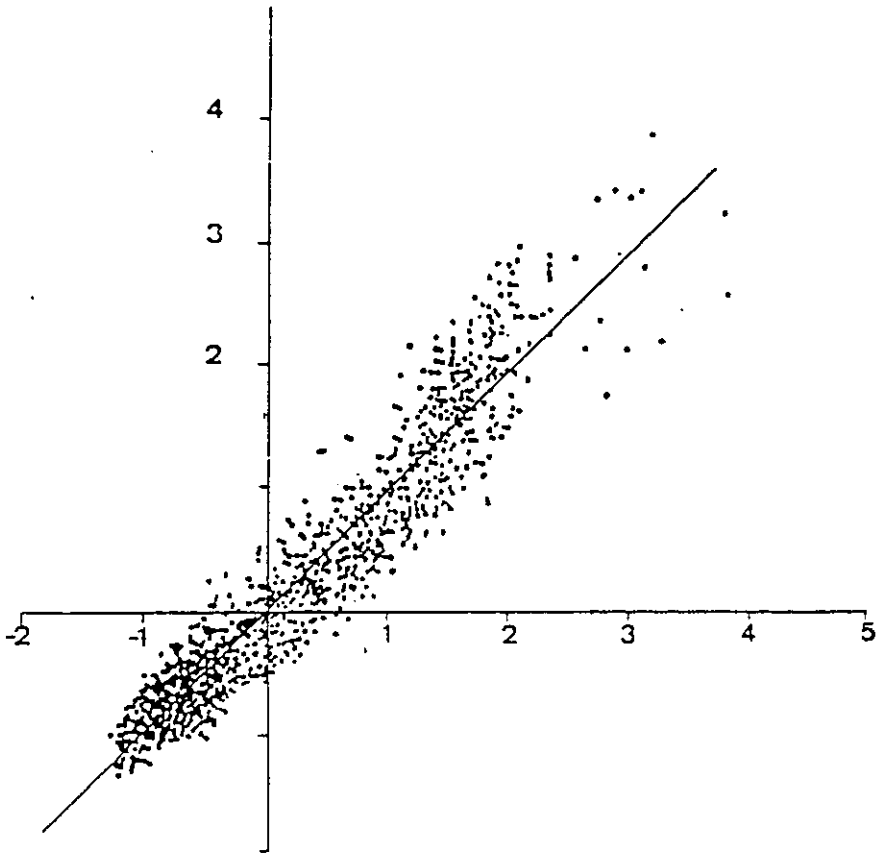

Figure 2.6: Standardized DG/DG_{cs} vs. standardized σ correlation. From Mejon (79).

Katsoulis [139] estimates $[DG_{cs}]$ using the mean monthly atmospheric water vapour content, the albedo of the area and the monthly average dust depletion for Athens (Greece) using a method indicated by Fritz and McDonald [93]. Comparing his estimates by A-regression with those obtained with formulae used by other researchers he concludes that the A-regression gives the best results.

Capderou [65], using a formula of Perrin de Brichambout [202], calculates $[DG_{cs}]$ as the sum of $[DD_{cs}]$ and $[DB_{cs}]$. He assumes

$$IB_{cs} = IE\ sin(h)\ exp(-\frac{T}{0.9 + \frac{9.4}{m}}),$$

where h is the solar altitude,

$$m = \frac{0.89^z}{sin(h)}$$

is the corrected optical air mass (z is the altitude in kilometers), and T is a factor depending on the absorption of solar radiation by water vapour and molecular and aerosol diffusion.
The diffuse irradiance is taken as $ID_{cs} = IE\ \mathcal{D}(T,h)$, where $\mathcal{D}(T,h)$ is a complex function (not reported).
He obtains $[DG_{cs}]$ by integrating on the day the quantity $IB_{cs} + ID_{cs}$.
Using monthly average values for $[DG_{cs}]$ and experimental monthly averages of DG and σ measured at five stations in Algeria, he finds and assumes valid for the whole country the formula:

$$\frac{[DG]}{[DG_{cs}]} = 0.32 + 0.69\ [\sigma].$$

Childs *et al* [69] use cubic splines to fit $[DG]/[DG_{cs}]$ vs. $[\sigma]$ for three towns in Malaysia (Kuala Lumpur, Penang and Kota Baru), using three years of measurements. They use the $[DG_{cs}]$ values already computed by Chuah [72].
The curves, obtained for each month, are used to estimate $[DG]$ values for three other localities in Malaysia (Malacca, Ipoh and Kuala Trangganu) for which data relative to one year are available. The obtained percentage errors are less than those which would be arise by symple linear A-regression.

2.2.2 Prescott- and Iqbal-like regressions

We have seen that the DG_{cs} or the DG_{cls} values which appear in all A-regressions must be either calculated by some irradiance model or approximately inferred from empirical daily data. Unfortunately the required measurements are often not available to designers or researchers, so that A-regressions cannot be used even in the presence of relative sunshine data. For this reason Prescott [204] first proposed using the modified formula

$$\frac{[DG]}{[DE]} = a + b\,[\sigma]$$

in which the extra-atmospherical daily irradiation DE substitutes the *clear sky* daily irradiation DG_{cs}. Of course, this implies that $a\,[DE]$ can be assumed to be an estimate of $[DG_{ov}]$ (i.e. $[DD_{ov}]$) and $(a + b)\,[DE]$ an estimate of $[DG_{cs}]$. For that which concerns the reliability of both these estimates, which relate to extreme values of $[\sigma]$, the same remarks already made relative to A-regressions are valid.

In the following we will refer to regression formulae such as

$$\frac{[DG]}{[DE]} = f([\sigma], [\xi])$$

as P-regressions. Here too ξ indicates a set of climatological parameters, other than σ, which can be eventually absent. Unless otherwise specified, the function f will be a first degree plynomial in $[\sigma]$.

Penman [200], as reported by Lewis [162], finds $a = 0.18$ and $b = 0.55$.

Black *et al.* [48] perform the fit analyzing data for five localities. They find coefficient ranges $[0.15, 0.30]$ for a, $[0.50, 0.55]$ for b and $[0.69, 0.80]$ for $a + b$. Using values from 32 stations they also estimate overall coefficients $a = 0.23$, $b = 0.48$, and assume that these values can be used with sufficient reliability for regions located between 35^{o} S and 65^{o} N.

Glover and McCulloch [101], analyzing P-regressions for various sites, conclude that, for all practical purposes, the coefficient b could be considered constant, with mean value 0.52 and standard error 0.005, whereas for a the relationship

$$a = 0.29\ cos\ \Phi$$

where Φ is the latitude, can be adopted.

Hounam [124], using 458 monthly values relative to 6 Australian stations with observations ranging from 3 to 10 years, obtains

$$\frac{[DG]}{[DE]} = 0.26 + 0.50\,[\sigma].$$

Page [194] extensively uses P-regressions to calculate monthly average daily global irradiations (on tilted surfaces) for sites belonging to the latitude range $40^o\ S - 40^o\ N$, and Löf *et al.* [165] report a list of a and b coefficients for different climates and latitudes.

Schuepp [227], in order to account for the misfits in the linear P-regressions when $[\sigma]$ is either too small or too large proposes the nonlinear relationship

$$\frac{[DG]}{[DE]} = \frac{[DG_{cs}]}{[DE]} + \sqrt{a\,[\sigma]^2 + b\,[\sigma]}.$$

A similar relation is given by Masson [177], who suggests

$$(1 + \frac{[\sigma]}{a})^2 - \frac{(\frac{[DG]}{[DE]} - \frac{[DG_{cs}]}{[DE]})^2}{b^2} = 1$$

Frère *et al.* [91] analyze the a and b coefficients for several stations with latitudes between $35^o\ S$ and $50^o\ N$ and propose a graphical relationship between these parameters and $[\sigma]$ (see Fig. 2.7).

Sayigh [224] finds for the linear P-regression the specification

$$\frac{[DD]}{[DE]} = 0.30 - 0.025\,[\sigma].$$

Iqbal [132] , while estimating the monthly average $[DG]$ on inclined surfaces, proposes the regression formula

$$\frac{[DD]}{[DG]} = 1 - [\sigma]$$

to calculate the ensemble monthly average $[DD]$ (on horizontal surfaces) using average relative sunshine and the corresponding average daily global irradiation. He studies data from four sites in Canada

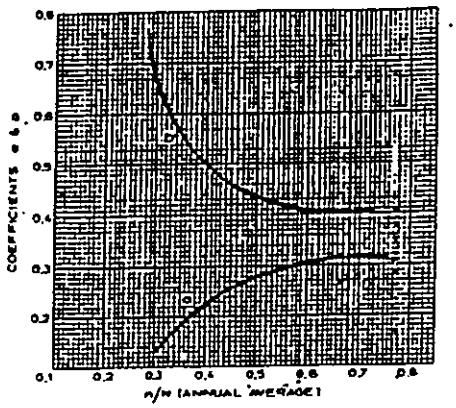

Figure 2.7: Relationship between a and b coefficients for P-regression and $[\sigma]$. From Frère *et al.* (75)

(Montreal, Winnipeg, Edmonton and Vancouver), using tables of measured $[DG]$ existing for the four localities in the climatological literature. The $[DG]$ values on tilted surfaces estimated using his fit for $[DD]$ (horizontal) are in good agreement with other results found in literature.

Katsoulis and Papachristopoulos [140] fit P-regression to determine a and b coefficients for Athens, Thera (500 m a.s.l) and Magoulina (1200 m a.s.l.), using 16 years of data. They find $a = 0.26$, $b = 0.71$ for Athens, $a = 0.27$, $b = 0.61$ for Magoulina and $a = 0.28$, $b = 0.67$ for Thera, with overall values $a = 0.316$, $b = 0.661$.
These last values are used to estimate $[DG]$ for 32 greek localities. It is found that the correlations between observed and estimated monthly values, calculated for localities where both $[DS]$ and $[DG]$ are available, are not uniformly high, even for data taken at the same station. Thus the authors conclude that for Greece this method gives poor overall estimates.

Rietveld [218], examining several published values of a an b for the linear P-regression, finds the relationship

$$a = 0.10 + 0.24\,[\sigma]$$

$$b = 0.38 + 0.08\,\frac{1}{[\sigma]}.$$

This results is believed to be applicable anywhere in the world.

Hay [118] notices that the empirical coefficients of the P-regressions show substantial temporal and spatial variations, and attributes these variations and the scattering of data points around regression lines to two main causes: a) the discrepancy between the "true" DS and the daily sunshine time interval measured with Campbell-Stokes recorders, which fail to respond to bright sunshine until the sun is some 5° above the horizon ([60]); b) the discrepancy between the diffuse irradiation DD' which comes directly from the DE depletion and the measured diffuse irradiation DD which results from multiple reflection among ground, clouds and atmosphere.
He accounts for the first cause by choosing as effective DS_o the quantity

$$DS'_o = \frac{arccos(\frac{cos\ 85^o - sin\ \Phi\ sin\ \delta}{cos\ \Phi\ cos\ \delta})}{7.5}$$

i.e. the astronomical daylength for solar zenith angle $\leq 85°$ (Φ is the latitude and δ the solar declination).
The second cause, which is important mainly in presence of clouds and high ground albedo, is accounted for by calculating DG' as

$$DG' = DG\ \{1 - \alpha\ (\alpha_a\ \sigma + \alpha_c\ (1 - \sigma))\}$$

(see [119]), where α, α_a and α_c are the albedo coefficients of the ground, the atmosphere and the clouds respectively.
He assumes constant values $\alpha_a = 0.25$ and $\alpha_c = 0.60$ and tests the regression[4]

$$\frac{DG'}{DE} = a + b\ [\sigma']$$

using data covering about 30 years from 9 stations sparsely located in Western Canada, with very different altitudes, latitudes and climates. Comparing the scatter plots of $[DG]/[DE]$ vs. $[\sigma]$ and $[DG']/[DE]$ vs. $[\sigma']$ an evident scatter reduction is observed. The mathematical analysis of the regressed line quantifies this reduction (see Fig. 2.8).
The obtained regression formula, generally suggested to estimate $[DG]$ given $[DE]$ and the ground albedo α, is given by

$$\frac{[DG]}{[DE]} = \frac{0.1572 + 0.5566\ [\sigma']}{1 - \alpha\ (0.25\ [\sigma'] + 0.60\ (1 - [\sigma']))}$$

[4]We will indicate DS/DS'_o with σ'.

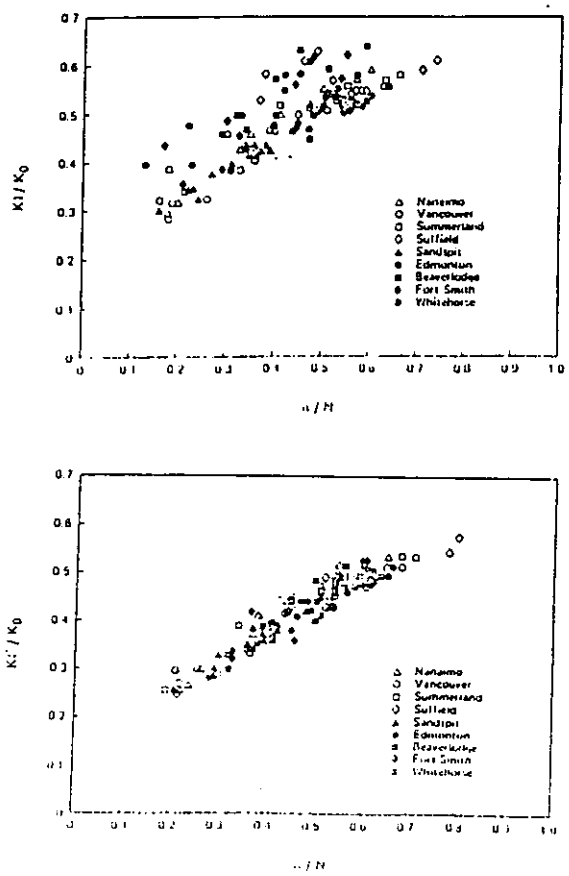

Independent variable	n/N	n/N'
Dependent variable	$K\downarrow/K_0$	$K\downarrow'/K_0$
Intercept	0.280	0.157
Slope	0.493	0.557
Coefficient of determination	.0.6775	0.905
Standard error of residuals	-0.047	0.024

Figure 2.8: Graphical and numerical comparison of classical and Hay corrected P-regression. From Hay (79).

Berger [41], using a formula suggested by Perrin de Brichambau [201], finds the individual daily estimates

$$DD = DG\,\{(sin(\phi-\delta))^{0.01} - 0.21\,\sigma - 0.55\,\sqrt{\sigma} + 0.8\,\sigma\,(1-\sigma)\}$$

for the region of Carpentras and

$$DD = DG\,\{(sin(\phi-\delta))^{0.01} - 0.31\,\sigma - 0.45\,\sqrt{\sigma} + 0.3\,\sigma\,(1-\sigma)\}$$

for the region of Trappes (both localities in France), where ϕ and δ are the latitude and the solar declination.

Mejon *et al.* [179], using 6 years of daily data at Carpentras (France) try to fit month by month

$$\frac{DB}{DE} = a\,(\sigma+b)^c$$

finding (for the corresponding logarithmic relation) correlation coefficients ranging from $r = 0.9451$ to $r = 0.9858$. They test their result using one year of independent daily data. By linearly fitting the calculated vs the observed DB values they find accounted variances in the range $[0.86, 0.98]$, depending on the month.

Iqbal [131], using irradiation data of three canadian localities (Toronto, Montreal and Goose Bay) relative to about 10 years and records of daily bright sunshine relative to about 30 years, studies the three relationships:

$$\frac{[DD}{[DG]} = a_1 + a_2\,[\sigma],$$

$$\frac{[DD}{[DE]} = a_5 + a_6\,[\sigma] + a_7\,[\sigma]^2,$$

$$\frac{[DB}{[DE]} = a_8 + a_9\,[\sigma] + a_{10}\,[\sigma]^2,$$

(cofficients a_3, a_4 refer in his article to a different regression). Results are reported in Fig. 2.9. He finds the performance of the first equation generally higher than that of the second to predict $[DD]$ (if, of course, $[DG]$ is known).

Source of Data	Coefficient a_1	Coefficient a_2	Standard Error of Estimate	Number
Montreal	0.7294	-0.5337	0.0228	(2a)
Toronto	0.7860	-0.6142	0.0394	(2b)
Goose Bay	0.8281	-0.7044	0.0223	(2c)
Montreal plus Toronto	0.7650	-0.5900	0.0277	(2d)
Montreal, Toronto and Goose Bay combined	0.7910	-0.6350	0.0317	(2e)

Source of Data	Coefficients a_5	Coefficients a_6	Coefficients a_7	Standard Error of Estimate	Number
Montreal	0.0945	0.6336	-0.7398	0.0163	(4a)
Toronto	0.2427	0.0439	-0.1161	0.0187	(4b)
Goose Bay	-0.1017	2.0408	-2.7905	0.0273	(4c)
Montreal plus Toronto	0.2020	0.1775	-0.2421	0.0196	(4d)
Montreal, Toronto and Goose Bay combined	0.1633	0.4778	-0.6555	0.0267	(4e)

Source of Data	Coefficients a_8	Coefficients a_9	Coefficients a_{10}	Standard Error of Estimate	Number
Montreal	-0.2536	1.8690	-1.6494	0.0163	(7a)
Toronto	-0.1844	1.4578	-1.0868	0.0311	(7b)
Goose Bay	-1.0576	6.2283	-7.4988	0.0173	(7c)
Montreal plus Toronto	-0.1791	1.4561	-1.1169	0.0253	(7d)
Montreal, Toronto and Goose Bay combined	-0.1763	1.4497	-1.1193	0.0250	(7e)

Figure 2.9: Regression coefficients for various relationships. From Iqbal (79).

In the following, we will speak of I-regressions to indicate formulae such as

$$\frac{[DD]}{[DG]} = f([\sigma],[\xi]).$$

where ξ retains the previously indicated meaning and,as before, f will be in general a first order polynomial in $[\sigma]$.

De Almeida and Rosa [76] and Biga and Rosa [45] study the P- and I-regressions relative to individual days

$$\frac{DG}{DE} = a + b\,\sigma$$

and

$$\frac{DD}{DG} = c - d\,\sigma$$

using 5 years of data for Lisboa (Portugal). For each particular month they divide the data according to the magnitude of σ (ten classes of about 15 points each) and average DD and DG within each class. They then compute the linear regressions. Results are reported (see Fig.2.10) for the regression coefficients. The authors claim that the correlation coefficients are not less than 0.98 for the P-regression and not less than 0.93 for the I-regression.
The same formulae, fitted on annual basis, give correlation coefficients of 0.98 and 0.99 respectively.
Moreover, following Nicolet and Dogniaux [185] the authors express DG and DD as

$$DG = DD + DB_{cs}\,F'(\sigma)$$

and

$$DD = DD_{cs}\,\sigma + DD_{ov}\,F''(\sigma)$$

where as customary the indices ov and cs stan for completely overcast and cloudless day respectively, and $F'(\sigma)$, $F''(\sigma)$ are in principle arbitrary functions subject to the conditions $F'(0) = 0$, $F''(0) = 1$ and $F''(1) = 0$. They are able to deduce the relationships

$$\frac{DB_{cs}\,F'(\sigma)}{DE} = 0.017 + 0.228\,\sigma + 0.419\,\sigma^2$$

and

$$\frac{DD_{ov}\ F''(\sigma)}{DE} = 0.218 + 0.176\,\sigma - 0.491\,\sigma^2$$

which, due to the previous relations, are in fact fits for DB/DE and $(DD - DD_{ov})/DE$ respectively (see Fig. 2.11).

Flocas [90], using 15 years of irradiation and sunshine measurements at Athens (Greece), obtains P-regression coefficients $a = 0.20$ and $b = 0.51$, with a regression correlation coefficient $r = 0.92$. Using the Frère *et al.* [91] empirical relationships, values $a = 0.31$ and $b = 0.41$ would be obtained. Though the coefficients are different, estimates of monthly $[DG]$ using the two pair of values are not so contrasting, and they are both in satisfactory agreement with measured data. The author prefers to use the first pair of values both for their agreement with values previously found in literature and because it gives a more precise annual [DG] mean.

Neuwirth [183] analyzes the P-regression coefficients a and b previously calculated ([182]) using many decades of irradiation and sunshine measurements at 19 stations in Austria.
In order to take into account their slight variation from month to month and their dependence on the altitude of the measuring station a.s.l., he classifies a and b for six classes of altitudes and for the four seasons. Moreover, for each season a quadratic fit of both a and b vs. the altitude is performed (see Fig. 2.12).

Lewis [162] compares DG values calculated using the formulae of Penman [200], Black [48], Fritz [92] and Masson [177] to the irradiation and sunshine measurements performed during one year at Lusaka (Zambia). He concludes that Black's specification of the P-regression

$$[DG] = [DE]\,(0.23 + 0.48\,[\sigma])$$

gives the most appropriate estimates. He also compares various formulae founded in literature to estimate the ratio $[DD]/[DG]$, and chooses that by Sayigh [224]

$$[DD] = [DG]\,(0.30 - 0.025\,[\sigma])\ .$$

Barbaro *et al.* [22] use data of monthly mean irradiations and relative sunshine measured at three Italian localities (Palermo, Macerata and

Month	a	b	c	d
January	0.26	0.48	0.90	0.75
February	0.23	0.57	0.96	0.84
March	0.23	0.59	0.94	0.83
April	0.24	0.55	0.94	0.81
May	0.23	0.56	0.90	0.78
June	0.23	0.55	0.93	0.83
July	0.29	0.46	0.78	0.67
August	0.23	0.49	0.89	0.78
September	0.25	0.48	0.91	0.82
October	0.23	0.47	0.91	0.77
November	0.23	0.45	0.94	0.81
December	0.21	0.50	0.95	0.82
YEAR	0.24	0.52	0.93	0.81

Figure 2.10: A- and I-regression coefficients. From Biga and Rosa (79).

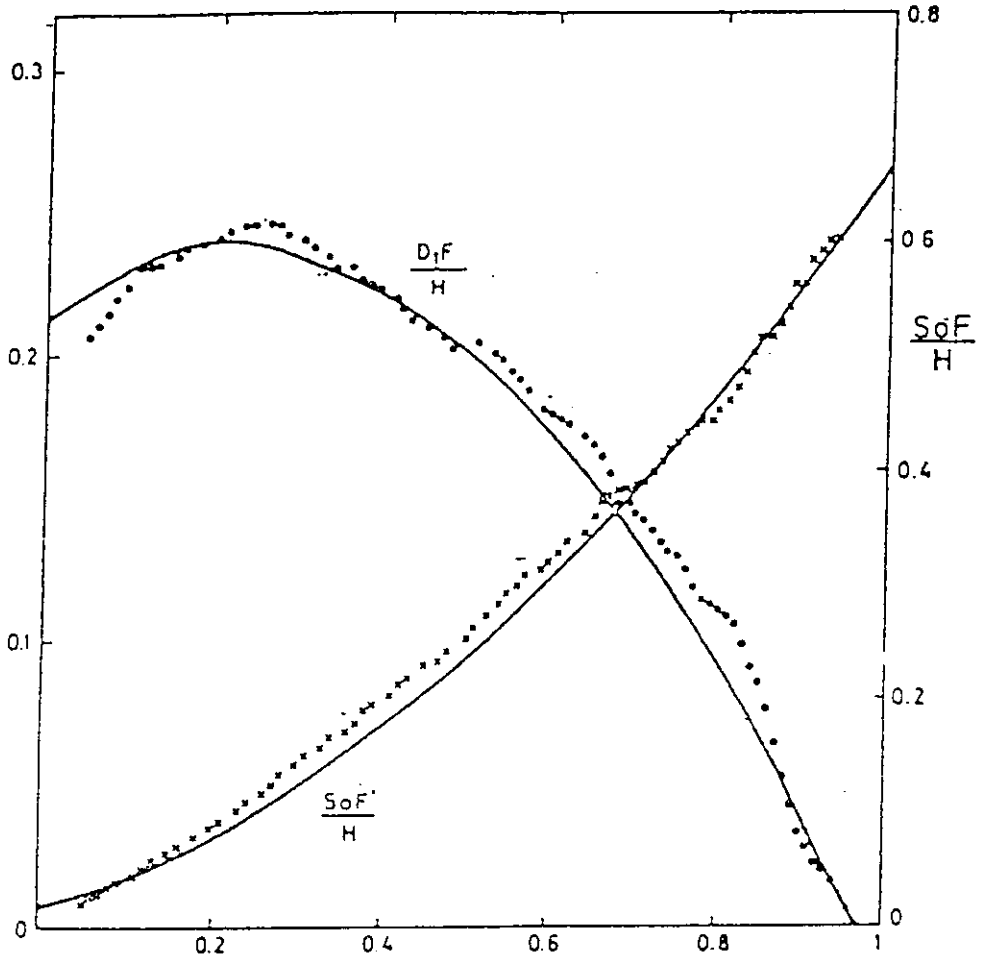

Figure 2.11: Comparison between calculated and smoothed DB/DE and $(DD - DD_{ov})/DE$. From Biga and Rosa (79).

altitude a.s.l		winter	spring	summer	autumn
100-300 m	a	0.18	0.21	0.21	0.18
	b	0.51	0.49	0.47	0.51
300-500 m	a	0.22	0.21	0.21	0.20
	b	0.48	0.49	0.48	0.49
500-1000 m	a	0.23	0.24	0.22	0.21
	b	0.41	0.45	0.46	0.42
1500 m	a	0.23	0.25	0.17	0.20
	b	0.51	0.48	0.56	0.53
2000 m	a	0.36	0.38	0.22	0.27
	b	0.36	0.36	0.54	0.54
3000 m	a	0.43	0.44	0.33	0.36
	b	0.36	0.32	0.46	0.40

	A_0	A_1	A_2
winter	0.1494	0.1192	-0.0117
spring	0.1711	0.1261	-0.0108
summer	0.2051	0.0234	0.0078
autumn	0.1917	0.0210	0.0073

	B_0	B_1	B_2
winter	0.5498	-0.2062	0.0492
spring	0.5403	-0.1813	0.0395
summer	0.4972	-0.0693	0.0199
autumn	0.4921	-0.0428	0.0091

Figure 2.12: P-regression a and b coefficients for different altitudes and seasons, and their quadratic regression coefficients vs. altitude for the four seasons. From Neuwirth (80).

Genova) during different numbers of years. They compare, among other things, the relative merits of the formulae

$$\frac{[DD]}{[DG]} = a_1 + a_2\,[\sigma] + (a_3\,[\sigma]^2)$$

$$\frac{[DD]}{[DE]} = a_1 + a_2\,[\sigma] + (a_3\,[\sigma]^2)$$

used by various authors to estimate $[DD]$. The quadratic terms can be included or excluded from the fitting procedure, and results are evaluated by minimizing the sum of the squared *relative* errors Γ and considering the two quantities

$$\Phi = \sqrt{\frac{\Gamma}{n}}$$

and

$$\Omega = \frac{\Gamma}{n-m}$$

where n is the number of points and m the number of parameters. Results are reported in Fig. 2.13.

The authors conclude that the linear form of the second relationship is preferable, both for its prediction performances and because requires only sunshine measurements.

Sfeir [229] fits the P-relationship with data for two sites in Lebanon, one on the coast and the other in the interior, using about 10 years of data. For the coastal area the coefficients a and b, calculated by twelve monthly regressions, show a seasonal trend which the author fits by

$$a = 0.230 + 0.055\ sin(30\ (m-3))$$

and

$$b = 0.738 - a$$

where m designates the month of the year. In fact, the standard error of a with respect to its annual mean is 0.042, whereas it is 0.023 with respect to the sinusoidal fit.

A P-regression between monthly averages is also performed, both in its original form and with the corrections suggested by Hay. Results are reported in Fig. 2.14, showing no dramatic differences.

STATION	a_1	a_2	ϕ
Palermo	0.6603	-0.5272	0.0947
Macerata	0.6603	-0.5717	0.0833
Genova	0.5866	-0.4264	0.0838
PA - GE	0.6178	-0.4704	0.0939

STATION	a_1	a_2	a_3	ϕ
Palermo	0.7434	-0.8203	0.2454	0.0940
Macerata	1.0297	-2.1096	1.5193	0.0717
Genova	0.8159	-1.3289	0.8668	0.0829

STATION	a_1	a_2	ϕ
Palermo	0.2626	-0.1391	0.0903
Macerata	0.2989	-0.1577	0.0682
Genova	0.1532	0.0283	0.0428
PA - GE	0.2036	-0.0562	0.1025

STATION	a_1	a_2	a_3	ϕ
Palermo	0.2205	0.0126	-0.1292	0.0899
Macerata	0.3627	-0.4259	0.2678	0.0662
Genova	0.1717	-0.0461	0.0725	0.0428

Figure 2.13: Linear and quadratic regression coefficients of $[DD]/[DG]$ (above) and $[DD]/[DE]$ (below) vs. $[\sigma]$. From Barbaro (81a).

	$\bar{H}_h/\bar{H}_o$ vs $\bar{n}/\bar{N}$			$\bar{H}_h'/\bar{H}_o$ vs $\bar{n}/\bar{N}'$		
	A	B	Coef. of determination	A	B	Coef. of determination
COAST	0.23	0.49	0.90	0.20	0.46	0.90
INTERIOR	0.22	0.57	0.94	0.15	0.55	0.94
ALL DATA	0.20	0.57	0.86	0.16	0.53	0.92

Figure 2.14: Comparison between the original and the Hay-corrected P-regression. From Sfeir (81).

Sears *et al.* [228] investigate, using one year of accurate radiation measurements at Davis(California), the individual daily relationships

$$\frac{DG}{DE} = a' + b' \sigma$$

$$\frac{DB}{DE} = a'' + b'' \sigma$$

$$\frac{DD}{DG} = a''' + b''' \sigma$$

The analysis is performed month by month. The authors find, except for the month of June (which gives strange results due to very specific local circumstances), coefficients of determination in the ranges $[0.81, 0.98]$, $[0.87, 0.96]$ and $[0.88, 0.98]$ for the three equations respectively.
The related regression coefficients range in the intervals $[0.17, 0.31]$, $[-0.7, -0.02]$ and $[0.97, 1.59]$ for a', a'' and a''' and $[0.42, 0.61]$, $[0.54, 1.41]$ and $[-0.81, -1.55]$ for b', b'' and b'''.

Majmudar [172] fits the corrected Hay [118] formula to monthly [DG] measured during one year at Sringar (Kashmir). An approximate fixed value 0.25 is assumed for the albedo coefficient, and a fairly good agreement between observed and calculated data is obtained.

Scerri [225], using 24 years of irradiation and sunshine data for Malta, perform linear regressions for $[DD]/[DG]$ and $[DD]/[DE]$ vs. $[DS]/[DS_{max}]$, where $[DS_{max}]$ is the maximum value of DS recorded for any day of the considered month during the whole experimental period.
He finds

$$\frac{[DD]}{[DG]} = 0.832 - 0.626 \frac{[DS]}{[DS_{max}]}$$

with linear correlation coefficient $r = -0.995$, standard deviation of the slope 0.0175 and standard deviation of the intercept 0.0132.
The second regression gives

$$\frac{[DD]}{[DE]} = 0.385 - 0.215 \frac{[DS]}{[DS_{max}]}$$

with correlation coefficient 0.97. The values of the parameters are found to be similar to those which can be deduced from Glover and McCulloch [101] for the latitude of Malta.

Andretta *et al.* [11] analyze irradiation and relative sunshine monthly averages, calculated for a period of about 10 years at 28 Italian stations. They find a general P-correlation

$$\frac{[DG]}{[DE]} = 0.23 + 0.37\,[\sigma]$$

with correlation coefficient $r = 0.796$. If performed on individual station data the correlations are much better, with r generally higher than 0.90 and root mean square error $\simeq 0.015$. The two parameters a and b for each locality and the corresponding regression correlation coefficient are reported.

On the other hand, correlations performed on each month, considering all localities together, gives a much worse determination (r ranges from 0.50 in March to 0.87 in November). Nevertheless these twelve fits are evaluated as statistically compatible with the overall fit already quoted.

The authors analyze the sources of errors and conclude that the estimated error for $[DG]/[DE]$, using the previously calculated overall coefficients, is given by

$$\Delta = 0.027 + \frac{0.017}{\sqrt{M}}$$

where M is the total number of available experimental years. Thus, they claim that no significantly better result can be expected using longer observation periods, most of the error coming from the inherent imperfect correlation between the concerned variables.

Hawas and Muner [117] try to fit the P-regression, both in its classical form and in the modified form suggested by Hay, to monthly averaged data from 18 locations in India relative to about 15 years. They find for the classical P-regression overall coefficients $a = 0.299$ and $b = 0.448$, with correlation of determination $r^2 = 0.993$. The same relationship is shown to hold for individual sites.On the other hand, they find for Hay's corrected regression the specification

$$\frac{[DG']}{DE} = 0.249 + 0.429\,[\sigma'] \ ,$$

with no dramatic reduction in the scatter of the experimental points.

Ahmad *et al.* [4], in order to draw solar irradiation maps for Iraq on the basis of reliable irradiation data for few stations in the country, analyze different possible statistical relationships between solar irradiation and other climatological parameters. They finally choose relative sunshine duration as the best predictor of monhly $[DG]$ through linear P-regression, and obtain the values: $a = 0.3019$, $b = 0.3135$ for Mosul; $a = 0.4153$, $b = 0.2340$ for Baghdad; $a = 0.6573$, $b = 0.0228$ for Basra.
A quadratic P-regression is also performed, but gives very slightly improved results.

Lewis [160] looks for the best predictive formula for $[DD]$ given $[DG]$ using data from two stations in Zimbabwe (Salisbury and Bulawayo) for which long term monthly means of these quantities exist. He concludes that, among others, the best results are given by the I-regressions

$$\frac{[DD]}{[DG]} = 0.754 - 0.654\,[\sigma] \qquad (r = -0.9912)$$

for Bulawayo and

$$\frac{[DD]}{[DG]} = 0.7794 - 0.689\,[\sigma] \qquad (r = -0.9651)$$

for Salisbury. He uses the Bulawayo regression to estimate $[DD]$ for other 3 stations in Zimbabwe.

Bamiro [19], while comparing different formulae to estimate $[DG]$ on the basis of 5 years of measurements in Ibadan(Nigeria), reports the P-regression coefficients (for monthly averages) $a = 0.35$ and $b = 0.27$, which give correlation coefficient $r = 0.78$. A slight improvement is obtained if $[DS]$ is related to 12 hours, instead of to $[DS_o]$ (in this case $a = 0.34$, $b = 0.29$, $r = 0.80$).

Khogali *et al.* [143] test the P-regression using reliable data from Sana'a (Yemen) relative to 2 years, obtaining $a = 0.262$, $b = 0.454$ and $r = 0.97$. The same regression, performed using values of $[DG]$ estimated by the formula by Barbaro *et al.* [25] with $K = 13$ (see below), gives $a = 0.35$, $b = 0.36$ and $r = 0.995$. The authors also

test the I-regression for six localities in Yemen (from 2 to 5 years of measurements), obtaining

$$\frac{[DG]}{[DE]} = 0.92 - 0.83\,[\sigma] \quad (r = 0.97)$$

Mani and Rangarajan [176] use the Hay modified P-regression to fit $[DG]$ data measured at 16 stations in India during periods ranging from 8 to 21 years. They assume a mean ground albedo coefficient 0.20 for all stations, and for each station they calculate the coefficients for the relationship

$$\frac{[DG']}{[DE]} = a + b\,[\sigma']$$

The obtained ranges are 0.156 to 0.313 for a, 0.378 to 0.521 for b and 0.860 to 0.975 for $a+b$. The agreement between computed and observed values of $[DG]$ is within $2\%-5\%$ in most cases. The authors suggest that a minimum of 5 years for each location is needed to obtain reliable estimates.

Lewis [161] compares ten different empirical regression formulae to $[DG]$ data from Harare (Zimbabwe), finding that the simple P-regression gives the most reliable results. He obtains the formula

$$[DG] = [DE]\,(0.317 + 0.464\,[\sigma])$$

with standard errors 0.013 for a and 0.020 for b and coefficient of determination $r^2 = 0.983$. This equation is used to estimate monthly average global irradiations at three selected localities in Zimbabwe.

Cerquetti *et al.* [66] test the correlations

$$\frac{[DG]}{[DE]} = a + b\,[\sigma]$$

$$\frac{[DB]}{[DE]} = b'\,[\sigma]$$

$$\frac{[DD]}{[DG]} = a'' + b''\,[\sigma]$$

using about 20 years of measurements at Macerata (Italy). Their monthly regressions show correlation coefficients ranging in the intervals $[0.69, 0.95]$ for the first formula, $[0.72, 0.96]$ for the second and $[0.53, 0.78]$ for the third.

Ögelmann *etal.* [189], using about 4 years of data for Ankara and Adana (Turkey) test the quadratic relationship

$$\frac{DG}{DE} = a_o + a_1 \sigma + a_2 \sigma^2$$

They obtain for a_0, a_1 and a_2 the values 0.181, 0.875, -0.361 for Adana, 0.221, 0.705, -0.217 for Ankara and 0.204, 0.758, -0.250 for both localities together, with an average difference of $\sim 2\%$ and a maximum difference of 0.10 between the combined and the individual fits. Since the scatter of experimental points is $\pm 50\%$ at $\sigma = 0$ and $\pm 15\%$ at $\sigma = 0.9$ they assume the common fit coefficients is valid for both locations.

The authors also test the "monthly averaged" formula

$$\frac{[DG]}{[DE]} = a'_o + a'_1 [\sigma] + a'_2 [\sigma^2]$$

which, using the previously determined coefficients and taking into account the statistical relationship

$$[\sigma^2] = [\sigma]^2 + var(\sigma)$$

they rewrite as

$$\frac{[DG]}{[DE]} = 0.204 + 0.758 [\sigma] - 0.250 ([\sigma]^2 + var(\sigma))$$

Using this formula and 57 monthly values they find agreements up to 3.8% for Adana and 6.9% for Ankara. Moreover, they are able to find their data for the relationship

$$var(\sigma) = 0.035 + 0.326 [\sigma] - 0.433 [\sigma]^2$$

which, combined with the previous one, gives the monthly formula:

$$\frac{[DG]}{[DE]} = 0.195 + 0.677 [\sigma] - 0.142 [\sigma]^2$$

Comparison with experimental values at other five stations in Turkey shows a satisfactory agreement. For $[\sigma] = 1$ one has $\frac{[DG]}{[DE]} = 0.73$, whereas Ångström [12] suggests (for lower latitudes indeed) 0.80. Finally, the authors show that a linear fit of their quadratic formula would give, between a and b coefficients, the relation

$$a = 1.00 - 2.38\, b + 1.76\, b^2$$

which satisfactorily accounts for the well-known pairwise variability of these parameters in P-regressions depending on seasons and sites.

Rao *et al.* [207], while studying the regression of DD/DG on DG/DE as it emerges from two years of measured data at Corvallis (Oregon), calculate the I-relationship

$$\frac{DD}{DG} = 1.007 - 0.9316\, \sigma$$

obtaining coefficient of determination $r^2 = 0.925$ and standard error of the estimate equal to 0.080.

Capderou [65], using data from five stations in Algeria, calculates the I-regression

$$\frac{[DD]}{[DG]} = 0.61 - 0.45\, [\sigma]$$

He notes that this relationship could not be used outside the range $0.5 \leq [\sigma] \leq 0.9$.

Hutchinson *et al.* [127] use data from 11 Australian stations, covering periods from 5 to 9 years of measurements, to fit the Hay corrected linear P-regression to individual daily data. They group data for each month and find accounted variances from 77.2% to 92.0%, with a and b coefficients ranging in the intervals $[0.188, 0.266]$ and $[0.448, 0.534]$ respectively.

Benson *et al.*[40], after discussing the relative performances of Campbell-Stokes, Normal Incidence Pyrheliometer and Foster Sunshine Switch for the precise determination of sunshine lengths, study correlations of DG/DE, DD/DG and DB/DE vs. NIP-σ on the basis of about 2 years of precise measurements at Atlanta (Georgia).

They analyze quadratic P-regressions for DG/DE and DB/DE and a linear I-regression for DD/DG and obtain

$$\frac{DG}{DE} = 0.24 + 0.71\,\sigma + 0.26\,\sigma^2$$

$$\frac{DD}{DG} = 1.00 - 0.90\,\sigma$$

$$\frac{DB}{DE} = 0.31(0.26)\,\sigma + 0.26(0.23)\,\sigma^2$$

(the unit coefficient in the second regression is taken as fixed and the values between parenthesis into the third regression refer to the period April-September).
The authors also analyze the effects of turbidity of the atmosphere on DD/DB $(DB > 0)$, DD/DG, DG/DE and the effects of precipitable water content on DB/DB_{normal}, DD/DB, DG/DE.
Finally they investigate the correlations between monthly averages, and find (coefficient values within parenthesis refer to the previously indicated months)

$$\frac{[DB_{normal}]}{[DE_{normal}]} = 0.545(0.445)[\sigma]$$

$$\frac{[DD]}{[DG]} = 0.66(0.88) - 0.61(0.80)[\sigma]$$

$$\frac{[DG]}{[DE]} = 0.18(0.60) + 0.24(0.53)[\sigma]$$

$$\frac{[DB]}{[DE]} = 0.06(0.03) + 0.31(0.26)[\sigma] + 0.36(0.42)[\sigma]^2.$$

Rao *et al.* [208] comment on some results of the P-regression they obtain on the basis of three years of very reliable data measured at Corvallis (Oregon). Coefficients $a = 0.207$ and $b = 0.560$ (with $r^2 = 0.92$) result from complete regression, and $a = 0.234$ and $b = 0.520$ (with the same r^2) for regression excludig points with $\sigma = 0$. The values 0.767 and 0.754 respectively corresponding to $\sigma = 1$ both fall within the range found in literature. They notice that the large range 0.05 to 0.325 for DG/DE when $\sigma = 0$ (see Fig.2.15) can be

explained both by differences in the trasmissivity of clouds and by the fact that $\sigma = 0$ does not mean $DB = 0$, due to the sensitivity of the Campbell-Stokes instruments (the threshold varying between 4.2 and 16.8 $kJ\ m^{-2}\ min$ depending on the atmosphere turbidity and humidity and on the moisture content of the sunshine card).

The authors conclude that $DG/DE \leq 0.20$ when $\sigma = 0$ is a good approximation and that no significant variation in the linear regression estimate for DG_{cs}/DE ($\sigma = 1$) appears when data for $\sigma = 0$ are excluded from the analysis.

Ibrahim [128] fit monthly P-regression for seven cities in Egypt with latitudes from $23°58'\ N$ to $31°20'\ N$, using data covering from 2 to 22 years, depending on the city. They find a coefficients ranging from 0.14 to 0.70 and b coefficients ranging from 0.03 and 0.61. A remarkable feature of their results is that, in despect of those large variations, the range for $a+b$, i.e. the estimated $[DG_{cs}]/[DE]$, results very narrow: $[0.73, 0.77]$.

Soler [237] tests both linear and quadratic P-regressions for five localities in Spain, using two years of data. Regressions are performed within each month of the year. He finds an annual trend for $[DG_{cs}]/DE$ (i.e. the estimated value of $[DG]/[DE]$ when $[\sigma] = 1$), both for the linear and the quadratic relationships. No tentative mathematical fit of this trend is nevertheless performed.

Turton [251] estimates P-regression coefficients for a group of 25 tropical localities (latitudes between $19°14'S$ and $22°32'N$). He finds, using 300 monthly observations, $a = 0.30$, $b = 0.40$ with correlation coefficient $r = 0.84$. Regressions for climatical subgroups are also performed, obtaining the worst linear correlation coefficients.

Jain and Jain [136], using monthly averages of daily global irradiation and relative sunshine measured at 8 stations in Zambia during about 7 years and monthly average ground albedo coefficients, compare the original linear P-regression with other three linear regressions which take into account multiple reflections between ground and atmosphere and clouds, reduction in DS_o due to the sensitivity of Campbell-Stokes recorders and both effects together (see [118]). They do not find significant improvements using the three "corrected" formulae with respect to the first, and assert that relevant improvement can perhaps be obtained only at higher latitudes and for higher

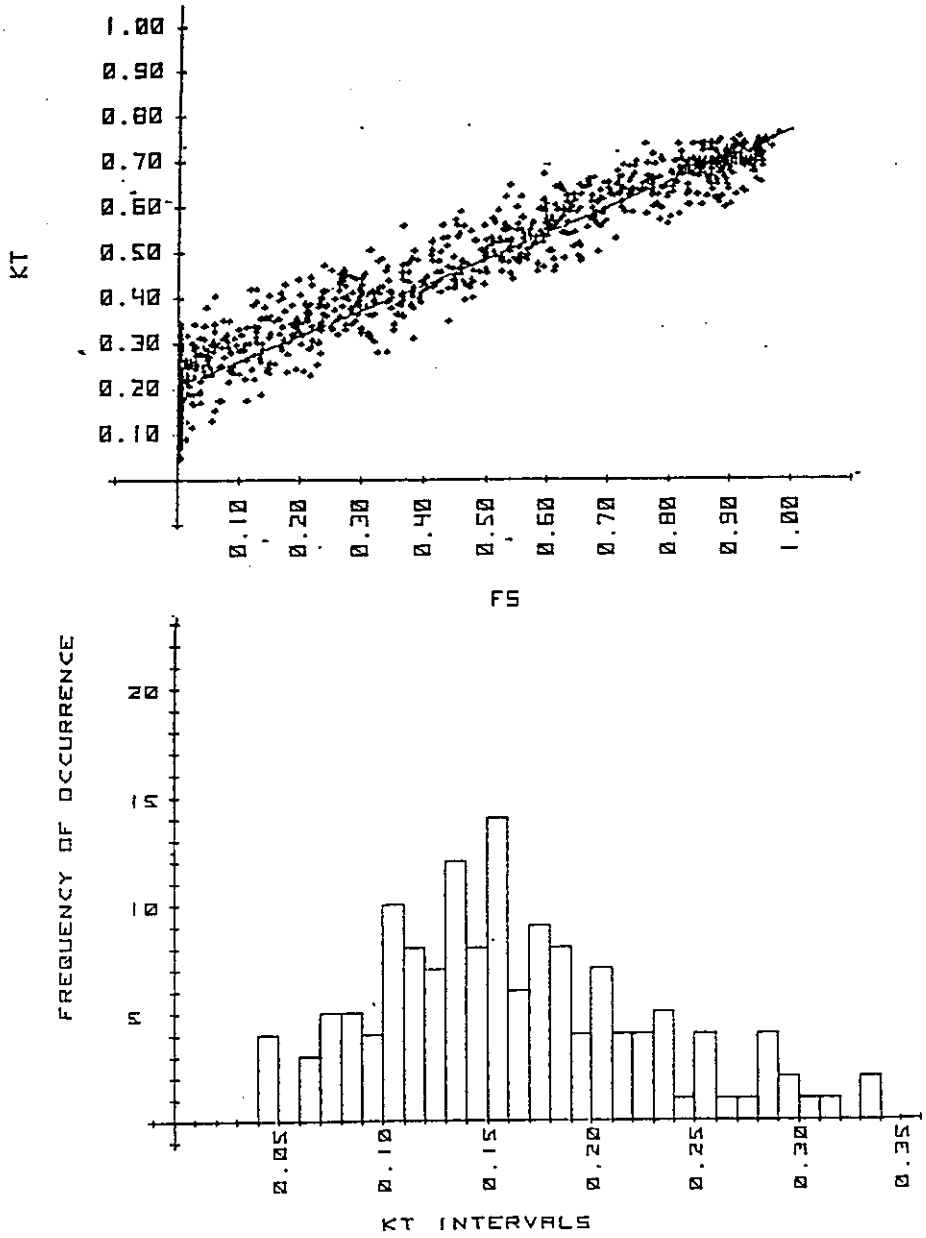

Figure 2.15: Scatter diagram for DG/DE vs. σ and DG/DE frequency distribution for $\sigma = 0$. From Rao *et al.* (85).

ground albedo coefficients. They conclude by advising for Zambia the relationship

$$\frac{[DG]}{[DE]} = 0.240 + 0.513\,[\sigma]$$

Gopinathan [107] suggests the extended I-regression

$$\frac{[DD]}{[DG]} = a + b\,\frac{[DG]}{[DE]} + c\,[\sigma]$$

to estimate $[DD]$ knowing both $[\sigma]$ and $[DG]/[DE]$. He obtains regression coefficients $a = 0.879$, $b = -0.575$, $c = -0.323$ for locations in Southern africa. He also tests the formula on data for New Dehli, Poona and Madras (India) [106] and finds better performances against the simple linear I-regression. In this case the regression coefficients are found to be $a = 1.194$, $b = -0.838$, $c = -0.446$ with correlation coefficient $r = 0.973$.

Gopinathan [108], using a and b parameters for P-regression and $[\sigma]$ values relative to 40 locations spread all around the world, is able to obtain the regressed relationships

$$a = -0.309 + 0.539\,cos\Phi - 0.069\,h + 0.290\,[\sigma]$$

$$b = 1.527 - 1.027\,cos\Phi + 0.0926\,h - 0.359\,[\sigma]$$

where Φ is the latitude and h the hight a.s.l.
These formulae are used to calculate a and b for another 14 stations in the latitude range $34°S$ to $54°N$ and estimations of $[DG]/[DE]$ are performed (see Fig.2.16) using the obtained values.
Results are compared with those obtained with the Rietveld [218] and Glover and McCulloch citeGlover58 models using the mean bias error, root mean square error and mean percentage error as indicators. The merits of the author's approach clearly appear, mainly if one considers that only geo-topographical knowledge is required in addition to sunshine data.

Al-Hamadani *et al.*[6] test the simple I-regression and the I-regression linearly inplemented by a DG/DE linear term using the individual daily data relative to about 2 years of measurements for a station near Baghdad (Iraq). They subdivide the data into four seasonal groups

Location	Latitude ϕ (degrees)	Elevation h (km)	Mean S/S_o	a	b	$a+b$	Present model MBE	Present model RMSE	Present model MPE	Rietveld MBE	Rietveld RMSE	Rietveld MPE	Glover and McCulloch MBE	Glover and McCulloch RMSE	Glover and McCulloch MPE
Buenos Aires	34.58 S	0.025	.577	.300	.477	.777	.513	1.729	4.4	−.636	1.004	3.8	−.660	1.086	3.3
Sydney	33.87 S	0.042	.558	.297	.478	.775	1.102	1.674	6.8	−.071	1.188	4.7	.093	1.175	4.1
Maseru	29.19 S	1.571	735	.266	.512	.778	.188	.254	0.9	.196	.358	1.2	.186	.341	0.9
Alexander Bay	28.57 S	0.021	.750	.380	.358	.738	−1.652	2.056	6.6	−1.991	2.369	7.9	−2.005	2.371	7.9
Bulawayo	20.15 S	1.343	.689	.304	.440	.744	−1.177	1.201	5.6	−1.303	1.549	6.0	−.440	.576	2.2
Penang	5.3 N	0.003	.560	.390	.303	.693	.997	1.310	6.3	−1.890	2.112	8.8	− 438	.961	4.2
Ibadan	7.43 N	0.228	.435	.336	.373	.709	1.307	1.336	8.3	396	1.211	5.9	1.842	1.921	11.0
Ilorin	21.3 N	0.015	.650	.381	.338	.719	−1.280	1.622	6.2	−1.887	2.112	8.8	−1.056	1.372	5.4
New Delhi	28.58 N	0.216	.665	.342	.407	.749	−.305	1.219	4.8	−1.113	1.481	5.5	−.780	1.511	4.7
Cairo	30.08 N	0.112	.800	.381	.362	.743	.933	1.008	5.8	1.199	1.313	6.6	.877	.942	5.2
Albuquerque	35.05 N	1.620	.775	.245	.558	.803	−1.566	1.665	7.4	−2.060	2.176	9.1	−2.667	2.780	12.4
Roma	41.8 N	0.131	556	.245	.574	.819	.125	607	5 1	−.908	1.283	4.8	−1.528	1.980	7.5
Venezia	45.5 N	0 006	446	.198	.648	846	− 231	.935	6.5	−1.169	1.494	7.2	−1 527	2.297	10 8
Hamburg	53.63 N	0.014	.344	.109	796	.905	182	.673	7.5	.192	.452	4.6	− 899	1.079	9.4

Figure 2.16: Comparison between the Gopinathan, Rietveld and Glover and McCulloch [DG] estimation methods. From Gopinathan (88c).

(Winter, Spring, Summer and Autumn in that order) and obtain (read ordered components for each season)

$$\frac{DD}{DG} = (0.782, 0.734, 0.897, 0.771) - (0.655, 0.687, 0.790, 0.646)\,\sigma$$

with correlation coefficients $r = (0.953, 0.950, 0.939, 0.963)$ for the simple regression and

$$\frac{DD}{DG} = (0.923, 0.951, 1.093, 0.856) - (0.429, 0.565, 0.507, -0.275)\,\frac{DG}{DE} - (0.497, 0.471, -0.629, 0538)\,\sigma$$

with $r = (0.960, 0.957, 0.962, 0.966)$ for the implemented one.
Analogous correlations between the corresponding monthly averages give

$$\frac{[DD]}{[DG]} = 0.650 - 0.494\,[\sigma]$$

and

$$\frac{[DD]}{[DG]} = 0.962 - 0.758\,\frac{[DG]}{[DE]} - 0.277\,[\sigma]$$

2.2.3 Miscellaneous regressions containing sunshine

Regression formulae of DG vs σ with DG_{cs} or DE as normalizing quantities do not exhaust tentative correlations which have been performed between global irradiation and sunshine.

Ukraintzev [252] suggests a linear equation between $[DG]$ and $[DS]$, but some authors([42], [5]) show that the linear dependence underestimates the true values in summer and overestimates them in winter.

Sivkov [232] [231] proposed the relationship

$$[DG] = 4.9\,[DS]^{1.31} + 10500\,(sinh_n)^{2.1} \quad [cal/cm^2]$$

where h_n is the noon solar height on the 15th of the given month.

Masson [177], as reported by Lewis [162], advises the formula

$$[DG] = 0.042\ (60 + \sqrt{1406.2\ [DS]^2 + 7426.6\ [DS]})$$

to estimate the global solar irradiation from absolute sunshine only.

Swartman and Ogunlade [246] give for $[DG]$ the three formulae [5]

$$[DG] = 1.875\ [\sigma]^{0.360}\ [DR]^{-0.150} \quad (DS > 0)$$

$$[DG] = 14.451 + 17.593\ [\sigma] - 10.137\ [DR]$$

$$[DG] = 0.0419\ 460^{0.607([\sigma]-[DR])}$$

Reddy *et al.* [212] suggest the formula

$$[DG] = \alpha\ K\ 10^2\ exp\{\Phi\ ([\sigma_*] - \frac{[DR]^{1/3}}{100} - \frac{1}{T_m})\}$$

where $[DG]$ is measured in $cal/cm^2\ day$, $\alpha = 1.53$, Φ is the latitude in radians, σ_* the ratio of the bright sunshine relative to 12 hours, T_m the maximum air temperature in Celsius degree, and

$$K = \frac{0.2}{1 + 0.1\Phi}[DS_o] + \psi_{ij}\ cos\Phi$$

is a suitable latitude dependent expression which contains a climatical and seasonal factor ψ_{ij} ($i = 1, 2$ refer to onshore or inner region and $j = 1, \ldots, 12$ to the months of the year).

Reddy [211] also suggests the alternative formula

$$[DG] = 100\ K\ \frac{(1 + 0.8\ [\sigma])(1 - 0.2\ [\frac{r}{m}])}{\sqrt{[DR]}}$$

in which the fraction r/m of rainy days during the month appears. He checks his relationship with data by Poona and Trivandrum (India). Tests performed with other localities show large prediction errors.

Sabbagh *et al.* [221] and Sayigh [223] use the Reddy first formula, and Sayigh claims that an "Universal Formula" can be obtained by expressing the α coefficient as a function of the latitude given by

$$\alpha = 1.7 - 0.458\ \Phi$$

[5] We recall that R in this review indicates the relative humidity

They call ψ_{ij} *relative humidity factor* and give to its first index a different range of variation ($i = 1, 2, 3$ for $[DR] < 60\%$, $60\% < [DR] < 70\%$, $70\% < [DR]$ respectively).

Barbaro *et al.* [25], analyzing 13 years of daily data for 31 Italian stations, modify Sivkov's regression as

$$[DG] \;=\; K\,[DS]^{1.24}\,h_n^{-0.19} \;+\; 10550\,(sin\;h_n)^{2.1} \;+\; 300\,(sin\;h_n)^3$$

where $K = 8, 9.5, 11$ for three climatically homogeneous Italian zones. They claim a prediction error not greater than 10%.

Almanza and López [7] assert that the use of A-regressions or P-regressions is inappropriate to coherently map solar irradiation for a region such as Mexico, due to its topographycally induced abrupt changes of climate even among geographically closed sites. Thus they chose to apply the Reddy's formula [211] to data for 38 locations in Mexico taken over periods ranging from 7 to 30 years and believe that the obtained estimates are precise to within $\pm 10\%$.

Goldberg *et al.* [105] compare their model for estimating DG [104], which is based on physical atmospherical quantities, with the empirical models of Liu and Jordan [163] [164], Reddy [212] and Barbaro *et al* [25].
Results obtained for three latitudes ($30°N$, $40°N$ and $50°N$) and regressions against measured data at two locations are considered. They conclude that, but for Reddy's model (which gives discrepancies increasing with latitude), the tested models can be satisfactorily used to predict weekly or even daily values of DG.
Reddy [214] replies that, in fact, his model also works comparably well, even at the latitudes used by Goldberg, if a simple factor accounting for the daylength variations is introduced, this factor not being needed in the original use of the model for Indian localities.

In the SOLMET derived data base [238] hourly global values are estimated from hourly relative sunshine σ_h and a precipitation indicator p ($p = 0$ or $p = 1$) as

$$HG \;=\; HG_{cs}\,(b_o \;+\; b_1\,\sigma_h \;+\; b_2\,p$$

where the *clear sky* HG_{cs} is calculated in terms of the zenith angle θ as

$$HG_{cs} \;=\; a_o \;+\; a_1\,cos\;\theta \;+\; a_2\,(cos\;\theta)^2 \;+\; a_3\,(cos\;\theta)^3.$$

Tables for the a and c coefficients are presented relative to 26 sites.

Ezekwe and Ezeilo [87] compare, analyzing the data from Nsukka (Nigeria) and taking averages over eight 1.5- month periods (see [85]), five formulae taken from literature to estimate $[DG]$. These are: 1) the customary P-regression; 2)-3)-4) the three formulae given by Swartman and Ogunlade (see [246]); 5) the formula by Sabbagh *et al.* (see [221]). The authors use the first formula of Swartmann multiplied by a factor $\alpha \simeq 0.82$ for days with dusty haze.
For P-regression values $a = 0.276$ and $b = 0.648$ are obtained, being fairly constant throughout the eight considered year periods (variation: $\pm 3\%$). The authors assert that data are found to be consistent with model 2) (overall relative error: $\pm 6\%$) and sometimes with model 1) (overall relative error: $\pm 10\%$). Other models show poor agreement, except for model 5) in November, a period with minimal cloud cover or dusty haze occurrence, confirming the Sabbagh conditions.

Sfeir [229] uses about 10 years of data at two sites in Lebanon to fit a model for $[DG]$ based on the work of Cole [73] and Barbaro *et al.* [24], but using the method due to Hay [118] to correct for multiple reflections. In calculating the atmospheric attenuation for clear sky, the dust content (particles/cc) is estimated from the visibility observations as indicated by McClatchey *et al.* [178].
The obtained estimates show a good agreement with the data, except for $[DG_{cs}]$, this fact being possibly due to the ambiguity in calculating it by estrapolation of a previously fitted P-regression to $[\sigma] \to 1$.

Badescu [16] tests, in conditions of a temperate-continental climate, the model due to Barbaro *et al.* [24] to calculate $[DG]$, $[DD]$ and $[DB]$. He uses monthly averages of $[\sigma]$ (25 years), $[DT]$ (29 years) and $[DR]$ (31 years) measured at Jassy (Romania), and fixes at 0.2 the ground albedo coefficient and at 300 *particles* cm^{-3} the average dust content of the atmosphere.
Results show deviations up to -24.7% of the estimated to the observed values if the albedo effects are ignored and up to -15.3%, with about 75% of cases in the range $\pm 7.5\%$, if the albedo is taken into account.

Ahmad *et al.* [4], already quoted in the previos subsection, try to fit monthly averaged irradiations data relative to a few years for Mosul, Baghdad and Basra (Iraq) vs. relative sunshine and climatological parameters. They use different formulae reported in literature and

obtain (for Baghdad)

$$[DG] \;=\; 9243\,[\sigma]^{-1.928}\,[DR]^{1.316}$$

with average error 14% and maximum error 35%,

$$[DG] \;=\; 8.199\;exp\{0.946\;([\sigma]-[DR])\}$$

with average error 1.2% and maximum error 24% and

$$[DG] \;=\; 3010 \;+\; 10609.5\,[\sigma] \;-\; 5.2887\,[DR]$$

with average error 2.6% and maximum error 46%. Notice that the very different orders of magnitude of the coefficients (units are not univocally reported) are probably due to some misprint.
However, all the three regression have evidently poor and possibly dangerous forcasting performances.

Onyango [192] uses the formula of Sayigh [223] to calculate, from very reliable data recorded during over 20 years in certain meteorological stations in Kenya, the relative humidity factor ψ which appear in that formula as proportional to $[DG]$. He finds that from December to June no dependence of the humidity factor on the index i is evident, and perform a best fit for ψ_{ij}, dependently on $[DR]$, for the other months. He uses his results to estimate $[DG]$ for other 6 sites in Kenya, 3 sites in Tanzania and 1 site in Uganda, obtaining a good agreement with measured data ($\pm 10\%$).

Bamiro [19] uses data relative to 5 years at Ibadan (Nigeria) to compare the merits of different formulae used to estimate $[DG]$ from sunshine and/or other meteorological parameters. He reports results of his analysis for the relationships:

$$[DG] \;=\; a\,[\sigma]^{b}\,[DR]^{c}$$

$$[DG] \;=\; \alpha\,K\;exp\{b\;\Phi\;([\sigma] \;-\; \frac{[DR]^{1/3}}{100} - \frac{1}{T}\}$$

$$[DG] \;=\; K\,(C_0 \;+\; C_1T[\sigma] \;+\; C_2[DR]^{1/2}) \;+\; C_3[DR] \;+\; C_4[DR]T^{1/2} \;+\; C_5[DR][\sigma]$$

The first equation was investigated by Swartman and Ogunlade [246], the second is the equation of Reddy [212], the third is an equation similar to that also proposed by Reddy [212] [211] except for the last term. The authors find that the second equation, with the modification $(\frac{[DR]}{100})^{1/3}$ in place of $\frac{[DR]^{1/3}}{100}$, gives better performances relative to the first. It allows $[DG]$ to be estimated with percentage errors exceeding only in few cases $\pm 10\%$ and with a correlation coefficient $r = 0.91$.

The third equation is tested against the data using a number of different choices relative to the retained terms in the multiple regression. Among various sensible combinations, that obtained fixing $C_3 = 0$ (the other coefficients assume by regression the values $C_0 = 1.15$, $C_1 = 0.08$, $C_2 = -0.15$, $C_4 = 0.04$ and $C_5 = -0.23$) gives the best results ($r = 0.96$ and relative errors rarely $> \pm 7\%$)

Nevertheless, the formula obtained by fixing $C_3 = C_4 = C_5 = 0$ also gives good agreement and requires less variables (it offers a correlation coefficient $r = 0.93$).

Seasonal fits, performed by dividing the year into eight 1.5 month periods, indicates that the third formula with $C_3 = 0$ and the first give comparable good results (r ranges from 0.66 to 0.94).

Finally, the author uses the third formula with $C_3 = 0$ to estimate the monthly average daily diffuse irradiation $[DD]$ from its values when $[\sigma] = 0$.

Khogali *et al.* [143] test the Sivkov relationship [232] [231], as modified by Barbaro *et al.* [25] (see above), to estimate $[DG]$ for Sana'a (Yemen), using a few years of precise measurements. This relationship, originally proposed for latitudes in the range 35^o N to 65^o N, was previously tested by the authors and found to be applicable with a good degree of accuracy to latitudes in the range 4^o N to 19^o N by appropriately adjusting the climatical factor K [142].

They fix to $K = 13$ and find estimates which correspond, with a maximum error of 6%, to the measured data. The same formula, tested with data from a distinct group of 5 localities (from 2 to 5 years of measurements), gives maximum errors of about 12%, with 75% of cases within $\pm 6\%$.

Barra [26] tests, on 28 Italian localities for which a long term of monthly averages of climatological quantities are available, the

Reddy [212] first formula. The author finds that the a factor cannot be considered constant during the year, at least for temperate regions. By best fitting he gets

$$a = 1.15\,(1 + 0.4\,cos\frac{\pi}{6}(j+6))$$

where j is the month number.
Comparison for all months and locations shows that the ratio between calculated and observed values ranges between 0.90 and 1.10. Since the error of the experimental values is evaluated as being no lower than 10%, the obtained degree of accuracy is judged satisfactory.

2.3 Irradiation values vs. other data

When sunshine data are not available one can try to relate irradiation values to other climatological data. The most common observations connected with irradiation are likely to be the cloud cover inspections, usually performed (in oktas or tenths of the sky which result covered by clouds) three or more times during each day. One must take into account that cloud cover observations retain sufficient reliability only if they are done by trained observers, mainly because psycological and perspective errors are likely to arise.

Coherently with the Ångström formula using sunshine data, Savinov [148] proposed the relationship

$$[DG] = [DG_{cs}]\,(1-(1-a)[DC]),$$

which implies the assumption

$$[\sigma] = 1 - [DC].$$

The Ångström-Savinov formula can be transformed to give the two-coefficient regression relationship

$$DG = DG_{cs} - ([DG_{cs}] - [DG_{ov}])\,[DC].$$

Kondratiev [148] suggested substituting the linear relationship with a parabolic one. On the other hand, Albrecht [5] advised using the more general relationship

$$[DG] = [DG_{cls}]\,(a + b\,(1-[DC]),$$

which corresponds to the general linear A-regression (see above).

Haurwitz [44] [43], in his investigations on the relationships between global irradiation and cloudiness performed using 11 years of hourly observations at Blue Hill (Massachussets), presents correlations of global irradiance to solar altitude γ, cloud amounts and cloud densities or cloud types. For cloudless sky irradiance he gives the formula

$$IG_{cs} = 1098 \sin\gamma \exp\{\frac{-0.057}{\sin\gamma}\} \quad [W\ m^{-2}]$$

Black [47], using data from many parts of the world, proposes the quadratic regression

$$\frac{[DG]}{[DE]} = 0.803 - 0.340\,[DC] - 0.458\,[DC]^2 \quad ([DC] \leq 0.8)$$

Lumb [167] correlates hourly values of global irradiation and cloudiness measured during three years aboard two weather ships in the North Atlantic Ocean, and derives regression lines for HG/HE vs. solar altitude for 9 classes of cloudiness defined by different combinations of total cloud cover and amounts of low, middle and high clouds.
He proposes, for cloudless sky relative irradiance, the formula

$$\frac{IG_{cs}}{IE} = 0.61 + 0.20 \sin\gamma$$

where γ is the solar altitude.

Bossolasco et al. [55], analyzing six years of measurements at Genova and M.Capellino (Italy) using the Albrecht correlation, find $a = 0.20$, $b = 1.03$ for Genova and $a = 0.18$, $b = 1.18$ for M.Capellino. From a more detailed analysis, following the method of Lumb, they group all cloudiness data (observed at 8 a.m. and 2 p.m) into seven classes dependig on the cloud type (other classes are scarcely represented in the data):

C	$Cloudtype$
0.1	=

$0.2 - -0.5$	Cu
$0.6 - -0.8$	Cu
$0.9 - -1.0$	Cu
$0.9 - -1.0$	ASt, ACu
$0.2 - -0.5$	$Ci, CiSt$
$0.6 - -1.0$	$Ci, CiSt$

and associate to each C-measurement both the value of HG relative to the previous hour and the average $sin\ \gamma$. They plot HG vs. $sin\ \gamma$ distinguishing between the various classes and find a linear relationship for classes 1, 2 and 6 and a non linear dependence for the other classes (see Fig. 2.17).

They also study the behaviour of HD (values between 1 p.m. and 3 p.m.), normalizing the measured values with the values of HD_{cs}, determined by enveloping the minima during the year of the measured HD_{cs} values. The authors plot HD/HD_{cs} vs. C for *high clouds* (Ci, CiSt, AlSt, AlCu) and *low clouds* (Cu, StCu, CuNe, Ne), finding very different trends (see Fig. 2.18)

Norris [186] reviews attempts to divide cloud reports into classes of trasmissivity for prediction use. He calculates linear regressions between global radiation measurements and total cloud cover using three hourly synoptic observations during one year at Melbourne (Australia). He concludes that the correlation of cloudiness with irradiation has poor prediction performance.

Lund [168] correlates 9 years of daily global radiation with measurements of temperature, snow cover, wind, sunshine, cloudiness, pressure and precipitation at Blue Hill, Massachussets. He finds that DS is the best specifier of DG, followed by DC.

Bennet [37] claims the usefulness of opaque sky cover as an important correlate of irradiation values.

Fitzpartick and Nix [89] linearly relate $[DG]/[DE]$ to $[DR]$ using data from 11 Australian stations, finding a significant correlation coefficient $r = -0.81$ when $[DR] \geq 45\%$. They use this relationship to estimate monthly mean of daily global solar irradiation for 277 Australian stations.

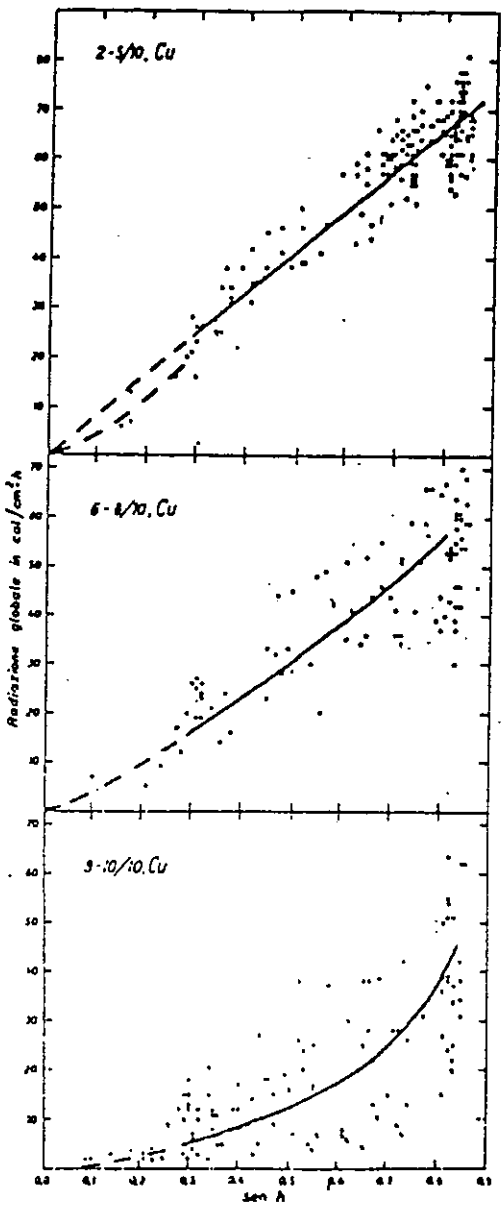

Figure 2.17: HG vs. $sin\ \gamma$ for various cloud types. From Bossolasco (65).

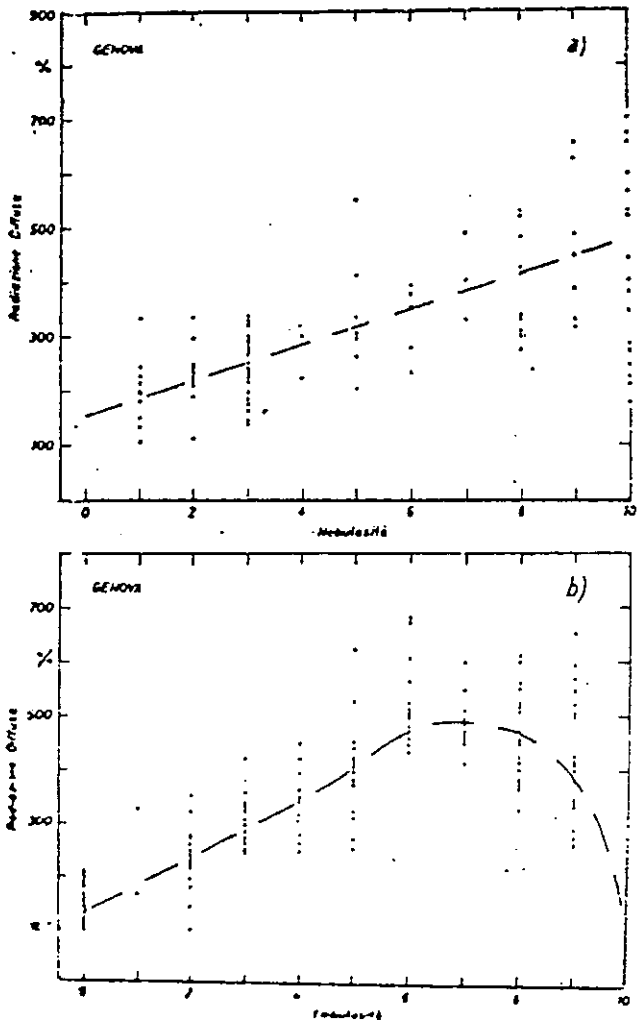

Figure 2.18: HD vs HC for two cloud types. From Bossolasco (65).

Parker [198] extends the work of Lumb to observations taken during 2 years at the island of Gan (equatorial Indian Ocean), introducing a set of 12 classes of sky cover conditions appropriate to tropical climates. He adds three linear terms to the linear regression considered by Lumb in the amount of low, middle and high clouds respectively, as proposed by Gadd and Keers [94].

Daneshyar [75] estimates $[DG]$ both by the formula due to Reddy [212] and as sum of $[DB]$ and $[DD]$, calculated using a method due to Paltridge [197] [196]. He takes in the latter case

$$[DB] \;=\; (1 - [DC]) \sum HB(\theta)\; cos(\theta)$$

where the sum is calculated over all hourly zenith angles θ during the day, and

$$HB(\theta) \;=\; 81.738\; (1 - exp\{-0.075\; (\frac{\pi}{2} - \theta)\} \quad [cal/cm^2\; hr]$$

The values of HD are assumed to be linear in the zenith angle and the cloud cover:

$$HD(\theta) \;=\; 0.123 \;+\; 0.181\; (\frac{\pi}{2} - \theta) \;+\; 10.43\; HC$$

and the daily value is obtained by summation:

$$[DD] \;=\; \sum HD(\theta).$$

The calculation is performed for the 15th of each month (daily sum terms refer 1/4 hourly values) whereas the needed $[DC]$ values are monthly averages obtained using 10 years of data.
Comparisons between experimental data and values of $[DG]$ obtained by both methods are performed for Teheran (four years of measurements) and Karag (one year). See Fig.2.19.
An average prediction error of about 2.0% is obtained with the second method of estimation, which is then used to predict monthly $[DG]$ values for 34 chosen localities of Iran.

In the SOLMET derived data base [238] hourly global values are estimated, if hourly sunshine is not available, from opaque cloud amount HC and a precipitation indicator p ($p = 0$ or $p = 1$) as

$$HG \;=\; HG_{cs}\; (c_o \;+\; c_1\; HC \;+\; c_2\; HC^2 \;+\; c_3\; HC^3 \;+\; c_4\; p)$$

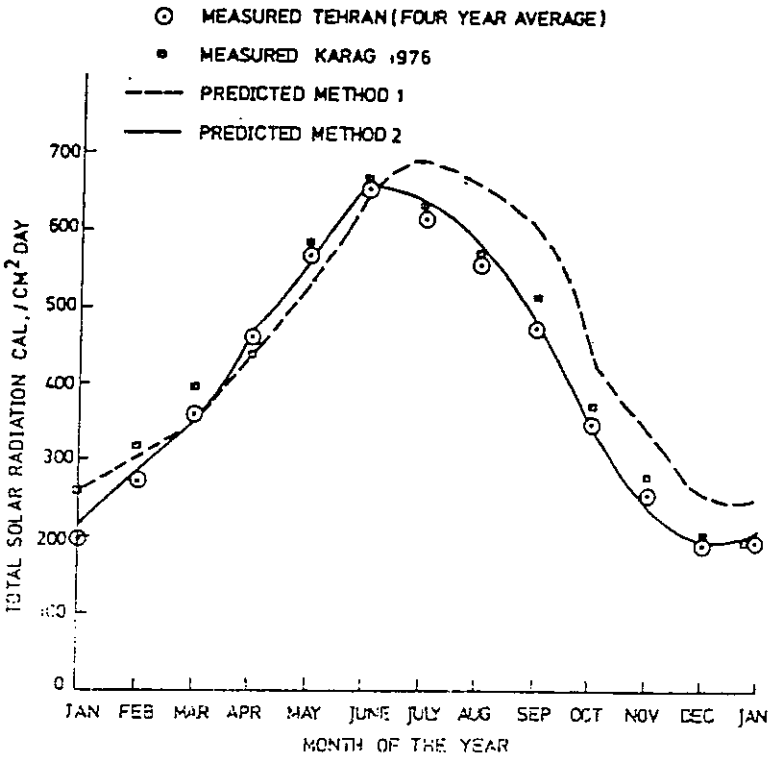

Figure 2.19: Comparison between observed and calculated (two methods) [DG] values. From Daneshyar (78).

where the *clear sky* HG_{cs} is calculated in terms of the zenith angle θ as

$$HG_{cs} = a_o + a_1 \cos\theta + a_2 (\cos\theta)^2 + a_3 (\cos\theta)^3.$$

Tables for the a and c coefficients are presented relative to 26 sites. Coefficients $a_o - a_3$ have in general different values for the morning and the afternoon, and a_o also changes with the month.

Mejon *et al.* [179] use 9 years of observation at Carpentras (France) to fit the individual daily values

$$\frac{DG}{DE} = a (DC)^2 + b\, DC + c$$

where DC is evaluated (in oktas) as the average of the observed cloudiness at four time during each day. The authors find for the various months determination coefficients which vary from $r^2 = 0.77$ to $r^2 = 0.87$ (see Fig. 2.20).

They also relate the daily beam irradiation to the cloudiness:

$$\frac{DB}{DE} = a\, DC + b$$

using 6 years of daily values at Carpentras, and performing the fit month by month. The correlation coefficients oscillate in the range $[0.85, 0.91]$, that is to say the accounted variances are in the range $[72\%, 82\%]$. The scatter cloud is nevertheless too wide, the standard deviations of the residuals varying between 0.06 and 0.10 depending on the month.

Modi and Sukhatme [15] analyze and correlate $[DG]/[DE]$ with other weather data for 18 Indian localities, using about 10 years of irradiation measurements and 30 years of weather data monthly averages. They choose as independent variables: sunshine hours , percent sunshine , all cloud cover, low cloud cover, pressure, average of maximum and minimum temperature, relative humidity, vapor pressure, wind speed, precipitation. The authors conclude that citywise regression analysis indicate $[\sigma]$ as the best predictor for $[DG]$.
Monthwise analysis for two groups of stations indicates all cloud $[DC]$ and $[\sigma]$ as the best possible predictors(see Fig. 2.21).

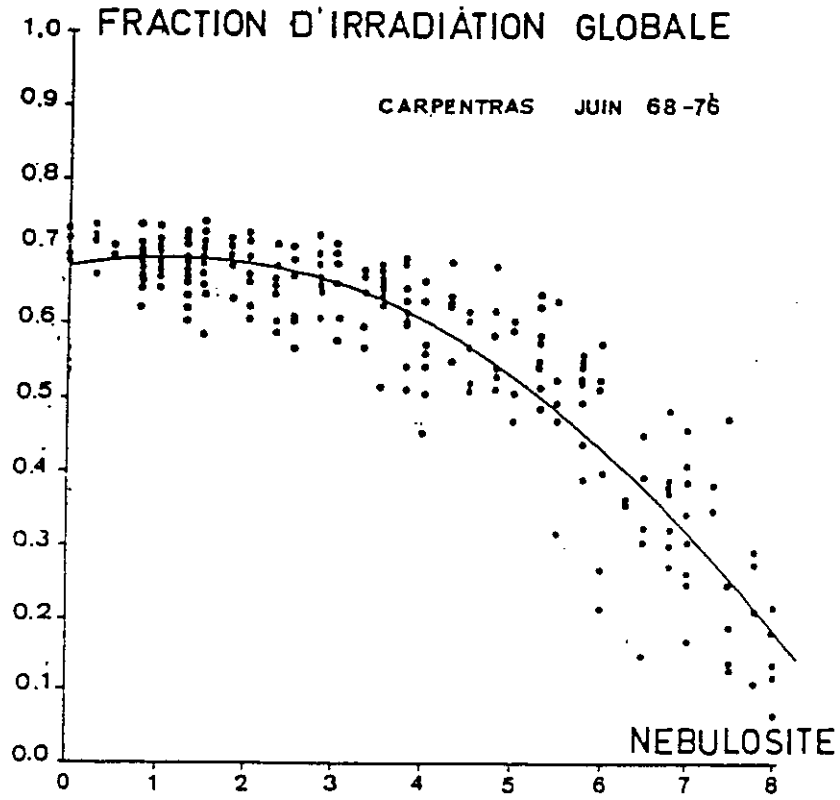

Figure 2.20: Scatter diagram for DG/DE vs. DC. From Mejon *et al.*(65).

	% possible sunshine				Sunshine hours				All clouds				Precipitation			
	100A	100B	$100r^2$	$\bar{s}$	100A	100B	$100r^2$	$\bar{s}$	100A	-100B	$100r^2$	$\bar{s}$	100A	-100B	$100r^2$	$\bar{s}$
Ahmedabad	28	480	94	3.0	26	45	91	3.7	76	45	96	2.0	70	15	94	1.0
Bangalore	18	640	95	3.9	16	57	94	4.4	86	59	91	5.0	69	15	95	5.4
Bhavnagar	28	470	96	2.8	28	41	88	5.3	78	49	88	5.1	71	20	96	3.7
Calcutta	28	420	99	1.3	24	41	97	1.8	68	36	93	3.1	63	09	99	3.7
Goa	30	480	98	2.1	28	43	96	2.9	84	59	87	5.6	69	10	98	3.5
Jodhpur	33	460	92	2.0	25	48	78	3.8	80	47	79	2.7	74	21	92	2.0
Kodaikanal	32	550	95	2.9	31	47	93	3.1	90	67	89	4.6	75	14	95	4.1
Madras	30	440	87	3.5	27	40	94	2.6	78	42	84	3.9	66	11	87	3.8
Mangalore	27	430	94	4.2	25	39	95	4.0	78	49	83	7.4	65	09	94	5.7
Minicoy	26	390	96	1.4	25	39	95	2.0	75	48	91	2.7	60	08	96	2.9
Nagpur	27	500	98	1.6	24	46	96	2.7	79	48	92	4.4	70	12	98	3.0
New Delhi	25	570	93	3.0	15	60	82	4.8	77	52	84	4.2	71	17	93	2.4
Poona	31	430	98	1.9	29	39	99	1.2	76	44	94	3.6	70	11	98	2.3
Shillong	22	570	98	3.0	18	53	91	5.2	83	64	83	6.5	65	10	98	7.5
Srinagar	35	400	81	4.7	39	26	82	4.7	70	37	44	8.3	57	22	81	10
Trivandrum	37	390	89	2.5	35	35	88	2.6	77	22	94	2.1	66	07	89	2.8
Vishakha-patnam	28	470	98	1.2	26	42	93	2.6	80	48	93	3.4	68	14	98	6.0
Average				2.6				3.4				4.6				4.1

	Percent possible sunshine			Precipitation			All clouds		
	$a \times 10^3$	$b \times 10^3$	$\bar{s}$	$a \times 10^3$	$-b \times 10^4$	$\bar{s}$	$a \times 10^3$	$-b \times 10^4$	$\bar{s}$
J	608	246	4.2	640	71	4.1	638	38	3.8
F	487	202	4.7	699	27	4.9	734	303	4.7
M	364	364	3.5	669	147	3.0	729	357	3.5
A	462	177	3.0	634	66	2.7	641	98	3.4
M	555	42	4.3	627	58	3.6	805	455	3.7
J	293	442	6.3	536	41	8.1	993	797	8.7
J	209	640	7.0	573	79	10.8	1234	1174	7.1
A	416	117	8.8	453	00	9.4	676	328	9.2
S	424	126	11.0	537	36	11.2	977	820	8.0
O	522	00	3.5	522	00	3.0	549	50	3.8
N	390	290	6.0	596	56	7.4	669	311	4.9
D	451	194	3.8	634	124	3.3	681	264	3.9
Average			5.5			6.0			5.4
J	490	239	2.0	709	147	1.4	730	200	2.0
F	567	165	0.8	717	61	0.7	730	113	0.9
M	608	119	2.3	711	98	1.9	743	241	1.8
A	561	152	2.1	597	103	1.8	729	199	1.5
M	469	263	1.6	704	135	1.3	711	172	1.4
J	352	385	2.3	641	59	1.5	702	301	4.1
J	267	532	3.7	567	69	4.0	745	481	7.2
A	171	519	3.3	491	19	8.0	826	583	4.1
S	354	387	3.7	663	82	2.8	729	333	3.2
O	289	479	1.3	711	98	1.0	725	191	2.5
N	279	487	2.2	724	224	1.6	742	283	2.0
D	442	287	2.0	693	277	2.1	690	68	2.3
Average			2.3			2.3			2.8

Figure 2.21: Coefficients for linear regressions of $[DG]/[DE]$ vs. various climatological quantities: fixed station (above) and two fixed month cases (below). From Modi and Sukhatme (79).

Notaridou and Lalas [188], while studying the distribution of global and net irradiation over Greece, calculate the monthly average daily global irradiation as

$$[DG] = [DG_{cs}] (1 - a [DC] - b [DC]^2)$$

where $[DG_{cs}]$ is calculated using physical atmospherical quantities. They notice that, but for months from June to September, the calculated values are lower than the observed, and attribute this discrepancy to overestimation of the cloudiness by ground based observers when clouds are mainly of convective nature (see next section).

Scerri [225] computes, using 24 years of irradiations and cloud cover measurements at Malta, the three correlations

$$\frac{[DD]}{[DE]} = 0.156 + 0.171 [DC] \qquad (r = 0.99)$$

$$\frac{[DG]}{[DE]} = 0.769 - 0.360 [DC] \qquad (r = 0.88)$$

$$\frac{[DD]}{[DG]} = 0.178 + 0.469 [DC] \qquad (r = 0.95)$$

The last relationship is in agreement with that given by Liu and Jordan [163]. Similar results were also found by Choudbury [71] in New Dehli (India) and by Mani and Chacko [174] in Poona(India).

Mani *et al.* [175] use the Ångström-Savinov formula to carry out an extensive study of the global irradiation over the Indian Ocean and its adjoining continents.

Kasten and Czeplak [138] perform a very extensive study on the dependence of solar irradiation on the amount (in oktas)and type of clouds using 10 years of continuously recorded hourly measurements at Hamburg (Germany). They subdivide the data into four seasonal groups and within each group into classes of equal mean hourly solar altitude γ by intervals $\Delta\gamma = 10°$. Only hourly values such that the reported cloud amount for the concerned hour is identical to that of the previous hour are examined (this condition is fulfilled by more than 25000 observations). The hourly irradiations are converted to mean hourly irradiances.

For both global and diffuse irradiance no relevant seasonal differences are noticed in their dependence on cloud cover C and solar altitude γ, so that yearly average results and graphs can be considered.
For the global irradiance (see Fig.2.22) a mathematical fit gives

$$\frac{\overline{IG}}{\overline{IG_{cs}}} = 1 - 0.75\, C^{3.4}$$

where the *clear sky* irradiance can be parametrized by

$$\overline{IG_{cs}} = 910\ sin\gamma - 30 \quad [W\ m^{-2}].$$

For the diffuse irradiance a more complex trend comes out, because of the well-known effect due to the reflection from side-walls of the clouds, which is relevant mainly in correspondence to intermediate cloud cover. For $\gamma > 20^o$ a rather good approximation for the diffuse fraction is found to be

$$\frac{\overline{ID}}{\overline{IG}} = 0.3 + 0.7\, C^2$$

The influence of the cloud type is studied by grouping all hourly data corresponding to completely overcast sky into the five classes: Cirrus=Ci,Cc,Cs; Altus=Ac,As; Cumulus=Sc,Cu; Stratus=St and Nimbostratus=Ns. As in the foregoing analysis, data are subdivided depending on the season and solar altitude, and only hours are considered with cloud cover type identical to that observed in the previous one. The fulfilled cases are about 4700, with Ci and Ni cases poorly represented.
As before, no relevant seasonal differences are noticed. Some of the yearly graphs are reported in Fig.2.22.

Garg and Garg [96] show, using data from 14 stations in India, that the empirical relation holds

$$\frac{[DG]}{[DE]} = 0.414 + 0.400\,[\sigma] - 0.0055\,[W_{at}]$$

where W_{at} is the water vapour content per unit volume (g/m^3).

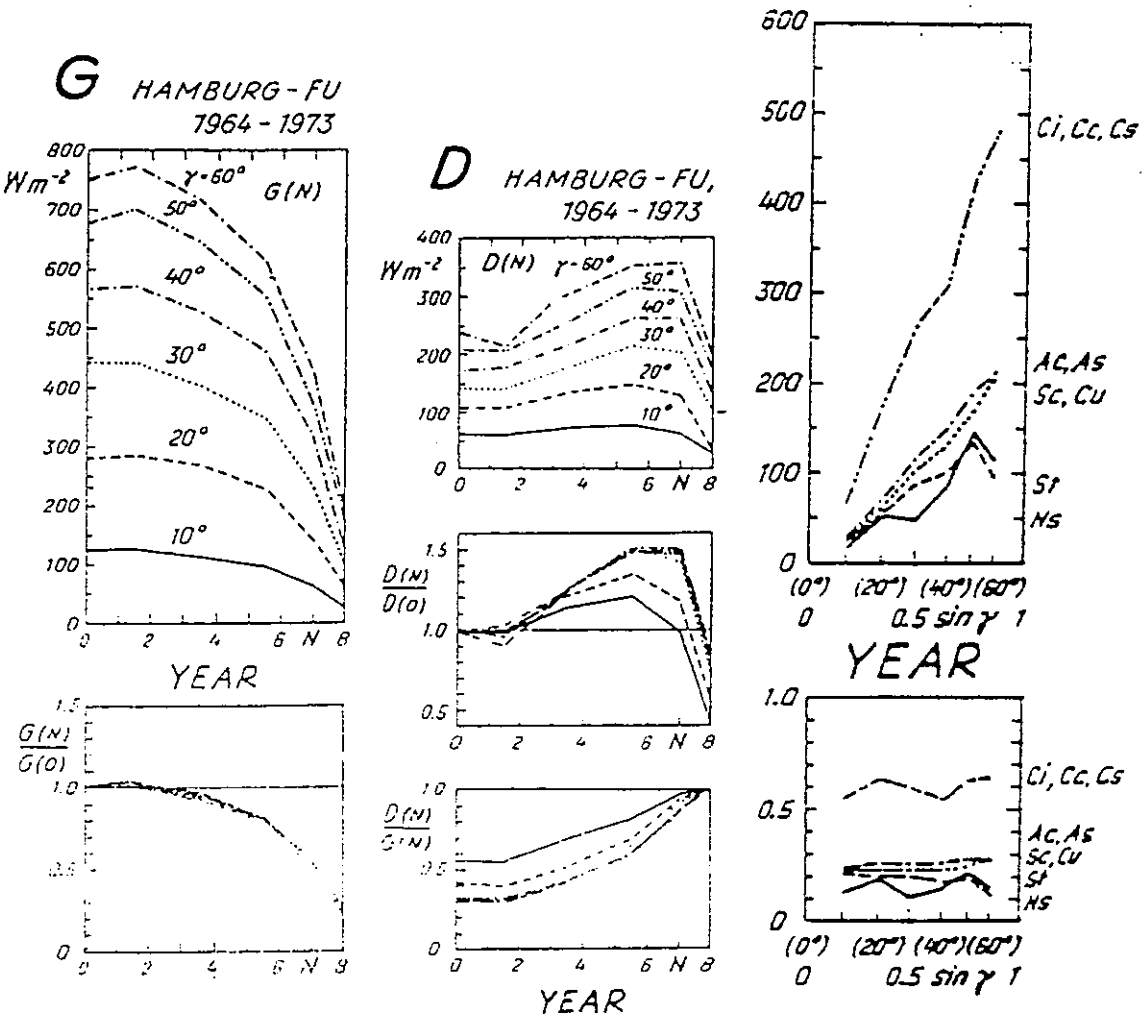

Figure 2.22: Relative solar global and diffuse irradiances vs. cloud cover and global vs. *sin* γ for different types of clouds. From Kasten and Czeplak (80).

Hussain [126], studying data of seven locations in North and Central India covering a period of about 20 years, finds similar correlations:

$$\frac{[DG]}{[DE]} = 0.394 + 0.364\,[\sigma] - 0.0035\,[W_{at}] \quad (r = 0.94)$$

$$\frac{[DD]}{[DE]} = 0.306 - 0.165\,[\sigma] - 0.0025\,[W_{at}] \quad (r = 0.85)$$

In order to perform the two fits he calculates the atmospheric vapour content (g/m^3) from the relative humidity and the temperature (Celsius degrees) by

$$[W_{at}] = [DR]\,(4.7923 + 0.3647\,[T] + 0.0055\,[T]^2 + 0.0003\,[T]^3$$

Comparison with measured values at Madras (South India) show a satisfactory agreement.

Reddy *et al.* [216] and Reddy [215] suggest and use the empirical simple model

$$[DG] = a + b\,\Phi + c\,[DP]^{1/3}$$

to deduce $[DG]$ from the latitude Φ (in degrees) and the mean monthly precipitation $[DP]$. Reddy [215] calculates the regression coefficients using data from 15 locations in Brazil and independent data from 23 location for testing purposes. He notices that percent deviations $\leq 5\%$ are more than 50% and percent deviations $\leq 10\%$ are more than 80% off all occasions. Moreover, the majority of $\geq 10\%$ deviations are relative to 2 sites, probably due to instrument calibration errors. He concludes that, almost for the examined region (northeast Brazil) the model could be reasonably used.

2.4 Sunshine vs. other climatological data

The most obviously quantity related to relative sunshine is the cloud cover.

Bennet [39] suggests as satisfactory a statistical linear relationship between $[\sigma]$ and $[DC]$ of the kind[6]

[6]The quantity $1 - \sigma$ is sometimes called *cloud shade*.

$$[DC] = 1 - [\sigma].$$

Mani *et al.* [175], assume as more reliable the relationship

$$[DC] = 1 - [\sigma'].$$

where σ' is the relative sunshine corrected as suggested by Hay [118] (see above).

Malberg [173] finds the linear relationship

$$[DC] - [1 - \sigma] = 0.240 - 0.0018\ L$$

holds for latitudes L between $30°N$ and $70°N$.

Reddy [213] studies the interdependence between $1 - [\sigma]$ and $[DC]$ for Indian latitudes and finds that they are best related by the equations

$$1 - [\sigma] = [DC]\ exp\{-0.25\ \sqrt{[DC]}\} - 0.02 - 0.08cos\ 4L$$

for latitudes $L \leq 45°$ and

$$1 - [\sigma] = [DC]\ exp\{-0.25\ \sqrt{[DC]}\} + 0.06$$

for $L \geq 45°$.

Exell [85] considers average relative monthly sunshine (measurements from 1950 to 1968) and cloudiness (measurements from 1951 to 1970) at about 20 stations in Thailand and does not find the linear relationship suggested by Bennet. Nevertheless he notices that, when individual scatter diagrams for each station are made, irregular regression patterns emerge which are similar for stations geographically close to each other. Thus he estimates relative sunshine from cloudiness at stations without sunshine recorders from the regression patterns at eventually existing nearby stations, and claims that the accuracy is better than 0.5 $hr\ day^{-1}$.

Hoyt [125] shows that, when using long term averages, sunshine data give an estimate of cloud cover more reliable, if compared with satellite and aircraft observations, than the C-values reported by a

ground-based observer. He finds, analyzing measurements at 72 stations in USA, that ground observations of cloud cover tend to overestimate the cloud amount, mainly because of projection problems and perspective errors.
Moreover a latitude dependence of the difference $[DC] - [1 - \sigma]$ is suggested for latitudes L between $20°N$ and $50°N$ as

$$[DC] - [1 - \sigma] \;=\; (0.176 \pm 0.016) \;-\; (0.0009 \pm 0.0003)\; L$$

Berger [41] claims that, at first approximation, the statistical relation holds

$$\sigma \;=\; 1.15 \;-\; DC$$

with an error of about 10%.

Barbaro *et al.* [21] correlate the monthly mean relative sunshine $[\sigma]$ to the "monthly mean state of the sky", determined by the numbers n_1, n_2, n_3 of the clear, mixed and overcast days in every month of the year deduced from several years. The qualifiers *clear*, *mixed* and *overcast* are related to different cloud cover fractions depending on their evaluation in oktas or tenths. The negative influence of the fog is accounted by a "fog factor" and the particular atmospheric conditions typical of each locality are accounted by a factor $K < 1$.
The suggested formula reads

$$[\sigma] \;=\; K\,(1 - \alpha\,\frac{\nu}{n})\,\frac{a\,n_1 \;+\; b\,n_2 \;+\; c\,n_3}{n}$$

where $n = n_1 + n_2 + n_3$. They apply this formula to data from 31 Italian stations relative to 5 years of measurements. The fog factor α is taken as $1/3$ for the period November-January and $1/6$ otherwise. The coefficients a, b, c are computed by minimizing the overall relative deviation between calculated and observed values. Sites with the same values of these regression coefficients are grouped into seven helioclimatic groups so that intermonthly comparisons can be performed within each group. Yearly results for the seven groups are reported in Fig. 2.23.

Raju and Kumar [205] suggest the linear relationship

$$[DC] - [1 - \sigma] \;=\; 0.25774 \;-\; 0.0008\; L$$

GROUP	a	b	c	K	
				Nov	Dec-Jan
I	0.9	0.6	0.2	1.0	1.0
II	0.9	0.6	0.2	1.0	0.9
III	0.9	0.6	0.2	0.9	0.8
IV	0.8	0.6	0.2	0.9	0.8
V	0.8	0.5	0.2	0.9	0.8
VI	0.8	0.5	0.1	1.0	1.0
VII	0.8	0.5	0.1	0.9	0.8

Figure 2.23: Regression coefficients for $[\sigma]$ vs. *status of the sky*. From Barbaro *et al.* (81b)

for latitudes between $8°N$ and $36°N$. for the dependence of $[DC] - [1 - \sigma]$ on the latitude L.

Rangarajan *et al.* [206] analyze the relationship between sunshine duration and cloud cover using data from 20 stations in India with 10 years of reliable observations of both quantities. They test the validity of the Mani *et al.* equation [175]

$$[DC] = 1 - [\sigma']$$

(monthly averages). They notice that the empirical r.h.s. quantity is almost sistematically lower than [DC], thus confirming Hoyt's remarks [125], with maximum differences when $0.4 < [DC] < 0.7$ (see Fig.2.24. The authors attribute this result to the fact that, mainly during *mixed* days, clouds with vertical extents appear to fill a greater fraction of the sky when located near the horizon than when they are overhead.

They fit the data with a cubic polynomial, and find, grouping the station into two distinct latitude classes,

$$1 - [\sigma'] = 0.22\,[DC] + 0.55\,[DC]^2 + 0.10\,[DC]^3 \quad (8°N - 20°N)$$

and

$$1 - [\sigma'] = 0.45\,[DC] + 0.30\,[DC]^2 + 0.15\,[DC]^3 \quad (20°N - 36°N)$$

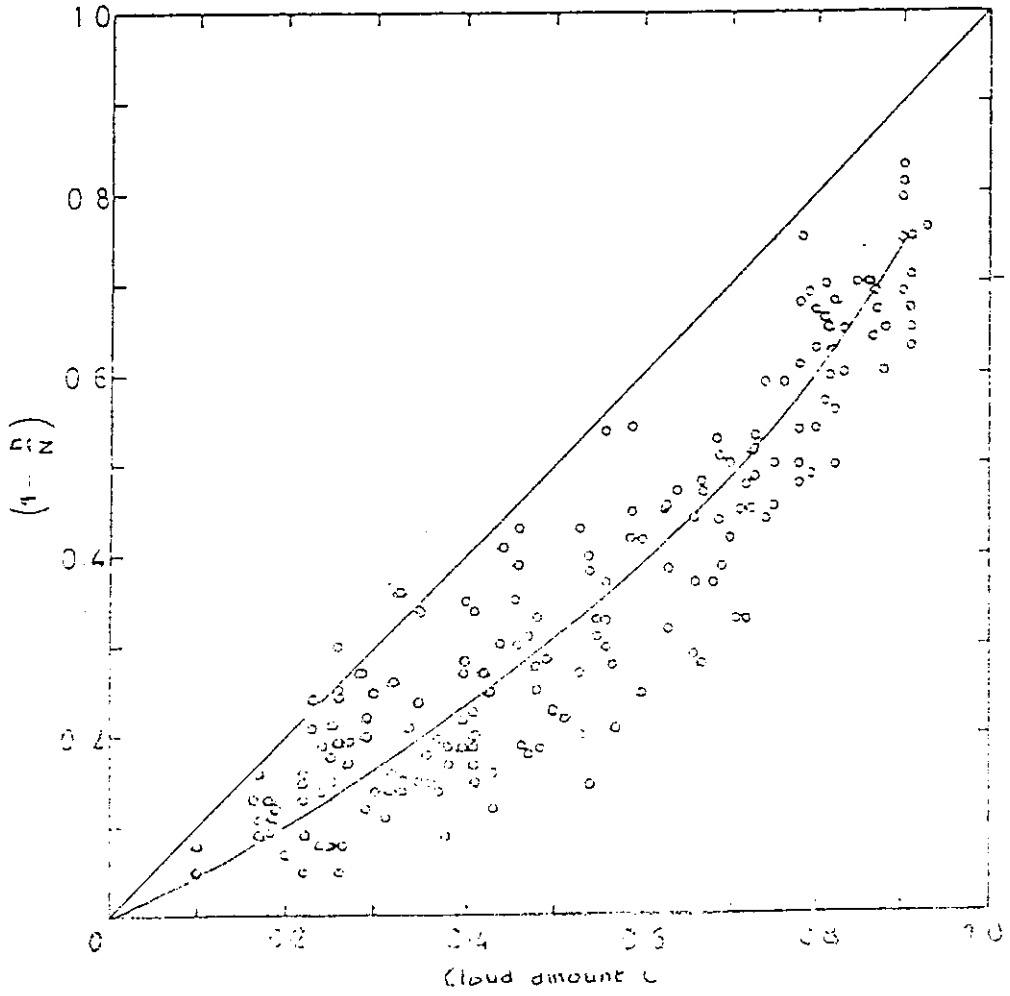

Figure 2.24: Relationship between $1 - [\sigma']$ and $[DC]$. From Rangarajan (84).

Harrison and Coombes [116] investigate the relationship of the observed cloud cover C with the corresponding ***cloud shade*** using as data base the hourly values measured at 43 Canadian weather stations for a period of more than 10 years. Only sunshine measurements corresponding to a solar altitude $\geq 5^{o}$ are analyzed. The hourly values are averaged over each day and each month resulting in about 500 experimental pairs. They fit the data with the quadratic relationship

$$1 - [\sigma] \;=\; l\,[HC] \;+\; m\,[HC]^2$$

obtaining $l = 0.159$ and $m = 0.837$ (see Fig.2.25).

A linear fit of $[HC] - (1 - [\sigma])$ to the latitude L (degrees) gives

$$[HC] - (1 - [\sigma]) \;=\; (0.305 \pm 0.028) \;-\; (0.0024 \pm 0.0005)\; L,$$

thus confirming data in literature about the decrease of this "discrepancy" with increasing latitude.

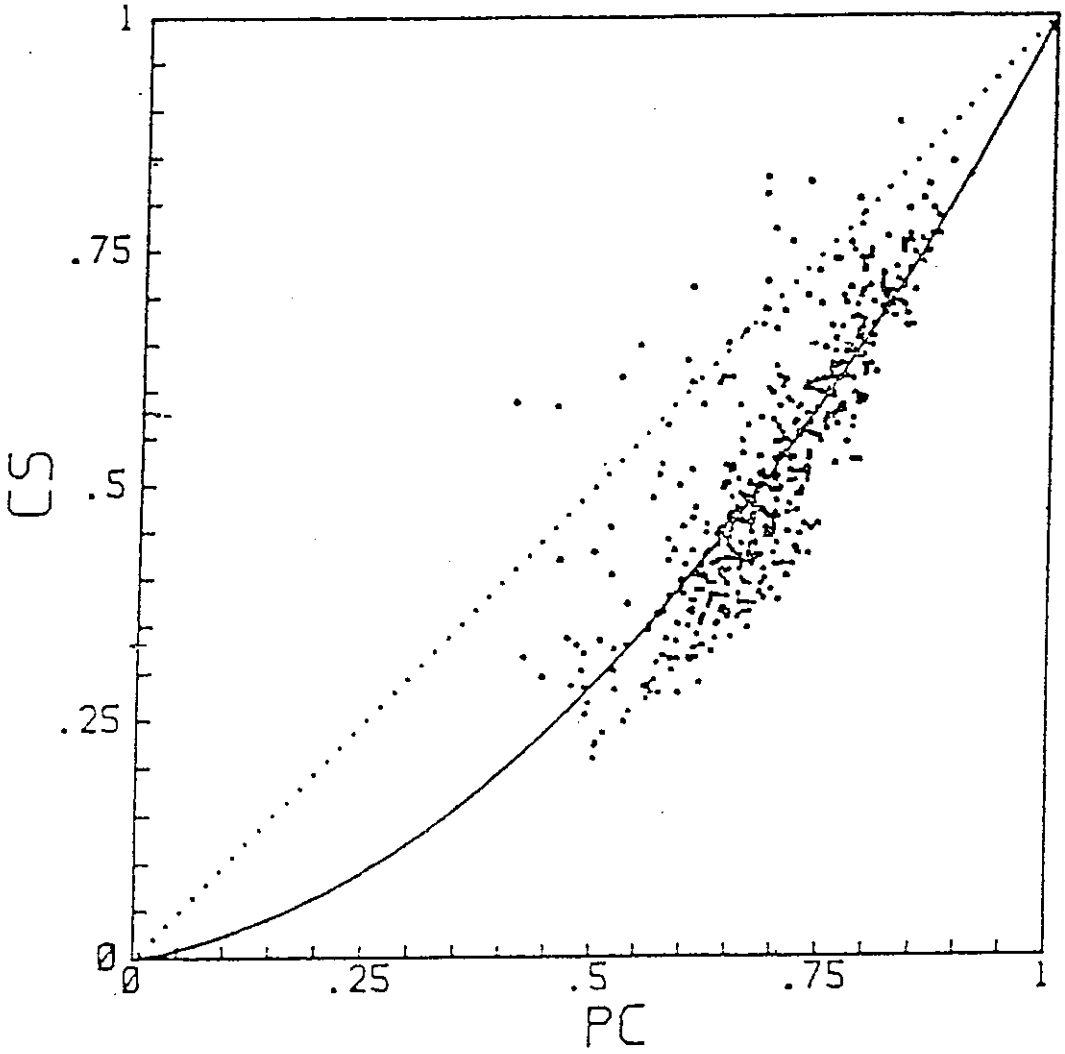

Figure 2.25: Scatter diagram and quadratic fit for $[1-\sigma]$ vs. $[HC]$. From Harrison and Coombes (86).

Chapter 3

SOLAR TIME SERIES MODELLING

3.1 Generalities about stochastic sequences

As already stated in the Introduction, the solar climate of a given locality is described by a family of stochastically periodic processes (essentially IB(t) and ID(t)). These processes are not necessarily defined only in terms of their periodic first order distribution (in these case they would be *purely random processes*). In general, knowledge about higher order distributions, i.e. joint distributions of the concerned quantities at two or more distinct times, is needed.

In order to unify the reading of the various approaches suited by different researchers to study this topics, let us briefly recall a few concepts and nomenclature, without any pretence of rigour or completeness.

3.1.1 Stochastic sequences

A *stochastic process* is an infinite family of random variables $\{x(t), t \in \Re\}$, where the range $\Re$ of the "time" label can be continuous or countable. In the latter case one can identify $\Re$ with the set of the integers and speak of *stocastic sequence* $\{x_i\}$. Since both for practical and theoretical reasons climatology deals with time series (i. e. realization of stochastic sequences), we will limit ourselves to

stochastic sequences discussion.

A stochastic sequence $\{x_i\}$ (s.s.) is completely determined if one knows all the joint cff's

$$F(x_n, x_{n+1}, \ldots, x_{n+j}) = Prob\{X_n < x_n, X_{n+1} < x_{n+1}, \ldots, X_{n+j} < x_{n+j}\}$$

for every integer $n \in \Re$ and every j=0,1,2..... Here and in the following we use the symbol F with a colloquial meaning in order to avoid the rigorous but somewhat cumbersome notation

$$F_{X_n, X_{n+1}, \ldots, X_{n+j}}(x_n, x_{n+1}, \ldots, x_{n+j})$$

which distinguishes among different *numbers* of concerned random variables $(X_n, X_{n+1}, \ldots, X_{n+j})$ and therefore different *functions* "F".

The "dependence" of the distribution of X_n on the past sequence history is described by the *conditional* cff's

$$\Phi(x_n | x_{n-1}, x_{n-2}, \ldots, x_{n-j}) = \frac{F(x_{n-j}, \ldots, x_{n-2}, x_{n-1}, x_n)}{F(x_{n-j}, \ldots, x_{n-2}, x_{n-1})}$$

These conditional distributions are the direct tools to classify a s.s. in terms of Markov order, in the following way:

$$\Phi(x_n | x_{n-1}, n_{n-2}, \ldots) = F(x_n) \qquad \Rightarrow Markov\ order\ zero$$

$$\Phi(x_n | x_{n-1}, n_{n-2}, \ldots) = \Phi(x_n | x_{n-1}) \qquad \Rightarrow Markov\ order\ one$$

$$\Phi(x_n | x_{n-1}, n_{n-2}, \ldots) = \Phi(x_n | x_{n-1}, x_{n-2}) \qquad \Rightarrow Markov\ order\ two$$

and so on.

In other words, given some information on the past history of a s.s., its Markov order indicates the number of the more recent distinct past values, which the future probabilistic evolution depends on. Thus, a zeroth order s.s. (purely random s.s.) does not "remember " its past, a first order (properly Markov s.s.) "remembers" only its more recent known value, a second order its more recently known pair of values, and so on.

For a first order s.s. the functions $\Phi(x_n | x_{n-1})$ and $F(x_n)$ (or alternatively the unique cff $F(x_{n-1}, x_n)$) suffice to describe its probabilistic structure.

An important possible property of a s.s. is *stationarity*, which means invariance of all joint cff's by change of the time origin:

$$F(x_n, x_{n+1}, \ldots, x_{n+j} = F(x_{n+m}, x_{n+m+1}, \ldots, x_{n+m+j}) \quad (\forall m) \quad (\forall j)$$

In practical investigation one is often led to be satisfied with inspections about a *second order* or *wide sense* stationarity

$$F(x_n, x_{n+1}) = F(x_{n+m}, x_{n+m+1}) \quad (\forall m)$$

which implies

$$F(x_n) = F(x_{n+m})$$

and

$$\Phi(x_{n+1}|x_n) = \Phi(x_{n+m+1}|x_{n+m})$$

Finally, we recall the concept of *ergodicity* of a stationary s.s., i.e. the property that any single *realization* of the process shows almost surely (i.e. with probability equal to 1) distributions of any order of the taken values which coincide with the respective process distributions of the same order. Thus, by analyzing a single realization of an ergodic s.s. one gets (almost surely) full information about the process.

3.1.2 Stochastic chains

If a s.s. $\{x_n\}$ can only take a *countable* (finite or infinite) set of values, one speaks of *stochastic chain* (s.c.). In practical climatological research one often divides the range of variability of a given stochastic quantity into a number of intervals and categorizes it depending on the interval to which it belongs. For example, the relative daily sunshine DS/So is often categorized as 0.05, 0.15, 0.25, ..., 0.95 if it belongs to [0.0, 0.1], [0.1, 0.2], and so on. Thus stochastic chains are frequently met in empirical works.

An important class of s.c. is that of homogeneous Markov s.c.'s, which are characterized by constant one step conditional probabilities. If one indicates with integer numbers i, j, k,... the discrete set of values a s.c. can take, this means that

$$P_{i,j} = Prob\ \{x_{n+1} = j \mid x_n = i\}$$

does not depend on the "time" n.

The square matrix $||P_{ij}||$ is called the "transition matrix" of the chain. One easily sees that, if

$$p_i(n) = Prob\ \{x_n = i\}$$

then

$$p_j(n+1) = \sum_j p_i(n)\ P_{ij}$$

or symbolically

$$\overline{p}(n+1) = \overline{p}(n)\overline{\overline{P}}$$

where $\overline{p}$ represent the row vector having as elements the probabilities of the various distinct allowable values, and the symbol $\overline{p}\overline{\overline{P}}$ represent the customary row by column product of a vector with a matrix. In general

$$\overline{p}(n+k) = \overline{p}(n)\overline{\overline{P}}^k$$

An homogeneous Markov s.c. is not necessarily stationary. For example, if

$$\overline{\overline{P}} = \begin{pmatrix} 0 & 1 \\ 1 & 0 \end{pmatrix}$$

and

$$\overline{p}(n) = (a, b) \qquad (a + b = 1)$$

then

$$\overline{p}(n+1) = (b, a)$$

so that the probabilities of the two concerned states are indefinitely exchanged (notice that $\overline{p} = (0.5, 0.5)$ is left unchanged).

It may happen that

$$\lim_{k\to\infty} \overline{p}\ \overline{\overline{P}}^k = \overline{q}$$

for *every* initial probability vector $\overline{p}$. In this case the chain is called *ergodic* and the asymptotic transition matrix

$$\overline{\overline{Q}} = \lim_{k\to\infty} \overline{\overline{P}}^k$$

exists and is such that its lines are equal one to the other, and each of them to the stationary probability vector $\overline{q}$.

It is obvious that, if

$$\overline{q} = \overline{q}\overline{\overline{P}}$$

and $lim\ \overline{\overline{P}}^k$ exists, then the chain is ergodic. An ergodic chain is asymptotically stationary, since it is Markovian and

$$Prob\{x_n = i, x_{n+1} = j\} = p_i(n)\ P_{ij} \rightarrow q_i P_{ij}$$

and both factors are independent from n.

3.1.3 ARMA stochastic sequences

A s.s. is said to be Autoregressive of order p and Moving Average of order q, sinthetically ARMA(p,q), if it can be expressed by

$$x_n = \sum_{j=1}^{p} \Phi\ x_{n-j} - \sum_{k=1}^{q} \Theta_k\ r_{n-k} + r_n$$

where $\{r_n\}$ is a stationary purely random s.c. independent from $\{x_n, x_{n-1}, \ldots\}$ [57]. ARMA s.s are often utilized as models for empirical time series. In particular, the ARMA(1,0) s.s.

$$x_n = \Phi\ x_{n-1} + r_n \qquad (\mid \Phi \mid\ < 1)$$

has been used in the last years in modeling solar climatological time series. One easily deduces that

$$(1\ -\ \Phi)\ \langle x_n \rangle = \langle r_n \rangle$$

so that is in general assumed without any loss of generality that

$$\langle r_n \rangle = \langle x_n \rangle = 0$$

This is of course not necessary. For istance, the model

$$x_n = \Phi\ x_{n-1}\ +\ (1\ -\ \Phi)\ r_n$$

with both $\{x_n\}$ and $\{r_n\}$ ranging between 0 and 1 can be utilized with some profit to simulate ratios as DD/DG, DG/DE, DS/DS_o and so on.

It is often erroneously claimed that an ARMA(1,0) s.s. is asymptotically normally distributed. Since, by iteration, one gets asymptotically

$$x_n = \sum_{j=0}^{\infty} \Phi^j \, r_{n-1}$$

one can believe that the "central limit theorem" holds. In fact this theorem holds if the infinite independent random variables which sum up do not have vanishing variances. This is not the case of the ARMA(1,0) process, since the variances of $\{\Phi^j \, r_{n-j}\}$, i.e. $\{\Phi^{2j} \, \sigma_r^2\}$ are fast vanishing with increasing j. The more the Φ parameter is small, the more the distributions of r_n and x_n are similar.

3.1.4 DARMA stochastic sequences

We also recall the recently introduced Discrete ARMA (DARMA) s.s. [134] [135], limiting ourselves to briefly describe the DAR(p) case. A DAR s.s. of orede p is defined by the sheme

$$x_n = \alpha_n \, x_{n-k_n} + (1 - \alpha_n) \, y_n$$

where $\{y_n\}$ is a purely random stationary s.c. with probabilities f_i (where the index i ranges onto the discrete set of the allowable values), $\{\alpha_n\}$ is a purely random stationary s.c. which can only take the values 1 or 0 (with given probabilities Φ, $1-\Phi$), and k_n is another purely random s.c. which can assume the values $k_n = 1, 2, \ldots, p$ with probabilities $q_1, q_2, \ldots, q_p$.

The parameter p is the Markov order of the s.c.. If p=1 the chain is properly markovian. In this case, since

$$x_n = \alpha_n \, x_{n-1} + (1 - \alpha_n) \, y_n$$

indicating by i, j the generical values which y_n can assume, one obtains

$$Prob\{x_n = j \mid x_{n-1} = j\} = Prob\{\alpha_n = 0\} \; Prob\{y_n = j\} + Prob\{\alpha_n = 1\}$$

and

$$Prob\ \{x_n = j \mid x_{n-1} = i \neq j\} = Prob\ \{\alpha_n = 0\}\ Prob\ \{y_n = j\}$$

so that one obtains the transition matrix

$$P_{ij} = \delta_{ij}\ [(1 - \Phi)\ f_j\ +\ \Phi]\ +\ (1 - \delta_{ij})(1 - \Phi)\ f_j$$

The DAR s.c.'s allow modeled time series $\{x_n\}$ to be obtained with a *given* discrete distribution, i.e. the given $\{y_n\}$ distribution.

3.2 Solar Irradiation Time Series

Though no theoretical reason seems to exist, most authors agree on the fact that the sequences of daily solar irradiations (or related quantities) can be satisfactorily described as first order Markov sequences. Some researchers (see below) have modeled with this class of processes even the sequences of hourly values, but some doubt exists that the Markov scheme can hold for sequence steps less than one hour. On the other hand, weekly or monthly valued time series are likely to be almost purely random. Thus, since daily or hourly time series are central topics in solar statistical climatology, one is mainly concerned with (first or second order) Markovian models.

Note that the previously cited agreement on the first order Markov model does not mean that the concerned stochastic sequences *are* realizations of first order processes. Some discrepancies can arise, especially in tropical regions. For example, Exell ([85] and [83]), analyzing five years of data for Bankok, finds that the chains obtained by classifing the DG sequences into three broad contiguous classes are appreciably better modeled by a second order stochastic chain than by a first order one, as the chains of rainy days are [59].

In temperate latitudes however, these discrepancies are more less pronunced. For instance, Bois et al. [53], in order to check the dependence of DG/DG_{cs} on the same quantity at previous days, construct the anticumulative conditional distribution

$$G_{>}(x;k) = Prob\ \{DD/DG_{cs}(n)\ >\ x \mid DG/DG_{cs}(n\ -\ k)\ >\ x\}$$

and

$$G_<(x;k) = Prob\ \{DD/DG_{cs}(n)\ >\ x \mid DD/DG_{cs}(n\ -\ k)\ \leq\ x\}$$

Examples are reported (see Fig. 3.1), based on ten years of daily measurements at Carpentras (France), for the months of March and June. The authors suggest fitting curves of this kind by third order polynomials. As a remarkable result, no appreciable differences between $G_>$ and G_- are noticed for $k > 1$. This means that the concerned process is first order Markovian.

The fact that solar time series are generally not purely random has some consequences on the solar statistical climatology. As pointed out by Skaggs *et al.* [233], the persistence causes complications in time series statistics since it implies a loss of information. Confidence limits estimation, hypothesis testing and general modelling can be appreciably influenced [154] [170] [171]. One can describe the loss of information over a period of N steps by the effective number of independent samples

$$N_0 = \frac{\sigma^2(x)}{\sigma^2(\overline{x})}$$

where $\overline{x}$ is the serial average, or by the characteristic persistence time

$$T_0 = \frac{N}{N_0}$$

The standard error of the mean can be estimated by [59]

$$\sigma(\overline{x}) = \frac{\sigma(x)}{N}\ \{N\ +\ 2\ [(N\ -\ 1)\ r_1\ +\ (N\ -\ 2)\ r_2\ +\ \ldots +\ r_{n-1}]\}^{\frac{1}{2}}$$

where r_j is the serial correlation coefficient at lag j. For a first Markovian order sequence one has

$$\sigma(\overline{x}) = \frac{\sigma(x)}{\sqrt{N}}\ \left(1\ +\ \frac{2r_1}{1\ -\ r_1}\ \left(1\ -\ \frac{1}{N}\ \frac{1\ -\ r_1^N}{1\ -\ r_1}\right)\right)^{\frac{1}{2}}$$

The authors, using 17 years of measured DG at St. Paul,Canada, calculate to five lags the autocorrelation coefficients (before and after

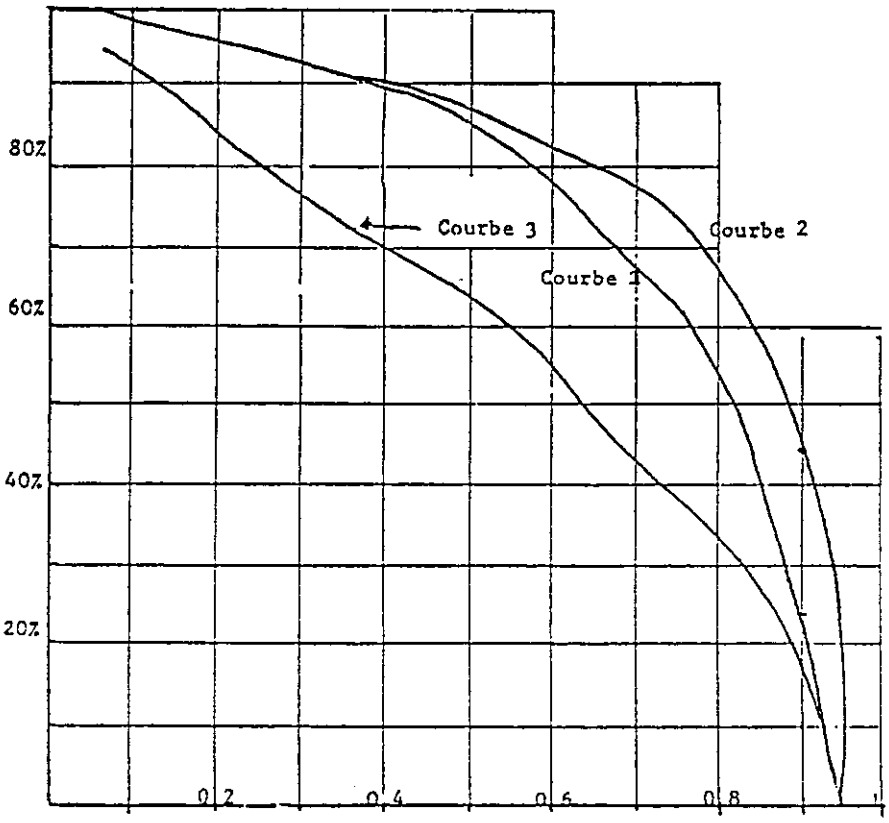

Figure 3.1: Anticumulative distribution for DG/DG_{cs} (1) compared with the corresponding anticumulative conditional distributions, given that the previous day DG/DG_{cs} value is above (2) or below (3) the present value. From Bois (78).

having removed, with a simple two harmonic fit, the trend of DG during the year). The monthly characteristics times are reported, together with their values calculated with a method by Chervin [67]. The monthly effective number of independent daily values is also reported (see Fig. 3.2 and Fig. 3.3).

Results show a detrendized characteristic time ranging from 1.19 to 1.78 days. September is shown to be the more "persistent" month and January the less "persistent".

3.3 Sequences Analysis

Another method of investigating persistence in a time series consists of analyzing the frequencies of the sequences of consecutive values belonging to some class in terms of their length.

Bois et al. [53] perform this analysis on the data of Carpentras (see above) and report results relative to August (period: 1964 ÷ 1975). They investigate the class of sequences of DG/DG_{cs} values greater or less than 0.7 and compare the empirical frequencies with those calculated using one–step conditional probabilities. The two frequency distributions are practically indistinguishable, and this confirms the Markov character of their DG/DG_{cs} time series. A further confirmation is given by the exponential decreasing of the "stable" frequencies from the three–day length on (see Fig. 3.4 and Fig. 3.5).

Bénard *et al.* [33][34][35] study, using eleven years of daily data for Trappes (France) and Huallao (Perù), the length probabilities for "stable" sequences. They calculated $\langle DG \rangle(n)$ and $\sigma_{DG}(n)$ during the year ($n = 1, \ldots, 365$), solve the non stationarity problem by dividing the year into months, and quantizing the $DG(n)$ range in three intervals, defined by two cuts at values DG_{min} and DG_{max} (these values are chosen to depend on $\sigma_{DG}(n)$). A sequence is called *stable* if all its DG values belong to the central interval. Three fixing criteria for $\langle DG \rangle(n)$, DG_{min} and DG_{max} are examined, and for each of these the probabilities of stable sequences with length from 1 to 7 days are calculated during the year, together with the conditional probabilities of obtaining a stable sequence of $d + 1$ days given that a stable sequence of d days has already occurred.

Month	Lag (Days) 1	2	3	4	5
January	.14	.02	.08	.02	.06
February	.17	.06	.02	-.10	-.02
March	.25	.05	.03	0	0
April	.24	-.04	-.08	-.11	-.07
May	.29	.05	.04	-.05	-.08
June	.20	.08	-.04	-.06	0
July	.13	.03	-.04	-.08	-.10
August	.31	.10	.05	.02	.01
September	.35	.09	0	.01	.03
October	.33	.11	.03	-.02	-.10
November	.25	.04	-.04	-.06	-.05
December	.20	.08	0	-.03	-.06

Month	Lag (Days) 1	2	3	4	5
January	.09	-.02	.05	-.01	.04
February	.17	.02	.01	-.09	-.02
March	.22	.02	.01	-.02	-.03
April	.23	-.05	-.09	-.11	-.07
May	.28	.04	.04	-.06	-.09
June	.20	.08	-.03	-.06	0
July	.12	.02	-.04	-.09	-.11
August	.24	.02	-.03	-.04	-.06
September	.29	.01	-.07	-.05	-.01
October	.28	.07	-.01	-.06	-.14
November	.22	.01	-.07	-.09	-.08
December	.20	.01	-.03	-.03	-.05

Figure 3.2: Average serial correlations for DG, before and after removing the yearly trend. From Skaggs (82).

Month	Type of Estimate		
	Trend	No. Trend	Chervin
January	1.31	1.19	1.52
February	1.39	1.39	1.09
March	1.64	1.54	2.23
April	1.60	1.57	1.39
May	1.78	1.74	2.04
June	1.48	1.48	2.27
July	1.29	1.26	2.13
August	1.86	1.60	2.79
September	2.02	1.78	3.22
October	1.94	1.74	2.13
November	1.64	1.54	2.67
December	1.48	1.48	2.48

Figure 3.3: Characteristic time intervals, in days, between independent daily values, calculated before and after removing the yearly trend. From Skaggs (82).

- Séquences de jours dépassant le seuil 70%

Longueur en jours :	1	2	3	4	5	6	7	8	9	10	11
Nombre de séquences :	8	17	11	5	3	7	5	1	4	6	1

- Séquences de jours n'atteignant pas ce seuil :

Longueur en jours :	1	2	3	4	5	6	7
Nombre de séquences :	43	15	4	2	1	2	2

- Séquences de jours dépassant ce seuil :

Longueur en jours :	1	2	3	4	5	6	7	8	9	10	11
Nombre de séquences:	7	14	11	8	6	5	4	2	2	2	1

- Séquences de jours n'atteignant pas ce seuil .

Longueur en jours :	1	2	3	4	5	6
Nombre de séquences:	45	14	6	2	1	1

Figure 3.4: Experimental (above) and calculated (below) frequency distributions of DG/DG_{cs} sequences with values greater or less than 0.70. From Bois (78).

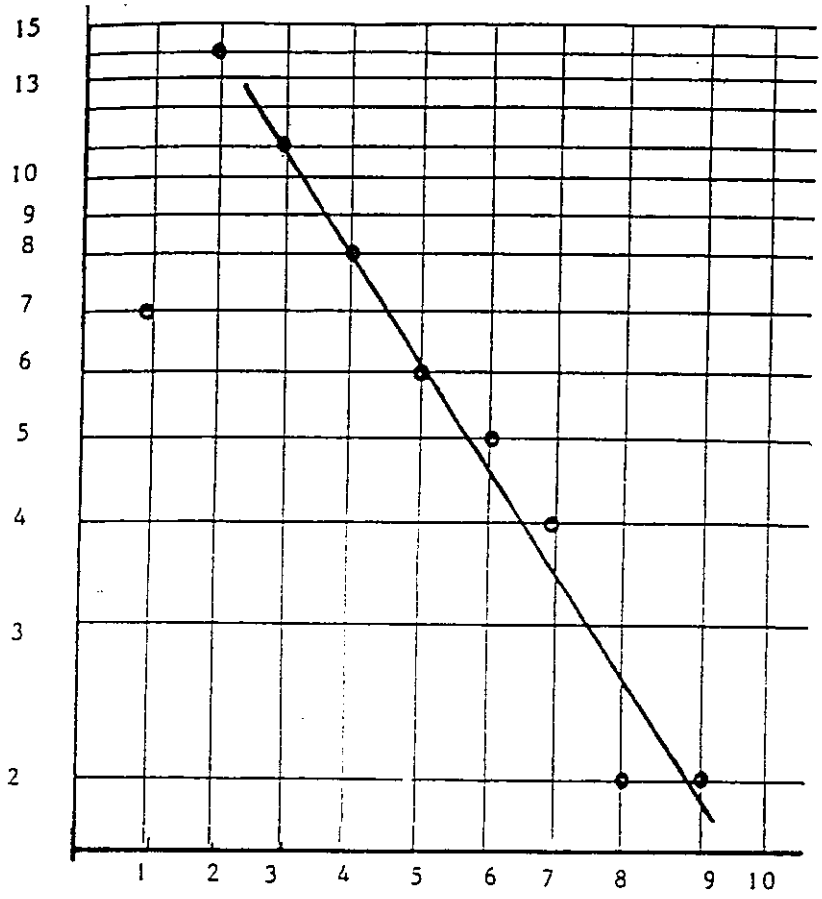

Figure 3.5: Frequencies of DG/DG_{cs} sequences with values greater than 0.70 *vs.* the sequence length. From Bois (78).

The results are graphically reported for both the localities (see Fig. 3.6 and Fig. 3.7) showing fluctuations both in absolute and in conditional probabilities and, for some months, behaviours which are not compatible with markovianity.

Goh [102], using daily data relative to 14 years at Singapore, investigates on the yearly occurrences of sequences with $DG < DG_{cs}$. This choice is somewhat customary for researches on solar energy utilizability, mainly in order to evaluate the right dimension of the storage, as suggested and illustrated by Lougeay and Brazel [166] (Fig. 3.8).

Goh shows examples of this investigation by choosing the values of DG_{cs} as $DG_{cs} = 100(100)400\ cal/sqcm$ (see Fig. 3.9).

Gandino [95] performs a similar analysis using 15 years of data at ISPRA (Italy). He examines sequences of overcast days, of days with DD/DG ratio greater then 0.7 and of days with DG/DE ratio greater then 0.5. In all cases a strong nonstationarity during the year is shown.

In conclusion, it is worthwhile noticing that the frequency length distribution for sequences of values, say of DG, belonging to a specified class gives an immediate view of the dynamic solar climatology for a given locality. Nevertheless, the same information can be *calculated* if one has some stochastic model which simulates the empirical time series.

3.4 Continuously Valued Sequence Models

3.4.1 Autoregressive models

In 1977 two works were published, which could be assumed to be the basic examples of application of the continuous values sequences to solar climatology. Both works use the Markov autoregressive model AR(1) applied to daily solar irradiation time series.

Brinkworth [58], analyzing 8 years of data for Brackell (U.K.), subdivides each year into six periods of 61 days, placed summetrically

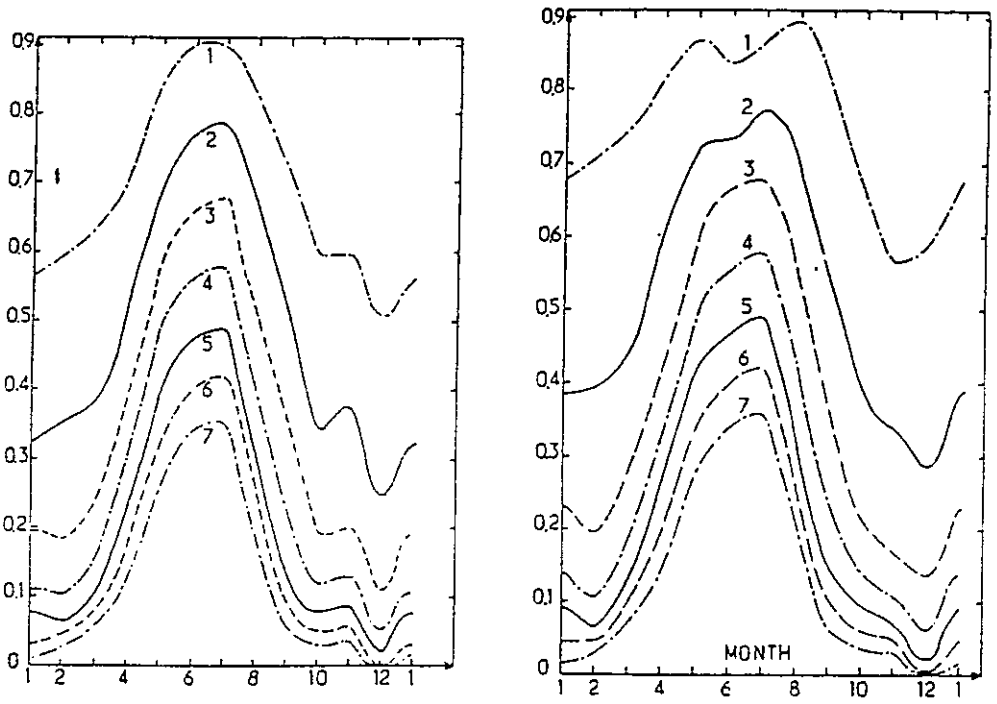

Figure 3.6: Yearly evolution of the probability that a DG sequence is composed by n=1,...,7 *central* values, with two different definitions of *central* day. From Bénard79

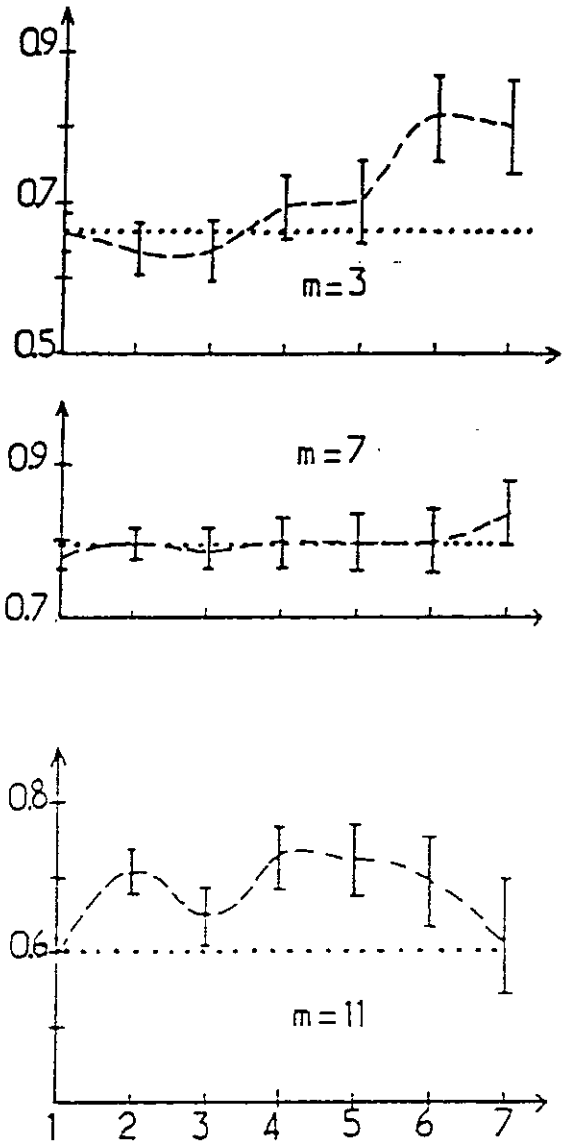

Figure 3.7: Conditional probabilities that, given a sequence of d *central DG* values, the sequence of $d+1$ *central* values is obtained — as a function of $d+1$. Months: March, July and November. From Bénard (79).

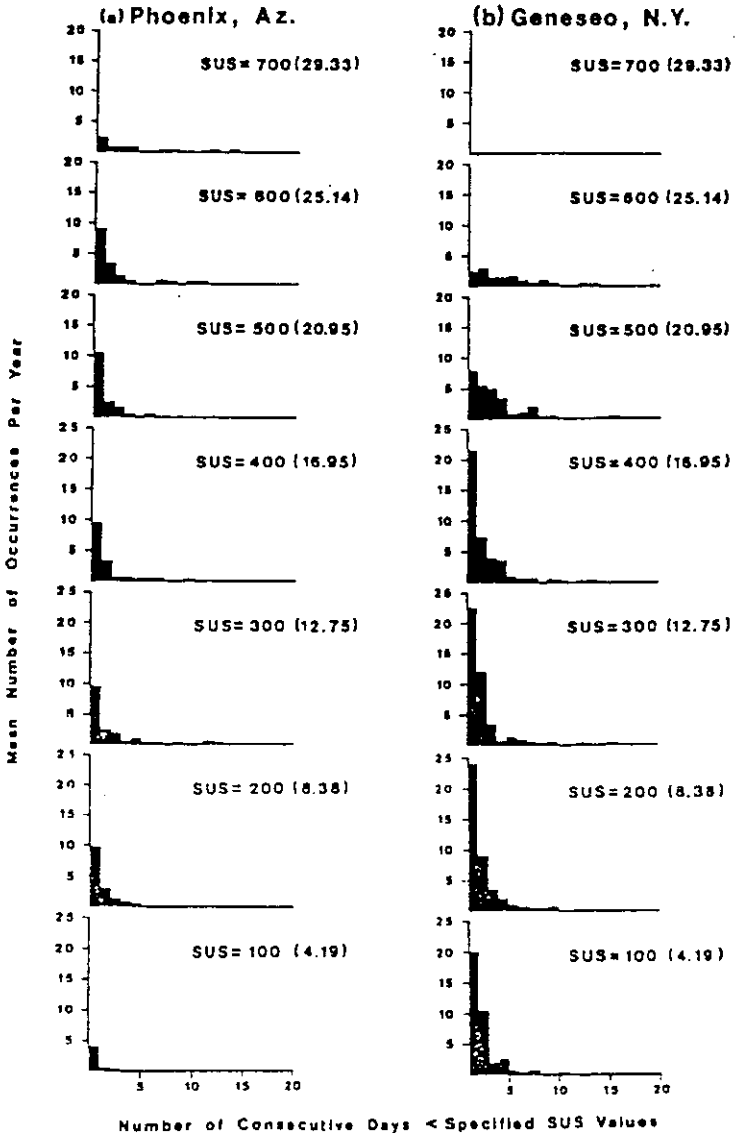

Figure 3.8: Frequency distributions of consecutive day periods with *DG* less than a given threshold (SUS). From Lougeay (84).

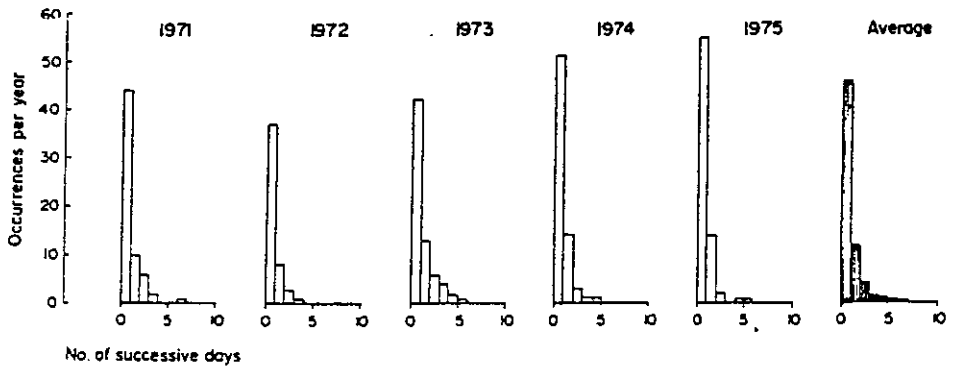

Figure 3.9: Frequency distributions of periods of successive days with DG less than a given threshold (12.57 $MJ/m^2\ d^1$). From Goh (79).

with respect to solstices, and for each period calculates the (linear) trend of the experimental data with the least squares fit. Thus, for each period, the data are expressed by

$$DG(n) = B + C\,n + Q(n)$$

(n =day number) where Q(n) is a random fluctuation with variance σ_Q^2 and correlation function r(k) (calculated for $k = 1,\ldots,5$). The author finds that the Q values are *fairly* symmetrically distributed about zero and calculates for each period the first order autocorrelation coefficient $R(1)$. Then, setting

$$Q(n) = R(1)\ Q(n-1) + r(n)$$

and applying the theoretical formulae for AR(1) sequences, he finds the variance of the (supposed) gaussian random noise $r(n)$:

$$\sigma_r^2 = (1 - R(1))^2\ \sigma_Q^2$$

Thus, for each period, he is able to simulate the residual time series by choosing at random the initial Q value and using an uncorrelated *stationary* gaussian process $\{r(n)\}$, with $\langle r(n)\rangle = 0$ and σ_r^2 given by the previuos relation.

Goh and Tan [103] perform the same kind of analysis and test the same simulation model on hourly values HG, using 14 years of hourly

data for calculating the average HG value for each hour of the year and one single year for stochastic modelling. The authors consider the time series

$$x(n) = HG(n) \; - \; \langle HG(n) \rangle$$

where n indicates a given hour of the year (only hours between 6 a.m. and 6 p.m. are considered). Serial autocorrelation and partial autocorrelation are calculated, which suggest to the authors the use of an AR(1) model

$$x(n) = \Phi \; x(n-1) \; + \; r(n)$$

with $\phi = 0.670$.

Both the previously quoted pioneering articles suffer from one or more of the following defects:

1. no check on the *normality* of the series to be simulated $x(n)$ or of the empirical series of the residuals $r(n)$ is performed, and nevertheless both simulations use a normal "white noise" $r(n)$ (this automatically produces a normal $x(n)$);

2. no check on the *pure randomness* of $r(n)$ is performed (or on its lack of autocorrelation in the case that $r(n)$ is gaussian);

3. no check is performed on the *independence* of $r(n)$ from the past values of $x(n)$ (this independence is essential for the Markov property to hold);

4. in the case of Goh and Tan, no account is given either to *seasonal trends* or to the *nightbreaking* of the (hourly) sequence;

5. no check is performed on the similarity of the empirical *joint distribution* of (x_n, x_{n+1}) and the simulated one.

In 1979 Mustacchi et al [181] tested different models to simulate the HG/HE time series. Among the AR(p) $(p = 1, \ldots, 6)$ models they verified that, for a sample of about 8000 hourly measurements for each of the two Italian localities, the AR(2) is sufficient to account

for the autocorrelational structure. They choose ($x = HG/HE$) respectively

$$x_n = 0.759\ x_{n-1} + 0.096\ x_{n-2} + r_n$$

for Ispra and

$$x_n = 0.601\ x_{n-1} + 0.127\ x_{n-2} + r_n$$

for Vigna di Valle (Italy). The authors notice that neither the empirical HG/HE nor the model residuals r_n are normally distributed while the modeled HG/HE series is, due to the normality of the employed white noise $r(n)$ (see Fig. 3.10 and Fig. 3.11).

Moreover, they notice a high degree of cross correlation between $\{r(n)\}$ and $\{x(n)\}$. For these reasons they conclude the invalidation of the AR and suggest other stochastic models. To overcome the non gaussianity problem they suggest a previous variable trasformation (Gaussian Mapping), which puts the $\{x(n)\}$ series in correspondence with an artificial $\{y(n)\}$ series, built with the following xy relation

$$\frac{1}{\sqrt{2\pi}} \int_{-\infty}^{y} dt\ e^{-\frac{t^2}{2}} = F(x)$$

where F(x) represents the empirical cff for $\{x(n)\}$. Thus, they choose to apply an AR model to the $\{y(n)\}$ series and finally antimap the resulting model to obtain the modeled $\{x(n)\}$. Results seem quite satisfactory but for a slight loss of memory (possibly due to the truncation errors in the mapping – antimapping procedure). Seasonality is not taken into account in the mapping step, i.e. the *yearly* HG/HE distribution is mapped onto the gaussian distribution. Moreover, the problem of night breaking is not considered. Finally, no check is applied to the joint distribution of the pairs (x_n, x_{n+1}) of the simulated versus the empirical values.

In 1980 Sfeir [230] uses a bivariate stochastic sequence model $\{(DG(n),\ T(n)\}$, where $T(n)$ is the daily average dry bulb temperature, to simulate the performance of solar heating and hot – water systems. Both quantities are assumed to be normally distributed (and perfectly cross – correlated), and suggestions are given to estimate their standard deviations, if they are not known, from the

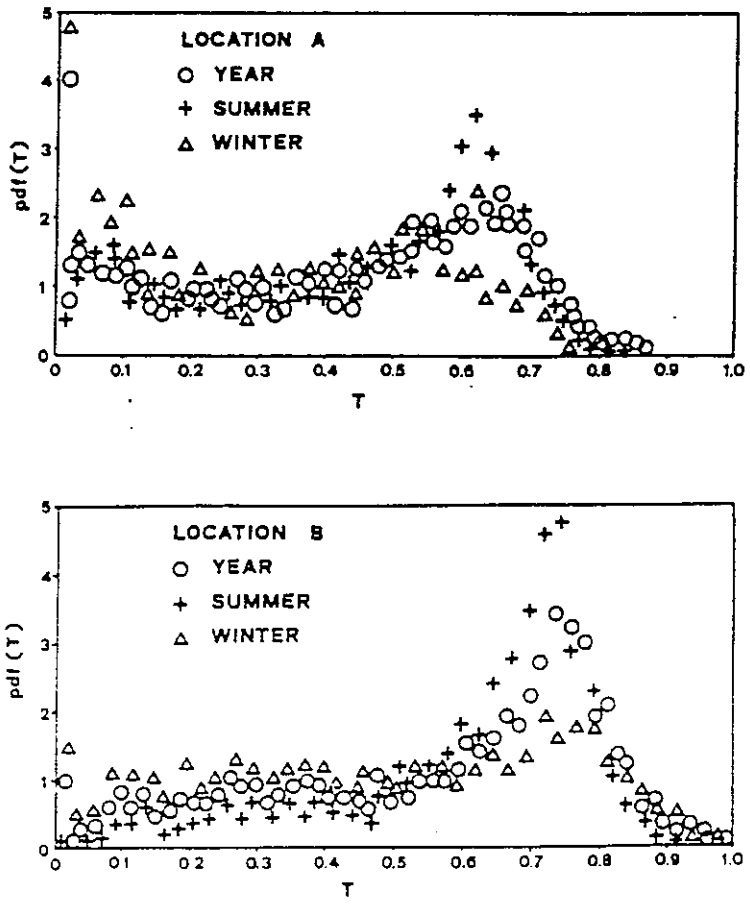

Figure 3.10: The *fdf*s of HG/HE in two Italian localities. From Mustacchi (79).

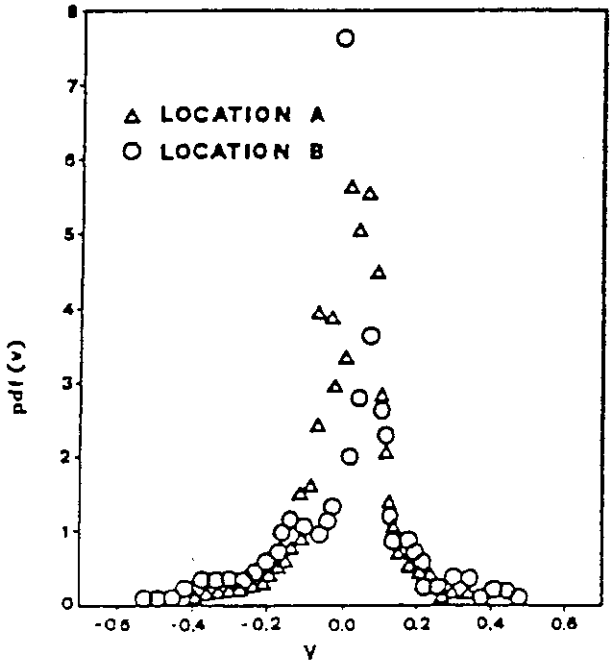

Figure 3.11: Probability density function of residuals in an ARMA(2,0) simulation of HG/HE sequences. From Mustacchi (79).

maxima and the minima of the data. Purely random series are simulated, which give performance results comparable to those obtained with the f–chart method. The author claims that no more involved assumptions about the statistical properties of DG seem to be warranted, due to the minimal accuracy of the available meteorological data (in 1980).

Biga and Rosa [46] analyze the months of January and July at Lisbon on the basis of 8 years of daily measurements. They verify that the DG/DE sequences cannot be attributed to a purely random underlying process, but also verify that the long persistence of autocorrelation is not accounted for by a first order Markov model. The spectral densities, both in January and July, show some periodicity peaks which are clearly not compatible with Ar(1) processes. Referring to the work of Brinkworth, the authors point out the evidence of intrinsic climatical differences between Lisbon and Bracknell.

Engels et al. [81] suggest that, due to the evidence of non normality of the distributions of the DG/DE or DG/DG_{cs}, the AR models or other models which give inherently gaussian results could not be used in simulating time series of these quantities.

In the same year Bartoli et al [28] analyze three years of DG/DE values for 18 Italian localities looking for AR(1) models. For each month m of the year they consider the detrendized variable

$$u(n) = DG/DE(n) \; - \; \langle DG/DE \rangle_m$$

They use the rank test [141] at a confidence level $\alpha = 0.05$ to check the pure randomness of the residual series

$$r(n) = u(n) \; - \; \widehat{\rho}_m \, u(n-1)$$

where $\widehat{\rho}_m$ is the estimated first order autocorrelation coefficient. Due to the positive result they accept the AR(1) model, and look to the distribution of $\widehat{\rho}_m$ among different months and stations. For each station, the series

$$w(m) = \widehat{\rho}_m \; - \; \overline{\rho}$$

where $\overline{\rho}$ represents the average of the $\hat{\rho}_m$'s is found to be purely random, and use of the F–test [226] does not reveal differences in the ρ

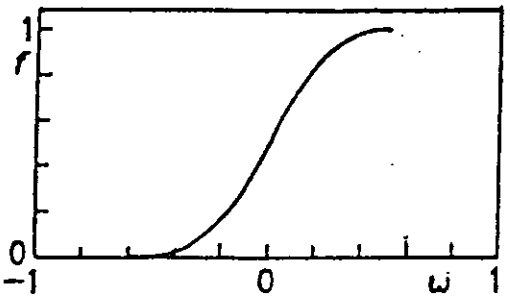

Figure 3.12: Cumulative frequency distribution of AR(1) residuals. From Bartoli (81).

– distribution among stations. Then the authors assume a unique ρ distribution for all Italian station.

In conclusion, they propose the use of an AR(1) monthly model, with a random ρ parameter. The *cff* of the residuals, with the choice of $\rho \in (0.2, 0.3]$, and the *fdf*s of the standardized DG/DE, given various values of the monthly average $\overline{DG/DE}$, are shown (see Fig. 3.12 and Fig. 3.13).

In a subsequent work [9], the same authors improve their model by applying the gaussian mapping technique to the $DG/DE(n)$ sequence, i.e. using the modified AR(1) series

$$y_n = \rho\, y_{n-1} + r_n$$

where, given for each month m the cff $F_m(DG/DE)$, the correspondence between y and DG/DE is given by

$$\frac{1}{\sqrt{2\pi}} \int_{-\infty}^{y} dt\; e^{-\frac{t^2}{2}} = F_m(DG/DE)$$

For ρ they use the fixed value $\rho = 0.25$, which is the expexted value of the monthly ρ distribution (Fig. 3.14).

Since $F_m(DG/DE)$ is assumed to only depend on $\overline{DG/DE}$ (the standard curves [163] or the analogous curves found by the same authors in previous works being assumed valid) the authors claim that

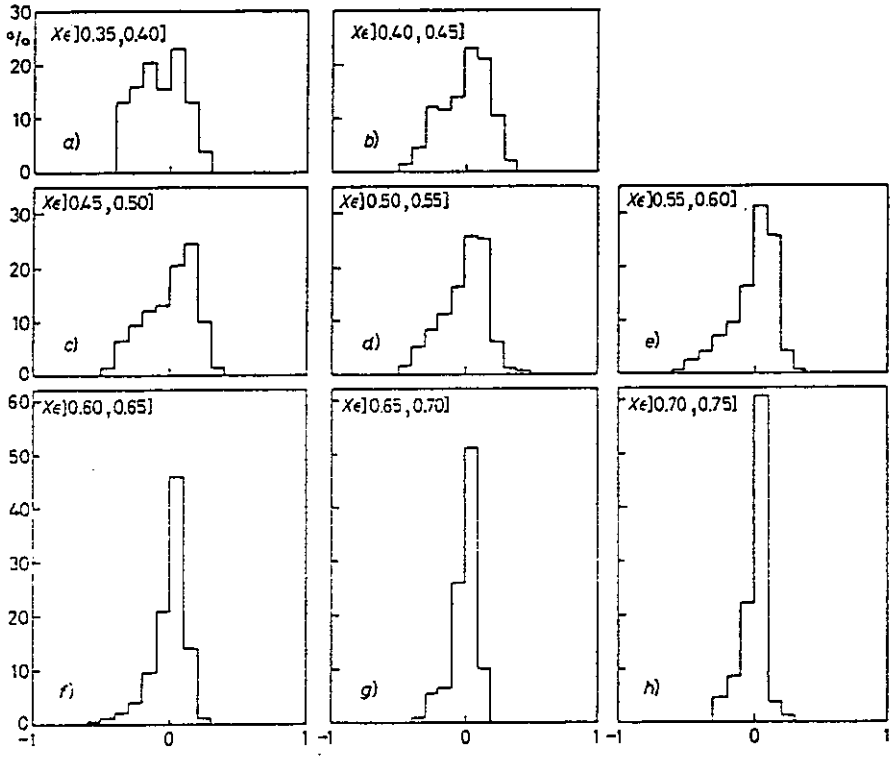

Figure 3.13: Frequency distribution densities of the AR(1) residuals for various ranges of $\overline{DG/DE}$. From Bartoli (81).

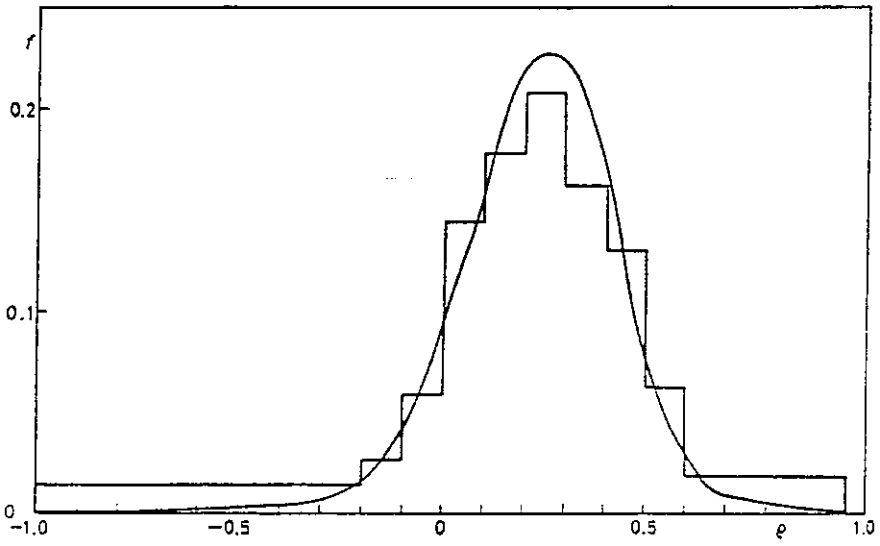

Figure 3.14: Experimental (histogram) and theoretical (continuous line) *fdf* of the first-order autocorrelation coefficient. From Amato (85).

the sole knowledge of $\overline{DG/DE}$ for a given month in a given locality is needed in order to model stochastic $DG/DE(n)$ series for that month in that locality.

Boileau [51] and Boileau *etal.* [114] analyze the $DG(n)$ series for three localities (Trappe (France), Carpentras (France) and Huallao (Peru)) using respectively 11, 9 and 9 years of daily measurements. Referring to previous articles [50] [52] for examples of seasonal modeling and of moving average modeling MA(2) for the difference $DG(n) - DG(n-1)$, they investigate the stochastic serial characteristics for

$$u(n) = \frac{DG(n) - \langle DG(n) \rangle}{\sigma_{DG(n)}}$$

where average and variance, for each day n, are previously calculated and then smoothed by a moving average of suitable length or by Fourier fitting with one harmonic.

They choose to simulate the empirical series with an AR(1) model with white gaussian noise, and to cut the anomalous negative values or the anomalous high values, which can appear in the simulations, by fixing a lower limit $e(n)$ and an upper limit $E(n)$. These limits are deduced by Fourier fitting the empirical lower and upper $DG(n)$ extreme values for each of a set of consecutive (15 days long) periods of the year. The resulting simulated series being normally distributed, the author chooses to apply the AR(1) model to a suitable transformed sequence $DG^*(n)$. He first considers a modified lower limit sequence $e^*(n)$ given by

$$e^*(n) = 2 \langle DG(n) \rangle - E(n)$$

except when $e^*(n) \leq e(n)$, in which case the $e^*(n)$ value is set equal to $e(n)$. Secondly, he consider a modified $DG^*(n)$ series, whose values are equal to the $DG(n)$ values when $\langle DG \rangle \leq DG(n)$ and otherwise with $DG^*(n)$ given, for each day n, by

$$DG^*(n) = \langle DG(n) \rangle + (DG(n) - \langle DG(n) \rangle) \frac{DG(n) - e^*}{DG(n) - e}$$

The modified series is more symmetrical about its mean $\langle DG^*(n) \rangle$ than the original $DG(n)$. The standardized series

$$u^*(n) = \frac{DG^*(n) - \langle DG^*(n) \rangle}{\sigma_{DG^*(n)}}$$

is finally modeled by the AR(1) process, and anomalous high and low values of the resulting simulated $DG(n)$ cut by the chosen upper and lower extremes. Correlation coefficients 0.28 for Trappes, 0.31 for Carpentras and 0.25 for Huallao are found to give the best fits (see Fig. 3.15).

Amato *et al.* [8] apply the gaussian mapping technique to the twenty year long $DG(n)$ time series relative to 4 Italian stations. They map to a gaussian series the standardized variable

$$u(n) = \frac{DG(n) - \widetilde{DG}(n)}{\tilde{\sigma}(n)}$$

where, for each locality,$\widetilde{DG}(n)$ and $\tilde{\sigma}(n)$ are obtained by fitting the daily data set and the standard deviation for each day n of the year with two Fourier sums containing one and two harmonics respectively. After gaussian mapping, the AR(1) model is applied, with $\rho = 0.33$, and the resulting time series is antimapped. No seasonal changes are taken into account, in the sense that the gaussian mapping of the *yearly* u-distribution is performed, because the authors do not find appreciable differences between the distinct monthly u-distributions.

Comparison of the experimental and simulated DG marginal yearly distributions for each of the four localities gives a good agreement (Fig. 3.16), but no similar check is performed on the joint $(DG(n), DG(n+1))$ distributions.

Graham *et al.* [113] suggest that any time series modeling for hourly data can give biased results due to the unavoidable night breaking, though atmospheric conditions (which in fact account for the fluctuations of quantities as HG/HE or HB/HE) *do exist* during the night too, even if they are not measurable in terms of solar irradiation. For this reason they choose to work with DG/DE data, using a data base of 10 years for three canadian localities with very different climates. They subdivide the available data into 8 years for model identification and 2 years for model validation.

Due to the well known non gaussianity of the DG/DE distributions, they previously transform the original series performing a month by month gaussian mapping. As a consequence of the analysis of the autocorrelation and partial autocorrelation functions structure,

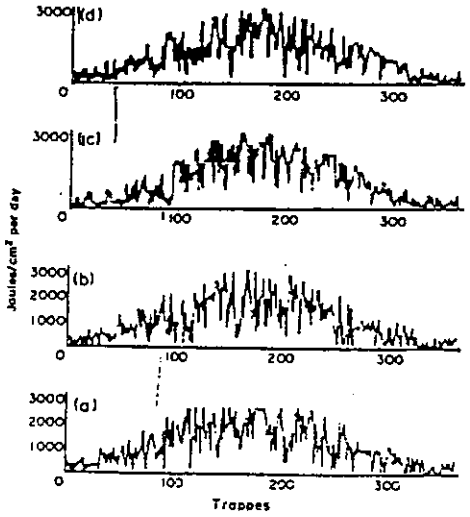

Fig. 4. Two years of simulated I_t obtained with model C in (a) and (b), with 2 yr of measured I_t in (c) and (d). Case of Trappes.

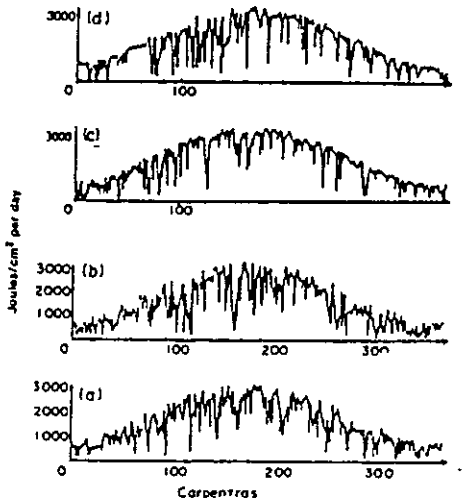

Fig. 5. Same as Fig. 4. Case of Carpentras.

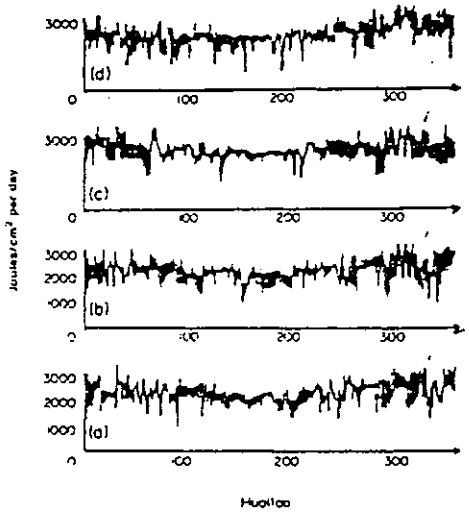

Figure 3.15: Comparison between two years of simulated $DG(n)$'s [(a) and (b)] and two years of measured values [(c) and (d)], in two french localities (Trappes and Carpentras) and at Huallao (Peru). From Boileau (83).

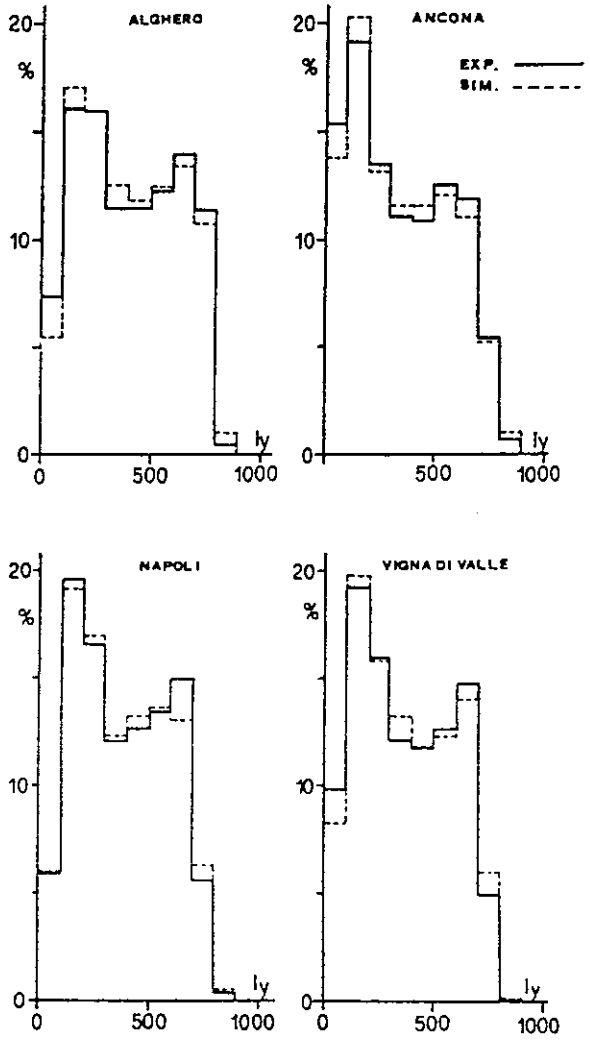

Figure 3.16: Comparison between observed (continuous line) and AR(1)–simulated (dashed line) *fdf*'s of *DG* relative to four Italian localities. From Amato (86).

the authors choose a first order autoregressive model with a unique autocorrelation coefficient $\Phi = 0.29$ for all three considered localities. The residual series is found, of course, to be normally distributed and its lack of autocorrelation is positively tested. After antimapping, the validation of the results is obtained by comparing, for each month, the average $\overline{DG/DE}$, the standard deviation, the skewness and kurtosis coefficients, and the minimum and maximum DG values obtained from a synthetic ten years long series with the corresponding original quantities. A close agreement is found (see Fig. 3.17).

3.5 Chain Models

3.5.1 Markov chain models

While much work using the Markov chain model has been done in the last decades to portray, for instance, the daily precipitation time series (see for a partial survey Chin [70]), this approach has seldom be used for simulating solar irradiation sequences. This is possibly due to the large samples needed to satisfactorily estimate all the transition probabilities when the marginal probabilities are classified in a somewhat fine way.

In 1978, Lestienne [157] analyzed the sequences of "bad" and "good" days at Odeillo (France), using more than three years of daily data. Each day was classified "bad" if the relative sunshine duration was less then 50% and "good" for the contrary. The author considered, month by month, the tetrachoric transition matrix

	good	*bad*
good	α	β
bad	γ	δ

where $\alpha = 1 - \beta$, $\delta = 1 - \gamma$ and

$$\beta = Prob\{day\ (n+1) = bad \mid day(n) = good\}$$

$$\gamma = Prob\{day\ (n+1) = good \mid day(n) = bad\}.$$

	K_t	σ_{K_t}	g_1	g_2	K_n	K_m
Jan	0.297	0.197	0.532	−0.971	0.023	0.751
Feb	0.390	0.228	0.184	−1.375	0.031	0.770
Mar	0.433	0.234	−0.051	−1.495	0.041	0.786
Apr	0.478	0.204	−0.291	−1.217	0.079	0.796
May	0.527	0.183	−0.683	−0.659	0.061	0.782
Jun	0.510	0.194	−0.586	−0.915	0.078	0.767
Jul	0.575	0.177	−1.149	0.148	0.072	0.768
Aug	0.535	0.183	−0.765	−0.597	0.065	0.760
Sep	0.528	0.204	−0.797	−0.695	0.066	0.773
Oct	0.412	0.228	−0.182	−1.480	0.027	0.749
Nov	0.321	0.198	0.335	−1.115	0.037	0.736
Dec	0.275	0.192	0.678	−0.771	0.017	0.772

Month	Mean $\bar{K}_t$	Std. dev. σ_{K_t}	Skewness g_1	Kurtosis g_2	K_n	K_m
Jan	0.319	0.198	0.458	−1.015	0.024	0.740
Feb	0.381	0.217	0.318	−1.219	0.033	0.770
Mar	0.411	0.240	0.012	−1.522	0.041	0.784
Apr	0.475	0.199	−0.263	−1.103	0.082	0.784
May	0.537	0.186	−0.730	−0.590	0.083	0.781
Jun	0.525	0.180	−0.614	−0.735	0.095	0.765
Jul	0.564	0.197	−1.060	−0.158	0.077	0.767
Aug	0.548	0.182	−0.803	−0.519	0.070	0.760
Sep	0.522	0.207	−0.755	−0.723	0.070	0.772
Oct	0.407	0.225	−0.188	−1.424	0.028	0.747
Nov	0.316	0.195	−0.332	−1.112	0.038	0.735
Dec	0.269	0.189	0.781	−0.506	0.018	0.766

Figure 3.17: Comparison of statistical parameters relative to experimental (above) and AR(1)–simulated (below) *DG fdf*s at Vancouver (Canada). From Graham (88).

	1974			1975			1976			1977			MOYENNE PONDEREE	
	p, q, r, s	α	δ	p, q, r, s	α	δ	p, q, r, s	α	δ	p, q, r, s	α	δ	$\overline{\alpha}$	$\overline{\delta}$
Janvier	17, 6, 5, 2	.74	.29	14, 5, 4, 7	.74	.64	23, 3, 3, 1	.88	.25	7, 9, 8, 6	.44	.43	0.77 ± 0.04	0.43 ± 0.07
Février	8, 5, 6, 8	.62	.57	9, 5, 5, 8	.64	.62	10, 4, 5, 9	.71	.64	9, 7, 6, 5	.56	.45	0.63 ± 0.06	0.58 ± 0.06
Mars	6, 5, 5, 14	.55	.74	5, 8, 8, 11	.27	.58	17, 5, 5, 3	.77	.58	15, 4, 4, 7	.79	.63	0.65 ± 0.05	0.61 ± 0.06
Avril	11, 5, 5, 8	.69	.62	12, 6, 6, 5	.67	.45	6, 6, 6, 11	.50	.65	12, 5, 4, 8	.71	.67	0.66 ± 0.05	0.61 ± 0.06
Mai	17, 5, 5, 3	.77	.58	6, 8, 7, 9	.43	.56	11, 5, 6, 8	.69	.57	11, 4, 4, 11	.73	.73	0.68 ± 0.05	0.59 ± 0.06
Juin	11, 5, 5, 8	.69	.62	10, 5, 6, 8	.67	.57	13, 6, 7, 3	.68	.30	14, 5, 5, 5	.74	.50	0.70 ± 0.05	0.51 ± 0.06
Juillet	18, 5, 4, 3	.78	.43	20, 4, 4, 2	.83	.33	18, 6, 5, 1	.75	.17	16, 4, 3, 7	.80	.70	0.79 ± 0.05	0.43 ± 0.07
Août	19, 5, 4, 4	.86	.50	13, 6, 6, 5	.68	.46	15, 6, 5, 4	.71	.44	11, 6, 6, 7	.65	.54	0.75 ± 0.05	0.49 ± 0.07
Sept bre	14, 6, 6, 2	.70	.25	9, 7, 6, 7	.56	.54	16, 5, 6, 2	.76	.25	23, 2, 3, 1	.92	.25	0.80 ± 0.04	0.34 ± 0.07
Octobre	13, 6, 6, 5	.68	.45	22, 3, 3, 2	.88	.40	8, 8, 8, 6	.50	.43				0.76 ± 0.06	0.43 ± 0.08
Novembre	10, 5, 5, 9	.67	.64	9, 9, 9, 2	.50	.18	14, 5, 5, 5	.74	.50				0.65 ± 0.06	0.43 ± 0.07
Décembre	22, 3, 3, 2	.88	.40	18, 4, 4, 4	.82	.50	7, 8, 8, 7	.47	.47				0.79 ± 0.05	0.54 ± 0.08

Figure 3.18: Estimates of α and δ transition probabilities for *tetrachoric DG* Markov chains at Odeillo (France). From Lestienne (78).

The asymptotic (stationary) probabilities are then given by

$$Prob\{good\} = \frac{\gamma}{\beta+\gamma}$$

$$Prob\{bad\} = \frac{\beta}{\beta+\gamma}.$$

By assigning the value 0 to bad days and the value 1 to good days a correlation sequence $c_n = (\alpha-\gamma)^n$ is found. In Fig. 3.18 the estimates for α and δ are reported.

The probability of a subsequence composed of exactly k good days is given by $(1-\beta)^{k-1}\beta$; that of a subsequence composed of exactly k bad days is $(1-\gamma)^{k-1}\gamma$. Thus the respective expected lenght are $1/\beta$

and $1/\gamma$. In Fig. 3.19 the comparison is shown between the empirical frequency distributions of these persistent sequences and the corresponding calculated distributions for purely random and Markovian sequences.

A slight underestimation for probability of long persistent sequences seems to indicate a correspondingly slight second order markovianity; nevertheless the overall comparison is quite satisfactory.

We note that the scheme of Lestienne is equivalent to a DAR(1) scheme with marginal probabilities $\gamma/(\beta+\gamma)$ and $\beta/(\beta+\gamma)$, and with parameter $\Phi = \alpha - \gamma$.

In a subsequent work [156], the same author applys his model to the study of the behaviour of the storage tank coupled to a solar power plant.

Petrie and McClintock [203], while describing a method to construct for simulation purposes a "typical week" relative to December, calculate a Markov transition matrix with five states, defining five solar day types:bad, poor, fair, good and excellent. This classification corresponds to the partition of DG given by $DG = 50[50]300$ *langleys*. Their data base consisted of eight December's (1956–1963) at Boston (US). The transition matrix is given by

	B	P	F	G	E
B	.356	.067	.111	.269	.178
P	.179	.205	.179	.308	.128
F	.178	.133	.289	.267	.133
G	.191	.161	.191	.279	.176
E	.070	.186	.163	.348	.233

Their "typical week" is built using the most probable transitions under the condition of recovering, as far as possible, the empirical relative frequency of each class during December and of being as short as possible. They choose a six–day period and the most probable sequence (E—G—P—G—F—B —>E.....).

Some relationship with the present topics is offered by the work of Lameiro and Bryson [151]. In developing a previous research [150], they examine the effects on the performance of a solar heating system on the assumption that the "climate+solar heating device" system can be described on hourly basis by a threevariate state: storage

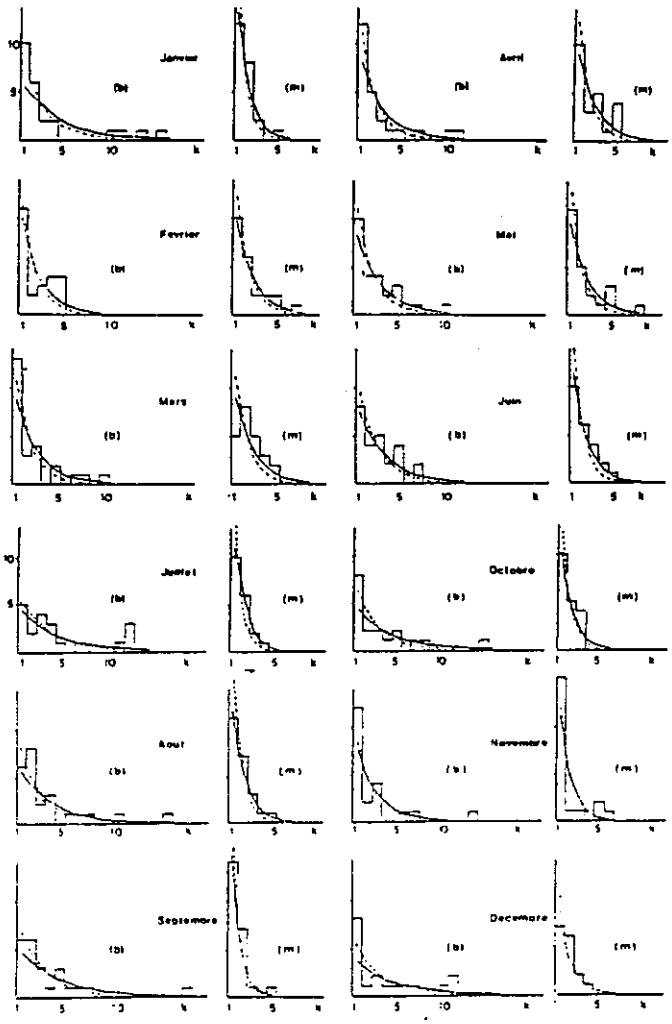

Figure 3.19: Monthly experimental and calculated *fdf*'s for sequences of *good* (b) and *bad* (m) days *vs.* sequence lengths (solid line). The dotted lines indicate frequencies for purely random simulations. Data from Odeillo (France). From Lestienne (78).

temperature T_s, global irradiation HG, ambient temperature T_a. The probabilistic evolution of this system state is then supposed to be governed by a Markov chain process.

In fact, due to computational limits, while T_s is discretized with a very fine grid (about 1 degree), the ambient temperature is assumed to be constant and HG is allowed to take only two values, i.e. 0 ("night" or "overcast" and 300 BTU/(h sqfoot) ("day"). This crude approximation is due to the main interest of the authors in comparing the predicted performance of the system with the more expensive real data simulation.

In a subsequent work, Lameiro and Duff [152] include the hot water demand level HW among the state parameters, but they only consider three possible deterministic "daily evolutions' for HW, which thus is not treated as a random variable. The performance indices are obtained, in both works, by calculation of the asymptotic stationary probability state for the system using the transition matrix.

In 1979, Mustacchi *et al.* [181], in an already quoted work on the HG/HE time series, find that the Markov chain model overcomes in reliability all other stochastic modelling approachs. They use a whole year of hourly measurements to estimate a 25x25 transition matrix with the marginal partition $HG/HE = 0[0.04]1$. After simulation, the (non normal) marginal probability is well recovered, while it results severely modified by AR models, as shown by Fig. 3.11 for Ispra,Italy.

A second order Markov chain (three dimensional transition matrix) shows, after simulation, only slight improvements with respect to the results obtained with the simpler first order process. Moreover, lack of sufficiently large sample does not allow reliable estimates for the elements of the transition matrix.

Exell [84], in setting up a random model for simulating daily and hourly global irradiation processes for Thailand, chooses a zeroth order (i.e. purely random) model for both DG/DG_{cs} and HG/HG_{cs}, where the "clear sky" quantities DG_{cs} and HG_{cs} are calculated with empirical formulae based on experimental data by methods found in literature [61]. These purely random chains do not completely account for experimental results, as one can see from Fig. 3.20, which shows the comparison between the observed and the calculated frequencies of consecutive "bad" solar day runs. Nevertheless, the author judges

	Length of run (days)				
	1	2	3	4	5
Bangkok					
Observed	32.0	9.4	3.4	1.8	0.8
Theory	43.8	9.2	2.2	0.6	0.2
Singapore					
Observed	45.6	11.8	4.0	1.6	0.8
Theory	49.3	13.4	4.0	1.2	0.4

Figure 3.20: Comparison between the observed and the calculated frequencies of *bad* solar day runs, for Bankok and Singapore. From Exell (81).

the overall results to be satisfactory in comparison with the simplicity of the algorithm.

Cammarata *et al.* [64], using one year of HG values measured at Catania, Italy, in 1967, set up for each season a 25x25 transition matrix for HG/HE, with marginal probabilities classified as HG/HE=0[0.04]1 as already done by Mustacchi *et al.*. Also these authors found a very good agreement between the experimental and the simulated marginal probabilities (see Fig. 3.21).

In 1988, Aguiar *et al* [3], assuming that the DG/DE sequences are first order markovian and using the Liu and Jordan result about the sole dependence of monthly DG/DE frequency distribution on the average value $\overline{DG/DE}$, built a set of ten 10x10 transition ma-

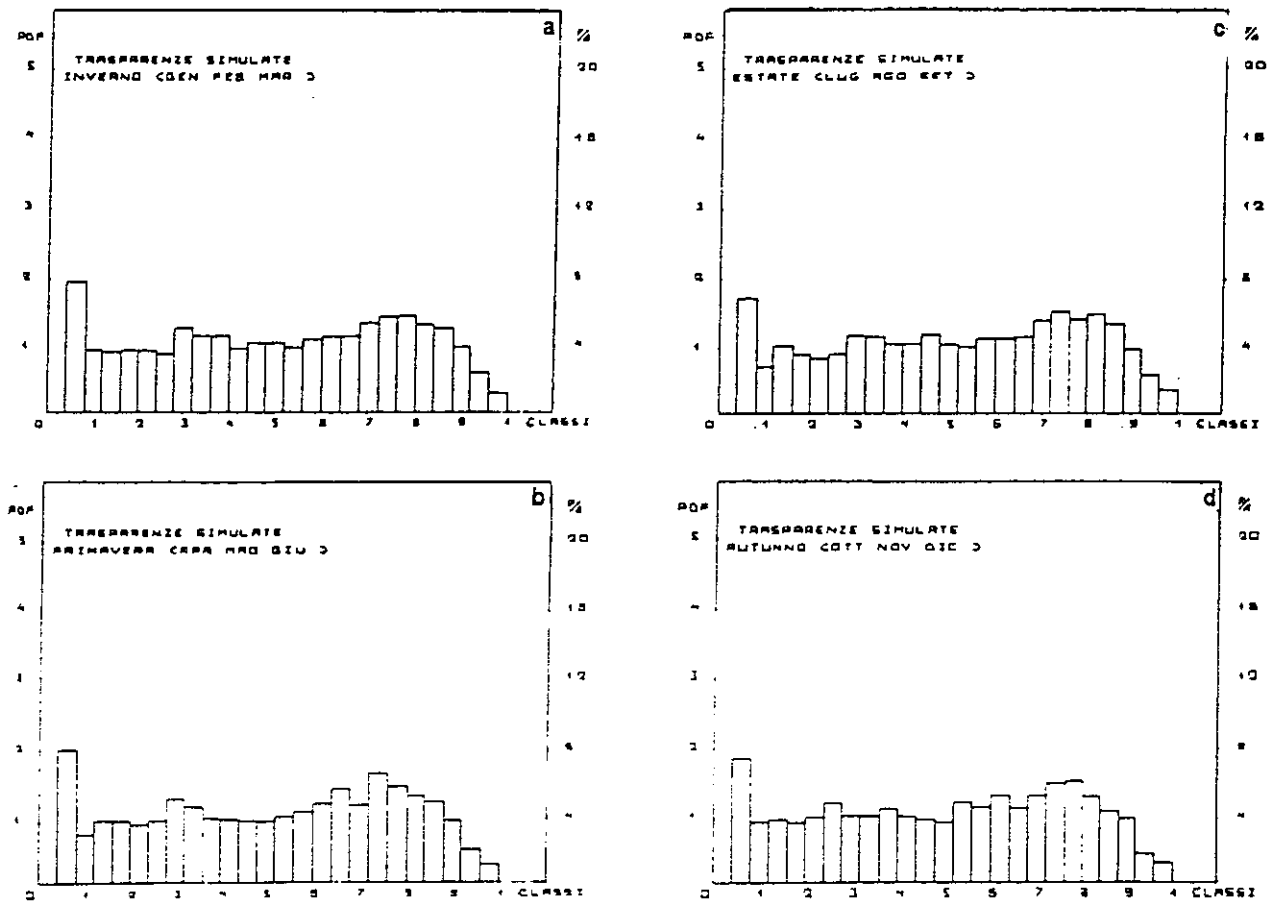

Figure 3.21: Four seasonal frequency distributions of HG/HE obtained through a 25x25 Markov matrix. Data from Catania (Italy). From Cammarata (82).

trices, each relative to a given $\overline{DG/DE}$ interval ($\overline{DG/DE}$= [0.,0.3], 0.3[0.05]0.7, [0.7,1.]).

They suppose that each of these matrices is *uniquely* determined by the marginal frequency distribution which must be equal to the standard corresponding $\overline{DG/DE}$-parametrized frequency distribution. In fact, this assumption does not take into account the variability of the correlation structure of a transition matrix for a given marginal probability.

The authors estimate the 1000 transition probabilities using 300 months of daily data relative to different years, ranging from 1965 to 1979, and to nine different localities in Portugal, France, Azores Islands, Madeira Islands, Mozambique and Macau. The numbers of months in each $\overline{DG/DE}$ class result 10, 4, 29, 46, 51, 63, 53, 18, 17, 9. They check this Markov matrices system using data from a set of 24 U.S. localities, not used to construct the matrices library, and found an overall good agreement ,by Smirnov test, between the yearly empirical and synthetical marginal distributions.

Some discrepancies are partly attributed to the unequality of the used $\overline{DG/DE}$ parameter values to the corresponding values resulting from averages of each simulated month. Nevertheless, even if one chooses to repeat each monthly simulation until coincidence of the two values is obtained, discrepancies remain (possibly due to the previously described lack of univocity in the determination of transition matrices by their $\overline{DG/DE}$ parameter).

Chapter 4

DISAGGREGATING GLOBAL RADIATION

4.1 Introduction

For many years solar radiation data primarily consisted of global irradiation data (on hourly, daily and often monthly basis) on horizontal surface. Since, for many applications, both the diffuse and the beam components of solar irradiation are needed the problem arose of investigating the statistical relationship betweeen the diffuse and the global components. Nowadays, data are allowable for both these quantities at many localities in the world. Nevertheless, for many other stations and relatively to the historically stored data, the problem of recovering the diffuse and the beam components from the global one is sill unsolved.

The fraction of the diffuse irradiation depends, at any on moment, both on geographical and astronomical factors (the altitude of the concerned locality, the zenith angle of the sun), and on climatological factors (the degree of turbidity, the amount of water vapour in the atmosphere, the extent and type of clouds and the albedo of the terrain). The climatological quantities vary in time in an unpredictable way, so that only *statistical* relationships can be obtained from the data. In fact, under the assumption that the *average* atmospheric characteristics of a given locality only depend on the period of the year, one can obtain regressed relationships for the diffuse irradiation

vs the global one, which are "almost" deterministic in their nature. Of course, these relationships represent averages and can depend on the concerned locality.

With whatever choice of the measuring time interval (X, say) the relationship between XB, XD and XG is obviously given by

$$XG = XD + XB \ .$$

As a consequence, any equation which relates two of the three quantities gives a complete knowlwdge about all other pairwise relations. The same conclusion holds of course if the previous quantities are *normalized* with the corresponding extra-atmospherical irradiation (XE), yelding the global, beam and diffuse *transmittivities* (XG/XE [1], XB/XE and XD/XE), or even with another quantity of the same group (typical are the cases of the *diffuse fraction* XD/XG and of the complementary *beam fraction* XB/XG).

Although the previous observations theoretically hold, we prefer, in this chapter, separately review and discuss two types of statistical regressions found in literature, i.e. those which connect transmittivities and those which connect *fractions* (diffuse or direct) to transmittivities (mainly global).

The reason is simply of a statistical nature, since, for instance, the average of XB/XG (and its variance) is not equal to the ratio of the averages of XB and XG (and so for the variances), so that some care must be applied in looking for and using *regressions* (which are in their essence conditional averages) concerning ratios between statistical quantities. Problems of this kind do not arise if the quantities to be compared are normalized with a non-statistical quantity, as XE is.

We finally note that some discrepancy can also arise concerning XB. The direct measurements of XB are usually performed with a sun tracking pyranometer, whereas the measurements of XD (or those consequently *calculated* of XB, given XG) are made with a fixed pyrheliometer equipped with an adjustable shadow ring or disk. Thus, due on one hand to the shadowing of a portion of the sky dome by the shadow ring and, on the other hand, due to possible spurious

[1] This quantity is also called *clearness index* by many authors

reflections of beam radiation on the sensor, XD measured with a pyrheliometer plus XB measured with a pyranometer rarely sums to XG.

4.2 Regressions between transmittances

Although Parmelee [199] first studied the relationship between DD and DG (or $DB = DG - DD$) for cloudless days, the very beginning of the inquiry about the statistical relationship between such variables dates from the work of Liu and Jordan [163].

These authors compare the empirical relationship between IB/IE and ID/IE with the theoretical one, as previously calculated by Kimball under the hypothesis of clear sky conditions. As experimental data, Liu and Jordan use the values of IB and IE measured at Hump Nountain (N.C.,USA) by More and Abbot [180], reduced by 2.5% to take into account changes in the Pyrheliometric scale. They find the empirical data lower than the theoretical data for all air mass values, and obtain the regressed relationship , independent from air mass,

$$\frac{DD}{DE} = 0.2710 - 0.2939 \frac{DB}{DE}$$

or

$$\frac{DD}{DE} = 0.3840 - 0.4160 \frac{DG}{DE} .$$

They also compare these relationships with the data for Blue Hill, Massachusetts, and Minneapolis, Minnesota, obtaining a quite satisfactory agreement, and suggest their use (under *cloudless sky* conditions) for all localities where the albedo of the terrain and the atmospheric contamination by dust are not greatly different from those of the concerned localities.

Relaxing the cloudless sky condition, Liu and Jordan statistically analyse, month by month, the regression lines for DD *vs* DG and for DD/DE vs DG/DE, using ten years of data for Blue Hill. They obtain a fairly definite empirical relationship (see Fig. 4.1).

Boes et al. [49], using one year of data from three US stations (Albuquerque, Blue Hill and Omaha), deduce a relationship between

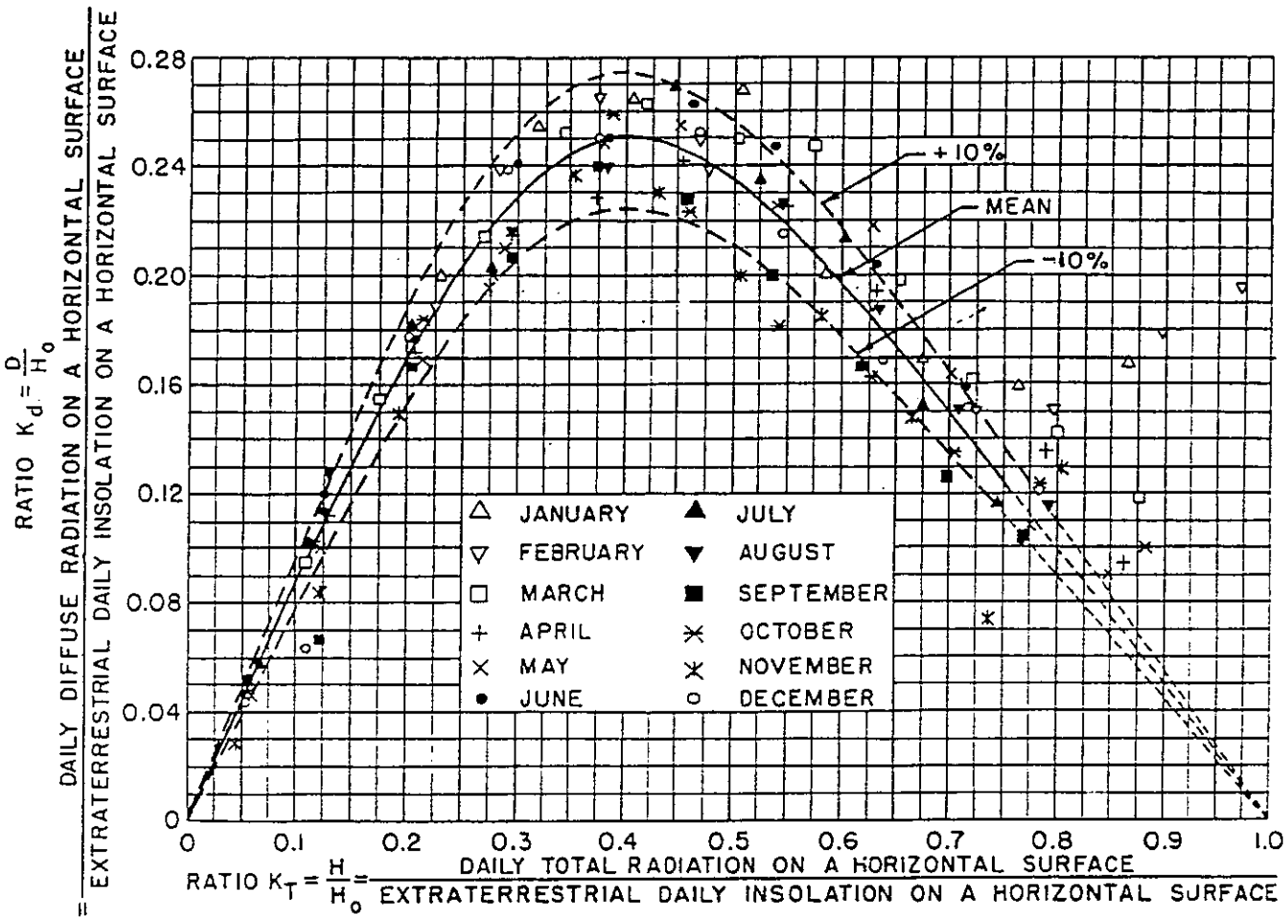

Figure 4.1: Regressed relationship between DD/DE and DG/DE. From Liu and Jordan (80).

the (hourly averaged) beam normal irradiance and the hourly global transmittance:

$$IB_n = 0.4kW/m^2 \quad (\alpha < 10^o, \frac{HG}{HE} > 0.5)$$

$$IB_n = 0\ kW/m^2 \quad (\frac{HG}{HE} \leq 0.3)$$

$$IB_n = -0.52 + 1.80\frac{HG}{HE}\ kW/m^2 \quad (0.3 < \frac{HG}{HE} \leq 0.85)$$

In the range $HG/HE > 0.85$ the data suggest values of IB_n ranging from 0.95 to 1.05, depending on the month.

Biga and Rosa [45] extensively analyze hourly and daily irradiation values measured over five years at Lisboa, Portugal. They find, both theoretically and experimentally, a linear correlation

$$\frac{HD}{HE} = c_1 - c_2\frac{HB}{HE}$$

betweeen the hourly diffuse and beam transmission coefficients under cloudless sky condition. No drastic dependence on the air mass is observed. In Fig. 4.2 the coefficients c_1 and c_2 are reported, together with the corresponding correlation coefficient, for each month. Of course, a linear regression consequently holds for HD/HE *vs* HG/HE.

An analysis of the correlation between beam and global irradiation is performed by Gordon and Hochman [109], who use 11 years of hourly horizontal global and normal beam irradiation measurements for Bet Dagan (Israel). The data set , filtered for basic inconsistencies, is composed of 2947 days (spanning 9 complete years) and 35343 hours. From this appreciable data base the authors generate joint frequency distribution for hourly, daily and monthly values of the beam and the global transmittance with intervals of 0.02. The authors do not analyse statistically these frequency distribution matrices, but use them to calculate regressions (i.e. conditional averages) for HB/HE *vs* HG/HE and viceversa, DB/DE *vs* DG/DE and viceversa and MB/ME *vs* MG/ME and viceversa. The regression curves are reported (see Fig. 4.3) together with the corresponding curve of Erbs *et al.* [82], which are based on a 65 month database for four stations in

Month	Regression Parameters c_1	c_2	Number of observations	Correlation coefficient
January	0.273	0.258	144	0.67
February	0.287	0.267	95	0.87
March	0.329	0.300	144	0.67
April	0.330	0.339	85	0.94
May	0.319	0.316	131	0.74
June	0.292	0.309	109	0.80
July	0.338	0.371	144	0.66
August	0.294	0.310	154	0.81
September	0.314	0.324	114	0.73
October	0.289	0.288	57	0.75
November	0.300	0.303	90	0.80
December	0.266	0.248	88	0.72
YEAR	0.303	0.303	1355	0.76

Figure 4.2: Coefficients of the regression equation of HD/HE vs HG/HE. From Biga and Rosa (79).

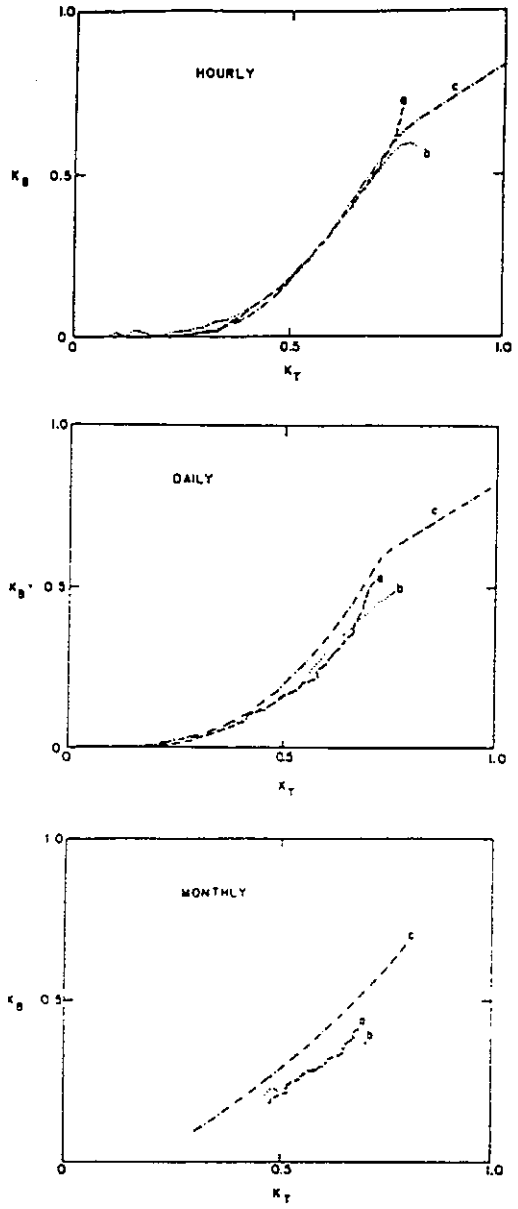

Figure 4.3: Hourly, daily and monthly beam *vs* global transmittance correlations [(a) abscissae *vs* ordinate regressions, (b) ordinates *vs* abscissa regressions, (c) Erbs *et al.* (82) regressions]. From Gordon and Hochman (84).

the USA and checked against 48 months of measurements for Highett, Australia.

The hourly regressions show an impressive agreement, whereas the agreement gradually disappears for daily and monthly regressions, due to the difference of the hourly and daily sequence patterns for different climates.

R. Bruno [62], using data from Hamburg (West Germany) relative to two years, analyses the regression of HD/HE vs. HG/HE over 4200 hourly data. He suggests the formula

$$\frac{HD}{HE} = a\,\frac{HG}{HE} + b\,sin(c\,\frac{HG}{HE})$$

where

$$a = 0.31 \qquad b = 0.139 \qquad c = 4.62 \ .$$

In order to model the HD values for simulation purposes, the author analyzes the dependence of the standard deviation σ of HD/HE on HG/HE, and proposes

$$\sigma = \alpha\,\frac{HD}{HE}\,\frac{HG}{HE}\,\frac{HG/HE-\beta}{HG/HE-\gamma}$$

where

$$\alpha = 0.81 \qquad \beta = 0.942 \qquad \gamma = 1.09 \ .$$

Neuwirth [183] looks for estimates of $[MD]$ from $[MG]$ (long-term averages referring to each single month of the year)

$$\frac{[MD]}{ME} = A_1 + B_1\,\frac{[MG]}{ME}$$

$$\frac{[MD]}{ME} = A_2 + B_2\,\frac{[MG]}{ME} + C_2\,(\frac{[MG]}{ME})^2.$$

He uses long-term monthly sums for Vienna, Salzburg and Sonnblick and reports the best coefficients (see Fig. 4.4). The same fitting formulae are also used in order to establish relationships between hourly values summed up (or averaged) during a whole month and a comparison between the observed and the estimated values is performed, showing a good agreement except for Sonnblick (3106 m a.s.l.).

location	form of regression
Vienna	$K = 1.059 - 1.193K_T$
	$K = 1.274\exp(-1.99K_T)$
	$K_d = 0.158 + 0.171K_T$
	$K_d = -0.072 + 1.494K_T - 1.813K_T^2$
Salzburg	$K = 0.854 - 0.862K_T$
	$K = 1.01\exp(-1.74K_T)$
	$K_d = 0.15 + 0.128K_T$
	$K_d = 0.274 - 0.459K_T + 0.669K_T^2$
Sonnblick	$K = 0.625 - 0.154K_T$
	$K_d = 0.086 + 0.366K_T$
	$K_d = -2.874 + 11.44K_T - 10.286K_T^2$

Figure 4.4: Regression formulae for the relationships between MD/ME, MD/MG and MG/ME using various regression curves. From Neuwirth (80).

Ideriah [130] compares the empirical relations of XD/XE and XG/XE (X represents *daily*, *weekly* or *monthly* time interval) with the corresponding curves of Liu and Jordan and of Ruth and Chant [219], using data for Ibadan, Nigeria. He finds that the Liu and Jordan curves underestimate the diffuse irradiation, whereas those of Ruth and Chant fit the Nigerian data despite appreciable scatter.

Garrison [97] studies measurements of hourly beam normal and global solar irradiation for Albuquerque (New Mexico), Fort Hood (Texas), Livermore (California), Meynard (Massachusets), Raleigh (North Carolina) and measurements of hourly diffuse and global solar irradiation for Highett, Australia. The length of the periods during which the data were collected ranges from one to four years. Although most of the data had previously be used by various authors to seek overall information about the relationships between diffuse and global irradiation, the study of Garrison mainly refers to the dependence of these relationships on air mass and time of the day and of the year, and on other variables affecting them.

As the first step, the author sorts the pair of corresponding HD/HE and HG/HE values into two dimensional frequency tables, with intervals of 0.03 for both quantities, for different solar elevation ranges, different solar hours and different months and seasons. Combined histograms for all data for each site year are also formed, which appear appreciably different, due to the obvious different climates (this can be shown by the analysis of the marginal frequency distribution of HG/HE). Garrison tests the hypothesis that the conditional frequency distributions of HD/HE given HG/HE (in a chosen 0.03 range) are given by similar overall matrices for different localities using a suitable defined *likelihood* L, defined as

$$L = \sum_i (N_i + 1)\ log(M_i + 1),$$

where N_i and M_i are the conditional (percent) frequencies in the i-th interval for the site under comparison and for the reference site respectively. The unit terms avoid taking the log of zero for empty intervals. In this analysis the ranges $0.42 - 0.78$ for HG/HE and $0 - 0.45$ for HD/HE are chosen. L takes its minimum value if $N_i + 1$ is proportional to $M_i + 1$ (under the condition $\sum_i M_i = constant$).

		Comparison Site											
Basis Site		(1)	(2)	(3)	(4)	(5)	(6)	(7)	(8)	(9)	(10)	(11)	Average Random
Maynard 75	(1)	100	81	74	78	42	65	67	68	46	58	25	
Maynard 76	(2)	83	100	76	84	63	75	80	69	51	55	20	
Highett 75	(3)	75	77	100	80	49	61	71	69	63	66	50	
Highett 76	(4)	77	83	79	100	52	73	77	72	57	58	23	
Livermore	(5)	68	80	72	74	100	66	82	57	49	50	28	
Ft. Hood	(6)	62	70	50	69	24	100	59	63	27	21	-27	
Raleigh	(7)	76	85	79	84	73	73	100	68	53	54	28	0
Albuquerque	(8)	62	59	59	64	9	56	44	100	51	43	6	
Albuquerque	(9)	42	41	55	50	2	30	22	56	100	57	39	
Albuquerque	(10)	61	55	68	61	13	38	41	52	63	100	62	
Albuquerque	(11)	52	47	67	54	16	30	36	49	62	72	100	

Figure 4.5: Relative likelihood values from comparison of annual histograms of HD/HG, HG/HE pairs for various sites. From Garrison (84).

The author linearly transforms the obtained L-values in order that the comparison of a site with itself gives 100 and comparison of a site with random data gives zero. Results are reported in Fig. 4.5.

Regression curves of HD/HE *vs* HG/HE (i.e. means of the HD/HE values for each HG/HE 0.03 interval) are also reported for each site and the dependence of these curves on solar elevation (intervals 4-20 deg., 20-40 deg., 40-60 deg.) and season (October-March and April-September) is shown for one site. Other similar curves are reported putting five sites together.The form of these curves appears to be most closely correlated with the average value of HG/HE for each case, and this value shows in turn a marked dependence on solar elevation, but no definitive conclusion is drawn. No dramatic depen-

dence of the concerned relations on the season is found.

Finally the author compares the daily regression of DD/DE *vs* DG/DE with the corresponding hourly, and discusses the origin of the differences.

In a subsequent work, Garrison [98] extends his study to thirty-three U.S. sites with latitudes between $25°N$ and $48°N$, except for Guam ($13.55°N$) and San Juan ($18.26°N$), and a great variety of longitudes, elevations a.s.l. and climatic conditions. The data include hourly values of global and beam irradiance (hourly values of diffuse irradiance for eight stations is also reported) betweeen 8 a.m. and 4 p.m.; they sum up to about 101 years of hourly global irradiation measurements for all 33 sites combined (an average of about three years per site) and to about 57 years of hourly beam irradiation measurements (an average of less than two years per site). For each site the mean surface albedo ($< A >$), mean precipitable water ($< P >$) and mean atmospheric turbidity ($< T >$) during Winter and Summer are also reported as taken from various references or suitably estimated.

Joint frequency histograms for HD/HE and HG/HE are built as in the previous work using intervals of 0.05. Different histograms are formed for pairs occurring in different solar elevation ranges, different months, different years and different sites. The next step consists of combining for each site the Winter months and the Summer months separately, according to solar elevation range and year, and combined for all years. The Summer months are taken to be June through September, the Winter months to be December through April, except for sites with noticeable snow cover (December through February), in order to have approximately uniform values of mean atmospheric precipitable water, turbidity and surface albedo over the period of months considered, and to still maintain a large data set. Analysis of these histogram leads to the separation of the 33 sites into 6 classes for Winter months and 6 classes for Summer months, according to given groups of ($< A >, < T >, < P >$) values.

Regression lines for HD/HE *vs* HG/HE are reported for the six Summer and the six Winter classes, distinguishing in each case different ranges of solar elevation (see Fig. 4.6).

The author claims that the large data set used in the study shows rather convincingly that climatic differences due to the latitude, alti-

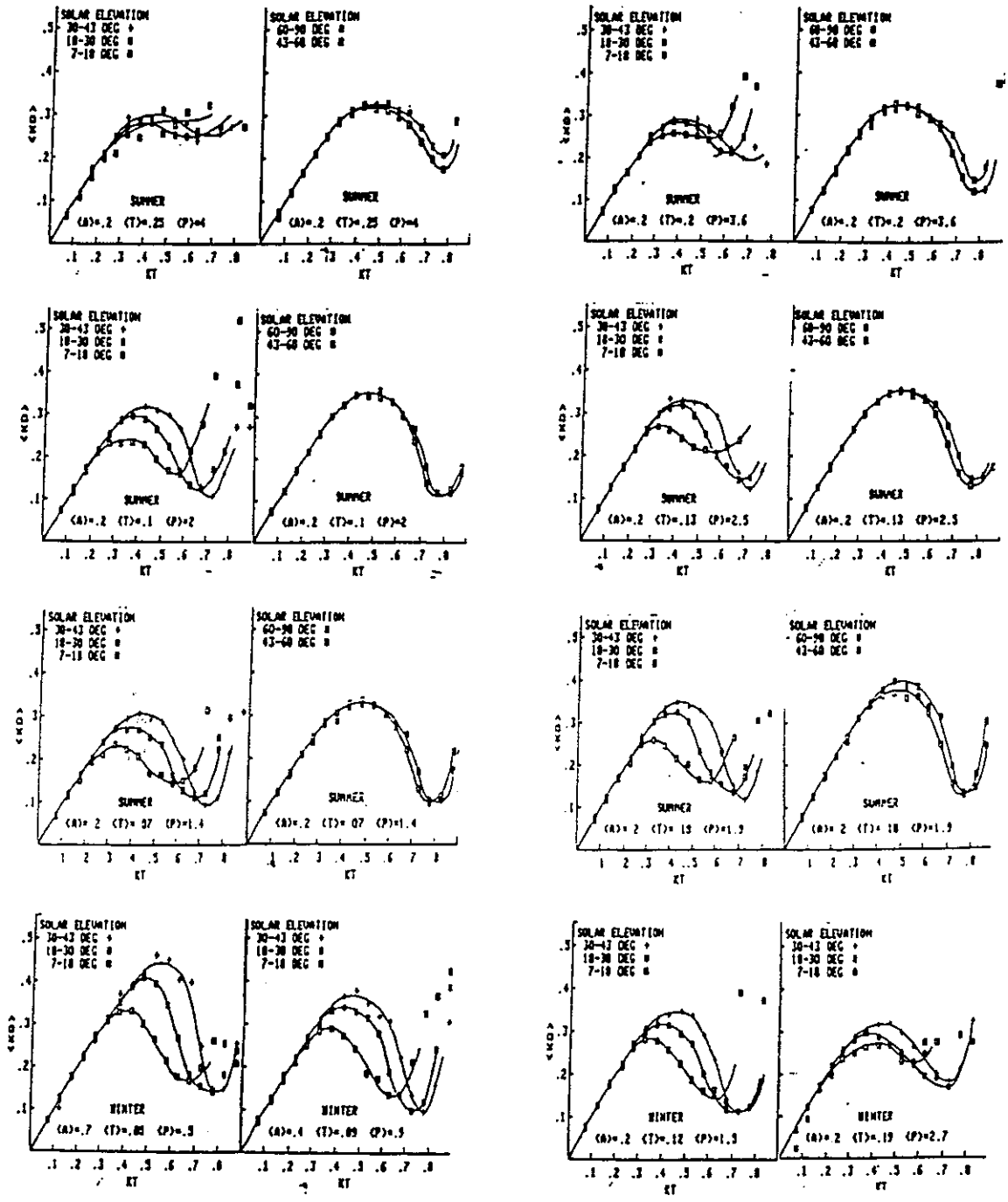

Figure 4.6: Regressions of HD/HG vs HG/HE for various climatical classes and solar elevations in Summer and Winter. From Garrison (85)

tude a.s.l. and other factors can be adequately summarized by groups of $(< A >, < T >, < P >)$ values, so that the regression of HD/HE on HG/HE is shown to depend on the three previous variables and on the solar altitude. He suggests a similar study for tropical sites and sites with latitudes greater than 48°.

Al-Hamadani *et al.* [6] fit the daily diffuse transmission coefficient DD/DE *vs* DG/DE with the formula

$$\frac{DD}{DE} = \frac{DG}{DE}(1 - e^{A\,(1-\frac{B}{DG/DE})})$$

The B coefficient represents the non zero intercept DG/DE value, while A determines the maximum DD/DE value. Substituting the experimental data, the formula

$$\frac{DD}{DE} = \frac{DG}{DE}(1 - e^{\frac{0.41}{B-0.45}(1-\frac{B}{DG/DE})})$$

is obtained, where $B = 0.74$ is the maximum (clear-sky) global trasmissivity.

4.3 Fractions *vs* global transmittance

As for the relationships between transmittances, the inquiry about statistical regressions between irradiation fractions and transmittances dates from the fundamental work of Liu and Jordan [163]. We recall that they use ten years of data from Blue Hill, Mass. (USA). The authors obtain the first regression of DD/DG *vs* DD/DE (Fig. 4.7), which has been in fact the reference point for many years for researchers in the field. The regression line suffers discrepancies for values of DG/DE greater than 0.75, a fact that the authors attribute to their choice of using a *fixed* value of DE for each month, so that for almost clear sky the imprecision of the ratio becomes important.

The regressed relation of DD/DG *vs* DG/DE suggests that an analogous relation can exist between the twelve pairs of *monthly* ratios $[MD/MG]$ and $[MG/ME]$, where $[\ldots]$ indicates the average over many years for a given month of the year. Indeed, Liu and Jordan shown this relationship (see Fig. 4.8) taking their data from Blue

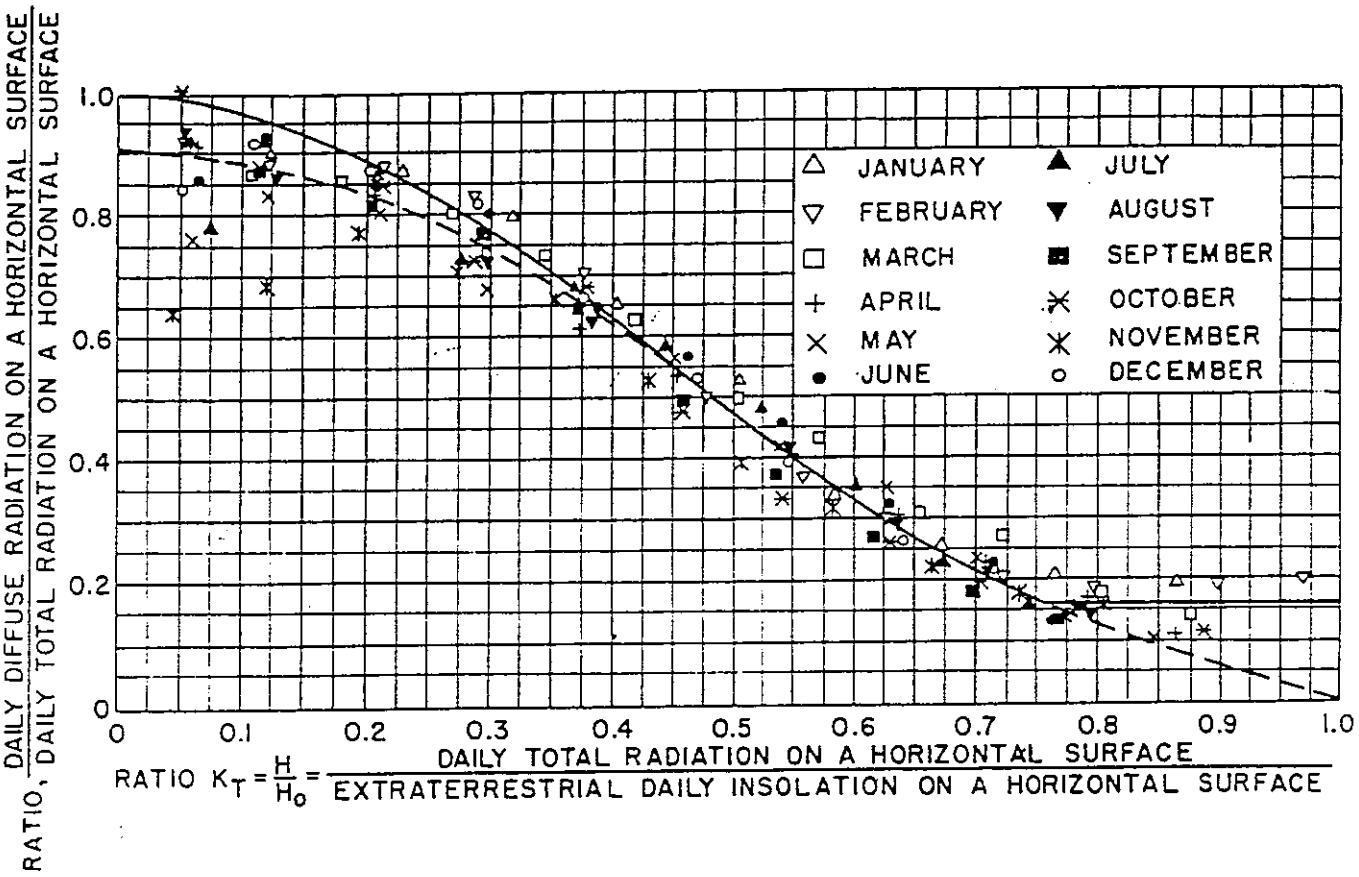

Figure 4.7: Regressed relationship between DD/DG and DG/DE. From Liu and Jordan (80).

Hill,Massachussets (ten years), Nice, France (three years), Helsingfors, Finland (four years) and Kew, London, U.K.(five years).

Page [194] develops a correlation for the monthly ratios MD/MG *vs* MG/ME using data from ten widely spread sites located between $40°N$ and $40°S$, obtaining

$$\frac{MD}{MG} = 1.00 - 1.13 \frac{MG}{ME} .$$

Choudhury [71] performs a similar analysis on daily data using measurements taken at New Dehli, India, and finds a linear relationship

$$\frac{DD}{DG} = 1.36 - 1.48 \frac{DG}{DE} .$$

Also Kalma and Fleming [137] study the correlations between the same quantities.

As already said, the empirical daily and monthly curves of Liu and Jordan (together with the monthly curve of Page) were considered for about twenty years as the main reference for deducing the daily or monthly diffuse irradiation from the corresponding global irradiation.

Nevertheless, the general assumption of the almost universal applicability of the L-J curves was in fact questioned by Ruth and Chant [219] who refer to four Canadian localities, finding generally higher values of the diffuse radiation compared to those of Liu an Jordan, and Orgill and Hollands [193]. The last authors and Bugler [63] give a correlation between the *hourly values* of the same quantities and report new regression curves.

Klein [146] develops a mathematical fit for the Liu and Jordan regression curve, originally reported only in graphical form:

$$\frac{MD}{MG} = 1.39 - 4.027\frac{MG}{ME} + 5.531(\frac{MG}{ME})^2 - 3.108(\frac{MG}{ME})^3 .$$

According to this author, Page's correlation fits data from India [71], from Israel [241], and from Australia [187] better than the Liu and Jordan's correlation.

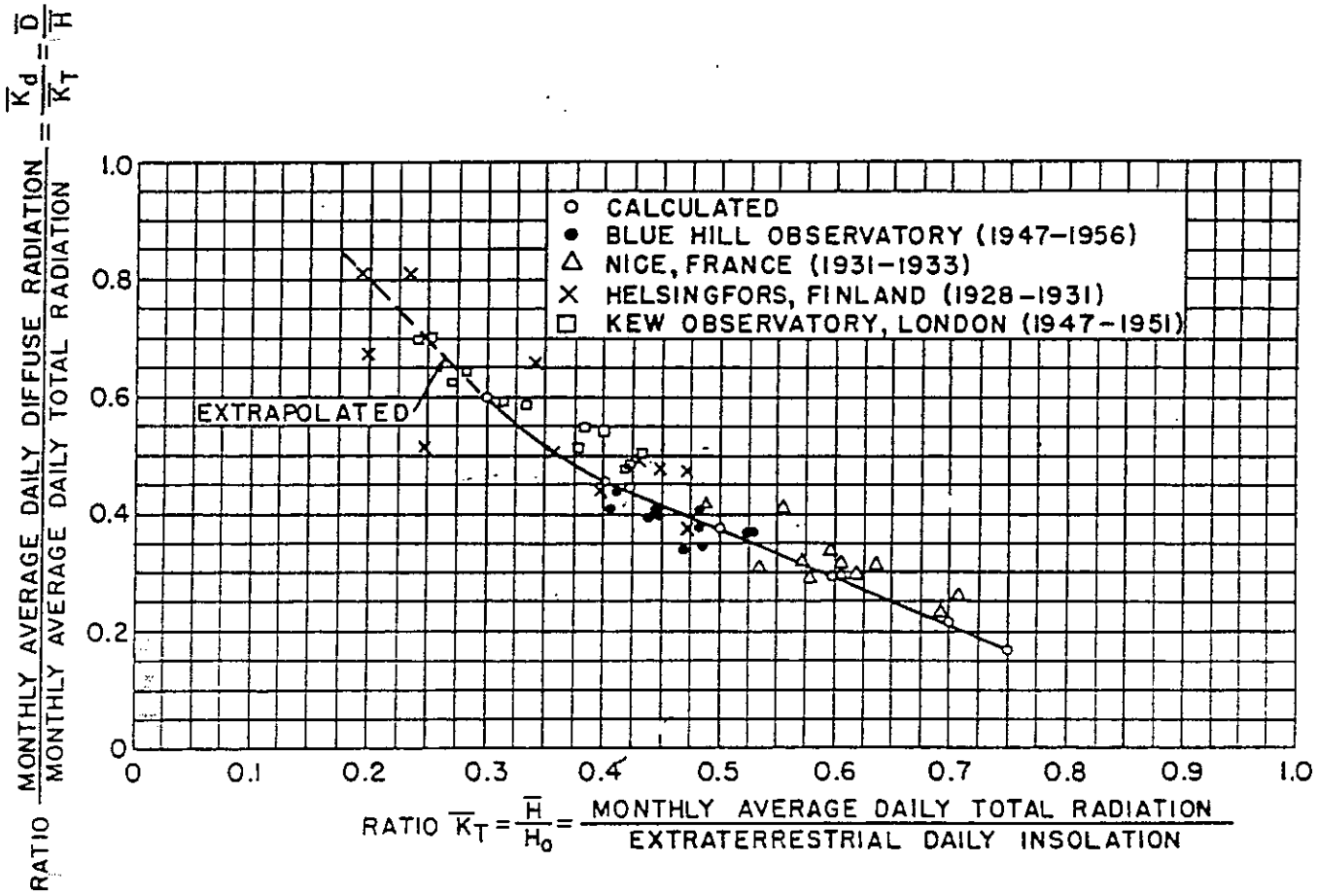

Figure 4.8: Regressed relationship between $[MD/MG]$ and $[MG/ME]$. From Liu and Jordan (80).

Tuller [249] also finds some discrepancies between the L-J relations and those relative to four Canadian localities. He suggests the regression curve

$$\frac{MD}{MG} = 0.84 - 0.62 \frac{MG}{ME} .$$

Nevertheless, the inclusion of the data from Resolute, Canada, which is inside the polar circle and gives anomalous results, makes this correlation not too reliable. The data from Resolute have been later recognized as "anomalous" both for latitudinal and for climatical (snow cover) factors.

Hay [119] presents a revised hourly relationship which incorporates information about local cloud cover and ground albedo.

In order to give a mathematical fit of the monthly regression, Ambrosone *et al.* [10] add the monthtly values ratio relative to Macerata (Italy) to the data of Liu and Jordan and suggest the fitting formula:

$$\frac{MD}{MG} = 1.65 \, (e^{-\frac{MG}{ME}} - e^{-1}) .$$

Modi and Sukhatme [15], while estimating the daily global and diffuse irradiation for many localities in India using climatological data, fit the monthly data for 12 Indian cities and find the linear regression

$$\frac{MD}{MG} = 1.4112 - 1.6956 \frac{MG}{ME}$$

for $0.34 \leq MG/ME \leq 0.73$, with a coefficient of determination $r^2 = 0.93$. They notice that this regression gives a much more diffuse fraction for India than that found by Liu and Jordan, mainly for lower values of MG/ME.

Biga and Rosa [45], analyzing hourly and daily irradiation values measured over five years at Lisboa, Portugal, deduce for the daily values the regressed line (see Fig. 4.9) :

$$\frac{DD}{DG} = 1.26 - 1.50 \frac{DG}{DE}$$

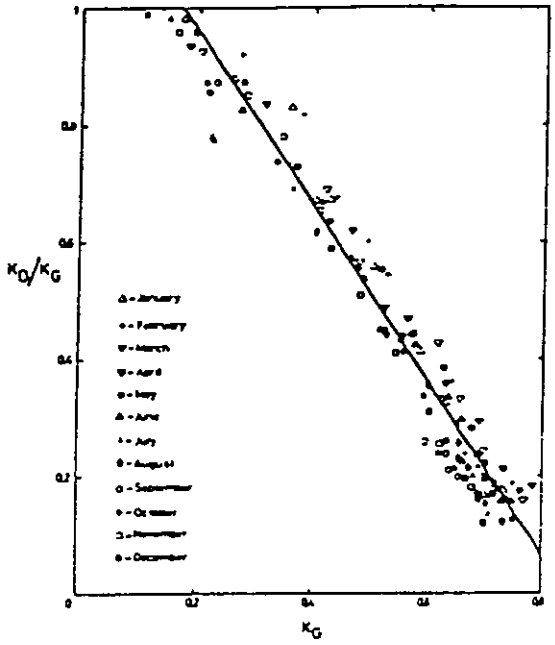

Figure 4.9: Regression of DD/DG *vs* DG/DE. From Biga and Rosa (79).

which applies fairly well over the whole range of observed DG/DE. Comparison with the corresponding coefficients of the Liu and Jordan and Choudhury regression is shown.

Iqbal [133], using about ten years of data for three Canadian localities, obtains the relationships

$$\frac{[MD]}{[MG]} = 0.958 - 0.982 \frac{[MG]}{[ME]}$$

for the combined Toronto-Montreal data, with a standard error of the estimate of 0.04, and

$$\frac{[MD]}{[MG]} = 0.914 - 0.847 \frac{[MG]}{[ME]}$$

adding to the previous data those for Goose Bay, resulting in a standard error of the estimate of 0.05. (see Fig. 4.10).

A comparison is performed month by month over the whole year between the measured values of MD and their estimates following the

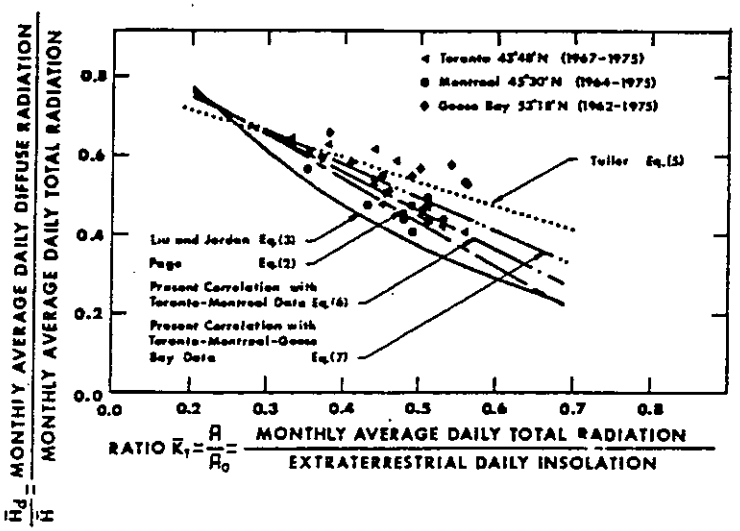

Figure 4.10: Regression between $[MD]/[MG]$ and $[MG]/[ME]$. From Iqbal (79).

regressed relationships found by the author and those of Liu-Jordan and Page.

A mathematical fit of the Ruth and Chant [219] daily regression curve (originally presented in graphical form only) is also performed, giving

$$\frac{DD}{DG} = 0.910 - 1.154\frac{DG}{DE} - 4.936(\frac{DG}{DE})^2 + 2.848(\frac{DG}{DE})^3 \ .$$

Collares-Pereira and Rabl [74] analyze data from Albuquerque (New Mexico), Fort Hood (Texas), Livermore (California), Maynard (Massachusetts) and Raleigh (N.Carolina) covering three years on average and regress DD/DG *vs* DG/DE obtaining a fourth degree polynomial fit

$$\frac{DD}{DG} = 0.99 \qquad [\frac{DG}{DE} \leq 0.17]$$

and

$$\frac{DD}{DG} = 1.188 - 2.272\frac{DG}{DE} + 9.473(\frac{DG}{DE})^2 - 21.856(\frac{DG}{DE})^3 + 14.648(\frac{DG}{DE})^4$$

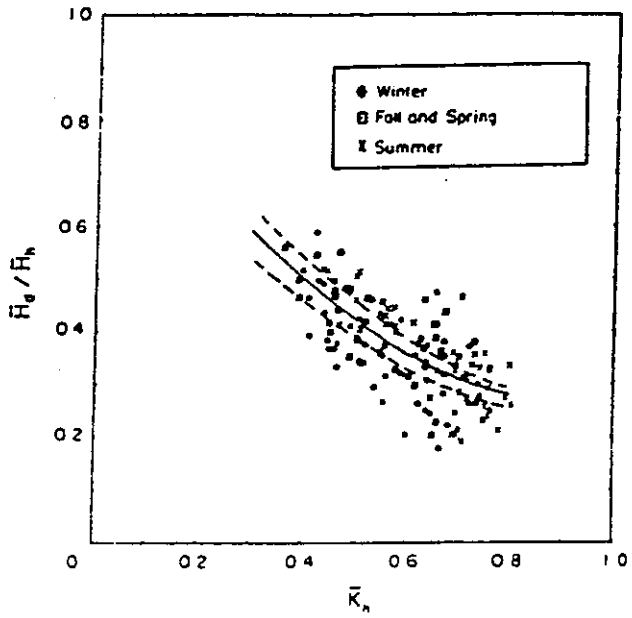

Figure 4.11: Regression of MD/MG *vs* MG/ME. From Collares-Pereira and Rabl (79).

for $0.17 \leq DG/DE \leq 0.8$.

The standard deviation of the fit is also reported for each 0.05 DG/DE interval. The values of DD/DG, generally higher than those of Liu and Jordan, are explained with the shade ring correction procedure used by the authors. A comparison between regressions on a seasonal basis does not reveal significant differences, but for very high values of DG/DE. The same authors also investigate the possible dependence of the regression MD/MG *vs* MG/ME on the season of the year. By choosing to distinguish the seasons by three sunset angle intervals ω_s, they obtain the parametrized fit (see Fig. 4.11)

$$\frac{MD}{MG} = 0.775+0.347(\omega_s-\frac{\pi}{2})-[0.505+0.261(\omega_s-\frac{\pi}{2})]\ cos[2(\frac{MG}{ME}-0.9)].$$

Moreover, in order to get a clearer demonstration of the seasonal trends, the authors average, for each season, the monthly points over DG/DE intervals of 0.05, obtaining fairly definite patterns which fit well with the previous formulae (see Fig. 4.12). A comparison with the fits of Liu and Jordan and of Page is also performed.

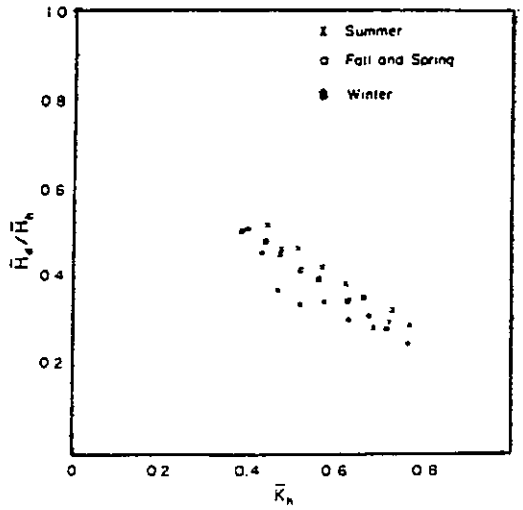

Figure 4.12: Values MD/MG (0.05 MG/ME interval averages) vs MG/ME. From Collares-Pereira and Rabl (79).

Neuwirth [183] looks for estimates of MD from MG using the formulae

$$\frac{MD}{ME} = A_1 + B_1 \frac{MG}{ME}$$

$$\frac{MD}{ME} = A_2 + B_2 \frac{MG}{ME} + C_2 (\frac{MG}{ME})^2.$$

He uses long-term monthly sums for Vienna, Salzburg and Sonnblick and reports the best coefficients (see Fig. 4.4). A comparison with the Liu and Jordan and with the Page formulae is made. The same four fitting formulae are also used to establish relationships between hourly values summed up (or averaged) during a whole month and a comparison between the observed and the estimated values is performed, showing a good agreement but for Sonnblick (3106 m a.s.l.).

Barbaro *et al.* [220] compute the linear regression coefficients for $[MD]/[MG]$ *vs* $[MG]/[ME]$ (long-term single month averages] using five years of data for five localities in Sicilia (Italy) (see Fig. 4.13).

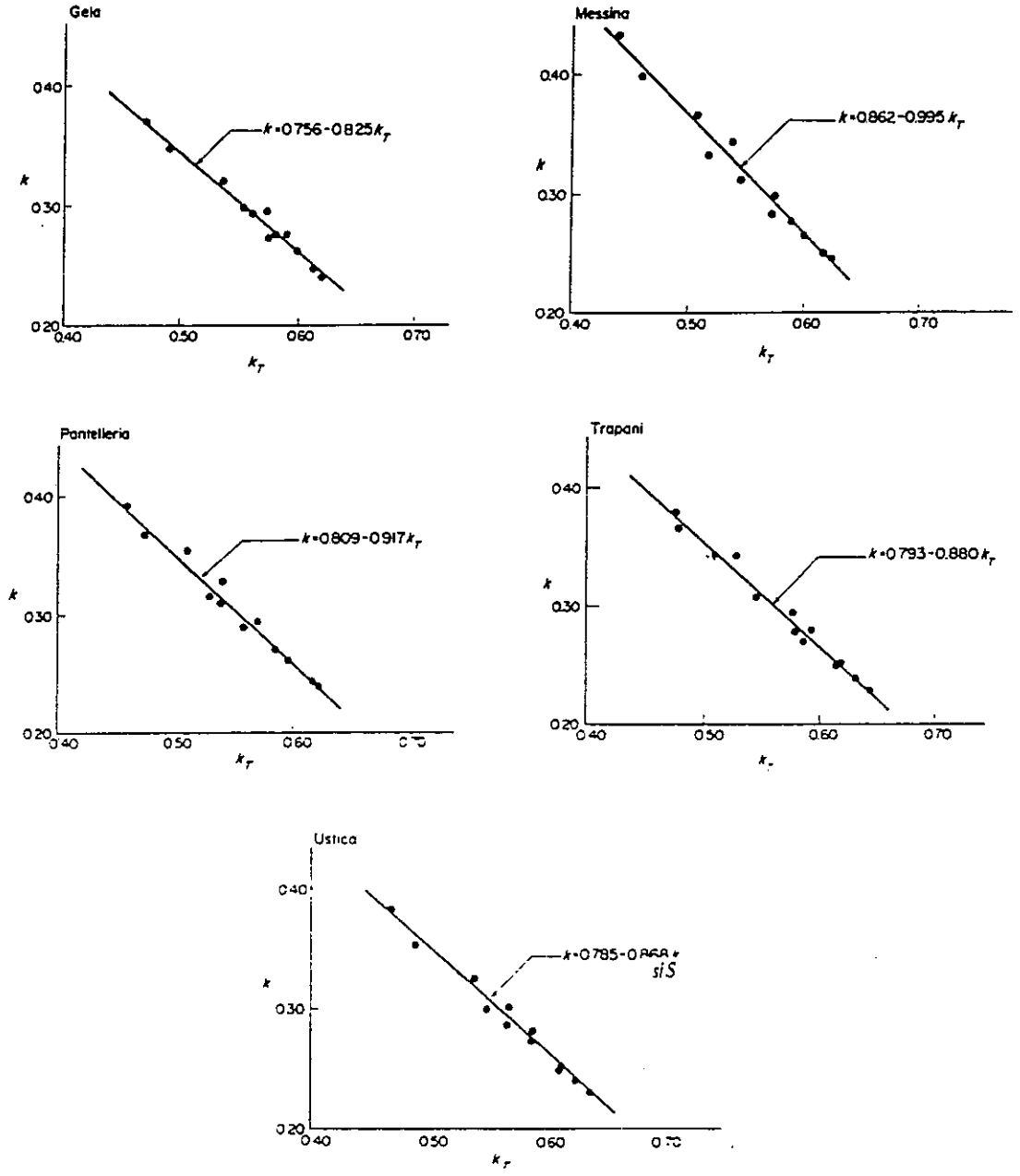

Figure 4.13: Regressions for $[MD]/[MG]$ *vs* $[MG]/[ME]$ for five localities in Sicilia (Italy). From Barbaro *et al.* (80).

The same authors [22] try a linear, quadratic and cubic polynomial fit using the same kind of data for the three Italian localities Palermo (2 years), Macerata(16 years) and Genova (4 years). In order to evaluate the accuracy of the fitting formulae they use the "relative standard error of the estimate"

$$\Phi = \sqrt{\frac{\Gamma}{n}}$$

where

$$\Gamma = \sum_{i=1}^{n} \left(\frac{v_{obs,i} - v_{calc,i}}{v_{obs,i}}\right)^2$$

is the sum of the squares of the relative deviations between observed and calculated values.

Their results are reported in Fig. 4.14. The authors also compare the actual monthly estimates MD with the experimental data and with the estimates obtained through the formulae of Page and Liu and Jordan (as fitted by Klein), and find their own fit performing very well.

Ezekwe and Ezeilo [87] compare one year of precise measurements at Nsukka, Nigeria, whose climate is characterized by a dry season (late November to early February), and during which the dust-bearing north-easterly trade winds can cause an harmattan haze to pervade the atmosphere on many days. When considered in general, the dry-season analysis gives results in good agreement with those of Modi and Sukhatme, yielding the regression (see Fig. 4.15)

$$\frac{DD}{DG} = 1.42 - 1.69 \frac{DG}{DE}.$$

The authors study the apparently clear days and the hazy days separately, and compare results with equations given by different researchers. In the former case, the data seem to agree more with the Page equation (see Fig. 4.16), in the latter with Orgill's correlation formula (see Fig. 4.17).

Scerri [225], analysing the solar irradiation climate of Malta on the basis of twenty five years of measurements, finds the linear correlation between average monthly values

STATION	a_1	a_2	ϕ
Palermo	1.0492	-1.3246	0.0918
Macerata	0.9918	-1.0336	0.0832
Genova	0.7273	-0.7770	0.0390
PA - GE	0.7801	-0.8537	0.0987

STATION	a_1	a_2	a_3	ϕ
Palermo	1.0896	-1.4797	0.1471	0.0918
Macerata	2.6845	-6.6848	4.6701	0.0724
Genova	0.6153	-0.2738	-0.5561	0.0381

STATION	a_1	a_2	a_3	a_4	ϕ
Palermo	13.9375	-76.2760	144.3846	-92.1480	0.0885
Macerata	1.2634	0.3801	-6.9645	6.3493	0.0723
Genova	1.1845	-4.2489	8.5833	-6.9198	0.0380

Figure 4.14: Coefficients and relative standard error of estimate for linear, quadratic and cubic fits of MD/MG *vs* MG/ME. From Barbaro *et al.* (81)

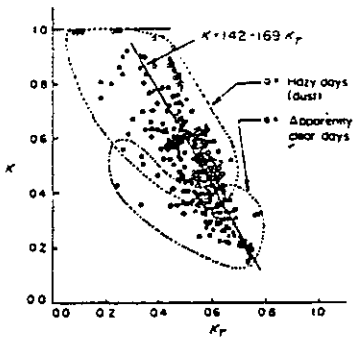

Figure 4.15: Relationship between DD/DG and DG/DE during dry season. From Ezekwe and Ezeilo (81).

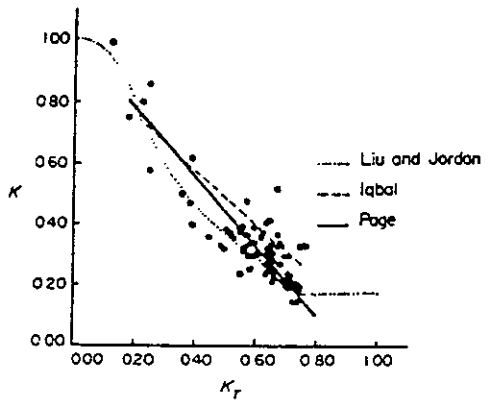

Figure 4.16: Relationship between DD/DG and DG/DE during dry season (bright days). From Ezekwe and Ezeilo (81).

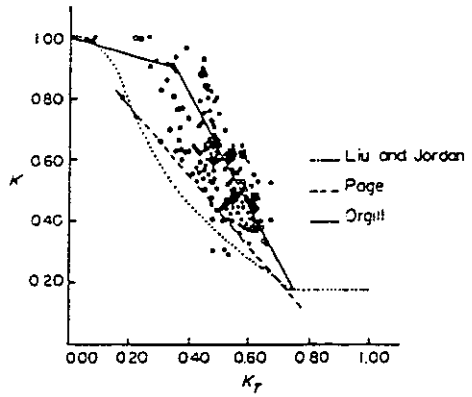

Figure 4.17: Relationship between DD/DG and DG/DE during dry season (hazy days). From Ezekwe and Ezeilo (81).

$$\frac{[MD]}{[MG]} = 1.103 - 1.179 \frac{[MG]}{ME}$$

whose coefficients compare favourably with a list compiled by Page [195].

An original approach for calculating the monthly diffuse irradiation and the monthly ratio MD/MG, based un the use of concurrent global solar irradiation measurements for a tilted and a horizontal surface is described by Kudish *et al.* [149]. The authors use one year of hourly values of global irradiation on horizontal (HG_h)and on a 39° South facing tilted surface (HG_t) at Beer Sheva, Israel. They perform the analysis month by month by classifying each hour as "clear" or "cloudy" in the following way. The first choice is made if the ratio $R = HG_t/HG_h$ is approximately equal to the corresponding ratio for the beam irradiation $R_b = HB_t/HB_h = cos(\theta_t)/cos(\theta_h)$, where θ_t and θ_h are the angles between the sun and the normals to the two surfaces. More precisely, they choose the attribute "clear" if

$$1 - \epsilon < \frac{R_b}{R} < 1 + \epsilon$$

where $\epsilon = 0.15$, and the attribute "cloudy" in the opposite case. Moreover, they assume that during a clear hour the diffuse irradiation comes mainly from the circumsolar region so that

$$R_b = R_d$$

whereas during a cloudy hour it comes isotropically from the whole sky dome, so that the known formula holds

$$R_d = \frac{HD_t}{HD_h} \frac{1 + cos\ s}{2} + \rho \frac{1 - cos\ s}{2},$$

where s is the slope of the surface and ρ is the albedo coefficient (they choose values from 0.2 to 0.7, obtaining quite small dispersions of the conclusive values). For each hour of the day the authors calculate (for both the clear and the cloudy hours groups): the average R_b and R, the number of hours in each group, the monthly average HG and the corresponding calculated DG. Since

$$R = R_b (1 - x) + R_d x$$

where

$$x = \frac{HD_h}{HG_h}$$

is the hourly diffuse fraction on horizontal surface, they determine the monthly average hourly diffuse fraction for cloudy hours as

$$\overline{x} = \frac{\overline{R_b} - \overline{R} + \rho \frac{1-cos\ s}{2}}{\overline{R_b} - \frac{1+cos\ s}{2}}.$$

The monthly average hourly diffuse fraction for clear hours is calculated using first both the Liu and Jordan formula for clear days (as formulated by Klein) and the Page equation to find DD/DG from DG/DE and then the average HD using, for each hour, the equation

$$\frac{HD}{DD} = \frac{HE}{DE}$$

due to Whillier [255] .

Starting from these data and from the relative frequencies of clear and cloudy hours the authors easily determine the monthly average diffuse fraction. Reported results show small sensitivity both to the assumed albedo value and to the equation used for clear days diffuse fraction calculation. Direct graphical comparison with the Liu and Jordan equation and with Page's equation is also performed (see Fig. 4.18).

Erbs *et al.* [82] recognize that considerable disagreement exists between HD/HG *vs* HG/HE, DD/DG *vs* DG/DE and MD/MG *vs* MG/ME, and that this disagreement can produce small or large differences on the annual estimated irradiation on tilted surfaces depending on the type of estimation (few percent for global, more than 10 percent for beam irradiation). The authors separately study the three types of relationships, using a set of accurate and complete hourly data measured at four U.S. localities during about two years.Three years of data recorded in Highett, Australia, are used to test the applicability of the results to other localities.

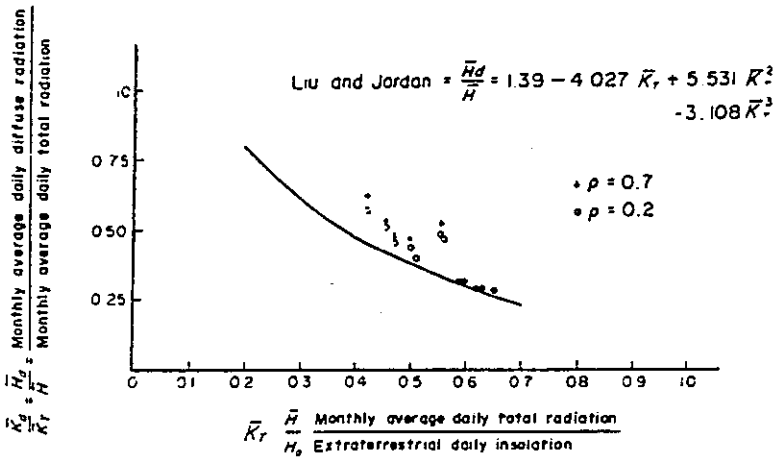

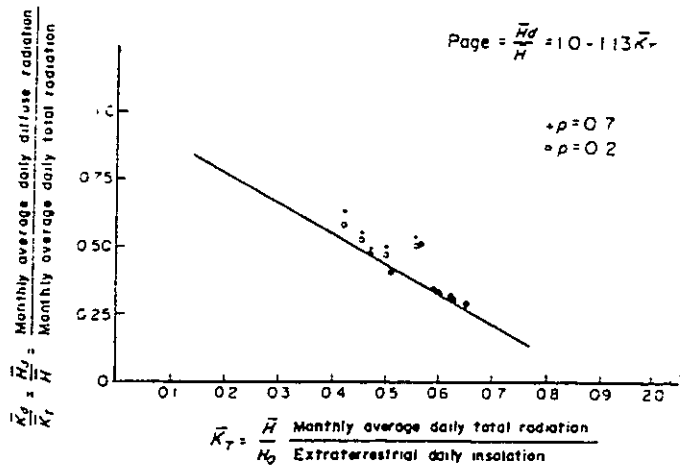

Figure 4.18: Comparison of the pairs MD/MG, MG/ME calculated by the author with those deduced from the formulae of Liu and Jordan (60) and Page (64). From Kudish (82).

The regression of HD/HG on HG/HE is analysed by subdividing the range of the latter quantity into intervals of 0.025. The regressed line is fitted by the formulae

$$\frac{HD}{HG} = 1.0 - 0.09\,\frac{HG}{HE}$$

for $HG/HE \leq 0.22$,

$$\frac{HD}{HG} = 0.9511 - 1.604\frac{HG}{HE} + 4.388(\frac{HG}{HE})^2 - 16.638(\frac{HG}{HE})^3 + 12.336(\frac{HG}{HE})^4$$

for $0.22 < HG/HE \leq 0.80$, and

$$\frac{HD}{HG} = 0.165$$

for $HG/HE > 0.80$.

For greater values of HG/HE (about 0.2 % of the data) no fit is attempted, due to the unsatisfactorily understood increasing of HD/HG (see Fig. 4.19), perhaps caused by spurious reflections of direct irradiation recorded as diffuse.

The "relative standard deviation"

$$\sigma = \sqrt{\frac{\sum^N (HD_m - HD_o)^2}{\sum^N HG}}$$

is somewhat independent from the location and about 95% of the data lie within plus or minus 2σ of the regressed values. Nevertheless, the large size of σ, due in part to seasonal variations in the average diffuse fraction, indicates the possibility of large errors in estimating the diffuse fraction for a particular hour. No significant improvements are obtained by regressing HD/HG *vs* HG/HG_{cs}, where HG_{cs} is the "clear sky" hourly global irradiation, whose beam component is calculated from a model developed by Hottel [122], whereas the diffuse component is calculated using the clear sky correlation of Liu and Jordan.

The daily correlation is studied, following the procedure of Collares-Pereira and Rabl [74], by seasonally dividing the data in three groups, depending on the sunrise hour angle ω_s:

$$\underline{Winter} \qquad \omega_s < 1.4208$$

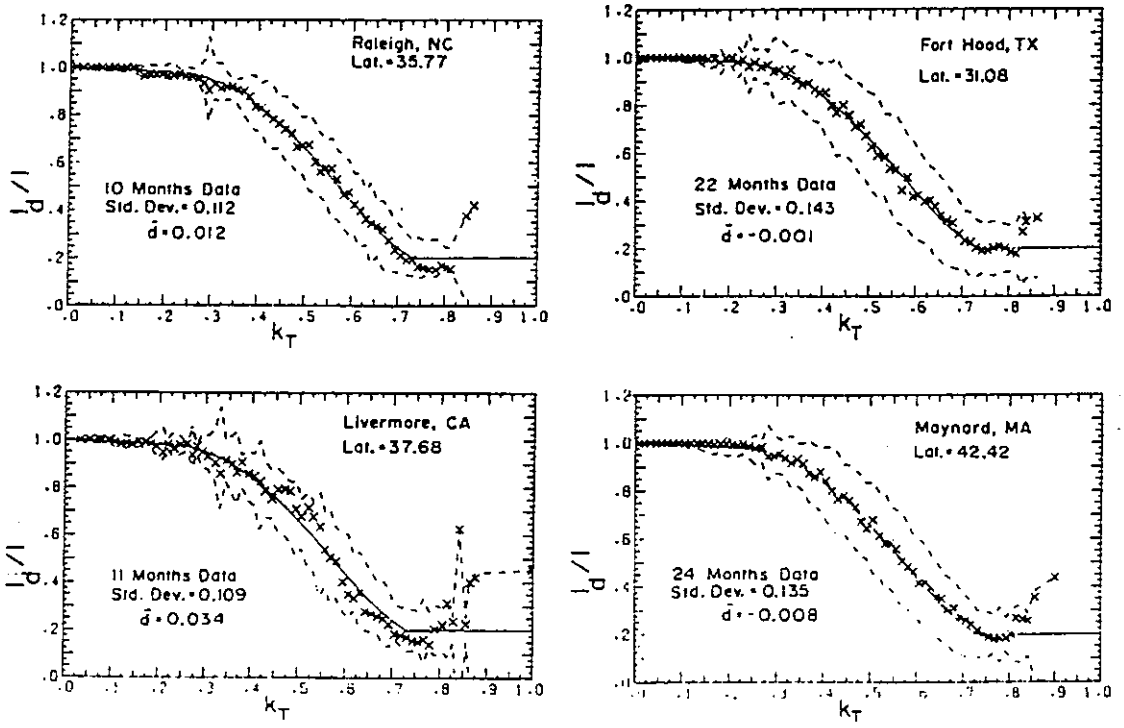

Figure 4.19: Regressions curves of HD/HG *vs* HG/HE for four U.S. sites. From Erbs *et al.* (82).

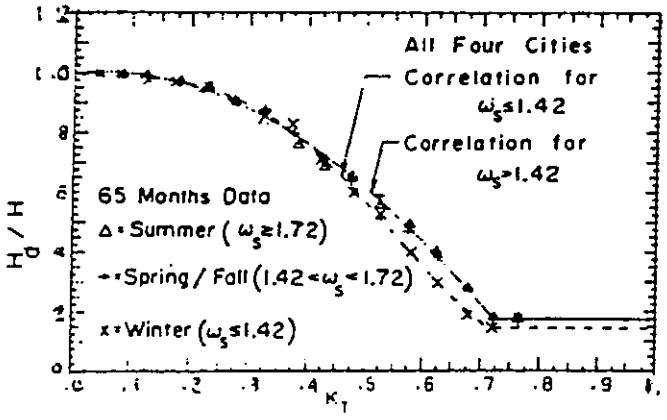

Figure 4.20: Regressions curves of DD/DG *vs* DG/DE for four U.S. sites together. From Erbs *et al.* (82).

Spring and Autumn	$1.4208 \leq \omega_s \leq 1.7208$
Summer	$\omega_s > 1.7208$.

The three regression are almost equal except for Winter and values of DG/DE greater than 0.45, where the diffuse fraction is lower (see Fig. 4.20).

Thus, two fitted equations are needed:

Winter

$$\frac{DD}{DG} = 1.0 - 0.2727\frac{DG}{DE} + 2.4495(\frac{DG}{DE})^2 - 11.9514(\frac{DG}{DE})^3 + 9.3879(\frac{DG}{DE})^4$$

for $DG/DE < 0.715$,

$$\frac{DD}{DG} = 0.143$$

for $DG/DE \geq 0.80$, and

Spring, Summer, Autumn

$$\frac{DD}{DG} = 1.0 + 0.2832\frac{DG}{DE} - 2.5557(\frac{DG}{DE})^2 + 0.8448(\frac{DG}{DE})^3$$

for $DG/DE < 0.722$,

$$\frac{DD}{DG} = 0.175$$

for $DG/DE \geq 0.722$.

Finally, the authors choose to investigate the monthly correlation following the suggestion of Liu and Jordan, i.e using the formula

$$\frac{MD}{MG} = \frac{\sum^N \frac{DD}{DG}\, x}{N < \frac{DG}{DE} >} \quad (x = \frac{DG}{DE})$$

based on the daily values, where $< DG/DE >$ is the average value which parametrizes the standard universal Liu and Jordan curves for the monthly frequency distributions of DG/DE. Thus, the authors use the appropriate L-J curve to choose N values of DG/DE corresponding to equally spaced cumulative frequency points and deduce the correlated values of $\frac{DD}{DG}$ from their daily regressions. In this way, monthly regressions with DG/DE ranging between 0.3 and 0.7 are obtained. They are fitted by the equations:

Winter

$$\frac{MD}{MG} = 1.391 - 0.3560\frac{MG}{ME} + 4.189(\frac{MG}{ME})^2 - 2.137(\frac{DG}{DE})^3$$

and

Spring, Summer, Fall

$$\frac{MD}{MG} = 1.311 - 3.022\frac{MG}{ME} + 3.427(\frac{MG}{ME})^2 - 1.821(\frac{MG}{ME})^3.$$

Moreover, a non seasonal monthly regression is given

$$\frac{MD}{MG} = 1.317 - 3.023\frac{MG}{ME} + 3.372(\frac{MG}{ME})^2 - 1.769(\frac{MG}{ME})^3.$$

Bartoli *et al.* [29], using about seven years of daily measurements recorded in Genova and Macerata (Italy) fit the daily diffuse fraction *vs* the globsl transmittance with the formulae

$$\frac{DD}{DG} = a + (1-a)\ exp[-\frac{b\ (DG/DE)^c}{1 - DG/DE}]$$

and

$$\frac{DD}{DG} = \alpha + \beta\frac{DG}{DE} + \gamma(\frac{DG}{DE})^2 + +\delta(\frac{DG}{DE})^3.$$

For the two functional forms they obtain respectively the parameter values

$$a = 0.154 \quad b = 1.062 \quad c = 0.861 \qquad (Macerata)$$

$$a = 0.0712 \quad b = 0.872 \quad c = 0.947 \qquad (Genova)$$

and

$$\alpha = 0.931 \quad \beta = -0.513 \quad \gamma = -1.849 \quad \delta = 1.613 \quad (Macerata)$$

$$\alpha = 0.879 \quad \beta = 0.324 \quad \gamma = -3.724 \quad \delta = 2.658 \quad (Genova)$$

Since both the regression curves give a root mean square deviation between observed and calculated value of 0.109 for Macerata and of 0.100 for Genova, the authors choose the trascendental curve, which needs only three parameters.Moreover, they calculate the dependence on DG/DE (step 0.01) of the variances of the experimental DD/DG values calculated with respect to both their local average values and the (trascendentally) fitted values. The variances are very similar in trend and order of magnitude, thus demonstrating that the errors in predicting the diffuse ratio, given the corresponding DG/DE value, are not due to the fit but to the intrinsic statistical indeterminacy of the data. Similar tests are performed on the calculated DD and DB.

Spencer [239] presents a comparison between four methods of estimating hourly diffuse from global solar irradiation. His database consists of about four years of half-hourly measurements in twelve Australian stations, and he uses all the stations to fit the data with a piecewise straightline curve following the method of Orgill and Hollands (see below). On the other hand comparison between different methods is performed using data of five stations of widely differing locations and radiation climates. The four methods are the following:

Bugler's method [63]

$$\frac{HD}{HG} = 0.94$$

for $HG/HG_{cs} \leq 0.4$,

$$\frac{HD}{HG} = \frac{1.29 - 1.19\,(HG/HG_{cs})}{1.00 - 0.334\,(HG/HG_{cs})}$$

for $0.4 \leq HG/HG_{cs} \leq 1$ and

$$\frac{HD}{HG} = 0.15$$

for $HG/HG_{cs} \geq 1.0$. The "clear sky" global irradiation HG_{cs} is evaluated from the beam irradiance using the curves of Rao and Seshadri [210] as given by Spencer [240], increased of 5% to allow for circumsolar diffuse irradiance, and from the diffuse irradiance component as suggested by Bugler [63]

$$ID = 16.0\,\alpha^{0.5} - 0.4\,\alpha \;\; W/m^2$$

(α is the solar altitude in degrees).

Liu and Jordan method [163]

$$\frac{HD}{HG} = 0.294\,\frac{HG}{HE} + 0.1445\,sin(4.97\frac{HG}{HE})$$

This formula is suggested by Bruno [62].

Boes et al. method [49]

$$IB_n = 0.4kW/m^2 \quad (\alpha < 10°, \frac{HG}{HE} > 0.5)$$

$$IB_n = 0\;kW/m^2 \quad (\frac{HG}{HE} \leq 0.3)$$

$$IB_n = -0.52 + 1.80\frac{HG}{HE}\;kW/m^2 \quad (0.3 < \frac{HG}{HE} \leq 0.85)$$

The value of the hourly averaged normal beam irradiance IB_n for $HG/HE > 0.85$ is taken as identically equal to 1 kW/m^2. From the

beam irradiance the diffuse component is easily deduced using the global irradiation.

Orgill and Hollands method [193]

$$\frac{HD}{HG} = 1.0 - 0.249\frac{HG}{HE} \quad (\frac{HG}{HE} \leq 0.35)$$

$$\frac{HD}{HG} = 1.557 - 1.84\frac{HG}{HE} \quad (0.35 \leq \frac{HG}{HE} \leq 0.75)$$

$$\frac{HD}{HG} = 0.177 \quad (\frac{HG}{HE} > 0.75)$$

Since this method is suggested by the authors to be accurate between latitudes of 43^oN and 54^oN, Spencer chooses to recalculate the coefficients from the data for each Australian location. For all locations he finds that in the low HG/HE values part of the regression curve the data do not support the non zero slope hypothesis of Orgill and Hollands, and so chooses to assign suitable constant values to each different fit in the intervals $DG/DE < 0.35$ and $DG/DE > 0.75$. In the complementary interval linear fits show correlation coefficients of about 0.99.

To choose the best method from the four, the author chooses to consider as predicting error those arising from estimates of HD instead than HD/HG. After an accurate analysis he concludes that the Orgill and Hollands method with appropriately modified coefficients performs best if the energy obtainable by solar radiation is the prediction task. Nevertheless Spencer judges that it is possible that the other formulae also perform similary well by modification of the related parameters for each location.

The regressions of MD/MG *vs* MG/ME due to Liu and Jordan [163] and to Page [194] have often been tested in various countries in the world outside the latitude range suggested by the authors. More or less different coefficients have been found in order to obtain appreciable correlation coefficients r (see, for instance, Lewis [160] for Zimbabwe with r ranging from 0.96 to 0.99 depending on the locality, Khogali *et al.* [143] for Yemen ($r = 0.96$) and Bamiro [19] for Nigeria ($r = 0.80$)).

For Ibadan, Nigeria, Ideriah [130] gives a comparison between the empirical relationships between XD/XG and XG/XE , where X=D (daily), X=W (weekly) or X=M (monthly) and the corresponding curves of Liu and Jordan and Collares-Pereira and Rabl [74]. He finds that the Liu and Jordan curves underestimate the diffuse irradiation, whereas the curves of Collares-Pereira and Rabl fit the Nigerian data well (nevertheless, an appreciable scatter affects the predicting power of the regression). We note that the diffuse "experimental" values used by Ideriah are in fact values calculated by a model by the same author [129].

A similar underestimation of the diffuse component by the Liu and Jordan curves is found by Desnica *et al.* [78] for three sites in Yugoslavia with different climates. The average error is about 6% per year, but in some months exceeds 15%.

About twenty years after the appearence of the Liu and Jordan correlations, and on the basis of the discrepancies between these curves and the data in various parts of the world, LeBaron and Dirmhirn [153] accurately analyse various effects which have some influence on the regression between the diffuse fraction and the clearness index. They use two years of measurements at two sites approximately $41°N$ latitude in Rocky Mountains, Utah (US), Salt Lake City, in an open valley, 1290m a.s.l., little horizon obstruction, relatively short-lived and intermittent snowcover and Snowbird, Hidden Peak, a mountain top, 3350 m a.s.l., with an entirely free horizon and undisturbed snowcover during Winter and early Spring. The first locality is geographically similar to Blue Hill, Mass., 1463 m a.s.l., where the data originally used by Liu and Jordan were measured. Daily data for both localities are compared with the L-J curves (see Fig. 4.21).

For Salt Lake City, the original curve appears adequate (but most of the values are slightly higher excpet under clear sky). For Snowbird the L-J curve appears to be completely inadequate and, in addition, the high scatter of the experimental points severely reduces the predictive power of any crude regression line. The authors then consider the effect of airmass, cloudiness, turbidity and and multiple reflection between surface and sky on the diffuse irradiance. Since the airmass can be calculated exactly, they first examine the statistical dependence of the diffuse radiation on the cloudiness (measured by

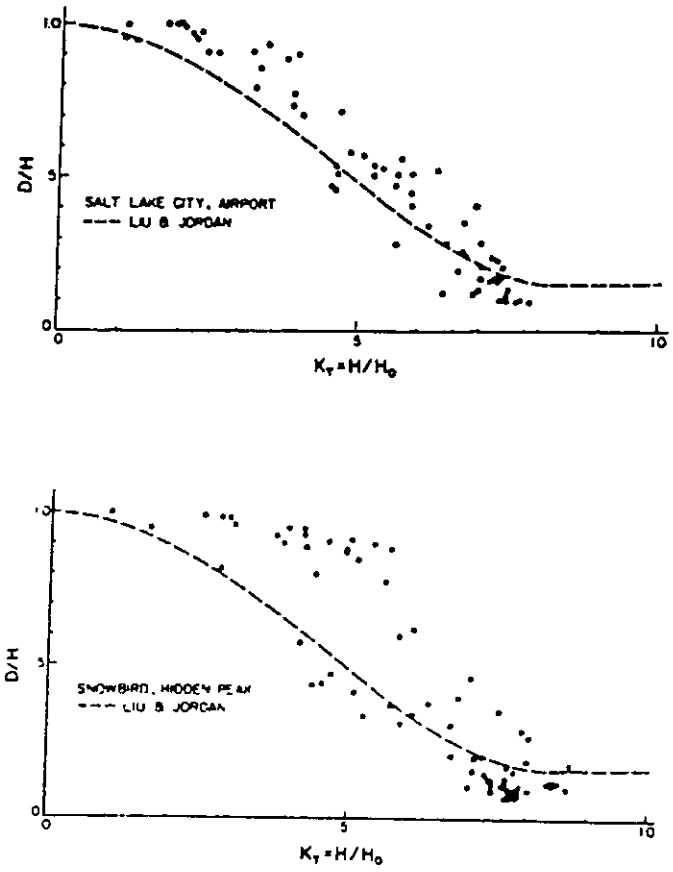

Figure 4.21: Comparison between experimental pairs DD/DG, DG/DE for two different sites in Utah(USA) and the corresponding curves of Liu and Jordan (60). From LeBaron and Dirmhirn (83).

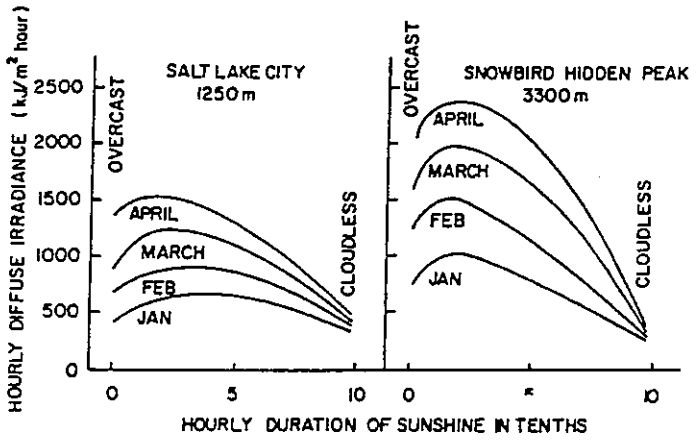

Figure 4.22: Comparison of hourly diffuse irradiance for localities with different altitude a.s.l. *vs* hourly relative sunshine. From LeBaron and Dirmhirn (83).

the relative sunshine in tenths of an hour) for both localities and for each month of the year during four hours around local noon (in order to enhance the effects). The behaviour of the two distinct groups of regressions is similar but it shows remarkable quantitative differences (see Fig. 4.22).

Turbidity is practically absent in the high elevation station, whereas it causes some spread of the experimental points, for clear sky, at the lower station. A seasonal effect due to multiple reflections between the ground and the sky is mainly due to the snowcover during Winter and early Spring, and it enhances the diffuse irradiance at Snowbird with respect with that in Salt Lake City (see Fig. 4.23). This effect causes the diffuse irradiance with snow covered ground to surpass 170% of that with snow-free ground at overcast sky.

On the grounds of this analysis the authors redraw the Liu and Jordan curves using homogeneous data by two intersecting criteria: a) low or high elevation and b) bare or snow covered ground (see Fig. 4.24).

Some differences in the trends of the curves are shown for bare

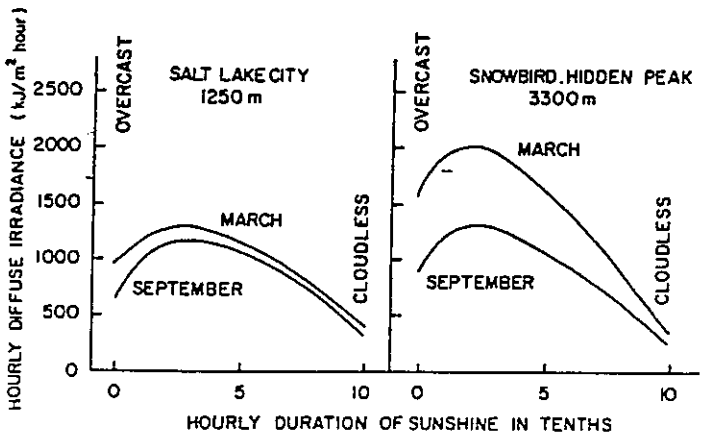

Figure 4.23: Comparison of hourly diffuse irradiance for localities with and without snow cover *vs* hourly relative sunshine. From LeBaron and Dirmhirn (83).

ground, mainly due to the lower scattering level of the diffuse irradiances at high elevation (and clear sky). The most striking difference arises when snow covered groud curves are compared: the multiple reflection causes the entire curve at high elevation to be drastically shifted to the right of the original L-J curve, and the increase in diffuse irradiance with cloudiness is much steeper, reaching its maximum at about $DG/DE = 0.4$. The authors conclude that mainly the effect of surface albedo is to be taken into account when using the Liu and Jordan relations and that it can explain most of the discrepancies found at middle latitudes.

Vignola and McDaniels [253] present correlations betweeen diffuse and global irradiation averaged over 1, 5, 10, 15, and 30 days for six locations in Oregon and Idaho (US), using data collected over a 2- to 4-year period. They calculate the daily diffuse irradiation starting from hourly values of the global irradiation and the normal beam irradiation from the formula

$$HD = HG - HB_n < cos\ \theta >$$

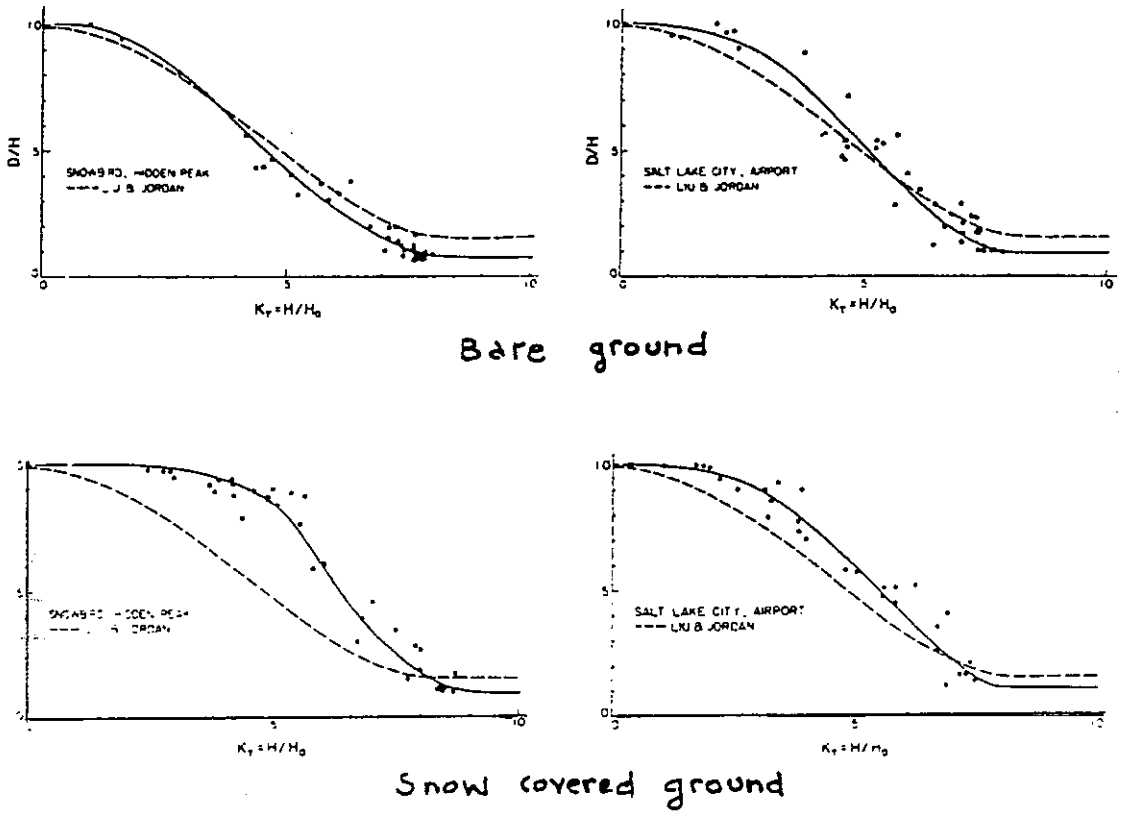

Figure 4.24: Suggested changes of the Liu and Jordan (60) relationship between DD/DG and DG/DE depending on height a.s.l. and ground albedo. From LeBaron and Dirmhirn (83).

where

$$< cos\ \theta > = \frac{\int d\omega\ (e^{-\alpha m} + e^{-\beta m})\ cos\theta}{\int d\omega\ (e^{-\alpha m} + e^{-\beta m})}$$

is a mean value of the cosine of the zenith angle, suitably averaged over each hour weighting the instantaneous value with the *air mass* (m) *transmission factor* (ω is the hour angle of the sun). The authors claim that this averaging procedure allows systematic errors to be avoided, with respect to the simple arithmetic mean, which can be as high as 2-3 % for DD on clear Summer days. The difference between the directly measured hourly totals and the air mass weighted calculated values is always less than 1%.

For each chosen period (1, 5, 10, 15 or 30 days) they calculate the average values of DD/DE and DG/DE, and finally they regress the ratio of the two quantities *vs* the second one. The moving average procedure is performed by successive steps of five days.

Linear regression fits are sufficient for all but the daily correlations, which require a third degree polynomial fit. Resulting coefficients are shown in Fig. 4.25.

The standard deviations for these fits regularly increase from about 0.05 to 0.09 by decreasing the length of the moving average period. Seasonal effects (August through January and February through July) are noticed, but not taken into account during the fitting procedure. Comparison of the results for daily and monthly regression with those of various authors is performed, showing noticeable differences (see Fig. 4.26).

In a subsequent work, the same authors [254] analyse the previously noticed seasonal effects by examining the residual differences between the measured diffuse fractions and those calculated from the over-all best-fit correlation. The residuals, both for daily and for 30-days regressions, are found to exhibit a pronounced sinusoidal yearly behaviour. Fitting sine terms on the residuals Vignola and McDaniels propose the modified regression formulae

$$\frac{MD}{MG} = a + b\,\frac{MG}{ME} + c\ sin(2\pi\frac{N-40}{365})$$

Site	30 day intervals a	b	15 day a	b	10 day a	b	5 day a	b
Burns	1.212	-1.516	1.171	-1.441	1.177	-1.444	1.198	-1.464
Corvallis	1.107	-1.290	1.131	-1.341	1.144	-1.351	1.197	-1.439
Eugene	1.091	-1.295	1.113	-1.338	1.141	-1.383	1.169	-1.414
Hermiston	1.020	-1.149	1.038	-1.169	1.047	-1.185	1.122	-1.305
Kimberly, Idaho	1.072	-1.298	1.078	-1.298	1.078	-1.291	1.133	-1.362
Whitehorse Ranch	1.094	-1.335	1.116	-1.365	1.123	-1.370	1.139	-1.377
All sites[a]	1.093	-1.313	1.104	-1.325	1.118	-1.341	1.155	-1.388

a. Except Corvallis

Site	a	b	c	d
Burns	0.868	1.690	-6.375	3.660
Corvallis	0.965	0.845	-4.430	2.325
Eugene	0.916	1.314	-5.985	3.750
Hermiston	0.926	1.270	-5.789	3.569
Kimberly, Idaho	0.821	1.934	-6.333	3.950
Whitehorse Ranch	0.894	1.433	-6.147	3.755
All sites[a]	0.921	1.218	-5.510	3.241

a. Except Corvallis

Figure 4.25: Empirical linear and cubic correlation coefficients for the regressions of $\overline{DD}/\overline{DG}$ *vs* $\overline{DG}/\overline{DE}$ for different (moving) averaging periods. From Vignola and McDaniels (84)

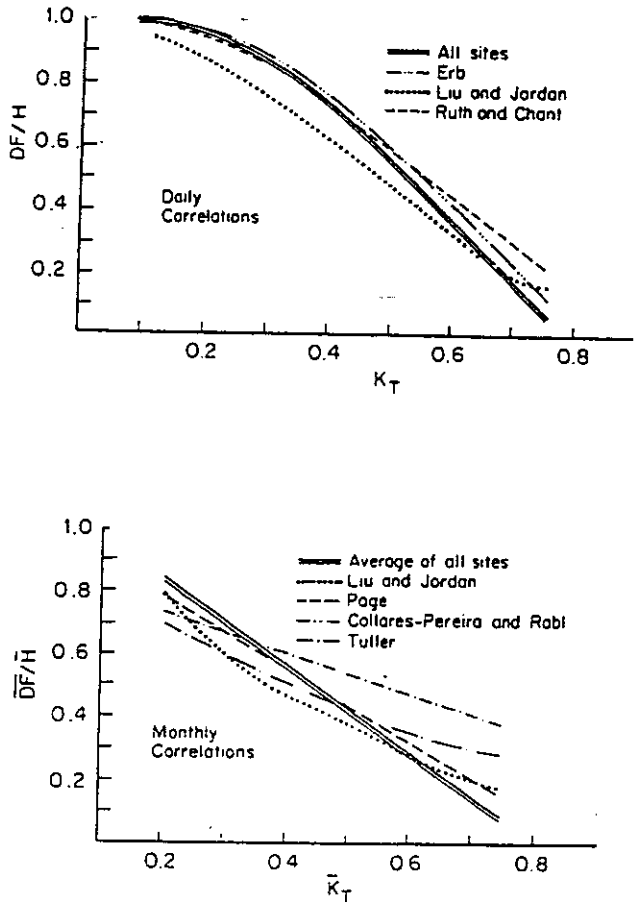

Figure 4.26: Comparison of various DD/DG *vs* DG/DE and MD/MG *vs* MG/ME correlations. From Vignola and McDaniels (84)

for 30-days regressions and

$$\frac{DD}{DG} = a + b\frac{DG}{DE} + c(\frac{DG}{DE})^2 + d(\frac{DG}{DE})^3 + (e+f\frac{DG}{DE})\, sin(2\pi\frac{N-40}{365})$$

for daily regressions, where N is the day number (or the median of the concerned 30 days in the first regression). Best fit coefficients are reported for each locality and all localities together. Finally, the authors discuss the possible explanations of the observed seasonal variation, and conclude that it is due to the combined effect of changes in air mass, water vapour and turbidity. This conclusion is supported by a study of the clear day solar noon transmission values.

Smietana *et al.* [236] use one-minute measurements of both diffuse and global irradiation during one year at Davis, California, to check the dependence of ID/IG on IG/IE. They find very different polynomial regression for days with different average sunshine and conclude that IG/IE is not sufficient to determine ID/IG. In a subsequent work, the same authors [235] provide a statistical comparison between one-minute, hourly and daily ratios obtained on the one hand by averaging the respective smaller time interval ratios and on the other hand by taking the ratio of the integrated values (see Fig. 4.27).

Rao *et al.* [207] use data measured at Corvallis, Oregon (USA) during 648 days to obtain the (85% accounted variance) fit

$$\frac{DD}{DG} = 1 \quad (\frac{DG}{DE} \leq 0.2)$$

$$\frac{DD}{DG} = 1.130 - 0.667\frac{DG}{DE} \quad (0.2 < \frac{DG}{DE} \leq 0.26)$$

$$\frac{DD}{DG} = 1.403 - 1.725\frac{DG}{DE} \quad (0.26 < \frac{DG}{DE} \leq 0.75)\ .$$

As previously noticed by Collares-Pereira and Rabl [74], the DD/DG values measured for $DG/DE \leq 0.2$ are with very few exceptions practically indistinguishable from unity (the authors substantiate this observations by analizing about 16000 one-minute global and beam normal measurements). Although the scatter diagram for higher values of DG/DE does not suggest the use of the second and higher order regression models, the fourth order polynomial fit

$$\frac{DD}{DG} = 0.9493 + 1.134\frac{DG}{DE} - 5.7688(\frac{DG}{DE})^2 + 4.5503(\frac{DG}{DE})^3 - 1.2457(\frac{DG}{DE})^4$$

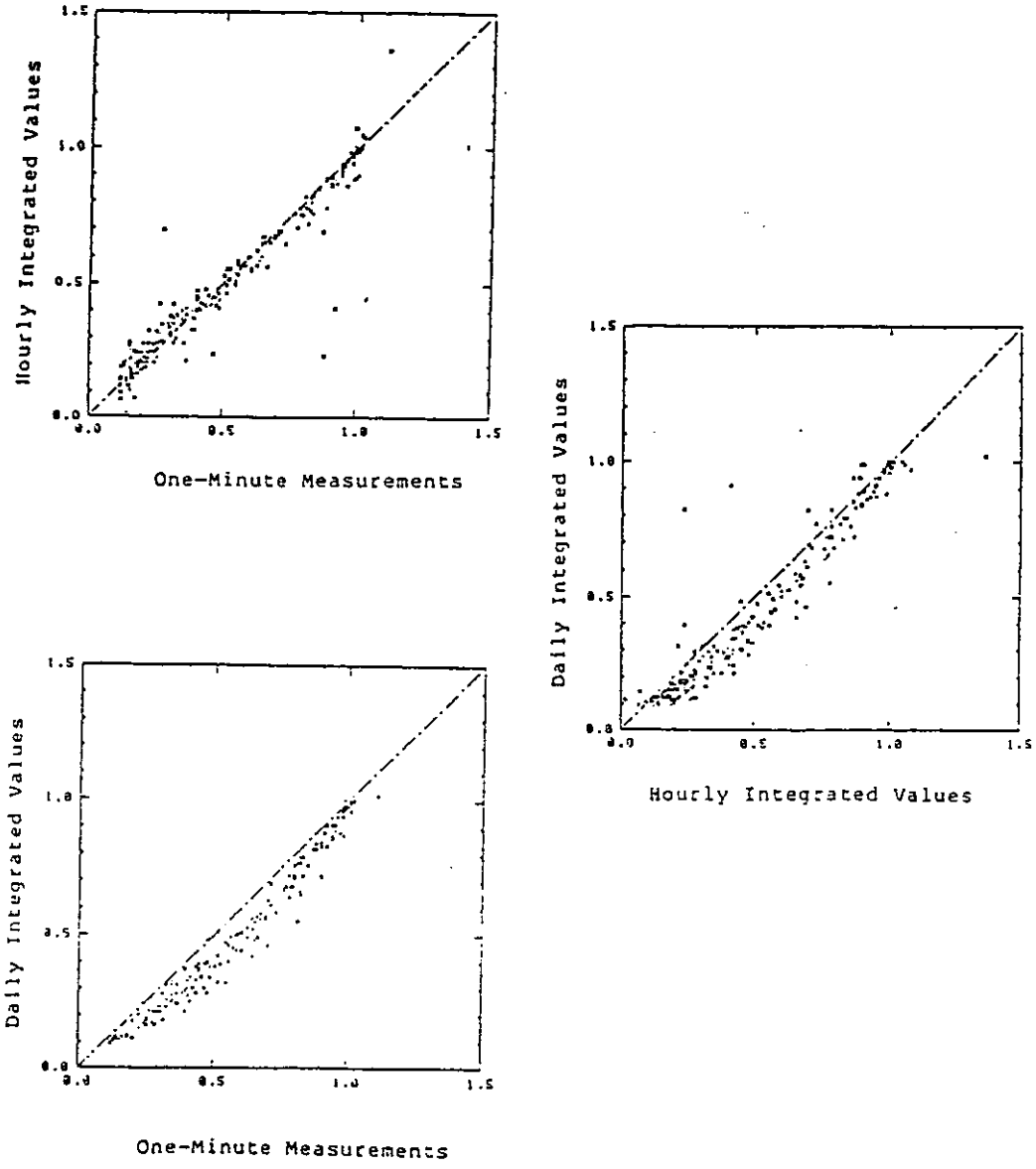

Figure 4.27: Comparison scatter plot of DD/DG calculated from one-minute, hourly or daily integrated values. From Smietana *et al.* (84).

is given for comparison with the results of other authors. The simple piecewise linear model is also seasonally fitted and compared with models of other authors.

Turner and Salim [250] compare the Stauter-Klein model for the diffuse fraction, as reported by Duffie and Beckman [80] (1980 edition) with a similar model fitted on their own data. They use about two years of hourly (in fact one-minute) measurements of direct normal, global and diffuse irradiation at Blytheville, Arkansas (USA). Both the Stauter-Klein model and the "Blytheville model" relate the hourly diffuse fraction to the *clear sky* clearness index HG/HG_{cs}, where HG_{cs}, the hourly clear sky global irradiation, is calculated from Hottel's model [122]. The first model reads

$$\frac{HD}{HG} = 1.0 - 0.1\,\frac{HG}{HG_{cs}}$$

for $0 \leq HG/HG_{cs} < 0.48$,

$$\frac{HD}{HG} = 1.11 + 0.0396\,\frac{HG}{HG_{cs}} - 0.789(\frac{HG}{HG_{cs}})^2$$

for $0.48 \leq HG/HG_{cs} < 1.10$, and

$$\frac{HD}{HG} = 0.20$$

for $HG/HG_{cs} \geq 1.10$, while the second is written as

$$\frac{HD}{HG} = 1.0 - 0.055\,\frac{HG}{HG_{cs}}$$

for $0 \leq HG/HG_{cs} < 0.48$,

$$\frac{HD}{HG} = 1.672 - 2.359\,\frac{HG}{HG_{cs}} + 2.638(\frac{HG}{HG_{cs}})^2 - 1.574(\frac{HG}{HG_{cs}})^3$$

for $0.48 \leq HG/HG_{cs} < 1.10$, and

$$\frac{HD}{HG} = 0.18$$

for $HG/HG_{cs} \geq 1.10$. The Stauter-Klein model predicts the measured diffuse data fairly well, and only small improvements are obtained with the second model fitted on the Blytheville data.

Ma and Iqbal [169] compare, using data for Bergen (Norway), Trappes (France), Montreal (Canada), Carpentras (France) and Toronto (Canada), eight different regression formulae for the monthly correlation between diffuse fraction and clearness index or relative sunshine. They use the *mean bias error* (MBE)

$$MBE = \frac{\sum_i (X_{i,calc} - X_{1,obs})}{N}$$

as an index of the long-term performance (under- or over-estimation), and the *rooth mean square error* (RMSE)

$$RMSE = \sqrt{\frac{\sum_i (X_{i,calc} - X_{1,obs})^2}{N}}$$

as an index of the short-term performance of the same fit. They find that, for monthly correlations, that of Page [194] gives the best results, with MBE remarkably low.

Lewis [159] tests, taking the RMSE as the sole index, the performances of the regression models of Liu and Jordan [163], Page [194], Collares-Pereira and Rabl [74], Iqbal [131], and Hay [118] in predicting the twelve long-term monthly averages of MD/MG and MG/ME measured at Huntsville, Alabama. He finds Hay's model performs best, with a $RMSE$ of 1.62 MJ/m^2day, followed by Page's model, with $RMSE = 1.71$ MJ/m^2day. The latter is nevertheless preferred for its greater simplicity.

The joint frequency distribution of HD/HG and HG/HE is analysed by Hollands and Crha [121] using ten years of hourly measurements for Toronto(Canada) and five years for Winnipeg(Canada). They subdivide the ranges of both quantities in twenty intervals, thus obtaining 400 bins which are to be filled with about 52000 pairs. The joint frequency graphs are reported for both localities (see Fig. 4.28).

The authors recognize that the joint distribution depends on both geographical and climatical factors, but they believe that this dependence can be resumed in the regression (i.e. conditional) curve

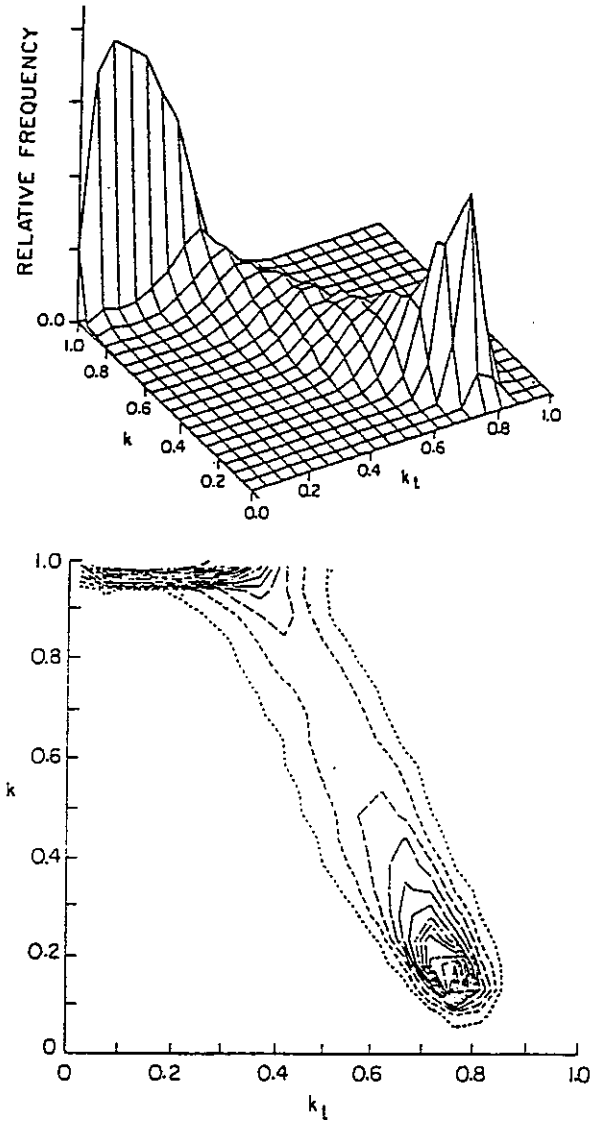

Figure 4.28: Joint relative frequency surface for the pairs HD/HG and HG/HE, and its projection with iso-frequency curves. From Hollands and Crha (87).

of HD/HG *vs* HG/HE. The conditional frequency distributions of HD/HG *given* HG/HE are fitted to the three parameter formula (here we put $k = HD/HG$ and $k_t = HG/HE$)

$$f(k|k_t) \;=\; C\;(k-k_l)\;(1-k)\;exp\lambda k$$

The lower boud k_l is fitted as a linear function of the conditional average (regressed value) $< k|k_t >$

$$k_l \;=\; 0.511\;\; < k|k_t > \;\; - \, 0.325$$

so that the two remaining free parameters C and λ can be calculated under the conditions

$$\int_{k_l}^{1} dk\; f(k|k_t) \;=\; 1 \qquad (normalization)$$

and

$$\int_{k_l}^{1} dk\; f(k|k_t)\; k \;=< k|k_t > \quad (average).$$

C and λ are to be calculated from implicit equations, but approximate explicit formulae are given by

$$C \;=\; \frac{\delta^3\; e^{-\lambda k_l}}{(1-k_l)^2(2+\delta+(\delta-2)exp\delta)}$$

$$\lambda \;=\; \frac{\delta}{1-k_l}$$

where, with

$$\eta \;=\; \frac{< k|k_t > -k_l}{1-k_l},$$

δ is given by the following three expressions:

$$\delta \;=\; -\frac{1+\eta+\sqrt{\eta^2-4\eta+1}}{\eta} \quad (\eta \leq 0.25)$$

$$\delta \;=\; 4.18\; sinh(4.72(\eta-0.5)) \quad (0.25 < \eta \leq 0.75)$$

$$\delta \;=\; \frac{1-\eta+\sqrt{\eta^2+2\eta-2}}{1-\eta} \quad (0.75 < \eta \leq 1.0)\;\; .$$

Both examples of (conditional) frequency density functions and a comparison between the (conditional) modeled and empirical cumulative frequency functions are reported, showing a fairly good agreement. The authors explicitely remark that the behaviour of the regressed k, which can depend on various geographical and climatological factors, is automatically embedded in the coefficients calculation, whereas it does not affect the general form of the suggested conditional frequency distribution.

Skartveit and Olsen [234] analytically express the regression curves of HD/HG *vs* HG/HE depending on solar elevation. With reference to the Garrison investigations they assert that the curves they construct can be considered as representing average curves with respect to values of surface albedo, atmospheric precipitable water and atmospheric turbidity typical for close to sea level snow-free conditions in Norway. The authors analyse 44687 hourly values of diffuse and global irradiation measured at Bergen (Norway), corresponding to solar elevation above 10^o; thus the period from early December to late January is removed, and a representative albedo of 0.15 can be attributed to the snow-free ground. Average precipitable water at cloudless sky is in the range $1-2\ cm$, and Schuepp turbidity coefficients are approximately in the range $0.05-0.10$.

The proposed model, setting as before $k = HD/HG$ and $k_t = HG/HE$ is

$$k = 1.00 \qquad (k_t \leq k_{t,0})$$

$$k = 1-(1-d_1)(a\sqrt{K}+bK+(1-a-b)K^2)$$

for $k_{t,0} < k_t \leq \alpha k_{t,1}$ where

$$K = 0.5(1+sin\ \pi(\frac{k_t-k_{t,0}}{k_{t,1}-k_{t,0}}-0.5))$$

and

$$k = 1-\alpha k_{t,1}\frac{1-f(\alpha k_{t,1})}{k_t}$$

for $k_t \geq \alpha k_{t,1}$. The paramaters $k_{t,0}$, $k_{t,1}$, d_1, a and b are determined by least square analysis, whereas α is determined assuming that the

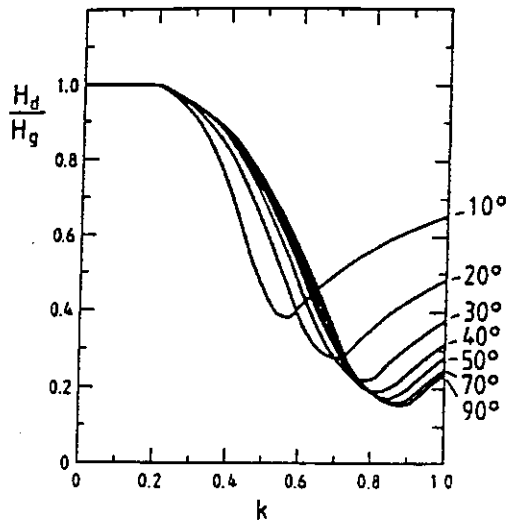

Figure 4.29: Modeled HD/HG *vs* HG/HE for various solar elevations. From Skartveit and Olseth (87).

derivative dk/dk_t is approximately continuous at $k = \alpha k_{t,1}$. The authors divide the data in groups corresponding to solar elevation intervals of 5^o and look for minimum least squares between the proposed formula and the conditionally averaged $< k|k_t >$ grouped in k_t-intervals of 0.05. They find the values

$$k_{t,0} = 0.20$$

$$k_{t,1} = 0.87 - 0.56\ e^{-0.06h}$$

$$\alpha = 1.09$$

$$d_1 = 0.15 + 0.43\ e^{-0.06h}$$

$$a = 0.27$$

$$b = 0.00$$

(see Fig. 4.29).

Skartveit and Olsen test their model against verification samples collected from several close to sea level stations (ten years of observations from Aas, Norway, and five years from Vancouver, Canada).

Moreover, for comparison they use regressions curves taken from literature ([133], [97]). Though some minor discrepancies appears, attributed to different climatic conditions, the model seems to fit fairly well the averages of the verification samples.

A simulated radiation data analysis for five different typical sky conditions is performed by Zangvil and Aviv [257], who study changes in daily relationship between DD/DG and DG/DE uniquely due to different season and latitude (i.e. mean daily solar altitude). The authors use continuously measured data at Sede Boqer, Israel, during 30/6/83 (uniformly clear sky, albedo: 0.35, precipitable water: 1.5 cm) and 22/6/83 (uniformly hazy sky, albedo: 0.35, precipitable water: 2.5 cm) to assign to each solar altitude between 0^o and 82^o (solar noon) a pair $(ID/IG, IG/IE)$ under the given sky conditions. Values for solar altitudes greater than 80^o are extrapolated. With the same data they construct, for each solar altitude, an *overcast day*, $(ID = IG = ID_{hazy})$, a *partly cloudy day* (by combining with equal weights the clear sky with an overcast sky for which $ID = ID_{clear}$), and a *cloudy sky* (by combining hazy sky and overcast sky with weights 0.1 and 0.9 respectively).

With these data Zangvil and Aviv are able to build five types of *simulated* days for each latitude and day of the year (the solar altitudes are easily calculated). They choose the latitudes 0^o N, 15^o N, $23^o27'$ N, 30^o N, 45^o N and 60^o N, and the days 22 December (Winter solstice), 21 March (spring equinox) and 22 June (Summer solstice). The seasonal dependence of the DD/DG, DG/DE relationship is very small at the equator and increases with increasing latitude.Moreover, it depends on the sky condition, being largest for clear sky condition and smallest for overcast sky condition. For a given sky condition, if DD/DG is greater than $0.7-0.8$ then DG/DE increases from Summer to Winter, whereas it decreases from Summer to Winter in the opposite case.

The latitude dependence is larger in Winter and smaller in Summer, and depends on the sky condition, being largest for hazy sky and smallest for overcast sky.

Both seasonal and latitudinal variations take place along lines which have orientations similar to the standard models of the DD/DG vs DG/DE regression. From an inspection of the deduced figures, the

authors suggest that two distinct paths exist from clear to overcast sky. On one hand through hazy or thin clouds of small optical depth which gradually thicken: this path would have relatively large values of DD/DG and DG/DE and will lie above the line describing known models. On the other hand, through partly cloudy conditions with clouds of large optical depth: in this case the regression line would lie under the line describing known models. This fact, together with the customary mixture of different solar altitudes, can explain the scattering of the experimental points in the daily scatter plots. Finally the authors briefly discuss how these considerations can influence the monthly or yearly regressions.

Becker [30] fits monthly means of beam irradiation vs monthly means of global irradiation using data measured during about nine years at Chiva-Chiva, Panama. Changing his MB/MG into $1 - MD/MG$ the regressed relationship reads

$$\frac{MD}{MG} = 1.14 - 1.26\,\frac{MG}{ME} \qquad (r^2 = 0.90)$$

with some improvement in determination (and different coefficients) when the monthly values are suitably grouped. The author also tests a logarithmic regression and finds

$$log(MB) = -1.98 + 2.33\ log(MG) \qquad (r^2 = 0.90)$$

In this case too, some improvement is obained by suitably grouping the different months of the year.

Lalas *et al.* [79] test, both for daily and monthly regressions, data from three localities in Greece: Athens (890 days), Rodos (567 days) and Kythnos (362 days). For the daily correlation they find

$$\frac{DD}{DG} = 0.98 \qquad (\frac{DG}{DE} < 0.22)$$

$$\frac{DD}{DG} = 1.36 - 1.60\frac{DG}{DE} \qquad (0.22 \leq \frac{DG}{DE} \leq 0.80)$$

with determination coefficient $r^2 = 0.883$. No seasonal difference or some significant difference between locations appears, except for

Summer days in Athens, which correspond to higher diffuse irradiation (especially for large DG/DE values). Higher order fits do not significantly improve the determination coefficient.

For monthly measurements, the authors calculate the linear regression

$$\frac{MD}{MG} = 1.27 - 1.45\,\frac{MG}{ME} \quad (r^2 = 0.941)$$

In this case too, no relevant differences between stations appear. The resulting correlations give higher values of diffuse radiation, especially in cloudy or partly cloudy days, than the standard one of Liu-Jordan or the latest one of Erbs *et al.*.

Gopinathan [107], tests four formulae to fit monthly values, using data from six locations in Southern Africa, and chooses, mainly for its semplicity,

$$\frac{MD}{MG} = 1.017 - 1.159\frac{MG}{ME} \quad (r = 0.930)$$

whose coefficients agree well with those given originally by Page. In a subsequent work, the same author [106], fitting monthly data for Dehli, Madras and Poona (India) with different regression formulae, finds that the simple standard linear regression requires different coefficient for different localities and chooses the mixed linear regression

$$\frac{MD}{MG} = 1.194 - 0.838\frac{MG}{ME} - 0.446\frac{SS}{SS_o}$$

where SS/SS_o is the monthly relative sunshine ($r = 0.973$). He recommends this relationship in order to calculate the monthly diffuse irradiation for locations in India with an average error of about 10%.

Also Al-Hamadani *et al.* [6] find, using some years of daily measurements for Baghdad,Iraq, that adding the relative sunshine as second independent variable the diffuse fraction *vs* clearness index relationship performs best. For daily measurements they obtain correlation coefficients in the range $0.957 - 0.966$ for the four seasons, whereas for monthly regression they obtain

$$\frac{MD}{MG} = 0.962 - 0.758\frac{MG}{ME} - 0.277\frac{SS}{SS_o}$$

with a correlation coefficient $r = 0.964$.

Suehrcke and McCormick [244] emphasize the importance of the relationship between the "instantaneous" relationship between diffuse fraction and clearness index in order to estimate the solar collector performances, due to the generally non linear behaviour of the solar energy conversion devices. They work with approximately one year of instantaneous measurements of global and normal beam irradation at one-minute intervals, taken at Perth, Australia. First, they determine the instantaneous diffuse fraction regression on air mass m on clear sky condition as

$$(\frac{ID}{IG})_{cs} \;=\; 0.0336 \;+\; 0.0477\, m$$

They notice that no correlation exists between the water vapour content and the diffuse fraction, indicating that the water vapour is responsible for selective absorption of solar radiation, but not for scattering. The corresponding regressed relation for the clearness index is given by

$$(\frac{IG}{IE})_{cs} \;=\; 0.877\; e^{-0.0933\; m}$$

All measurements are subsequently divided into the four air mass classes $1.0 \leq m \leq 1.1$, $1.4 \leq m \leq 1.6$, $1.8 \leq m \leq 2.2$, $2.7 \leq m \leq 3.3$, and for each class the regression of ID/IG vs IG/IE is calculated, with 0.02 IG/IE intervals (see Fig. 4.30).

Regression lines constitute a "regular" ($IG/IE \leq 0.8$) part, where the diffuse fraction decreases with increasing clearness index, and an "abnormal" part, where the diffuse fraction increases too. The latter results to be invariably associated with partly cloudy skies, were cloud edges reflect on the sensor an extra amount Δ of irradiation, (which is recorded as diffuse and results in an increase in both measured ID and IG), so that it results

$$(\frac{ID}{IG})_{measured} \;=\; \frac{ID+\Delta}{IG+\Delta}\;\cdot$$

The regression lines are empirically fitted with the formulae

$$\frac{ID}{IG} \;=\; 1-[1-(\frac{ID}{IG})_{cs}][\frac{IG/IE}{(IG/IE)_{cs}}]^{4.4}$$

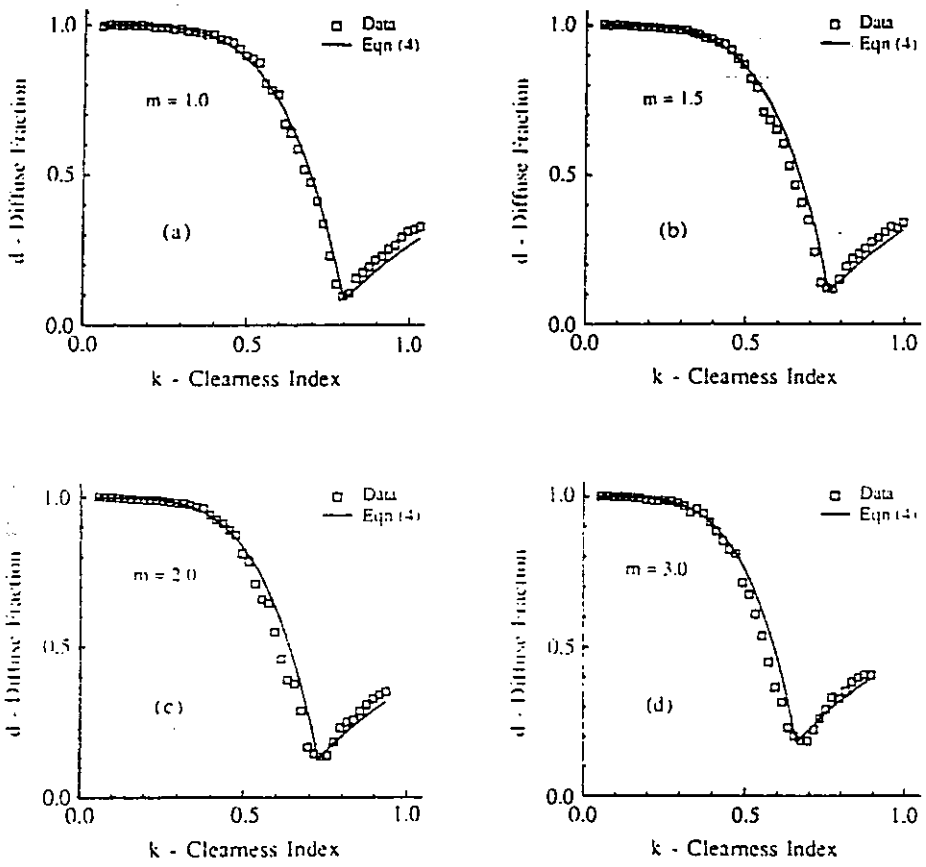

Figure 4.30: Regressions of ID/IG *vs* IG/IE for different values of the air mass m. From Suehrcke and McCormick (88).

for $IG/IE \leq (IG/IE)_{cs}$, and

$$\frac{ID}{IG} = (\frac{ID}{IG})_{cs}\frac{(IG/IE)_{cs}}{IG/IE} + 1 - \frac{(IG/IE)_{cs}}{IG/IE}$$

for $IG/IE \geq (IG/IE)_{cs}$. After developing a simplified model for instantaneous diffuse fraction, the authors discuss the differences between the istantaneous and the daily and monthly regressions and show how, given a same daily clearness index, very different values of the daily diffuse fraction can arise.

Kierkus and Colborne [144] develop relationships for estimating the daily and monthly diffuse fraction and try to determine the degree to which these relationships are dependent on the ground albedo as influenced by snow cover. They use an average of twelve years of hourly diffuse and global irradiation measurements from eight Canadian sites and find an overall fit given, with no snow cover, by (see Fig. 4.31)

$$\frac{DD}{DG} = 0.98 \quad (\frac{DG}{DE} \leq 0.11)$$

$$\frac{DD}{DG} = 0.944 + 0.672\frac{DG}{DE} - 3.22(\frac{DG}{DE})^2 - 0.618(\frac{DG}{DE})^3 + 2.568(\frac{DG}{DE})^4$$

for $0.11 < DG/DE < 0.84$,

$$\frac{DD}{DG} = 0.15 \quad (\frac{DG}{DE} \geq 0.84)$$

and, with snow cover,

$$\frac{DD}{DG} = 0.99 \quad (\frac{DG}{DE} \leq 0.22)$$

$$\frac{DD}{DG} = 0.931 + 0.123\frac{DG}{DE} + 3.072(\frac{DG}{DE})^2 - 12.682(\frac{DG}{DE})^3 + 9.071(\frac{DG}{DE})^4$$

for $0.22 < DG/DE < 0.84$,

$$\frac{DD}{DG} = 0.201 \quad (\frac{DG}{DE} \geq 0.84) \ .$$

With respect to the monthly regressions, the authors plot MD/MG vs MG/ME, distinguishing between months which have all their days

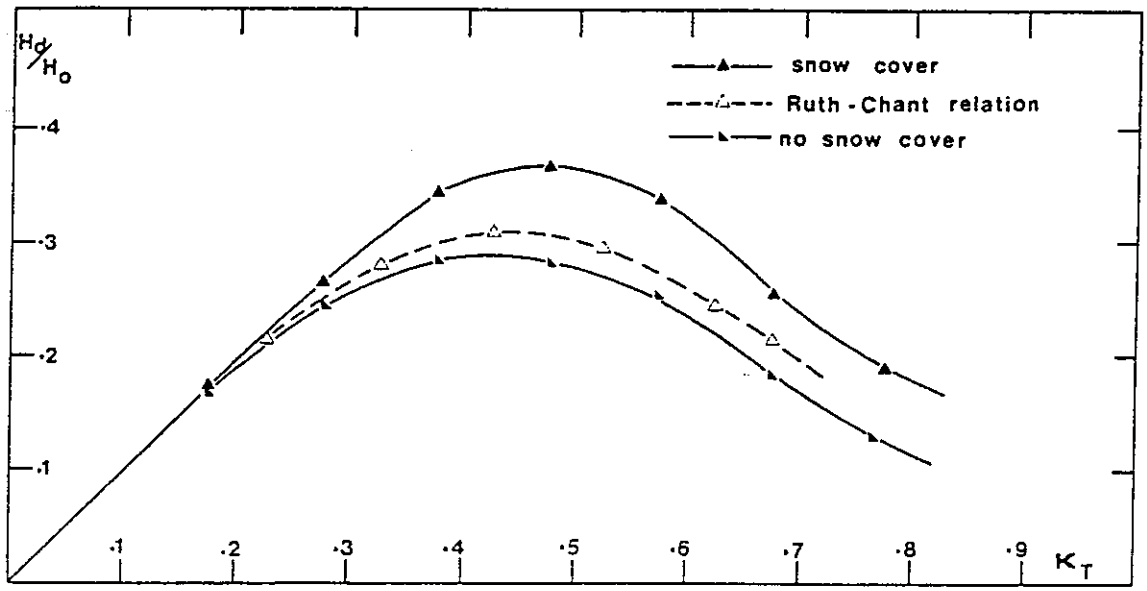

Figure 4.31: Regression lines for DD/DE *vs* DG/DE based on daily values averaged over eight sites, with and without snow cover, compared with the Ruth and Chant (76) regression. From Kierkus and Colborne (89).

either with snow cover or without snow cover. In the latter case the linear relationship is found

$$\frac{MD}{MG} = 0.95 - 1.019 \frac{MG}{ME} ,$$

whereas in the former case no fit is performed, due to the large scatter of the experimental points. Nevertheless, a higher diffuse radiation fraction (about +30%) clearly appears from the plotted points with respect to the no snow cover case.

Newland [184] studies relationships for daily and monthly data using eleven years of measurements at Macao, South China. For monthly data he obtains the linear regression

$$\frac{MD}{MG} = 1.020 - 1.157 \frac{MG}{ME} \quad (r = -1.157)$$

whose coefficients are very similar to those of Page's original formula. The similarity is even greater if the regression is made on the twelve long-term (eleven years) averages for each month of the year (equation coefficients become 1.003 and −1.141, with a correlation coefficient $r = -0.9804$).

The scatterplot of the daily values, after division of the DG/DE axis in 0.05 width intervals and averaging of DD/DG in each interval gives the regression curve

$$\frac{DD}{DG} = 0.9713 + 0.5614\frac{DG}{DE} - 3.3534(\frac{DG}{DE})^2 - 1.0339(\frac{DG}{DE})^3 + 0.5136(\frac{DG}{DE})^4$$

for $0.10 < DG/DE < 0.71$ and,

$$\frac{DD}{DG} = 0.18 \quad (\frac{DG}{DE} \geq 0.71) .$$

Seasonal dependence of the daily correlation is shown, using fourth degree polinomials for Winter, Summer and equinox data. The variations are attributed to the different solar altitudes, as predicted by Zangvil and Aviv [257], while no relevant dependence on climatical parameters such as high cloud cover or high humidity or high precipitable water is noticed (probably due to the somewhat constant or slighlty varying values of these quantities during the year).

Bibliography

[1] A.S.E. Ackermann. The utilisation of solar energy. *Annual Report of the Smithsonian Institution*, 141–166, 1915.

[2] J. Adnot, B. Bourges, D. Campana, and R. Gicquel. Utilisation de courbes de frequence cumulees pour le calcul des installation solaires. In R. Lestienne, editor, *Analise Statistique des Processus Meteorologiques Appliquee a l'Energie Solaire*, pages 9–40, C.N.R.S., Paris, 1979.

[3] R.J. Aguiar, M.Collares-Pereira, and J.P. Conde. Simple procedure for generating sequences of daily radiation values using a library of markov transition matrices. *Solar Energy*, 40:269–279, 1988.

[4] I. Ahmad, N. Al-Hamadani, and K. Ibrahim. Solar radiation maps for Iraq. *Solar Energy*, 31:29–44, 1983.

[5] F.H.W. Albrecht. Methods of computing global radiation. *Geofisica Pura e Applicata*, 32, 1955.

[6] N. Al-Hamadani, M. Al-Riahi, and K. Tahir. Estimation of the diffuse fraction of daily and monthly average global radiation for Fudhaliyah, Baghdad (Iraq). *Solar Energy*, 42:81–85, 1989.

[7] R. Almanza and S. Lopez. Total solar radiation in Mexico using sunshine hours and meteorological data. *Solar Energy*, 21:441–448, 1978.

[8] U. Amato, A. Andretta, B. Bartoli, B. Coluzzi, V. Cuomo, F. Fontana, and C. Serio. Markov processes and Fourier analysis

as a tool to describe and simulate daily solar irradiance. *Solar Energy*, 37:179–194, 1986.

[9] U. Amato, A. Andretta, B. Bartoli, B. Coluzzi, V. Cuomo, and C. Serio. Stochastic modelling of solar-radiation data. *Il Nuovo Cimento*, 8C:248–258, 1985.

[10] G. Ambrosone, A. Andretta, B. Bartoli, F. Bloisi, S. Catalanotti, B. Coluzzi, V. Cuomo, S. De Stefano, G. Formisano, V. Silvestrini, G. Troise, and L. Vicari. Disponibilita' e raccolta della radiazione solare. *Condizionamento dell'Aria Riscaldamento Refrigerazione*, Febbraio:101–109, 1978.

[11] A. Andretta, B. Bartoli, B. Coluzzi, V. Cuomo, M. Francesca, and C. Serio. Global solar radiation estimation from relative sunshine hours in Italy. *Jour. of Applied Meteorology*, 21:1377–1384, 1982.

[12] A. Angström. On the computation of global radiation from records of sunshine. *Arkiv fur Geofisik*, Band 2, Hefte 5:41, 1956.

[13] A. Angström. Recording solar radiation. *Medd. Stateus Meteor. Hyd. Anstalt.*, 3:4–10, 1929.

[14] A. Angström. Solar and terrestrial radiation. *Q. J. Roy. Met. Soc. A. J.*, 50:121–126, 1924.

[15] V. Modi ans S.P. Sukhatme. Estimation of daily total and diffuse insolation in India from weath data. *Solar Energy*, 22:407–411, 1979.

[16] V. Badescu. A verification of the atmospheric model proposed by Barbaro et al. for computing direct and diffuse solar radiation. *Solar Energy*, 26:459–460, 1981.

[17] D.G. Baker and J.C. Klink. *Solar radiation reception, probabilities, and areal distribution in the north-central region*, page 225. *Agricultural Experiment Station, University of Minnesota*, North Central Reg. Res. Publ., 1975.

[18] A. Baloutkis and Ph. Tsalides. Stochastic simulation model of hourly total solar radiation. *Solar Energy*, 37:119–126, 1986.

[19] O.A. Bamiro. Empirical relations for the determination of solar radiation in Ibadan, Nigeria. *Solar Energy*, 31:85–94, 1983.

[20] S. Barbaro, G. Cannata, and S. Coppolino. Monthly reference distribution of daily relative sunshine values. *Solar Energy*, 31:63–67, 1983.

[21] S. Barbaro, G. Cannata, S. Coppolino, C. Leone, and E. Sinagra. Correlation between relative sunshine and state of the sky. *Solar Energy*, 26:537–550, 1981.

[22] S. Barbaro, G. Cannata, S. Coppolino, C. Leone, and E. Sinagra. Diffuse solar radiation statistics for Italy. *Solar Energy*, 26:429–435, 1981.

[23] S. Barbaro, G. Cannata, S. Coppolino, and E. Sinagra. The reference frequency distribution of daily relative sunshine from different locations. *Solar Energy*, 33:19–24, 1984.

[24] S. Barbaro, S. Coppolino, C. Leone, and E. Sinagra. An atmospheric model for computing direct and diffuse solar radiation. *Solar Energy*, 22:225–278, 1979.

[25] S. Barbaro, S. Coppolino, C. Leone, and L. Sinagra. Global solar radiation in italy. *Solar Energy*, 20:431–435, 78.

[26] O.A. Barra. Estimation of the solar radiation from meteorological data in the Italian climatic area. *Solar Energy*, 31:427–428, 1983.

[27] B. Bartoli, S. Catalanotti, V. Cuomo, M. Francesca, C. Serio, V. Silvestrini, and G. Troise. Statistical correlation between daily and monthly averages of solar radiation data. *Nuovo Cimento*, 2C:222–234, 1979.

[28] B. Bartoli, B. Coluzzi, V. Cuomo, M. Francesca, and C. Serio. Autocorrelation of daily global solar radiation. *Il Nuovo Cimento*, 4C:113–122, 1981.

[29] B. Bartoli, V. Cuomo, U. Amato, G. Barone, and P. Mattarelli. Diffuse and beam components of daily global radiation in genova and macerata. *Solar Energy*, 28:307–311, 1982.

[30] P. Becker. Monthly average solar radiation in Panama. Daily] and hourly relations between direct and global insolation. *Solar Energy*, 39:445–453, 1987.

[31] W.A. Beckman, J.W. Bugler, P.I. Cooper, J.A. Duffie, R.V. Dunkle, P.E. Glaser, T. Origome, E.D.Howe, T.A. Lawand, P.L. van der Mersch, J.K. Page, N.R. Sheridan, and S.V. Szokolay. Unit and symbols in solar energy. *Solar Energy*, 21:65–68, 1978.

[32] J.A. Bedel. Solar energy recovered by a flat plate collector. In *EC Contractor's Meeting*, pages 170–176, Brussels,18–19 October 1982.

[33] C. Benard. Statistical analysis of insolation data applied to the study of thermal storage systems. In G. Chassagne, C. Depuy, and M. Levy, editors, *Solar Energy Conversion and Application*, pages 193–199, Cargese 19 Juin–2 Juillet 1977.

[34] C. Benard, Y. Body, and A. Wirgin. On the method of stochastic time series for the characterisation of the stability of solar insolation. In F. de Winter and M. Cox, editors, *Proceedings of the ISES Congress*, pages 338–345, Pergamon Press, January 1978.

[35] C. Benard, Y. Body, A. Wirgin, and D. Gobin. *Caracterisation de la stabilite de l'intensite solaire en France et au Perou par l'analyse temporelle de series aleatoires.* C.N.R.S., Paris, 1979.

[36] P. Bendt, M. Collares-Pereira, and A. Rabl. The frequency distribution of daily insolation values. *Solar Energy*, 27:1–5, 1981.

[37] I. Bennet. Correlation of daily insolation with daily total sky cover, opaque sky cover and percentage of possible sunshine. *Solar Energy*, 12:391, 1969.

[38] I. Bennet. Frequency of daily insolation in Anglo North America during June and December. *Solar Energy*, 11:41–55, 1967.

[39] I. Bennet. Monthly maps of mean daily insolation for the United States. *Solar Energy*, 9:145–158, 1965.

[40] R.B. Benson, M.V. Paris, J.E. Sherry, and C.G. Justus. Estimation of daily and monthly direct diffuse and global solar radiation from sunshine duration measurements. *Solar Energy*, 32:523–535, 1984.

[41] X. Berger. *Etude du climat en region nicoise en vue d'applications a l'habitat solaire.* C.N.R.S., Paris, 1979.

[42] T.G. Berland. Methods for climatological computations of global radiation. *Meteor. Hydrol.*, 6, 1960.

[43] B.Hourwitz. Insolation in relation to cloud type. *J. Met.*, 3:123–124, 1946.

[44] B.Hourwitz. Insolation in relation to cloudiness and cloud density. *J. Met.*, 2:154–156, 1945.

[45] A.J. Biga and R. Rosa. Contribution to the study of the solar radiation climate of Lisbon. *Solar Energy*, 23:61–67, 1979.

[46] A.J. Biga and R. Rosa. Statistical behaviour of solar irradiation over consecutive days. *Solar Energy*, 27:149–157, 1981.

[47] J.N. Black. The distribution of solar radiation over the earth's surface. *Arch. Met. Geoph. Biokl.*, 7:165–189, 1956.

[48] J.N. Black, C.W. Bonython, and J.M. Prescott. Solar radiation and the duration of sunshine. *Q. J. Roy. Met. Soc.*, 80:231–235, 1954.

[49] E.C. Boes, I.J. Hall, R.R. Prarie, R.P. Stromberg, and H.E. Anderson. Distribution of direct and total solar radiation availabilities for the usa. *Sandia Rep.*, Aug.1976.

[50] E. Boileau. Discussion d'un modele statistique en meteorologie solaire. *Rev. Phys. Appl.*, 14:343–347, 1977.

[51] E. Boileau. Use of simple statistical models in solar meteorology. *Solar Energy*, 30:333–339, 1983.

[52] E. Boileau and B. Guerrier. Comparaison de modeles statistiques saisonniers et non saisonniers en meteorologie solaire. *La Meteorologie*, VI Serie:115–130, 1979.

[53] Ph. Bois, J. Goussebaile, M.J. Mejon, and G. Vachaud. Analyse de donnees d'energie solaire en vue des applications. In G. Chassagne, C. Depuy, and M. Levy, editors, *Solar Energy Conversion and Application*, pages 171–191, Cargese 19 Juin–2 Juillet 1977.

[54] Ph. Bois and M.J. Mejon. Analyse du gain d'information en fonction du pas de temps de mesure du rayonnement directe. exemple de Saint-Chamas a l'echelle de la minute. In R. Lestienne, editor, *Analise Statistique des Processus Meteorologiques Appliquee a l'Energie Solaire*, pages 145–157, C.N.R.S., Paris, 1979.

[55] M. Bossolasco, G. Cicconi, I. Dagnino, A. Elena, and G. Flocchini. Ricerche sulla radiazione solare:I. *Anno Geofisico Internazionale 1957-58 & 1959-63*, 47–65, 1965.

[56] B. Bourges and F. Lasnier. Statistical distribution of solar radiation (hourly sums): Cumulative frequancy curves. In *EC Contractor's Meeting*, pages 177–181, Brussels,18–19 October 1982.

[57] E.P. Box and G.M. Jenkins. *Time series analysis, forecasting and control.* Holden Day, San Francisco, 1970.

[58] B.J. Brinkworth. Autocorrelation stochastic modelling of insolation sequences. *Solar Energy*, 19:343–347, 1977.

[59] C.E.P. Brooks and N. Carruthers. *Handbook of Statistical Methods in Meteorology.* Her Majesty's Stationary Office, London, 1953.

[60] C.F. Brooks and E.S. Brooks. Sunshine recorders: a comparative study of the burning glass and thermometric systems. *J. Meteor.*, 4:105–115, 1947.

[61] F.A. Brooks and W. Miller. Chapter 3. In A.M. Zarem and D.D. Erway, editors, *Intoduction to the utilisation of solar energy*, page 37, McGraw-Hill, New York, 1963.

[62] R. Bruno. A correction procedure for separating direct and diffuse insolation on a horizontal surface. *Solar Energy*, 20:97–100, 1978.

[63] J.M. Bugler. The determination of hourly insolation on an inclined plane using a diffuse irradiance model based on hourly measured global horizontal insolation. *Solar Energy*, 19:477–491, 1977.

[64] G. Cammarata, L. Marletta, F. Patane, and F. Patania. Analisi statistica dei dati storici di insolazione e simulazione di sequenze con il metodo di markoff. *Energie alternative HTE*, Anno 4:427–433, 1982.

[65] M. Capderou. *Atlas solaire de l'Algerie. Document preliminaire.* E.P.A.U., Alger, 1984.

[66] F. Cerquetti, C. Scuterini, and A. Murri. Correlations between total, diffuse and direct radiation and relative duration of sunshine. *Solar Energy*, 32:557–559, 1984.

[67] R. Chervin. Estimates of first– and second–moment climate statistics in GMC simulated climatic ensembles. *Journal of Atmospheric Science*, 37:1889–1902, 1980.

[68] L.S. Chia. Sunshine and solar radiation in Singapore. *Meteorol. Mag.*, 98:265, 1969.

[69] R.E. Childs, D.G.S. Chuah, S.L. Lee, and K.C. Tan. Analysis of solar radiation data using cubic splines. *Solar Energy*, 32:643–653, 1984.

[70] E.W. Chin. A secon order Markov chain model for daily rainfall occurrences. In *Conference on Hydrometeorology*, Am. Meteorol. Soc., Fort Worth, Texas, April 20–22 1976.

[71] N.K.D. Choudbury. Solar radiation at New Dehli. *Solar Energy*, 7:44–51, 1963.

[72] D.G. Chuah and S.L. Lee. Solar radiation estimates in Malaysia. *Solar Energy*, 26:33–40, 1981.

[73] R.J. Cole. Direct solar radiation data as input into mathematical models describing the thermal performance of buildings. I. A review of existing relationships which predict the direct component of solar radiation. II. Development of relationships. *Buildings and Environment*, II:173 and 181, 1976.

[74] M. Collares-Pereira and A. Rabl. The average distribution of solar radiation - Correlation between diffuse and hemispherical and between daily and hourly insolation values. *Solar Energy*, 22:155–164, 1979.

[75] M. Daneshyar. Solar radiation statistics for Iran. *Solar Energy*, 21:345–349, 1978.

[76] A.B. DeAlmeida and R.N. Rosa. Contribuicao para o estudo do clima radiativo de Lisboa. In *Conferencia Nacional de Fisica*, Lisbon, 23–24 Feb. 1978 1978.

[77] X. DeBoer. Calculation of global radiation with the aid of the relative duration of sunshine. *Arch. Met. Geoph. and Biokl.*, B10:xx, 1961.

[78] U.V. Desnica, N.B. Urli, and D. Desnica. Applicability of Liu-Jordan correlation in yugoslavia. *Solar Energy*, 32:435–437, 1984.

[79] M. Petrakis D.P. Lalas and C. Papadopoulos. Correlations for the estimation of the diffuse radiation component in Greece. *Solar Energy*, 39:455–458, 1987.

[80] J.A. Duffie and W.A. Beckman. *Solar Energy Thermal Processes.* John Wiley & Sons, New York, 1954.

[81] J.D. Engels, S.M. Pollock, and J.A. Clark. Observation on the statistical nature of terrestrial irradiation. *Solar Energy*, 26:91–92, 1981.

[82] D.G. Erbs, S.A. Klein, and J.A. Duffie. Estimation of the diffuse radiation fraction for hourly, daily and monthly-average global radiation. *Solar Energy*, 28:293–302, 1982.

[83] R.H.B. Exell. The fluctuation of solar radiation in Thailand. *Solar Energy*, 18:549–554, 1976.

[84] R.H.B. Exell. A mathematical model for solar radiation in South-East Asia (Thailand). *Solar Energy*, 26:161–168, 1981.

[85] R.H.B. Exell. The solar radiation climate of Thailand. *Solar Energy*, 18:349–354, 1976.

[86] R.H.B Exell and Md.M. Huq. The statistical distribution of hourly solar radiation amount in Thailand. *J. Sci. Soc. Thailand*, 4:16–26, 1978.

[87] C.I. Ezekwe and C.C. Ezeilo. Measured solar radiation in a Nigerian environment compared with predicted data. *Solar Energy*, 26:181–186, 1981.

[88] M. Fisz. *Probability theory and mathematical statistic.* John Wiley & Sons Inc., New York, 1978.

[89] E.A. Fitzpatrick and H.A. Nix. *The climatic factor in Australian grasslands*, chapter 1. ANU Press, Canberra, 1970.

[90] A.A. Flocas. Estimation and prediction of global solar radiation over Greece. *Solar Energy*, 24:63–70, 1980.

[91] M. Frere, J.Q. Rijks, and J. Rea. *Estudio agroclimatico de la zona andina.* Technical Report, FAO/UNESCO/OMM, Rome, 1975.

[92] S. Fritz. *Solar radiation energy and its modification by earth and its atmosphere.* American Meteorological Society, 1951. Compendium of Meteorology.

[93] S. Fritz and T.H. McDonald. Average solar radiation in the Unites States. *Heating and Ventil.*, 46:61–64, 1949.

[94] A.J. Gadd and J.F. Keer. Surface exchanges of sensible and latent heat in a 10-level model atmosphere. *Q. Jour. Roy. Met. Soc.*, 96:297–308, 1970.

[95] C. Gandino. Persistence of cloudy and sunny days at the southern foot of the Alps. *17 Tagun fur Alpine Meteorologie*, Berchtesgaden 21–25:November, 1982.

[96] H.P. Garg and S.N. Garg. Prediction of global solar radiation from bright sunshine hours and other meteorological parameters. In *Solar-India 1982. Proceedings of National Solar Energy Convention*, pages 1004–1007, Allied Publishers, New Dehli, 1982.

[97] J.D. Garrison. A study of solar irradiation data for six sites. *Solar Energy*, 32:237–249, 1984.

[98] J.D. Garrison. A study of the division of global irradiance into direct and diffuse irradiance at thirty-three U.S. sites. *Solar Energy*, 35:341–351, 1985.

[99] R. Gicquel. Cumulated frequencies diagrams. In C. Chassague, C. Dupuy, and M.Levy, editors, *Solar energy conversion and applications. Cargese, 19 Juin–2 Juillet 1977*, pages 201–208, 1978.

[100] R. Gicquel. Presentation statistique de donnes meteorologiques relatives a l'ensoleillement. *Rev. Intern. d'Heliotecnique (COMPLES)*, Janvier-June:3–7, 1977.

[101] J. Glover and J.S.G. McCulloch. The empirical relation between solar radiation and hours of sunshine. *Q. J. Roy. Met. Soc.*, 84:172–175, 1958.

[102] T.N. Goh. Statistical study of solar radiation information in an equatorial region (Singapore). *Solar Energy*, 22:105–111, 1979.

[103] T.N. Goh and K.J. Tan. Stochastic modelling and forecasting of solar radiation data. *Solar Energy*, 19:755, 1977.

[104] B. Goldberg and W.H. Klein. A simplified model for determining the spectral quality of daylight and the availability of solar energy at any location. In F. de Winter and M. Cox, editors, *Proceedings of the ISES Congress*, page x, Pergamon Press, New Dehli, India.1978.

[105] B. Goldberg, W.H. Klein, and R.D. McCartney. A comparison of some simple models used to predict solar irradiance on horizontal surface. *Solar Energy*, 22:407–411, 79.

[106] K.K. Gopinathan. Computing the monthly mean daily diffuse radiation from clearness index and percent possible sunshine. *Solar Energy*, 41:379–385, 1988.

[107] K.K. Gopinathan. Empirical correlations for diffuse solar irradiation. *Solar Energy*, 40:369–370, 1988.

[108] K.K. Gopinathan. A general formula for computing the coefficients of the correlation connecting global solar radiation to sunshine duration. *Solar Energy*, 41:499–502, 1988.

[109] J.M. Gordon and M. Hochman. On the correlation between beam and global radiation. *Solar Energy*, 32:329–336, 1984.

[110] J.M. Gordon and M. Hochman. On the random nature of solar radiation. *Solar Energy*, 32:337–342, 1984.

[111] J.M. Gordon and T.A. Reddy. Time series analysis of daily horizontal solar radiation. *Solar Energy*, 41:215–226, 1988.

[112] J. Goussebaile, M.J. Mejon, Ph. Bois, and G. Vachaud. *Critique et analyse de donnees journalieres d'insolation et de rayonnement.* C.N.R.S., Paris, 1979.

[113] V.A. Graham, K.G.T. Hollands, and T.E. Unny. A time series model for kt, with applications to global synthetic weather generation. *Solar Energy*, 40:83–92, 1988.

[114] B. Guerrier, E. Boileau, and C. Benard. Analyse statistique temporelle de l'irradiation solaire globale quotidienne: modelisation d'une variable reduite a l'aide de modeles statistiques A.R.M.A. *Rev. Phys. Appl.*, 15:93–102, 1980.

[115] C.L. Gupta, K.U. Rao, and T.A. Reddy. Radiation design data for solar energy applications. *Energy Menagement*, 3:299, 1979.

[116] A.W. Harrison and C.A. Coombe. Empirical relationship of cloud shade to point cloudiness (Canada. *Solar Energy*, 37:417–421, 1986.

[117] M.M. Hawas and T. Muner. Correlation between global radiation and sunshine data in India. *Solar Energy*, 30:289–290, 1983.

[118] J.E. Hay. Calculation of monthly mean solar radiation for horizontal and inclined surfaces. *Solar Energy*, 23:301–307, 1979.

[119] J.E. Hay. A revised method for determining the direct and diffuse components of the total shortwave radiation. *Atmosphere*, 14:278–287, 1976.

[120] K.G.T. Hollands and R.G. Huget. A probability density function for the clearness index, with applications. *Solar Energy*, 30:195–209, 1983.

[121] K.G.T. Hollands and S.J.Crha. A probability density function for the diffuse fraction, with applications. *Solar Energy*, 38:237–245, 1987.

[122] H.C. Hottel. A simple model for estimating the transmittance of direct solar radiation through clear atmosphere. *Solar Energy*, 18:129, 1976.

[123] H.C. Hottel and A. Willier. Evaluation of flat-plate solar collector performance. In *Conference on the use of solar energy:The scientific Basis, II. Part I.*, pages 74–104, 1955.

[124] C.E. Hounam. Estimates of solar radiation over Australia. *Austr. Met. Mag.*, 43:1–14, 1963.

[125] D.V. Hoyt. Percent possible sunshine and total cloud cover. *Monthly Weather Rev.*, 105:648–652, 1978.

[126] M. Hussain. Estimation of global and diffuse irradiation from sunshine duration and atmospheric water vapour content. *Solar Energy*, 33:217–220, 1984.

[127] M.F. Hutchinson, T.H. Booth, J.P. McMahon, and H.A. Nix. Estimating monthly mean values of daily total solar radiation for Australia. *Solar Energy*, 32:277–290, 1984.

[128] S.M.A. Ibrahim. Predicted and measured global solar radiation in Egypt. *Solar Energy*, 35:185–188, 1985.

[129] F.J.K. Ideriah. A model for calculating direct and diffuse solar radiation. *Solar Energy*, 26:225–228, 1981.

[130] F.J.K. Ideriah. On the relationship between diffuse an global solar radiation. *Solar Energy*, 31:119–124, 1983.

[131] M. Iqbal. Correlation of average diffuse and beam radiation with hours of bright sunshine. *Solar Energy*, 23:169–173, 1979.

[132] M. Iqbal. Estimation of the monthly average of the diffuse component of total insolation on a horizontal surface. *Solar Energy*, 20:101–105, 1978.

[133] M. Iqbal. A study of Canadian diffuse and total solar radiation data-i. monthly average daily horizontal radiation. *Solar Energy*, 22:81–86, 1979.

[134] P.A. Jacobs and P.A. Lewis. Discrete time series generated by mixtures. I: correlational and runs properties. *J. Roy. Stat. Soc.*, B 40:94–97, 1978.

[135] P.A. Jacobs and P.A. Lewis. Discrete time series generated by mixtures. II: asymptotic properties. *J. Roy. Stat. Soc.*, B 40:222–228, 1978.

[136] S. Jain and P.C. Jain. A comparison of the Ångström-type correlations and the estimation of monthly average daily global irradiation. *Solar Energy*, 40:93–98, 1988.

[137] J.D. Kalma and P.M. Fleming. A note on estimating the direct and diffuse components of the global radiation. *Arch. Met. Geoph. Biokl.*, 20:191–205, 1972.

[138] F. Kasten and G. Czeplak. Solar and terrestrial radiation dependent on the amount and type of clouds. *Solar Energy*, 24:177–189, 1980.

[139] B.D. Katsoulis. A method for estimating monthly global solar radiation. *Solar Energy*, 33:403–407, 1984.

[140] B.D. Katsoulis and C.E. Papachristopoulos. Analysis of solar radiation measurements at Athens observatory and estimates of solar radiation in Greece. *Solar Energy*, 21:217–225, 1978.

[141] M. Kendall and A. Stuart. *The advanced theory of statistics.* Charles Griffin Co. Ltd., London, 1977.

[142] A. Khogali. Solar radiation over Sudan. Comparison of measured and predicted data. *Solar Energy*, 31:45–53, 1983.

[143] A. Khogali, M.R. Ramadan, Z.E.H. Ali, and Y.A. Fattah. Global and diffuse solar irradiance in Yemen (Y.A.R.). *Solar Energy*, 31:55–62, 1983.

[144] W.T. Kierkus and W.G. Colborne. Diffuse solar radiation - Daily and monthly values as affected by snow cover. *Solar Energy*, 42:143–147, 1989.

[145] H.H. Kimball. Variations in the total and luminous solar radiation with geographical position in the United States. *Month. Weat. Rev.*, 47:769–793, 1919.

[146] S.A. Klein. Calculation of monthly average insolation on tilted surfaces. *Solar Energy*, 19:325–329, 1977.

[147] J. Klink. *A global solar radiation climatology for Minneapolis–St. Paul.* PhD thesis, University of Minnesota, Unpublished, 1974.

[148] K.Ya Kondratiev. *Radiation characteristics of the atmosphere and the earth's surface.* Amerind Publishing Co. Pvt. Ltd., New Dehli, 1973. Trans. from Russian.

[149] A.I. Kudish, D. Wolf, and Y. Machlav. A novel approach for calculating the monthly average daily fraction of diffuse solar radiation. *Solar Energy*, 28:181–186, 1982.

[150] G.F. Lameiro. *Stochastic models of solar energy systems.* PhD thesis, Colorado State University, 1977. 68 pp.

[151] G.F. Lameiro and M.C. Bryson. The effect of Markovian and discrete climate assumptions on the performance analysis of solar heating systems. *Journal of Applied Meteorology*, 17:386–389, 1978.

[152] G.F. Lameiro and W.S. Duff. A Markov model of solar energy space and hot water heating systems. *Solar Energy*, 22:211–219, 1979.

[153] B. LeBaron and I. Dirmhirn. Strengths and limitations of the Liu and Jordan model to determine diffuse from global irradiance. *Solar Energy*, 31:167–172, 1983.

[154] C. Leith. The standard error of time–averaged estimates of climatic means. *J. Appl. Meteorology*, 12:1066–1069, 1973.

[155] J.C. Leong and N.T. Soh. *An investigation of solar radiation in Singapore.* Mech. Engng. Dept. Report, Univ. of Singapore, 1973.

[156] R. Lestienne. Application du modele markovien simplifie a l'etude du comportement du stockage d'une centrale solaire. *Revue de Physique Appliquee*, 14:139–144, 1979.

[157] R. Lestienne. Modele markovien simplifie de meteorologie a deux etats. L'exemple d'Odeillo. *La Meteorologie*, 12:53–64, 1978.

[158] R. Lestienne, Ph. Bois, and Ch. Obled. *Analyse temporelle et cartographie de la matrice stochastique pour le modele Markovien dans le midi de la France.* C.N.R.S., Paris, 1979.

[159] G. Lewis. The applicability of diffuse solar radiation models to Huntsville, Alabama. *Solar Energy*, 38:55–57, 1987.

[160] G. Lewis. Diffuse irradiations over Zimbabwe. *Solar Energy*, 31:125–128, 1983.

[161] G. Lewis. Estimates of irradiance over Zimbabwe. *Solar Energy*, 31:609–612, 1983.

[162] G. Lewis. Irradiance estimates for Zambia. *Solar Energy*, 26:81–85, 1981.

[163] B.Y.H. Liu and R.C. Jordan. The interrelationship and the characteristic distribution of direct, diffuse and total solar radiation. *Solar Energy*, 4:1–19, 1960.

[164] B.Y.H. Liu and R.C. Jordan. A rational procedure for predicting the long-term average performance of flat-plate solar-energy collectors. *Solar Energy*, 7:53–74, 1963.

[165] G.O.G. Löf, J.A. Duffie, and C.O. Smith. *World distribution of solar radiation.* Engineering Experimental Station, Report N.21, University of Wisconsin, 1966.

[166] R.L. Lougeay and A.J. Brazel. A presentation of solar irradiation data suitable for solar energy application. *Solar Energy*, 33:409–415, 1984.

[167] F.E. Lumb. The influence of cloud on hourly amounts of total solar radiation at the sea surface. *Quart. Jour. Roy. Met. Soc.*, 90:43–56, 1964.

[168] I.A. Lund. Relationship between insolation and other surface weather observations at Blue Hill, Massachussets. *Solar Energy*, 12:95, 1968.

[169] C.C.Y. Ma and M. Iqbal. Statistical comparison of solar radiation correlations. Monthly average global and diffuse radiation on horizontal surfaces. *Solar Energy*, 33:143–148, 1984.

[170] R. Madden. Estimates of the autocorrelation and spectra of seasonal mean temparatures over North America. *Monthly Weather Review*, 105:9–18, 1977.

[171] R. Madden. Estimates of the natural variability of time–averaged sea–level pressure. *Monthly Weather Review*, 104:942–952, 1976.

[172] N.H. Majmudar. Availability of solar radiation and collection area requirement for solar heating of a laboratory in Sringar. *Solar Energy*, 28:263–264, 1982.

[173] H. Malberg. Comparison of mean cloud cover obtained by satellite photographs and ground based observations over Europe and the Atlantic. *Mon. Weat. Rev.*, 101:893, 1973.

[174] A. Mani and O. Chacko. Diffuse solar radiation ai Dehli and Poona. *Ind. J. Met. Geoph.*, 14:416–432, 1963.

[175] A. Mani, O. Chacko, V. Krishnamurthy, and V. Desikan. Distribution of global and net radiation over the Indian Ocean and its environments. *Arch. Met. Geoph. Biokli.*, B15:82, 1967.

[176] A. Mani and S. Rangarajan. Tecniques for the precise estimation of hourly values of global, diffuse and direct solar radiation. *Solar Energy*, 31:577–595, 1983.

[177] H. Masson. Quantitative evolution of solar radiation. *Solar Energy*, 10:119–124, 1966.

[178] R.A. McClatchey. *Optical properties of the atmosphere*, chapter 14. McGraw-Hill, New York, 1979.

[179] M.J. Mejon, J. Goussebaile, Ph. Bois, and G. Vachaud. Etude des liasons entre l'irradiation solaire journaliere et quelque variable meteorologique. Exemple des stations de Carpentras, Nice et Ajaccio. In R. Lestienne, editor, *Analise Statistique des Processus Meteorologiques Appliquee a l'Energie Solaire*, pages 106–143, C.N.R.S., Paris, 1979.

[180] A.F. More and L.H. Abbot. The brightness of the sky. *Smithsonian Miscellaneous Collection*, 71:1–36, 1920.

[181] C. Mustacchi, V. Cena, and M. Rocchi. Stochastic simulation of hourly global radiation sequences. *Solar Energy*, 23:47–51, 1979.

[182] F. Neuwirth. Beziehungen zwitschen den Monatswerten der Globalstrahlung und der Sonnenscheindauer in Österreich. *Arch. Met. Geoph. Biokl.*, B26:171–182, 1978.

[183] F. Neuwirth. The estimation of global and sky radiation in Austria. *Solar Energy*, 24:421–426, 1980.

[184] F.J. Newland. A study of solar radiation models for the coastal region of South China. *Solar Energy*, 43:227–235, 1989.

[185] M. Nicolet and R. Dogniaux. *Etude de la radiation globale du soleil.* Technical Report, Institut Royal Meteorologique de Belgique -Memoires XLVII, 1951.

[186] D.J. Norris. Correlation of solar radiation with clouds. *Solar Energy*, 12:107, 1968.

[187] D.J. Norris. Solar radiation on inclined surfaces. *Solar Energy*, 10:72–77, 1966.

[188] V.A. Notaridou and D.P. Lalas. The distribution of global and net radaition over greece. *Solar Energy*, 22:505–514, 79.

[189] H. Ögelman, A. Ecevit, and E. Tasdemiroglu. A new method for estimating solar radiation from bright sunshine data. *Solar Energy*, 33:619–625, 1984.

[190] J.A. Olseth and A. Skartveit. A probability density function for daily insolation within the temperate storm belts. *Solar Energy*, 33:533–542, 1984.

[191] J.A. Olseth and A. Skartveit. A probability density model for hourly total and beam irradiance on arbitrarily orientated planes. *Solar Energy*, 39:343–351, 1987.

[192] F.N. Onyango. On the estimation of global solar insolation. *Solar Energy*, 31:69–71, 1983.

[193] J.F. Orgill and K.G.T. Hollands. Correlation equation for the hourly diffuse radiation on horizontal surface. *Solar Energy*, 19:357–359, 1977.

[194] J.K. Page. The estimation of monthly mean values of daily totals short wave radiation on vertical and inclined surfaces for latitudes 40° North – 40° South. In *Proc. UN Conference on New Sources of Energy*, page 378 (vol.4), 1964.

[195] J.K. Page. *Methods for the estimation of solar energy on vertical and inclined surfaces*, pages 37–39. Pergamon Press, Oxford, 1979.

[196] G.W. Paltridge. *Solar radiation statistics for Australia.* Paper N.23, CSIRO, Division for Atmospheric Physics, Australia, 75.

[197] G.W. Paltridge and D. Proctor. Monthly mean solar radiation statistics for Australia. *Solar Energy*, 18:235–243, 1976.

[198] D.E. Parker. The effect of cloud on solar radiation receipt at the tropical ocean surface. *Met. Mag.*, 100:232–240, 1971.

[199] G.V. Parmelee. Irradiation of vertical and horizontal surfaces by diffuse solar radiation from cloudless skies. *ASHVE Transactions*, 60:341–358, 1954.

[200] H.L. Penman. Natural evaporation from open water, bare solids and grass. *Proc. Roy. Soc.*, A 193:120–145, 1948.

[201] Ch. Perrin de Brichambaut. Estimation des resources solaire en France. *Cahier AFEDES*, 1:, 1975.

[202] Ch. Perrin de Brichambaut and Ch. Vauge. *Le gisement solaire.* Technique & Documentation, Paris, 1982.

[203] W.R. Petrie and M. McClintock. Determining typical weather for use in solar energy simulations. *Solar Energy*, 21:55–59, 1978.

[204] J.A. Prescott. Evaporation from a water surface in relation to solar radiation. *Trans. Roy. Soc. Australia*, 64:114–118, 1940.

[205] A.S.N. Raju and K. Karuna Kumar. Comparison of point cloudiness and sunshine derived cloud cover in India. *Pageoph.*, 120:495, 1982.

[206] S. Rangarajan, M.S. Swaminathan, and A. Mani. Computation of solar radiation from observation of cloud cover. *Solar Energy*, 32:553–556, 1984.

[207] C.R.N. Rao, W.A. Bradley, and T.Y. Lee. The diffuse component of the daily global solar irradiation at Corvallis, Oregon (U.S.A.). *Solar Energy*, 32:637–641, 1984.

[208] C.R.N. Rao, W.A. Bradley, and T.Y. Lee. Some comments on Ångstr"om-type regression models for the estimation of the daily global solar irradiation. *Solar Energy*, 34:117–119, 1985.

[209] K.R. Rao and B.P. Lim. Solar energy availability at Singapore. In F. de Winter and M. Cox, editors, *Proceedings of the ISES Congress*, pages 448–453, Pergamon Press, January 1978.

[210] K.R. Rao and T.N. Seshadri. Solar insolation curves. *Ind. J. Meteorol. Geophys.*, 12:267–272, 1961.

[211] S.J. Reddy. An empirical method for the estimation of net radiation intensity. *Solar Energy*, 13:290–291, 1971.

[212] S.J. Reddy. An empirical method for the estimation of total solar radiation. *Solar Energy*, 13:289–290, 1971.

[213] S.J. Reddy. An empirical model for estimating sunshine from total cloud amount. *Solar Energy*, 15:281, 1974.

[214] S.J. Reddy. Estimation of global solar radiation. *Solar Energy*, 26:279, 1981.

[215] S.J. Reddy. The estimation of global solar radiation and evaporation throug precipitation - A note. *Solar Energy*, 38:97–104, 1987.

[216] S.J. Reddy, N.M. da Amorim, and M.da G. da S. Elpidio. A simple method for the estimation of global solar radiation over northeast brazil. *Pesq. Agropec. Bras.*, Brasilia 19:391–405, 1984.

[217] T.A. Reddy, S. Kumar, and G.Y. Saunier. Review of solar radiation analysis techniques for predicting long-term thermal collector performance: Applicability to Bankok data. *Renewable Energy Review J.*, 7:56, 1985.

[218] M.R. Rietveld. A new method for estimating the regression coefficients in the formula relating solar radiation to sunshine. *Agri. Meteorol.*, 19:243–252, 1978.

[219] D.W. Ruth and R.C. Chant. The relationship of diffuse radiation to total radiation in Canada. *Solar Energy*, 18:153–154, 1976.

[220] C. Leone S. Barbaro, S. Coppolino and E. Sinagra. An atmospheric model applied to some actinometric stations of Sicily. *Solar Energy*, 25:201–206, 1980.

[221] J.A. Sabbagh, A.A.M. Sayigh, and E.M.A. El-Salam. Estimation of the total solar radiation from meteorological data. *Solar Energy*, 19:307–311, 1977.

[222] G.Y. Saunier, T.A. Reddy, and S. Kumar. A monthly probability distribution function of daily global irradiation values appropriate for both tropical and temperate locations. *Solar Energy*, 38:169–177, 1987.

[223] A.A.M. Sayigh. Estimation of total solar radiation intensity. A Universal Formula. In *4th Course of Solar Energy Conversion*, ICTP, Trieste, 1977.

[224] A.A.M. Sayigh. Solar energy availability prediction from climatological data. In A.A.M. Sayigh, editor, *Solar Energy Engineering*, Academic Press, New York, 1977.

[225] E. Scerri. The radiation climate of Malta. *Solar Energy*, 28:353–356, 1982.

[226] H. Scheffe. *The analysis of variance*. John Wiley & Sons Inc., New York, 1959.

[227] W. Schuepp. Chapter 4. In N. Robinson, editor, *Solar radiation*, Elsevier, Amsterdam, 1966.

[228] R. Sears, R.G. Flocchini, and J.L. Hatfield. Correlation of total, diffuse and direct solar radiation with the percentage of possible sunshine for Davis, California. *Solar Energy*, 27:357–360, 1981.

[229] A.A. Sfeir. Solar radiation in Lebanon. *Solar Energy*, 26:497–502, 1981.

[230] A.A. Sfeir. A stochastic model for predicting solar system performance. *Solar Energy*, 25:149–154, 1980.

[231] S.I. Sivkov. On the computation of the possible and relative duration of sunshine. *Trans. Main Geophys. Obs.*, 160, 1964.

[232] S.I. Sivkov. To the method of computing the possible radiation in Italy. *Trans. Main Geophys. Obs.*, 160, 1964.

[233] R.H. Skaggs, D.G. Baker, and J.E. Liungkull. The influence of persistence and variability on the required solar radiation record lenght. *Solar Energy*, 28:281–287, 1982.

[234] A. Skartveit and J.A. Olseth. A model for the diffuse fraction of hourly global radiation. *Solar Energy*, 38:271–274, 1987.

[235] P.J. Smietana, R.G. Flocchini, R.L. Kennedy, and J.L. Hatfeld. Comparison of diffuse/global ratios calculated from one-minute, hourly and daily solar radiation data. *Solar Energy*, 32:417–423, 1984.

[236] P.J. Smietana, R.G. Flocchini, R.L. Kennedy, and J.L. Hatfeld. A new look at the correlation of k_d and k_t ratios and at global solar radiation tilt models using one-minute measurements. *Solar Energy*, 32:99–107, 1984.

[237] A. Soler. On the monthly variations in the atmospheric transmission for cloudless skies as inferred from the correlation of daily global radiation with hours of sunshine for Spain. *Solar Energy*, 37:235–238, 1986.

[238] SOLMET. *Hourly solar radiation surface meteorological observations.* Technical Report, Volume 2 - Final Report, TD-9724, 1979.

[239] J.W. Spencer. A comparison of methods for estimating hourly diffuse solar radiation from global solar radiation. *Solar Energy*, 29:19–32, 1982.

[240] J.W. Spencer. Computer estimation of direct solar radiation on clear days. *Solar Energy*, 13:437–438, 1972.

[241] G. Stanhill. Diffuse sky and cloud radiation in Israel. *Solar Energy*, 10:96–101, 1966.

[242] R.W. Stuart and K.G.T. Hollands. A probability density function for the beam transmittance. *Solar Energy*, 40:463–467, 1988.

[243] H. Suehrcke and P.G. McCormick. An approximation for v of the fractional time distribution of daily clearness index. *Solar Energy*, 39:369–370, 1987.

[244] H. Suehrcke and P.G. McCormick. The diffuse fraction of instantaneous solar radiation. *Solar Energy*, 40:423–430, 1988.

[245] H. Suehrcke and P.G. McCormick. The frequency distribution of instantaneous insolation values. *Solar Energy*, 40:413–422, 1988.

[246] R.K. Swartman and O. Ogunlade. Solar radiation estimates from common parameters. *Solar Energy*, 11:170–172, 1967.

[247] J.C. Theilacker and S.A. Klein. Improvement in the utilizability relationships. In *Proceedings of the Annual Meeting of ISES, U.S. Section*, page 271, Phoenix, 2–6 June 1980.

[248] J.F. Tricaud, Mrs Le Phat Vinh, and Mrs Parra. Statistical analysis of solar radiation data of a high altitude station. In *EC Contractor's Meeting*, pages 183–189, Brussels,18–19 October 1982.

[249] S.E. Tuller. The relationship between diffuse, total and extraterrestrial solar radiation. *Solar Energy*, 18:259, 1976.

[250] W.D. Turner and M. Salim. Comparison of two diffuse sky radiation models. *Solar Energy*, 32:677–679, 1984.

[251] S.M. Turton. The relationship between total irradiation and sunshine in the humid tropics. *Solar Energy*, 38:353–354, 1987.

[252] V.N. Ukraintzev. Cloudiness and sunshine. *Meteorol. Hydrol.*, 6, 1939.

[253] F. Vignola and D.K. McDaniels. Correlations between diffuse and global insolation for the Pacific Northwest. *Solar Energy*, 32:161–168, 1984.

[254] F. Vignola and D.K. McDaniels. Diffuse-global correlation: seasonal variations. *Solar Energy*, 33:397–402, 1984.

[255] A. Whillier. The determination of hourly values of total solar radiation from daily summation. *Archiv fur Meteorologie Geophysik und Bioklimatologie*, B7:197, 1956.

[256] A. Whillier. *Solar energy collection and its utilisation for house heating.* PhD thesis, MIT, Cambridge, Massachussets, 1953.

[257] A. Zangvil and E. Aviv. On the effect of latitude and season on the relation between the diffuse fraction of solar radiation and the ratio of global to extraterrestrial radiation. *Solar Energy*, 39:321–327, 1987.

Volume printed by the Ufficio Documentazione of the Department of Physics of the Genoa University